Improving construction sustainability by using glassy secondary materials as aggregate in concrete

Caroline Morrison

PhD Thesis

July 2005

In association with:

Sheffield University's Department of Engineering Materials
Building Research Establishment (BRE) Centre for Concrete Construction

Funded by the BRE Trust

Summary

This thesis reports experimental work, carried out as a PhD study, investigating the possible re-use of glassy secondary materials as aggregate in concrete. A study of the relevant literature suggested that slag from the Imperial Smelting Furnace method of zinc production (ISF slag) and Cathode Ray Tube (CRT) glass from end of life computer monitors and television screens would be promising materials to test. The main issues identified as being of most concern relating to the use of these materials were the potential for alkali-silica reaction (ASR) due to the glassy nature of the aggregate materials, in-service leaching of heavy metal ions, namely lead, zinc and barium from the aggregates and the possibility of a delay in set caused by the addition of these materials to concrete or mortar mixes.

A comprehensive study has been completed that has included characterisation of the secondary aggregate materials, their incorporation into concrete mixes and their effect on ASR, leaching and retardation of concrete set. Methods have been identified to minimise these potential problems where they have been shown to be an issue. These include the recommendation of various additions, depending upon the specific problem being overcome, ranging from cement replacement materials, such as pulverised fuel ash (PFA) and ground, granulated blastfurnace slag (GGBS) to chemical additions such as barium and calcium chlorides.

Overall, it has been shown that the ISF slag and CRT glass could prove to be useful secondary materials for use in the construction industry and it is hoped that their specification and use will be forthcoming as a result of this study.

Acknowledgements

The author would like to gratefully acknowledge the help and support of everyone who has made this research possible and in particular the BRE Trust who have provided the funding for this project. Many thanks to my supervisors from Sheffield University's Department of Engineering Materials, Dr. Russell Hand and Prof. John Sharp, as well as my industrial supervisor from BRE, David Richardson, who have provided constant technical and moral support.

Additionally, I would like to acknowledge the assistance and training that has been provided by the technical staff from both Sheffield University and BRE, without whom this work would not have been possible. In particular, I would like to express thanks to Heath Bagshaw, Neil Gape, Jacqui Hardcastle, Beverly Lane, Simon Lane, Len Liberty, Nik Reeves, Clive Tipple and Martyn Webb. Finally, I would like to thank Rebecca Hooper, Kevin Lardner and Ted Sibbick for their continued support and useful discussions.

Contents

Summary of abbreviations used in text

General

CRT = Cathode ray tube
ISF = Imperial smelting furnace (slag)
BGL = Bottle glass
TVS = Thames Valley sand
ASR = Alkali silica reaction
PFA = Pulverised fuel ash
GGBS = Ground, granulated blast furnace slag
DI = Deionised water
WEEE = Waste electrical & electronic equipment
RoHS = Restriction of hazardous substances
EA = Environment Agency
L/S = Liquid:Solid ratio
Na_2O_{eq} = alkali content, expressed as an equivalent concentration of sodium oxide

Cement compounds

CH = Calcium hydroxide/ $Ca(OH)_2$/ Portlandite
CC = Calcium carbonate/ $CaCO_3$/ Calcite
CaO = Calcium oxide/ Lime
CSH = Calcium silicate hydrate
C3S = $3CaO.SiO_2$/ Tricalcium silicate
C3A = $3CaO.Al_2O_3$/ Tricalcium aluminate

Experimental techniques

XRF = X-ray fluorescence
XRD = X-ray diffraction
SEM = Scanning electron microscopy
TEM = Transmission electron microscopy
EDS = Energy dispersive spectroscopy
SADP = Selected area diffraction pattern
ICC = Isothermal conduction calorimetry
TGA = Thermogravimetric analysis
TCLP = Toxicity characteristic leaching procedure
AAS = Atomic absorption spectroscopy
ICP-OES = Inductively coupled plasma – optical emission spectroscopy
XPS = X-ray photoelectron spectroscopy

1 Introduction

The use of secondary/ recycled materials in concrete has the potential to deliver significant benefits to the UK construction industry and the wider community. The use of such materials in construction will eliminate the need to landfill certain wastes. In turn, this will reduce the risk of any long-term damage to the environment through uncontrolled leaching from landfill sites and also extend the lifespan of sites in the immediate areas surrounding where the waste is generated/ collected.

The use of alternative materials as a replacement for primary, natural aggregates will reduce the consumption of natural resources and improve the sustainability of concrete construction. Legislation and various proposed directives are driving and promoting this kind of material reuse and recycling throughout every industry and this is leading to a wide range of potential materials being investigated.

This project is focussed on assessing the suitability of two such materials for use in concrete construction, namely waste Cathode Ray Tube (CRT) glass from end-of-life television screens and computer monitors etc. and slag from the Imperial Smelting Furnace (ISF) method of zinc production. It is hoped that the outcomes and information obtained from this work will be relevant to other glassy secondary materials that could potentially find use as aggregates in concrete.

There are several reasons why it would be beneficial to find a secondary use for these materials and divert them away from landfill disposal. In particular, both are known to contain lead and other heavy metals, which could be potentially damaging to the environment. There are several zinc-smelting plants around the world using the ISF method, which produce approximately one million tonnes of ISF slag per year. With the introduction and rapid acceptance of new technologies such as flat-screen televisions, it is anticipated that there will be a corresponding increase in the rate at which CRTs become obsolete. So it can be expected that considerable quantities of both of these materials will require disposal for some time to come, unless an alternative outlet can be found.

2 Literature review

Reuse and recycling has become an important consideration for many industries over the years, including the construction industry. The need to meet various environmental targets as well as to win public support has forced a general change in attitude, which has led to investigation into the reuse of many materials that would otherwise have been considered waste and most likely disposed of as landfill. The pressure to recycle is becoming more intense, with the introduction of many directives and legislation aimed at conserving energy and natural resources and, in particular, diverting potentially hazardous materials away from landfill sites.

2.1 Directives and taxes

In 1996 the UK landfill tax was introduced on materials being sent to landfill. The aim was to encourage waste producers to reduce the amount of waste being sent to landfill and to recover more value from the waste through recycling or composting where possible. It was also hoped that more environmentally friendly disposal methods would be adopted, which would help divert materials away from landfill. The rate of the tax was set at £2 per tonne for waste that was considered inert and a standard rate of £7 per tonne for all other waste (termed 'active' and described as 'waste that gives off emissions'). Since 1999, the standard rate has been steadily increasing up to £15 per tonne in 2005 and is set to increase further over the coming years to a medium- to long-term rate of £35 per tonne. The rate for inert waste has been frozen at £2 per tonne[1].

The recent EU Directive on Waste Electrical and Electronic Equipment (WEEE) is modelled on the End-of-Life Vehicle (ELV) Directive and is aimed at diverting hazardous substances away from landfill. This requires that 70% by weight of material classified under the Directive must be recycled and this target is expected to increase with time[2]. The associated Restriction of Hazardous Substances Directive (RoHS) aims to limit the inclusion of hazardous substances in electronic equipment, in order to minimise the potential harm that may result from improper disposal[3].

As well as increasing disposal costs and preventing certain materials being sent to landfill, other taxes have been introduced that will hopefully encourage recycling and reduce the demand on natural resources. The aggregate tax, that was introduced in April 2002, imposes a rate of £1.60 on every tonne of aggregate sold in the UK. The purpose of the tax was to address the environmental costs associated with quarrying operations, such as noise, dust, visual intrusion and damage to biodiversity[4].

However, as with many tax increases and directives that disadvantage certain parties, there was opposition to the tax from several organisations, representing the quarrying and aggregate industries. They argued that the tax disadvantaged UK producers compared to other countries and that there were no sufficient environmental bench

marks in place to assess the impact of the tax[5,6]. Consequently, this tax has been frozen at the rate of £1.60 for the time being.

Despite inevitable opposition to these taxes and directives, their introduction has led to the investigation and use of many secondary and recycled materials. There are several of these that have been utilised successfully by the UK construction industry, most providing their own significant benefits. Many waste materials have been found to be useful as aggregates or additives in concrete, or as raw materials in the manufacture of cements.

2.2 Successful use of secondary materials in concrete

Many recycled materials have been used successfully in concrete and construction applications. Due to the often variable nature of certain waste streams, some are most suited to use in low-grade applications, such as roadbase and fill materials, where they will generally provide cost savings over primary aggregates. Mixed crushed glass from recycled bottles and containers is often utilised as roadbase material[7,8] and recycled concrete from demolition waste can be used in foundations, as roadbase or fill material and also as aggregate in concrete[9,10].

However there are some materials that have found very specialised uses in concrete applications. Several secondary/ by-product materials have been found to possess pozzolanic properties, making them cementitious in the presence of a suitable activator. They can therefore be used as a cost effective replacement for Portland cement in concrete mixes, often bringing additional benefits such as improved workability and concrete durability. These include fly ash from coal combustion[11-15], iron blast furnace[11-13,16,17] and other slags[17-20,] and silica fume from the manufacture of silicon metal[11,13,20].

2.3 Other potential material sources

There are other materials that could potentially find secondary uses in concrete construction, but so far have only received limited investigation. These include china clay wastes[21] and rubber from the mechanical breakdown of used tyres[22-25], as well as the glass from waste cathode ray tubes (CRT) and slag from the Imperial smelting furnace (ISF) method of zinc production, which are considered here

2.3.1 CRT glass

The rapid adoption of new technologies, such as flat-screen and plasma televisions, is anticipated to cause a corresponding increase in the rate at which CRTs from TV screens and computer monitors become obsolete. Figure 2.1 shows the main components of a CRT within a typical computer monitor. The three distinct types of glass within a CRT are the plate/ screen glass, the funnel glass and the neck glass. The composition of each type is different and each may also vary between manufacturers. The funnel and screen are welded together using a lead frit/ solder glass in colour CRTs, whereas a steel frame is used in monochrome CRTs. Table 2.1 gives details of the relative composition of each different type of glass.

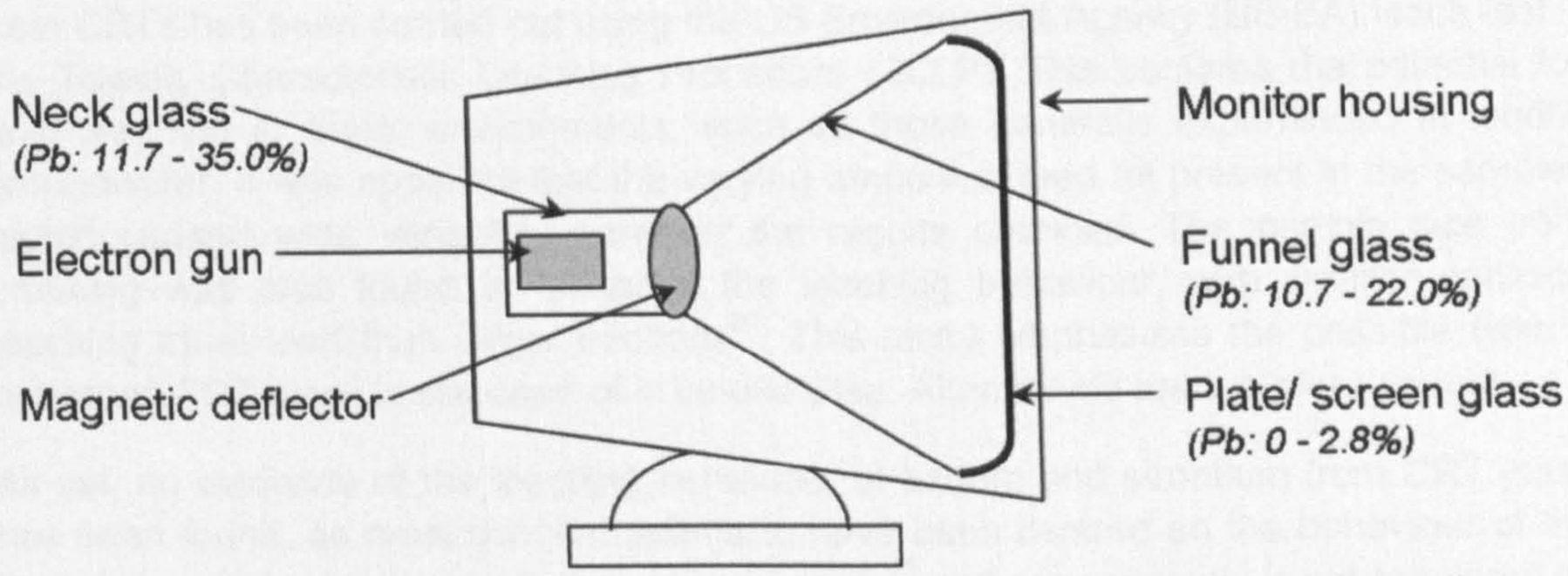

Figure 2.1: Diagram of main CRT components

Table 2.1: Composition of the different types of glass within a CRT[28]

Oxide %	Neck glass	Cone glass	Faceplate/ Screen glass
SiO_2	38.0 - 58.6	50.5 - 67.3	60.7 - 64.4
Na_2O	2.0 - 3.7	6.0 - 8.2	7.5 - 8.9
K_2O	10.9 - 16.5	7.1 - 10.2	6.9 - 10.6
CaO	0.1 - 2.1	0.3 - 5.3	0 - 4.2
MgO	0.8 - 1.0	1.5 - 3.7	0 - 1.8
BaO	0.7 - 6.8	0.8 - 12.3	0.2 - 13.6
PbO	11.7 - 35.0	10.7 - 22.0	0[#]
B_2O_3	1.4 - 2.8	0	0
Al_2O_3	0.9 - 3.1	1.8 - 5.1	1.7 - 3.9
TiO_2	0	0	0 - 0.6
CeO	0	0	0 - 0.3
SrO	0	0	0 - 10.5

[#] Although no lead is reported in the faceplate/ screen glass from this source, other sources[26,27] acknowledge the presence of lead in screen glass, particularly from older CRTs (0.1-2.8 wt%)

The WEEE Directive, mentioned earlier, is likely to strongly affect the disposal options available for CRT glass, as it can contain an average of between 8-25% lead oxide. The lead is used as radiation shielding, due to the ability of lead to absorb gamma rays and other forms of harmful radiation. There are also other heavy metals present in the various glass components, including barium (up to approx. 14%) and strontium (up to approx. 11%), which are often found in the plate/ screen glass of newer CRTs as an alternative to lead[26-29].

There is concern that the heavy metals present in CRTs would pose an environmental risk if they were to leach from the glass. A previous study into the leachability of lead

from CRTs has been carried out using the US Environment Agency (US EA) leach test – the Toxicity Characteristic Leaching Procedure (TCLP). This confirms the potential for lead leaching in acidic environments, such as those generally experienced in landfill groundwater. It was apparent that the varying amount of lead frit present in the samples tested caused wide variability between the results obtained. The particle size from crushing was also found to influence the leaching behaviour, with smaller particles leaching more lead than larger fractions[30]. This study emphasises the possible risks if untreated CRT glass is disposed of in landfill sites. Alternatives are therefore sought.

As yet, no evidence of the leaching behaviour of barium and strontium from CRT glass has been found, as most concern seems to have been centred on the behaviour of the lead. It is apparent that strontium is of low toxicity[31] and consequently is not regulated by organisation such as the UK Environment Agency in the same way as lead and barium.

However, both barium and strontium exist in a radioactive form, which are often found in many hazardous and high level radioactive waste streams. These have been investigated to some extent in relation to the vitrification and stabilisation of radioactive waste in glass. Barium was found to leach from glass into deionised water in apparently non-standard leach tests, though the leaching rate decreases over time and was further reduced by the inclusion of zinc oxide in the glass[32]. When analysed using the US TCLP, barium leaching was again reduced by the presence of phosphorus oxide in the glass[33]. No guidelines were given to assess whether the leaching observed in these studies were above or below any acceptance criteria. No leaching data could be found for strontium in glass.

TV manufacturers tend not to see recycled CRT cullet as a viable option due to the high quality requirements of the final glass and recycling into conventional glass recycling systems for the glass container industry is not a viable option due to its lead content[28]. However, there are several techniques that are currently under investigation with regard to the reuse of CRTs. These include refurbishment of waste electronic equipment where possible, otherwise separation and recycling of their component materials – glass-to-glass recycling, metals recovery and plastics recycling[34].

After being crushed and separated from other component materials, the leaded glass from CRTs may be sent to a lead refiner where the lead can be extracted and recycled. The glass replaces the silica normally used as a fluxing agent in the refining process[29]. Further studies have looked at the possibility of using a foaming process on the glass that does not require melting, thus preserving the chemical stability of the glass. The foamed product shows minimal lead leaching and it is thought that it could be used in applications such as thermal insulators, lightweight structural panels or filters[35]. Where it is possible to separate the panel/ screen glass, which often does not contain lead, there are more potential applications for reuse, including insulating glass fibre production, as tableware glass and in the production of ceramic glazes[26,27]. There is also research that suggests that ultrasonic accelerated leaching may be useful to remove the lead from CRT glass, allowing the glass to be recycled more readily into new products[36].

2.3.2 ISF slag

This ferro-silicate slag is a by-product of the Imperial Smelting Furnace (ISF) method of zinc production. Although the UK's ISF plant in Avonmouth closed in February 2003, a stockpile of 2.5 million tonnes of ISF slag still remains on the site[37]. Similar ISF plants exist around the world, producing just under a million tonnes of ISF slag annually[38]. Examples of typical ISF slag compositions are given in Table 2.2. The method used to determine these chemical compositions is not always specified, though one source[39] suggests the use of both X-ray diffraction (XRD) analysis in addition to atomic absorption spectroscopy (AAS) and plasma techniques.

Previous studies[39-44] have investigated the potential use of this type of slag material as an aggregate in concrete and mortars, the results from which have generally been positive. It has been shown that mortar and concrete samples, with a partial replacement of sand with ISF slag, give similar compressive strength results to control samples. The main concern to arise from these previous studies is the potential for the metal ions, zinc and lead, to leach from the slag into the surrounding environment, which would have health and environmental implications. It appears that generally the levels of leached ions increase in alkaline solutions when compared to water and increase further still in acidic solutions[39].

Table 2.2: Typical composition of ISF slags

Oxide or metal	Wt. % present in several ISF slags			
FeO	52.90	39.66	38.17	38.28
SiO_2	11.30	18.13	19.69	16.12
Al_2O_3	5.50	8.25	7.77	7.66
CaO	3.30	13.66	14.80	15.66
Zn	9.80	7.62	7.24	6.93
Pb	1.40	0.61	0.76	1.02
Cu	0.60	0.42	0.68	0.85
S	-	3.55	2.92	2.84
As	0.18	0.05	0.02	-
(Reference)	(39)	(45)	(45)	(41)

Additional studies are currently underway at BRE to investigate the use of this material as an aggregate in roadway construction – an area in which other similar materials, such as slag from steel production, have already been successfully utilised[46].

2.4 Potential barriers to use

Studies have indicated that there are several potential barriers that would need to be overcome in order for these particular materials to be accepted for use in concrete. These include the potential for alkali-silica reaction (ASR) in concrete caused by the

glassy nature of the aggregates, the risk of heavy metal ions leaching from the aggregates and the possibility of retardation of concrete set.

2.4.1 Alkali-silica reaction (ASR)

Although recycled glass may seem an attractive alternative to other aggregates for use in concrete, there is concern regarding the potential for alkali-silica reaction in concrete due to the high silica content of glass. ASR occurs in concrete when soluble alkali ions such as sodium and potassium react with certain sources of silica found in aggregate. This produces a gel that is able to absorb water. The water causes the gel to swell, which can lead to expansion and cracking of the surrounding concrete[47].

The main source of alkali ions is usually the cement, although they may come from the aggregate or from external sources such as de-icing salts, alkaline water or sea water[48]. During cement hydration, Portlandite (calcium hydroxide – $Ca(OH)_2$) is produced, which is present as a crystalline hydroxide. However, sodium and potassium hydroxides that form remain in the pore solution of the concrete. In this alkali environment, any silica present in the aggregate undergoes an acid/alkali surface reaction, which results in the formation of a gelatinous alkali-silicate gel. The reaction will proceed until either the available silica or the available alkali ions are used up, or until the concentration of hydroxide ions is so low that the reactive silica is no longer attacked[47].

The uptake of water causes a volume expansion in the alkali-silica gel. Some forms of silica react so slowly that there is sufficient time for this gel to expand into the surrounding pore network without causing a build up of internal stresses. Similarly, if the concrete is very porous, suggesting low quality concrete, any gel that forms is able to dissipate through the pore network and may not exert sufficient pressure on the concrete matrix to cause noticeable damage. However, if the concrete is of good quality with a low density of pores, the pressure caused by the formation of gel may lead to microcracking within the concrete. A characteristic feature of ASR damage is a random network of cracks known as map cracking[13,49-51].

The cracking itself may not always be sufficient to cause significant damage to a concrete member. However, it makes the concrete prone to other forms of attack from external agents that are able to infiltrate the concrete through the crack network that forms. Examples include carbonation of the concrete, sulfate attack, chloride attack on reinforcing steel and damage caused by cycles of freezing and thawing of water that may enter the structure[51,52].

The reactivity of different forms of silica-containing aggregate depends on the physical rather than chemical characteristics of the silica minerals and is linked to the degree of order within the silicate structure. A well ordered crystalline structure, which is unstrained, such as quartz, will normally be unreactive with respect to ASR. However opal, which has a very disordered structure, is frequently reported as being 'extremely reactive', although the extent of the reaction will be dictated by the particle size and the amount of reactive material present[51-57]. Amorphous glasses, with no crystalline silicate structure, would therefore be expected to be highly reactive.

It has been found, particularly with rapidly reacting forms of silica, that there is a specific proportion of reactive material within the aggregate that causes maximum expansion.

This maximum is called the pessimum content. If the silica content is low, any gel growth that occurs after the concrete hardens is generally insufficient to cause damage through cracking. The extent of the reaction (and therefore of the potential damage caused) will increase gradually as the level of the reactive components increases, until it becomes limited, either by the depletion of silica or the alkali in the pore fluid. If the silica content is sufficiently high, the reaction may be so rapid that it proceeds almost to completion before the concrete has hardened. In such instances, insufficient expansive forces will be developed to cause cracking[47].

2.4.2 Relationship between a pozzolanic reaction and ASR

The pozzolanic-type reaction, as mentioned earlier in section 2.2 in relation to PFA and GGBS, is very similar to the process that is experienced with ASR. For example, PFA contains amorphous silica. The particles are very fine and provide a large surface area for the reaction to occur. Hydroxyl ions in the pore solution from the cement (from $Ca(OH)_2$ during early hydration) attack the PFA particles, releasing silica ions. The silica then reacts with available alkali and water to form a silicate gel. During the early stages of hydration, the pore water is rich in calcium, so calcium silicate hydrate (CSH) gel is formed, which is the same strong binder that is normally formed during cement hydration[54].

When glass materials are present in a concrete mix, they too would be attacked by hydroxyl ions in the same way as PFA or other pozzolans. Again, if the reaction proceeds sufficiently quickly while calcium is still present in the pore water, CSH gel or a mixed calcium-alkali silicate hydrate gel will form (the alkali being either sodium or potassium). However, as in the case of ASR, if the reaction occurs very slowly (sometimes years after the concrete is placed), the calcium levels in the pore water will have been diminished by the continuing cement hydration reactions, leaving a pore solution rich in sodium and potassium. When these ions are taken up into the reaction product formed, a relatively mobile alkali-silicate gel forms without calcium, which is able to take in water and swell, causing damage to the surrounding concrete[54].

It follows that the main differences between the pozzolanic reaction and ASR is the speed at which the reaction takes place and consequently the amount of calcium that is available to stabilise the gel-product that forms from the reaction. The rate of the reaction will be controlled by the reactivity/ nature of the glassy silica-containing species and its relative particle size and surface area[58].

If the particle size of the reactive material is very fine (e.g. of cement consistency, or at least less than 38μm with glass[59]) the reaction will proceed so quickly that it will contribute to the binding properties of the cement during the hydration process and act as a pozzolan. In such an instance, the reaction product can be accommodated within the setting structure of the concrete. However, if the reactive particles are large (e.g. approximately 1200μm with glass) the reaction occurs more slowly and the reaction products do not form until the concrete has set (over a matter of months or years). By this time, an expansive, calcium-deficient gel product is more likely to form, which cannot be accommodated within the microstructure of the concrete. It is therefore likely to lead to expansive cracking and damage to the concrete member[58,60].

Once above the threshold particle size limit that separates the pozzolanic reaction from ASR, the alkali-silica reaction will occur more rapidly with smaller particles than larger particles. The absolute particle size limits will vary depending on the reactivity of the aggregate in question[61-65].

2.4.3 Methods to prevent ASR

A number of methods have been established to mitigate the damaging affects of ASR in concrete. These include reducing the permissible alkali level in a concrete mix, ensuring an environment of low relative humidity (less than 75%) and the selection of aggregates that are known to be unreactive[51,66]. There are also a range of additives that have been shown to prevent damaging expansion caused by ASR when included in a concrete mix. These include pulverised fuel ash (PFA – at levels of approximately 25-30% replacement of cement), ground granulated blast furnace slag (GGBS – at levels of approximately 40-50% replacement of cement) and silica fume (at levels between approximately 10-20% replacement of cement, depending on alkali content of the cement used and of the silica fume itself). These are thought to be effective due to their ability to incorporate more alkalis into secondary hydrates than they release into the pore solution of the concrete, thus overall reducing the alkali content and the pH of the mix[13,47,55,66-71].

It is also thought that such additives might be able to successfully prevent expansive reaction caused by ASR by producing non-expansive reaction products as opposed to gels that can swell by taking up water. Additives such as fly ash promote the formation of calcium alkali silicate hydrated gels while the concrete is in a fresh state[13]. As the gel becomes increasingly calcium rich (possibly derived from calcium hydroxide present as Portlandite or from lime (CaO) in the cement paste), it hardens and loses its ability to swell in the presence of moisture[49,53] (as discussed in section 2.4.2). This can also happen with gels in older concretes if they take up calcium from their surroundings. Therefore, it appears that when calcium is readily available, gels are less likely to cause expansive crack damage from ASR.

Use of lithium salts has also been adopted as a method to prevent deleterious expansion due to ASR. Lithium is in the same chemical group as sodium and potassium and competes with these ions for uptake into the reaction product. It is thought that it is effective at minimising damage caused by ASR because the reaction product formed is lithium silicate, which is relatively insoluble and does not absorb water. Lithium additions have been shown to have a pessimum proportion associated with them and so require additions in a mole ratio of $Li:(Na+K) > 1.2$[72-76]. The use of lithium compounds has also been shown to be an effective remedial measure for ASR-damaged concrete, particularly if it can be electrochemically driven into the concrete structure[77]. It has been used in combination with other concrete additives, such a PFA and superplasticisers, with minimal detrimental effects[78].

Since PFA and GGBS are by-products from coal fired power stations and iron smelting respectively, their use as pozzolans in concrete would not be expected to cause significantly increased costs, if at all. It is difficult to obtain relative prices for the use of additives such as PFA and GGBS, as their cost will very depending on their availability and the specific requirements of the mix that they are to be incorporated into. Although it might initially appear that they should bring about a cost saving by displacing some of

the Portland cement used, in reality the cost of concrete with these additives is probably much the same as it would be without, due to the recognised benefits that these additives are known to bring[79]. However, the use of lithium additions would use the same amount of Portland cement as well as incurring the cost of the additive itself. It has been suggested that, depending on the alkali content of a mix, the price per cubic yard[a] of concrete could increase by US$10-20 when lithium nitrate is used as an ASR mitigation technique in concrete[80].

2.4.4 Testing for ASR

The most reliable evidence that an aggregate material has, or may cause damage due to ASR is obtained from microscopic examination of concrete to identify the presence of ASR gel, internal cracking and aggregate particles that appear to have reacted[51]. Also petrographic examination of aggregate particles will often indicate whether an aggregate is likely to be susceptible to ASR[81].

Another useful gauge to assess whether expansion has occurred as a result of ASR in concrete is to measure length changes of concrete cores or prisms stored in a warm, humid atmosphere[51]. An example of such a test is BS 812-123:1999[82], which involves storing concrete prisms at 38°C for approximately a year. This test has been shown to give reliable results compared to similar exposure at 20°C. Although results from this method are obtained up to four times faster than under 'real' exposure conditions, it still requires a significant period of time before conclusions can be made about the reactivity of an aggregate[51,81]. Further test methods have been developed that use a higher temperature of 60°C (RILEM TC-ARP/01/20[83]) to accelerate the reaction further. However such tests still require exposure times of at least 20 weeks.

A more rapid test method for assessing aggregate materials would normally be preferred. Many potential techniques have been reviewed[84] and one of the most promising ultra-accelerated tests appears to be the NBRI (National Building Research Institute of South Africa) method that has been incorporated into RILEM and ASTM standards (RILEM TC 106[85] and ASTM C1260 - 94[86]). This method has been cited by several authors[87-90] and has been particularly useful for identifying reactive aggregates and those that have a 'pessimum' proportion associated with them[91].

The test involves soaking samples in 1M sodium hydroxide solution (NaOH) at 80°C for a period of 14 days. It is assumed that the NaOH provides sufficient alkali to cause expansion in samples due to ASR in the presence of a potentially reactive aggregate material. However, this method has its problems. It is generally not suitable for measuring the affect of mitigation techniques on the aggregates, as many such methods rely on reducing the alkali level within a concrete as their mode of prevention[92]. Also, the test has been shown to be ineffective in detecting reactivity of some aggregates that show late reaction[93,94] and has failed some aggregates that show satisfactory performance in real service conditions[84].

---

[a] 1 cubic yard = 0.76 cubic metres

2.4.5 Leaching of metal ions

It has already been stated that there is concern that the metal ions present in CRT glass and ISF slag could leach from the material, with potentially harmful results (sections 2.3.1 and 2.3.2). The ions that are of most concern are zinc and lead from the ISF slag and lead and barium from the CRT glass.

There appear to be two proposed mechanisms by which metal ions may be immobilised in cements to reduce leaching. The first and most preferable is through the formation of a chemical complex with the ions of concern, so they are not available to leach into the surroundings. The second is by physical immobilisation, preventing the movement of ions and retaining them within the pore structure of the cement[95]. Previous work on lead smelter slag suggests that lead may be subject to physical immobilisation, while zinc chemically complexes into the cement hydration products, hence lead and zinc are leachable at different rates and to different extents[96].

Previous leach testing that has been carried out on the ISF slag material did not follow an established method or standard, but did serve as a useful investigation into the leach behaviour of metal ions into various solutions[40]. This study suggested that PFA and GGBS may be able to reduce the leaching of metal ions from the slag by binding them up in some way. It was concluded that this would require further investigation, although other studies have also shown PFA to help reduce the leaching of metal ions and suggested similar absorption mechanisms[97,98]. Studies on other systems have found that the inclusion of GGBS reduced the levels of lead and chromium that were leachable from hardened cement[99]. It has been proposed that the reduction in the porosity of concrete containing GGBS compared to Portland cement alone may prevent the diffusion of metal ions through the pores. Since PFA is also known to reduce the pore volume of concrete it is thought that it too may be useful to immobilise metal ions in concrete. PFA and GGBS may therefore be capable of reducing leaching through a combination of both mechanisms mentioned above.

Until relatively recently there were no established standard test methods available for assessing leach behaviour of concrete and aggregates. Therefore, as with the research mentioned above, it must be assumed that individual tests have been devised to suit particular requirements and applications. Devising a test suitable for all possible requirements would be a very difficult task. Tests may be required to indicate the maximum leaching that would be possible from a material, or a more realistic simulation of in-service leaching conditions may be required. Any single test may be considered too severe or not severe enough.

Also, there are many factors that will influence the leaching behaviour of samples and the leaching characteristics of specific ions. For example, due to the changing nature of concrete as it ages, it has been suggested that samples should be allowed to cure for at least 2 months before testing and preferably for as long as 6 months. After this time, the impedance to leaching of ions offered by the concrete matrix is considered largely constant[100]. The pH of the test solution may also greatly influence the leaching behaviour of the ions being investigated, due to changes in ion solubility with varying pH. Examples of this can be seen in van der Sloot *et al*'s work, copied in Figure 2.2[101]. For example, lead and zinc ions are very soluble at a pH of 4. Their solubility decreased up to a pH of 7-8 for lead and 9-10 for zinc, then increases sharply again at higher pH values. Greater

leaching of lead and zinc ions would therefore be expected in strongly acidic or strongly alkaline environments. In contrast, variations in pH do not appear to influence the leaching of barium until a pH of 12 is reached, at which point leaching increases sharply[45,102].

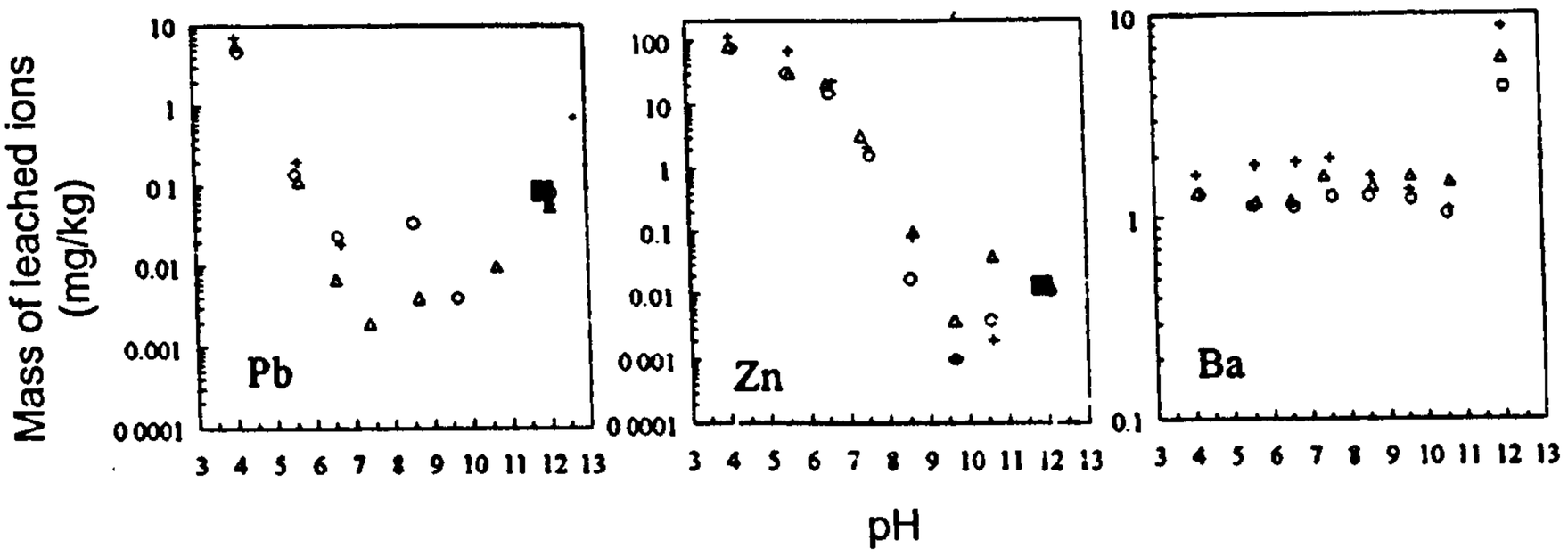

Figure 2.2: pH controlled leaching data for various elements, illustrating their different leaching characteristics (taken from Van der Sloot *et al*[101])

Van der Sloot *et al.* have recognised that no single test in isolation will give all the information necessary to fully understand the leaching behaviour of a particular material. They have proposed a comprehensive series of tests that show good agreement with different methods and experiments carried out on real samples in field conditions. These include tests to establish the maximum possible leaching of ions from a material, tests that provide predictions of leaching behaviour over time and compliance tests that can be used as a quick-check once the characteristic leaching behaviour of a material has been established. The work shows that one of the main influences on leaching is pH, as mentioned above, with each element having distinct leaching characteristics[101,102].

Several leach test methods now exists. Some are more severe than others, such as rapid shaking tests or those that use a tipping/ tumbler apparatus, while others are considered to be more realistic and representative of in-service conditions, such as washing and tank tests. Some of the types of test detailed here form part of the comprehensive testing that van der Sloot has proposed. Most are essentially compliance tests that can be used to provide relatively rapid results, once the general characteristics of a material are understood.

A series of draft standards for leach testing waste materials in water have recently been written, with the aim of characterising a 'realistic' leach behaviour of waste materials. Draft standard prEN XXXXX[103] covers leaching from monolithic wastes of regular shape and draft standard prEN 1744-3[104] covers leaching from aggregates in water. The tests involve mild agitation of the water and are carried out over a period of up to 48 hours. They do not cover leaching in solutions other than water and there is no guidance as to the levels of leached ions that may be considered 'acceptable' within the period of test. It is therefore assumed that results must be compared to standards for drinking water, or levels that are accepted for discharge into water courses.

Another test is the ASTM D3987[105] shake extraction test. This involves agitation of the sample in an end-over-end tumbler or similar, using water as the leaching solution at a liquid to solid ratio (L/S) of 20 (70g sample in 1400ml water) for 18 hours. A very similar

British/ European Standard also exists (BS EN 12457[106]) that uses an L/S of 10 for 24 hours. Both are suitable for testing granular materials, such as aggregate or crushed concrete, but not for monolithic samples. In spite of the similarity of these tests, the results from each cannot be directly compared due to the different L/S and time scales used, which highlights the problems associated with non-standard/ varying test methods. The BS/ EN leach test appears to have been recognised by the UK Environment Agency, who specify limits for this test to be applied to the acceptance of waste for landfill[107].

A similar test that has been widely used in the US is the US Environmental Protection Agency's Toxicity Characteristic Leaching Procedure (TCLP)[108]. This test is suitable for samples less than 10mm in diameter. Again, it involves agitation of a sample in an end-over-end tumbler, at an L/S of 20 (using at least 100g of sample), for 18 hours. However, in the TCLP, the pH of leach solution used is either 4.9 or 2.9, depending on the alkalinity of the solid phase of the waste initially.

This test was originally used to simulate leaching in landfill sites, which often experience acidic conditions. However, as the test became more common, it has since been applied to many leaching scenarios, for which it was not necessarily intended. This method has been criticised if used in more general applications as it does not take into consideration certain factors that are considered very important to leaching, such as pH and redox properties. It is also not possible to extrapolate potential long term effects from the data obtained and it does not give any indication of leaching mechanisms[109,110]. These observations show that it is important to consider and replicate as closely as possible the environmental conditions anticipated before selecting any of these test methods to assess the leaching behaviour of a material.

One main observation from these tumble-style leach tests is that the results are mainly a function of the mass of sample tested, with the grading of the samples being of secondary importance (for example, the tests are often specified for use on materials below 10mm, or 4mm). Measuring a sample's mass is obviously one of the simplest ways to standardise and batch up materials for testing, however the sample surface area to liquid volume ratio will also be influential on the leaching behaviour of any material. Comparison of results from different materials may not be reliable unless the same sample grading was used and the materials were of similar density, allowing the mass of sample tested to be equivalent. This raises concerns about the reliability of leaching standards such as these and the limitations of their use. However, once these factors have been identified and taken into consideration, such compliance tests to assess the behaviour of materials of a specific grading for a particular application should still be useful.

2.4.6 Retardation of concrete set

In addition to the environmental issues surrounding the leaching of heavy metal ions from these materials, there is concern that that the leaching of ions could be responsible for retardation in the concrete setting process if incorporated into a concrete mix.

Previous research suggests that the presence of the heavy metal ions lead and zinc in these secondary materials may be capable of causing a retardation affect on the cement

hydration process[40,111-120]. Microscopy and X-ray photoelectron spectroscopy (XPS) studies on lead nitrate in cement suggest that gelatinous lead (assumed to be lead hydroxide) precipitates are formed in the alkaline environment produced by the cement, which coat the surface of the cement grains and prevent their hydration[111,113]. Several further studies on both lead and zinc compounds in cement also suggest some sort of coating mechanism to explain their results, although they may not have direct evidence for it[116-120]. Lead and zinc are thought to behave similarly in a cement environment, as they both form insoluble hydroxides at high pH. However, one of the papers mentioned above[116] admitted that it was unclear how a precipitate could so rapidly cover the hydrating clinker particles with a membrane capable of preventing further hydration. Also, the discussion that followed another of the papers[120] raised the idea that the retarding species might not necessarily need to coat the cement grains in order to delay hydration, but that its presence may instead delay the nucleation of stable hydration products, such as Portlandite – $Ca(OH)_2$ and calcium silicate hydrates (CSH). This theory has also been supported in other literature[121].

This is particularly interesting when considered in light of findings of Arliguie *et al*[122]. They investigated the hydration of C_3S and C_3A in the presence of zinc. It was found that the zinc formed an insoluble calcium hydroxy-zincate compound ($CaZn_2(OH)_6.2H_2O$) before the formation of Portlandite ($Ca(OH)_2$) was detected to mark the start of the hydration process. This conversion relies on the availability of both calcium and hydroxide ions in the surrounding solution. If these ions were used up during the conversion to the insoluble zincate species, it would delay saturation of the surrounding solution with calcium and hydroxide ions (and thus delay the precipitation of Portlandite) until all of the zinc (assumed to be in the form of zinc hydroxide, $Zn(OH)_2$) had been converted. Although this paper still claims the involvement of some sort of coating layer to cause the delay, the idea of delaying the super-saturation of the solution with calcium and hydroxide ions may constitute a suitable mechanism on its own.

Other authors[120,123] have also noted the presence of the calcium hydroxy-zincate compound when examining the retardation of cement hydration with zinc, though they have not made the connection between the necessary depletion in calcium and hydroxide ions from the surrounding solution in order to form the zincate and the likelihood of this then preventing the super-saturation of the solution with respect to these ions, so delaying the precipitation of Portlandite. No equivalent hydroxy-plumbate compound has been detected, however you might expect zinc and lead to behave similarly due to their amphoteric character and hence their ability to form hydroxy-species at high pH. However, an equivalent tin containing hydroxy-compound, calcium hydroxy-stannate ($CaSn(OH)_6$) has been detected when tin(II) chloride was added to cement[124]. Tin(II) chloride was also shown to cause a delay in the concrete setting process, similar to that witnessed with zinc and lead[125].

Interestingly, when the calcium zincate was added to cement in place of the zinc oxide used initially, cement hydration was not delayed in the same way. This suggests that it is the process of converting from the initial form of zinc to the zincate (i.e. using up the available calcium and hydroxide ions that would normally form Portlandite) that is the cause of the retardation, rather than the zincate itself.

Although heavy metal ions have been shown to cause a delay in the hydration process of cement, there is evidence to suggest that at 28 days of age the compressive strength results obtained from samples containing these ions are equivalent to, if not higher than control samples[111,115]. There is also evidence to suggest that lead and chromium present in mixes containing GGBS as a cement replacement material do not appear to cause this delay in set, or affect the compressive strength results obtained at 28 days[99].

Other metal ions have been reported to cause varying degrees of retardation of cement. These include beryllium, arsenic, chromium, copper, mercury, antimony, vanadium and tin. However, the metals that consistently appear to cause the most severe retardation are lead and zinc[126]. Since tin has also been shown to cause a delay in set and the formation of a hydroxy-stannate compound, it is possible that some, if not all of these metals might be expected to retard by the same mechanism that is eventually proposed for lead and zinc.

2.5 Summary

Directives, taxes and legislation have been introduced to encourage the reuse of many materials that would otherwise be considered waste. Some such materials have been successfully utilised in concrete construction processes. Research into the possible secondary uses of CRT glass and ISF slag has been limited, although it is recognised that issues surrounding the use of these materials in concrete may include the potential for alkali-silica reaction, the leaching of heavy metal ions into the environment and retardation of the concrete setting process. It is preferable that these particular materials find secondary uses in concrete construction, so as to divert them away from landfill disposal and to provide cheap, yet suitable alternatives to quarried primary aggregates.

3 Experimental procedures

3.1 Overview of materials used during testing

3.1.1 ISF slag

The ISF slag used for this study was supplied by Britannia Zinc Ltd, who were an ISF zinc and lead production facility based in Avonmouth, in the South West of England. The plant ceased production during this research and closed in February 2003. However, a large stockpile of the slag material still remains on the site and other ISF plants around the world continue to produce the slag as a by-product material. The slag itself is a black, granular material, generally coarser in appearance than natural sand. It is assumed to have become vitrified on cooling to result in this form.

3.1.2 CRT glass

The CRT glass used for this study was supplied by Bruce Metals Ltd, who are essentially a metal reclamation and recycling company based in Sheffield, England[b]. They provide a computer recycling facility (mainly for businesses) through which they refurbish and re-sell viable computer equipment and recover any valuable metals from the remaining items that cannot be repaired and sold. Computer monitors and televisions are therefore crushed and the plastic and glass separated, so the metal components can be recovered. The resulting glass is crushed and mixed from all sections of a CRT. After crushing, separation of the various materials is difficult. Consequently, the CRT glass was contaminated with relatively small amounts of plastic and metal.

Initially, a relatively coarse grade of crushed CRT glass was provided for use in this study. When more glass was required, an additional crushing process had been adopted by the company, which resulted in a finer grade of crushed glass that resembled fine white sand. This finer grade of glass was used for the majority of the study.

3.1.3 Bottle glass

A sample of crushed, recycled bottle glass was obtained as a control material to which the performance of the CRT glass could be compared. This material is referred to as BGL in the following text. The BGL was supplied by Northern Cullet Ltd in Barnsley, England[c]. The glass did not appear to contain any contamination. The supplied grading of this glass was different to that of the CRT, so all BGL was re-graded to match the CRT glass before being used in any testing.

---

[b] Bruce Metals Ltd, March Street, Sheffield, S9 5DQ, UK

[c] Northern Cullet Ltd, Pontefract Road, Barnsley, S71 1HJ, UK

3.1.4 Inert/ control aggregates and cement

Various other crushed rock and natural sand aggregates were used during this study. They were provided by BRE's Concrete Laboratory[d] from their standard lab stock. The coarse aggregate used was Cheddar limestone crushed rock. The fine aggregate used, depending on testing, was either Cheddar limestone crushed rock (used as inert aggregate in mortars for ASR testing) or Thames Valley natural river sand (TVS; used as fine aggregate in other, non-ASR related control mixes). Table 4.2 gives details of these aggregates as well as their main reported physical properties.

The main cement used for this work was again supplied by BRE's Concrete Laboratory. It was of relatively low alkali content and the details are given in Table 4.3. A second cement was used when testing BGL mortars for ASR that was considered a high alkali cement. The details of this cement are given in Table 4.4.

3.2 Characterisation of materials

3.2.1 Particle density and water absorption

A sample of each aggregate was sent away to STATS laboratories[e] (a UKAS accredited test house) to accurately establish the particle density and water absorption of the material, in accordance with BS 812: Part 2: 1995[127]. These figures are used when designing concrete mixes in accordance with BRE Report BR 331, 'Design of normal concrete mixes'[128], as detailed in section (3.3.1).

According to this method, the sample is immersed in water for 24 hours, then drained. The aggregate is then exposed to a gentle current of warm air to evaporate the surface moisture, until it attains a 'free-running' condition, making it saturated and surface dry (SSD). The sample is weighed (A), then transferred to a container, which is then filled with water to a known level. The whole apparatus is weighed (B), before being emptied. The container is then re-filled with water to the same level and re-weighed (C).

The sample is then transferred to a tray and placed in an oven at 105°C for 24 hours, after which it is then allowed to cool to room temperature and re-weighed (D). The water absorption of the aggregate can then be calculated by subtracting the oven dried mass (D) from the SSD mass (A) and expressing it as a percentage of the dry mass. The particle density of the sample can be calculated from the formula D / D - (B - C).

3.2.2 Moisture content

The moisture content of the ISF slag and CRT glass was established so they could be used in their 'as received' damp state rather than drying them before use. This was due to concerns about respirable dust that might be mobilised during concrete mixing if dry aggregates were used. Three glass evaporating basins (approx. 100mm diameter, height 70mm) were labelled and weighed. Approximately 50g of the damp aggregate was then added to the basins and re-weighed. The basins were placed in an oven at 105°C and left overnight to dry. They were then removed from the oven and left to cool to room

---

[d] BRE, Watford, Hertfordshire, WD25 9XX, UK

[e] STATS Laboratories, Porterswood House, Porters Wood, St Albans, AL3 6PQ, UK

temperature. The basins were then re-weighed and the moisture content of the samples calculated from the change in weight, assuming all weight loss was due to water evaporation from the sample. An average of the three results was then taken and expressed as a percentage of the dry weight of the sample.

3.2.3 Grading of aggregates

Grading of the aggregate materials was carried out in accordance with BS 882[129], using limits imposed for a fine grade aggregate. This British Standard has since been superseded by BS EN 12620, under which the grading would now be classed as a 0/4 or 0/2 (MP) aggregate (the MP designation shows that it has been classed a medium grade fine aggregate based on the percentage passing a 0.50mm sieve)[130]. The sieve sizes used in accordance with the original BS 882 were 5.00, 2.36, 1.18, 0.60, 0.30 and 0.15mm. The mass of material retained on each sieve was recorded and the percentage of material passing through each sieve calculated. The ISF slag and two different gradings of CRT glass were analysed by this method.

3.2.4 XRF composition analysis

X-ray fluorescence (XRF) analysis was carried out on the aggregates by CERAM Research Ltd[f] using their own in-house method. The sample was ground down to a powder and then ignited at 1025°C, oxidising all elements within the sample. Those that formed gases will have been released. Of these, sulfur trioxide was analysed for.

3.2.5 XRD analysis

XRD analysis was carried out on the cement and ground aggregate materials, as well as on hydrating cement and mortar samples containing the aggregates. This was achieved by quenching the samples in acetone at various times after mixing. Times generally ranged from 2 hours up to 28 days of age, with the aim of establishing how the various components present varied during hydration.

Mortar samples containing the secondary aggregate materials were mixed in polythene sample bags, sealed and stored at room temperature. Periodically, some of the sample was removed from the bag and transferred to a pestle and mortar. Acetone was added to the mix and stirred/ ground into the sample. The acetone was allowed to evaporate, leaving a dry, granular sample, which was ground to pass a 63µm sieve before the XRD analysis was carried out. It was hoped that these results would indicate whether the presence of the secondary aggregate materials influenced the compounds formed during cement hydration.

Details of the mixes used for this work are given in Table 3.1. In each case the free water/cement ratio was 0.6 (once water absorption and moisture content of the aggregates was taken into consideration) and the cement/fine aggregate ratio (by volume, determined from the particle density) was 0.4, as with the full scale concrete mixes used for this work (section 5). The relevant values for water absorption, moisture content and density can be found in Table 4.1 and Table 4.2.

---

[f] CERAM Research Limited, Queens Road, Penkhull, Stoke-on-Trent, ST4 7LQ, UK

All samples for X-ray diffraction (XRD) analysis were first ground to pass a 63μm sieve. A sufficient quantity of the ground sample was then transferred to a square recess in an aluminium slide and levelled flush with the edges. A series of samples were then loaded into an automatic sample changer that was attached to the XRD equipment. A Philips PW1710 Reflection Diffractometer using Cu Kα radiation was used. The equipment was set to scan from 10 to 60 º2θ. Once the sample runs were complete, the data obtained was analysed using WinX^{POW} software, to match potential compounds present with the Powder Diffraction File database.

Table 3.1: Details of quenched mortar mixes used for XRD analysis
(In all cases the resulting water/cement ratio = 0.6 and the cement/aggregate ratio = 0.4 once water absorption, moisture content and density of the materials is taken into consideration)

Mix	Aggregate g	Cement g	Water g	Times quenched
Cement	0.0	70.0	42.0	2, 4, 6, 24 hours, 7 & 28 days
Limestone control	100.0	38.7	26.0	2, 4, 6, 24 hours, 7 & 28 days
CRT	100.0	38.9	23.4	2, 4, 6, 24 hours, 7 & 28 days
BGL	100.0	38.9	23.4	2, 4, 6, 24 hours, 7 & 28 days
ISF	100.0	25.6	15.4	2, 4, 6, 24, 30, 48, 51, 54, 72 hours, nominal 7 & 28 days from hydration

3.2.6 SEM and TEM analysis of aggregates

SEM was carried out on a Camscan scanning electron microscope or a JEOL JSM 6400 scanning electron microscope, both fitted with an Energy Dispersive Spectrometer (EDS) detector. The JEOL machine used a 'windowless' EDS system, which allowed the detection of elements of low molecular weight, such as oxygen. Samples were generally prepared as thin sections of ~30μm thickness (also used for optical microscopic examination, detailed later in section 3.4.3), or polished blocks of sample that had been impregnated with resin, which were carbon coated before being inserted into the sample chamber for observation.

TEM analysis was carried out on a Philips EM420 transmission electron microscope operating at 120kV, which was also fitted with an EDS detector. Samples had been prepared by grinding the materials by hand in a pestle and mortar, then mixing them with methanol. A few drops of the mix were taken up using a disposable pipette and dropped onto a 3.05mm diameter, 400 mesh (38μm) copper grid covered in a thin carbon film. Once the methanol had evaporated, the sample could be loaded into the sample chamber and viewed in the TEM. Selected area diffraction patterns (SADP) were also obtained during the examination of these samples, using a camera length of 660mm.

3.3 Concrete mixes containing the replacement aggregates

3.3.1 Concrete mix design

Concrete mixes were designed for this work based on the method given in BRE Report BR 331, 'Design of normal concrete mixes'[128]. This method aims to design concrete mixes to meet specific workability, strength and durability requirements. The mix proportions are calculated based on the weight of materials required to produce a unit volume of fully compacted concrete. Therefore the expected density of the fresh concrete and the relative density of the aggregates to be used must be known. The method results in the mix design being specified in terms of the weight, in kilograms, of the different materials required to produce one cubic metre of finished concrete.

All mixes were designed to achieve at least 30MPa compressive strength at 28 days of age, with a slump/ workability target range between 30-60mm. Where the density of a replacement aggregate differed from that of traditional/ control aggregate materials, a volumetric rather than a mass replacement was made.

All mixing was carried out in accordance with BS 1881: Part 125: 1986[131] in a UKAS accredited test laboratory. Various concrete mixers were used, depending on the volume of the required mix, though the mix method adopted was the same for each. Small mixes of approximately 3-5 litres used a 'Cretangle' pan mixer. Mixes of 5-9 litres used an 'FLS' forced action pan mixer and larger mixes of between 20-40 litres used an 'Eirich' forced action pan mixer. The aggregates were placed in the appropriate sized mixer and stirred for 30 seconds. With the mixer still turning, half the mix water was then added over a period of a further 30 seconds. Mixing then continued for a further 2 minutes. The aggregates were then allowed to stand for 10 minutes to enable any expected water absorption to occur. The cement was then added and the mixer started again. This point was taken as the 'start of hydration'. After 30 seconds, the remaining mix water was added over another 30 seconds. The mixer was then allowed to stir for a further 2 minutes.

A slump test was carried out 6 minutes after the start of hydration. The wet density was also calculated before samples were cast by filling moulds in two roughly equal layers on a vibrating table, expelling any air and allowing each level to compact. Sample surfaces were then levelled and finished by hand using a metal float.

A slight modification to this method was applied to concrete mixes containing the finer grading of CRT glass. This was to overcome problems that were experienced due to contamination of the glass with shards of aluminium and zinc metal. This will be discussed in greater detail in a later section (5.2). The aggregate was passed through a 2.36mm sieve to remove the largest metal particles. The above mixing routine was still followed, however the samples were additionally shaken on a vibrating table for approximately 1 minute, every 30 minutes, for 2 hours, in an attempt to expel any gas that was evolved within the wet concrete due to reactions involving the contaminant metals. Samples were topped up with further concrete after this displacement had occurred and finished by hand using a metal float.

Cast specimens were cured under damp sacking and polythene until they were demoulded, then wrapped in damp sacking and sealed in polythene bags until they were tested. Details of the cast specimens are given in the following sections.

3.3.2 Wet concrete testing

A slump measurement of the wet concrete has been taken as a measure of the workability of each mix. The slump test was carried out in accordance with BS 1881-102: 1983[132]. The slump cone was filled in three approximately equal layers, tamping the concrete with a metal rod 25 times after each addition of material to compact it. The surface of the cone was levelled off using a flat metal bar. The metal cone was then carefully lifted away from the concrete. The difference in height between the metal cone and the slumped concrete was measured with a metal rule to the nearest 5mm.

The wet density of each mix was calculated in accordance with BS 1881-107:1983[133]. A cylindrical metal container of known mass and volume was filled with concrete in five approximately equal layers, while being compacted on a vibrating table. The surface of the cylinder was levelled using a flat metal bar and any excess concrete cleaned from the outside of the container. The cylinder and concrete were then weighed. The density was calculated by subtracting the mass of the metal cylinder from the total weight and dividing the remainder by the known volume of the container. The density was then reported to the nearest 10kg/m^3.

3.3.3 Hardened concrete testing

Compressive strength testing was carried out on 100mm concrete cubes in accordance with BS 1881-116: 1983[134]. The test faces of the cubes were first scraped with a flat metal plate to remove any fins remaining on the edges after demoulding. The dimensions of the cubes were then measured to the nearest 1mm and the samples weighed to the nearest 1g. Since the samples had been stored under damp sacking and polythene before test and were therefore not saturated, the density of the cubes was determined using the volume, calculated from the measured dimensions. The condition of the test cube was then assessed (apparent porosity, damage to edges or corners, geometrically fit for test) and reported. Samples were then placed in a Controls C48 Compression machine and a load applied at a rate of 0.25 MPa/s to catastrophic failure. The compressive strength was then reported to the nearest 0.5 MPa.

3.4 Alkali-silica reaction

3.4.1 80°C testing of mortar bars

Rapid testing to assess the alkali-silica reactivity of the replacement aggregates has been carried out in accordance with the RILEM test method RILEM TC106-2: AAR accelerated test[85], with a slight modification to the material grading used. It is very similar to the ASTM C1260-94[86] test, as both are based on an original National Building Research Institute of South Africa (NBRI) test method. From this test an indication of potential aggregate reactivity can be obtained in a matter of days rather than weeks or

years. However, this test has its own limitations, which were highlighted previously (section 2.4.4).

The RILEM method recommends that the material follows a specific grading. It requires 10% of the material to be retained on a 2mm sieve, 25% each on 1mm, 500µm and 250µm sieves and 15% on a 125µm sieve. The grading of the CRT glass was rather fine and there was not a sufficient quantity of the larger fractions available to be able to re-grade the glass in order to meet the requirements of the standard. As mentioned earlier, it was decided that the ISF slag should not be dried prior to use due to the possibility of respirable dust, so drying and re-grading was avoided with the ISF slag also. Both materials were therefore used in their as-received grading. It was also felt that using an 'artificial' grading would not represent the materials' in service characteristics. However, when bottle glass was used as a comparison to the CRT glass in this test, it was re-graded to match that of the CRT glass, so it would provide a direct comparison.

The grading of the replacement aggregates were generally finer than the standard's recommendations. If, as argued previously (section 2.4.2), particles with a larger surface area to volume ratio are more susceptible to ASR, it might be expected that the results obtained from this testing would be potentially more severe than if the standard's grading were adopted. The results obtained are therefore relevant for this work, but could not necessarily be directly compared with other published literature that used the same test method.

Mortar bars were made, each 250mm x 25mm x 25mm with metal inserts at each end for measuring purposes. Each mix used 400g cement and a water/cement ratio of 0.47. The control mix used 900g of inert Cheddar limestone fine aggregate. This was replaced with first 10% by volume of the replacement aggregate, then with 20%, then increasing in each mix by 10% until the mortars were made with either 70% ISF slag or 100% CRT glass replacement. (Due to the density and nature of the ISF slag material, suitable mortar samples could not be obtained at replacement levels above 70% as the ISF slag would settle to the bottom of the sample moulds.) Samples were cast in this way in order to establish whether there was an optimum level/ pessimum proportion at which ASR would occur.

The mortars were mixed in a 'Hobart' paddle mixer, with a planetary driven blade and a mixing bowl approximately 5 litres in volume, in accordance with BS EN 196-1:1995[135]. The water and cement were placed into the mixing bowl and mixed at low speed for 30 seconds. The fine aggregate was then added steadily over the next 30 seconds. The mixer was then switched to high speed and run for a further 30 seconds, before being allowed to rest for 1 minute, 30 seconds. During this time any mortar adhering to the paddle or the mixing bowl was scraped back into the bulk of the mix using a spatula. Finally, the mixer was run at high speed for 60 seconds. Mortar bars were moulded in two approximately equal layers, paying attention to surround the metal measuring inserts, then compacted on a vibrating table. Samples were then stored for 24 hours under damp sacking and polythene, before being demoulded.

Each set of samples was then immersed in deionised water and placed in an oven at 80°C for 24 hours. After this time, samples were removed from the water, roughly patted dry with a cloth and measured using a length comparator. This figure was used as the

'zero' reading for the samples, as all other measurements were made after removal from solution at 80°C. Samples were then transferred to polypropylene Safepak containers with pre-heated 1M sodium hydroxide (NaOH) solution (40g NaOH pellets per litre of deionised water) and returned to the oven for storage at 80°C for 14 days. The NaOH provides sufficient alkali to cause expansion in the samples due to ASR in the presence of a potentially reactive aggregate material.

Samples were removed from their storage containers periodically for measurement purposes. Measurements were made using the length comparator, which was designed to accommodate the metal inserts that were cast into each prism. The apparatus had a digital gauge that measured accurate to 0.001mm. From the expansion measurements that were made, the percentage expansion, relative to the original sample length, could be calculated. Samples were then examined petrographically and using SEM to confirm whether ASR had occurred.

3.4.2 60°C and 38°C testing of concrete prisms

Long term testing (though still accelerated compared to field exposure conditions) to assess the alkali-silica reactivity of the replacement aggregates has been carried out using two different methods. Both measure the degree of expansion of concrete prisms that have been stored at elevated temperatures. BS 812-123: 1999[82] tests samples stored at 38°C for a minimum of 1 year. RILEM/ TC-ARP/ 01/20[83] tests samples stored at 60°C for 20 weeks.

Both methods require concrete prisms (200mm x 75mm x 75mm) to be cast with metal inserts at either end for measurement purposes. Mixing followed the method given in section 3.3.1. Once demoulded, samples were wrapped in twill cotton cloth and sealed inside polythene tubing. They were then placed in individual polythene bags, before being transferred to rigid, polypropylene Safepak containers with approximately 20-40mm of water in the base. Samples were raised above this water level using a plastic support. This set-up maintained a high relative humidity around the wrapped prisms during storage (reported to be >96% relative humidity[82]). Samples were measured periodically using a length comparator and examined microscopically in the same way as the samples discussed in the previous section on 80°C ASR testing.

Concrete prisms were cast containing ISF slag as 100% volume replacement for the fine aggregate (5-0mm) normally present in the mix, with a cement content of 300 kg/m^3, giving a calculated alkali content of 1.8 kg/m^3 Na_2O_{eq}[g]. Inert Cheddar limestone was used as the coarse aggregate, as detailed later in section 5.1. Further prisms were cast using mix water with additions of NaOH to provide an artificially elevated alkali content. This raised the total alkali content of the mix to 7.0 kg/m^3 Na_2O_{eq}, which had been used in previous studies[136] and simulates the highest level that might be anticipated in concrete.

The purpose of the series of CRT glass concrete mixes tested by these methods was to assess the effectiveness and suitability of established ASR mitigation techniques given in BRE Digest 330[51], as well as more recent guidance specified in the BRE Information

---

[g] Na_2O_{eq} = alkali content, expressed as an equivalent concentration of sodium oxide

Paper, IP1/02[72], to see if they could be successfully applied to this aggregate. These included partial replacement of cement with pulverised fuel ash (PFA) and ground granulated blast furnace slag (GGBS), as well as the use of lithium salts – lithium hydroxide monohydrate ($LiOH.H_2O$) and lithium nitrate ($LiNO_3$), in the concrete mix water.

BRE Digest 330[51] categorises aggregates into reactivity classes – low, medium and high. Appropriate guidance for the use of ASR mitigation techniques is then provided according to the anticipated aggregate reactivity. Low reactivity aggregates are those of rock types that have not been implicated in damaging ASR in field concrete's in the UK. According to the 38°C ASR test on concrete prisms, BS 812-123: 1999[82], aggregates may be deemed of low reactivity if the expansion of prisms does not exceed 0.10% within 12 months of testing. (They may be classed as unreactive if the expansion does not exceed 0.05% in 12 months.) The term normal reactivity covers most aggregates extracted in the UK. Aggregates may be considered of normal reactivity if the expansion in the 38°C prism test is between 0.10-0.20%. High reactivity aggregates are those that react at lower alkali levels than the more common UK concreting aggregates. Recycled aggregates, such as those processed from demolition waste, are generally classed as high reactivity, as there is little experience of the ASR behaviour of such aggregate sources. Aggregates are considered of high reactivity if the expansion in the 38°C prism test is above 0.20%.

All mitigation additives were initially used at a dose recommended for high reactivity UK aggregate materials. Later, further samples were cast with PFA and GGBS at a dosage recommended for normal reactivity aggregates for comparative purposes. As with the ISF slag mixes, CRT glass was used as 100% fine aggregate in the concrete, with inert Cheddar limestone as the coarse aggregate. Details of these mixes are given later in section 5.2.

3.4.3 Petrographic examination

Microscopic examination is an essential technique in the detection and confirmation of ASR in concrete and mortar samples. Optical microscopy was carried out on a research grade Carl Zeiss transmitted light polarising microscope using thin sample sections of approximately 30µm thickness. The sections were prepared by impregnating concrete/ mortar samples with an epoxy resin containing a fluorescent dye. The resin was made up using 10 parts resin to 1 part hardener, with the dye added at a concentration of 5g/L of epoxy resin. Once the resin had hardened (at least 8 hours in an oven set at 40°C), one side of the sample was finely ground on an 'Abwood' surface grinder. This used a diamond impregnated grinding cup wheel with an oil coolant. The oil coolant is preferred as various concrete features, in particular ASR gel, are sensitive to water. This provided a flat surface that was then lapped using a 'Logitech LP40 auto' lapping machine with 15µm aluminium oxide abrasive and oil lapping medium. The sample was then cleaned and glued to a frosted glass slide. The excess material was cut off the sample using a 'Beuhler Petro-thin' thin sectioning system, which used a continuous rim diamond cutting blade with an oil coolant. This left a slice of material approximately 300µm thick on the slide.

The remaining sample was gradually reduced to a thickness of approximately 35µm using the 'Logitech LP40 auto' lapping machine and the abrasive medium mentioned above. The final 30µm thickness was obtained by hand using a 15µm, then 9µm aluminium oxide oil abrasive on a glass plate. This reduced the sample to the desired thickness and removed any residual dirt remaining from the lapping process. The finished slide was then covered with a glass slip before it could be examined under the microscope.

3.5 Leaching of metal ions

As mentioned in an earlier section (2.4.5), leach testing is an area of some controversy. It therefore seems appropriate to give some justification to the methods that were chosen for this project work.

Relevant literature[101] has indicated the general leaching characteristics of a selection of metal ions with varying pH, including lead, zinc and barium. It was apparent that leaching of these ions would be greatest in solutions of pH 11 and above, which would be expected in wet concrete. Leaching of the aggregates in a high pH solution was therefore of interest, as well as in deionised water, to assess the availability of these metal ions in the concrete mix water and gauge whether they were likely to influence the retardation of setting concrete. Rapid, small-scale leach tests were also developed to give an indication of the leaching behaviour over time and potentially to suggest the possible mechanism(s) by which leaching was occurring (e.g. surface wash off, or diffusion controlled).

The leaching behaviour of concrete containing the replacement aggregate materials was obviously also important. If a concrete member were subject to leaching from rainwater or groundwater in the environment then the pH of the leaching solution would be dictated by the concrete itself. It was therefore accepted that leaching the concrete in deionised water, then measuring the final pH of the solution, would be most appropriate.

A tank-style leach test (see section 3.5.1 below) was chosen to approximately simulate potential in-service leaching of concrete cubes containing the aggregates. However, it was appreciated that if the concrete were to become damaged in any way that would expose the replacement aggregates, leaching might be expected to increase from the concrete. Concrete samples were therefore crushed to expose the aggregate surfaces and tested in a tumble-style leach test (see section 3.5.2 below), with the intention of simulating a worst case scenario for the leaching of metal ions from the concrete.

All solutions that were obtained from leach testing were analysed by inductively coupled plasma – optical emission spectroscopy (ICP-OES), which was carried out by a specialist laboratory[h], as the facility was otherwise unavailable. All sample solutions were vacuum filtered through 45µm membrane filters, transferred to 125ml HDPE plastic sample bottles, then fixed with concentrated nitric acid to preserve the solutions. All samples were at least analysed for the metal ions lead, zinc and barium. Some were additionally analysed for some, or all of the following: strontium, arsenic, calcium, silicon, sodium and potassium.

---

[h] Butterworth Labs Limited, 54-56 Waldegrave Road, Teddington, TW11 8NY, UK

3.5.1 Tank-style leach test of monolithic samples

The first method employed was a draft European Standard (CEN/TC 292, Draft prEN XXXX)[137] that is suitable for testing concrete cubes containing the secondary aggregates. This is a tank-style test that involves mild agitation of the liquid surrounding the sample and is supposed to better simulate potential in-service leaching. The surface area of the sample available for leaching is considered of greatest influence in this test. The leachant volume required (in ml) is five times the surface area of the sample under test (600cm^2), therefore 3 litres of water was used. Polypropylene containers were used for this leach testing rather than glass containers, since the aggregates under test are glassy in nature and the use of glass equipment could affect the results obtained.

3.5.2 Tumble-style leach test of aggregate and crushed concrete

This is a four-part British and European standard that appears to have been recognised by the UK Environment Agency (EA), aimed at assessing granular wastes and sludges (BS EN 12457 Parts 1-4)[106]. The various parts of this method are suitable for testing both the secondary aggregate material (<4mm grading) and crushed concrete containing the aggregates (>5<10mm grading). Guidance is given by the EA regarding the acceptable levels of certain heavy metal ions permissible in such leach tests, in order that they satisfy criteria set for the landfill of waste[107]. These figures can be used as a guide to assess the leach results obtained from this work, although it is realised that a different criteria might be used to ultimately assess the environmental suitability of the materials.

The method involves constant agitation of the sample in an end-over-end tumbler. It is relatively severe, with the intention of determining the maximum level of pollutants that are likely to be leached from a given material. It was hoped that this will give a worst case scenario of the leaching potential of the slag and the glass. Polypropylene containers were used rather than glass, so they did not affect the results obtained from the glassy aggregates being tested. (Although theoretically the polypropylene containers could contaminate the samples, it would be an organic contaminant, which would not affect the inorganic species being analysed for.) A liquid to solid ratio (L/S) = 10 is specified for this test. Therefore, 175g of sample was leached in 1.75 litres of deionised water, for a period of 24 hours.

A pH 13 buffer solution was also used for this work, replacing the deionised water in the leach tests, in order to simulate the behaviour of the aggregates in a high alkali environment, such as a concrete mix. The buffer was made up from 660ml of 0.2M NaOH and 250ml of 0.2M KCl, topped up to 1 litre with deionised water, for every litre of buffer required.

3.5.3 Variation on tumble-style leach test

As a means of testing smaller quantities of the materials, the tumble style leach test was varied as follows. Instead of using 175g of sample in 1.75 litres of solution, 35g of sample was leached in 350ml of solution. All other testing criteria remained the same and the L/S = 10 was therefore maintained. This method was used to test the ISF slag and CRT glass aggregates in association with PFA and GGBS.

3.5.4 Rapid small-scale tumble leach test of aggregate

This second method has also been used as a basis for designing a very rapid, small scale leach test, to give an indication as to how quickly metal ions are able to leach from the aggregates into solution. As a deviation from the standard, 35g samples (rather than 175g) of ISF slag and CRT glass were tested at a liquid/ solid ratio (L/S) of 10 for 15, 30 and 60 minutes only, rather than 24 hours. Aggregate samples were tested in de-ionised water and additionally in a pH 13 buffer solution, to simulate the high alkali environment of a concrete mix, as this could influence the availability of metal ions from the glass and the slag.

3.6 Retardation of concrete set

3.6.1 Scanning and transmission electron microscopy of ISF slag

SEM analysis was carried out on a Camscan scanning electron microscope with an Energy Dispersive Spectroscopy (EDS) detector. This microscope was fitted with a cryo-stage to allow examination of samples that have been effectively 'frozen' in liquid nitrogen. This technique was used to analyse mortar containing ISF slag, which was suffering from delayed setting. The ISF slag was passed through a 300µm sieve and a 150µm sieve. Only the material retained on the 150µm sieve was used in the mortar mix. This allowed better distinction between the finer cement particles and the aggregate particles under the microscope, due to their relative sizes. The mortar was mixed and stored for approximately 18 hours before being quenched in liquid nitrogen and transferred to the SEM, to ensure that the hydration of the mortar mix was being retarded while examined. It was then placed onto the cryo-stage and the surface fractured using a sharp blade before it was transferred into the SEM's sample chamber. The sample was then observed using secondary electrons to see if there was any evidence of phases coating the cement particles. An equivalent mortar containing a limestone control aggregate was examined for comparison. The control mortar was only stored for 1 hour prior to quenching in liquid nitrogen, so it too would be in the early stages of the hydration reaction.

TEM analysis was carried out on a Philips EM420 transmission electron microscope, which was also fitted with an EDS detector. Details of the sample preparation methods used were given in an earlier section (3.2.6).

3.6.2 XRD analysis

XRD analysis was carried out as described earlier in the section on characterisation of the materials (3.2.5).

3.6.3 Thermogravimetric analysis

Thermogravimetric analysis was carried out on my behalf by Beverley Lane at Sheffield University, using a Perkin-Elmer Thermogravimetric Analyser. Samples were heated over a range from 40 to 600°C at a rate of 10°C per minute in a flowing nitrogen atmosphere. The samples tested by this method were a selection from those that had been quenched for XRD analysis, discussed earlier in section 3.2.5. These included raw

cement and ISF slag samples as well as small scale ISF slag mortars that were quenched in acetone during their hydration period at 2, 24, 48 and 72 hours and cement alone that had been quenched after 24 hours hydration.

3.6.4 Isothermal conduction calorimetry (ICC)

A JAF Isothermal Conduction Calorimeter was used to track the heat evolution during the cement hydration process. This technique was seen to be more accurate than the larger-scale temperature monitoring that was carried out using concrete cubes and allowed the use of small (~30g) samples.

Samples were mixed externally then transferred to the calorimeter for testing. The mortars were made up in sealable polythene bags. The water was weighed into the bag, then any additive to be used weighed and dissolved in the mix water. The cement and aggregates were weighed out separately and mixed together in their dry state before being added to the bag and sealed. The mortar was then mixed by hand by manipulating the mortar within the bag for 1 minute. The bag was then secured around a metal disc to which was fixed a small (6 x 10mm) heater within an aluminium pot (approximately 60mm diameter) filled with oil. This was placed inside the calorimeter pot and submerged within a water bath maintained at 20°C. An electrical output proportional to the heat flow from the sample was generated. This was logged by a computer over the course of several days to track the progress of the hydration reaction within the sample. Once the sample run was completed, the output was calibrated by applying a known current to the system via the heater located within the aluminium sample pot. The computer then utilised the calibration data obtained and provided the output from the sample in units of Watts/kg against time.

The mortar samples used for this work were made from aggregate that had been ground to pass 150µm sieve, to allow even heat distribution throughout the sample when the cement hydrated. It was accepted that grinding the sample might increase the retardation experienced with the ISF slag, due to the higher surface area/ volume ratio that would result. However, any additives that showed promising results during this testing were incorporated into full-scale concrete mixes and tested using internal thermistors (as detailed in section 3.6.1) to assess their suitability.

The mortar mixes used the same cement/ aggregate ratio as the main concrete mixes used for this work (0.4). Inert Thames Valley natural sand aggregate (TVS, 5-0mm grading) was replaced by first 20%, then 40, 60, 80 and 100% by volume of ISF slag, to compensate for the different density of the two aggregate materials. The water/ cement ratio was increased for this testing compared to the main concrete mixes, from 0.60 to 1.00. This was decided after it had been established from the internal temperature monitoring of concrete samples that the water/cement ratio of a mix containing the ISF slag did not significantly influence its delaying behaviour (see Figure 8.19, section 8.6.1). The increase in water allowed a workable mortar to be made, despite the high surface area of the aggregates used.

It was established from this testing that a 60% volume replacement with ISF slag resulted in a delay in the setting process that was close to that experienced with the main ISF concrete mixes used for this work (approx. 40 hours to start of hydration with

60% ISF in calorimetry experiments compared to approx. 48 hours in the concrete testing). The 60% replacement level was therefore adopted to test the effect of various additives on the setting behaviour.

During thermistor testing of concrete containing NaOH for ASR testing purposes, it was noted that the NaOH appeared to prevent the delay in the setting process that was usually witnessed with the ISF slag. The equivalent concentration of this additive was therefore used in the calorimeter experiments as a comparison. Other additives, that had been suggested as possible set accelerators[11], were tested at an equivalent molar concentration to the sodium, so the effectiveness of various cations as accelerators could be compared. The molar concentration was calculated to be 0.00475 moles in the 30g (or equivalent) mixes tested in the calorimeter.

An established accelerator of concrete hydration is calcium chloride ($CaCl_2$), which is commonly used at a concentration of 2% of the mass of the cement[138]. This level was used for the calorimeter work and, again, other additives were tested at an equivalent molar concentration to the calcium from the $CaCl_2$, so various cations could be compared. The molar concentration was calculated to be 0.0015 moles in the 30g (or equivalent) mixes tested in the calorimeter.

These two molar concentrations were used as a 'high' and 'low' addition level for all of the additives tested. Various group I and II elements were trialled to see if they could overcome the delay in set that was experienced with the ISF slag and potentially indicate a possible mechanism by which the retardation was occurring. TVS mortars were also dosed with additions of lead and zinc oxide (each at 0.2g) to confirm that these ions produced a retarding effect on cement hydration and to give an indication as to the length of retardation that was caused by arbitrary additions of these metal ions. PFA and GGBS additions were tested at a 35% cement replacement in mixes containing the ISF slag. The mix details for the mortars are given in Table 3.2, while the additives used are shown in Table 3.3. The 60% ISF slag mix used with the additives is highlighted in bold. Additives marked with an asterisk (*) in the tables were mixed with the aggregates in their powder form, as they were simulating a species that would have come from the aggregate initially (i.e. Pb or Zn). All other additives were dissolved in the mix water before the cement and aggregates were added.

3.6.5 Temperature monitoring of ISF slag concrete

This technique appears to be similar to the embedded thermocouple method used by Bushnell-Watson & Sharp[139]. However, this testing has been carried out on larger volumes of concrete (150mm cubes) in insulated moulds, rather than small tubes of cement paste in a temperature controlled water bath. A temperature monitor (thermistor), attached to a length of 10mm diameter doweling, was placed in the centre of an insulated 150mm square mould. The thermistor was then connected to an 8 bit Grant Squirrel data logger. A second thermistor was also connected to the data logger to monitor the temperature external to the mould (ambient temperature). The mould was then filled with concrete and the logger set to record the temperature at intervals of 15 minutes, accurate to the nearest 0.5°C. The data logger was downloaded periodically throughout the course of the experiment, until the concrete within the mould had set.

Details of the concrete mixes tested by this method are given in Table 5.2. Additionally, several additives that had been shown to be useful at overcoming the delay in set caused by the ISF slag during testing by ICC were also scaled up and tested in concrete by this method. The additives included calcium nitrate (at low and high addition levels), calcium chloride (high addition), barium chloride (low addition), magnesium chloride and nitrate (both high addition) and potassium hydroxide (high addition). The actual quantities used are included in Table 5.3 in the section on concrete mixes.

Table 3.2: Mortar mixes used for ICC

Experiment	Cement (g)	TVS aggregate (g)	ISF aggregate (g)	Additives (g)	Water (g)	Total weight (g)
TVS control	8.5	21.5	0.0	0.0	8.5	30.0
TVS + ISF 20%	8.5	17.2	6.5	0.0	8.5	32.2
TVS + ISF 40%	8.5	12.9	12.9	0.0	8.5	34.3
TVS + ISF 60%	**8.5**	**8.6**	**19.4**	**0.0**	**8.5**	**36.5**
TVS + ISF 80%	8.5	4.3	25.8	0.0	8.5	38.6
ISF 100%	8.5	0.0	32.3	0.0	8.5	40.8
TVS + 0.2g ZnO*	8.5	21.5	0.0	0.2	8.5	30.2
TVS + 0.2g PbO*	8.5	21.5	0.0	0.2	8.5	30.2
ISF 60% + PFA (35% cement replacement)	5.5	8.6	19.4	3.0	8.5	36.5
ISF 60% + GGBS (35% cement replacement)	5.5	8.6	19.4	3.0	8.5	36.5

Table 3.3: Additives tested in association with ISF slag, by ICC

Cation → Anion ↓	Ca	Na	K	Mg	Li	Sr	Ba
Cl	X	X	X	X	X	X	X
NO_3	X	X	X	X	X		
OH	X	X	X		X		

4 Characterisation of materials

4.1 Physical properties

Table 4.1 gives the particle density, percentage water absorption, average moisture content and grading details of the replacement aggregates used in this study. Two grades of CRT glass were tested. Both were classed as 5-0mm aggregate, although one was towards the finer end of this limit (F) and the other towards the coarser boundary (C).

Table 4.1: Physical properties of the replacement aggregates

	ISF slag	CRT glass (C)	CRT glass (F)
Particle density on SSD basis (Mg/m^3)	3.88	2.91	2.91
Water absorption (% of dry mass)	0.2	0.2	0.2
Average moisture content (%)	1.57	2.09	1.15
Grading sieve sizes (mm)	Percentage of material passing		
5.00	99.76	99.68	99.76
2.36	98.42	77.53	99.41
1.18	85.61	44.00	98.51
0.60	48.75	21.24	78.86
0.30	10.69	10.38	31.17
0.15	1.93	5.18	1.57

It can be seen that the density of the ISF slag is significantly higher than that of the CRT glass, which in turn is generally higher than most natural aggregates (~2.6 Mg/m^3). The grading results obtained fall within the boundaries accepted for a medium grade sand, as defined by BS 882:1992[129], which should now qualify as a 0/4 or 0/2 (MP) fine aggregate under the more recent standard, BS EN 12620[130,140].

Other materials utilised in the work were standard lab-stock materials, whose physical properties have been provided by the supplier. Basic physical properties of the control aggregates are given in Table 4.2. These figures are used when designing concrete mixes according to the method given in section 3.3.1. Details of the cement used for the majority of this work are given in Table 4.3. An additional, high alkali cement was also used in some testing, the details of which are given in Table 4.4.

Table 4.2: Physical properties of control aggregates
(analysis by STATS Laboratories[i])

	Cheddar limestone	Cheddar limestone	Cheddar limestone	Thames Valley sand
Grading range (mm)	20-10	10-5	5-0	5-0
Particle density on SSD basis (Mg/m^3)	2.6	2.6	2.6	2.6
Water absorption (% of dry mass)	0.30	0.53	2.20	1.40
Average moisture content (%)	0 (dry)	0 (dry)	0 (dry)	0 (dry)

Table 4.3: Bogue analysis of Portland cement
(analysis supplied by Castle Cement Ltd[j])

Compound	wt %		wt %
SiO_2	21.1	Free CaO	1.6
Al_2O_3	4.7	Total alkali equivalent (Na_2O_{eq})	0.6
Fe_2O_3	2.7		
CaO	64.5		
MgO	1.3		
SO_3	3.3		
K_2O	0.7	Cement compounds	wt %
Na_2O	0.2	C_3S	52.6
Cl	<0.1	C_2S	20.4
Insoluble residue	0.5	C_3A	7.7
Loss on ignition	1.3	C_4AF	8.1

Table 4.4: Bogue analysis of high alkali Portland cement
(analysis by QED Independent Testing and Consultancy Ltd[k])

Compound	wt %		wt %
SiO_2	20.1	Free CaO	2.5
Al_2O_3	4.9	Total alkali equivalent (Na_2O_{eq})	1.4
Fe_2O_3	3.4		
CaO	61.6		
MgO	2.6		
SO_3	3.4		
K_2O	1.1	Cement compounds	wt %
Na_2O	0.5	C_3S	42.9
Cl	<0.1	C_2S	24.4
Insoluble residue	1.1	C_3A	7.4
Loss on ignition	1.9	C_4AF	10.2

[i] STATS Laboratories, Porterswood House, Porters Wood, St Albans, AL3 6PQ, UK
[j] Castle Cement Ltd, Ribblesdale Works, Clitheroe, Lancashire, BB7 4QF, UK
[k] QED Independent Testing & Consultancy Ltd, Bucknalls Lane, Garston, Watford, WD25 9XX, UK

4.2 XRF composition analysis

Table 4.5 shows the percentage (by mass) of each element present in the secondary aggregate materials in their fully oxidised state. Any elements that formed gases during the oxidation process will have been released from the sample and of these, sulfur trioxide was analysed for. It is notable that under the loss on ignition, the ISF slag sample actually shows a net gain in mass. This is most probably due to the oxidation of elements in the ISF slag.

Table 4.5: Results of XRF analysis of the aggregates (as mass %)

Oxide (%)		ISF slag	CRT glass	Bottle glass
Silicon dioxide	SiO_2	18.89	58.05	71.88
Titanium (IV) oxide	TiO_2	0.40	0.25	0.04
Aluminium oxide	Al_2O_3	8.52	2.98	1.02
Iron (III) oxide	Fe_2O_3	39.15	0.34	0.12
Calcium oxide	CaO	13.92	1.56	8.62
Magnesium oxide	MgO	2.05	0.71	3.79
Potassium oxide	K_2O	0.57	7.06	0.51
Sodium oxide	Na_2O	0.98	7.28	13.38
Phosphorus (V) oxide	P_2O_5	0.36	<0.02	<0.02
Chromium (III) oxide	Cr_2O_3	0.19	0.02	<0.01
Manganese (II, III) oxide	Mn_3O_4	1.12	0.02	0.01
Zirconium (IV) oxide	ZrO_2	<0.02	1.10	<0.02
Hafnium oxide	HfO_2	<0.01	0.02	<0.01
Lead (II) oxide	PbO	1.37	7.41	<0.02
Zinc oxide	ZnO	13.95	0.21	<0.01
Barium oxide	BaO	0.66	6.97	0.01
Strontium oxide	SrO	0.07	4.87	<0.01
Tin (IV) oxide	SnO_2	0.03	0.02	<0.01
Copper (II) oxide	CuO	0.62	0.62	<0.01
Cerium (IV) oxide	CeO_2	<0.01	0.20	<0.01
Arsenic (III) oxide	As_2O_3	0.36	<0.01	<0.01
Niobium (V) oxide	Nb_2O_5	<0.01	0.05	<0.01
Nickel (II) oxide	NiO	<0.01	0.02	<0.01
Loss/Gain on ignition (-/+)		6.19	-0.22	-0.15
Sulfur trioxide (remaining after LOI and fusion)	SO_3	3.77	<0.05	0.21
Total		97.02	99.98	99.53

The relatively low total for the slag sample is thought to be due to the presence of elements that were not analysed for by this XRF analysis, such as other transition metals. Several transition metals have been shown to be present in relatively small quantities (TiO_2 = 0.40%, Mn_3O_4 = 1.12%, CuO = 0.62%). If others that were not analysed for were present in similar quantities, they could potentially account for the ~3% shortfall witnessed.

The presence of lead and other heavy metal ions in the CRT glass and the ISF slag bias the composition results when considered on a mass basis. The main elemental composition has therefore been recalculated on a molar basis and summarised in Table 4.6. For this calculation to be made, the mass % totals in the previous table have been rounded to 100%. The values in Table 4.6 are therefore only approximate.

Table 4.6: Main elements present in the aggregates (as molar %)

Oxide (Molar %)		ISF slag	CRT glass	Bottle glass
Silicon dioxide	SiO_2	26.84	69.72	71.35
Aluminium oxide	Al_2O_3	7.13	2.11	0.60
Iron (III) oxide	Fe_2O_3	20.93	0.15	0.04
Calcium oxide	CaO	21.19	2.01	9.17
Magnesium oxide	MgO	4.34	1.27	5.61
Potassium oxide	K_2O	0.52	5.41	0.32
Sodium oxide	Na_2O	1.35	8.48	12.88
Lead (II) oxide	PbO	0.52	2.40	0.00
Zinc oxide	ZnO	14.63	0.19	0.00
Barium oxide	BaO	0.37	3.28	0.00
Strontium oxide	SrO	0.06	3.39	0.00

The addition of CaO to silicate glass is known to increase its durability up to a concentration of 10 mol%. At high pH (~10), silica (SiO_2) extraction will be high for low CaO glasses[141]. CRT glass might be expected to be of lower durability at high pH than the bottle glass, as it has a lower CaO content. If the silica is more readily available in the CRT glass, it would be expected to facilitate ASR.

The ISF slag is relatively low in silica compared to the glass samples. However the silica present is assumed to be amorphous, as indicated by the amorphous background hump on the XRD traces obtained (see section 4.3.3 below). The majority of the ISF slag is composed of iron, calcium and zinc, although this analysis does not indicate the form in which these ions are present, for instance whether they are present as metallic inclusions, oxides, or sulfides. The high CaO content may provide some durability to the glass structure, making it less prone to silica leaching at high pH and therefore less susceptible to ASR attack. However, the silica content may be sufficiently low to reduce the risk of ASR regardless of the CaO content.

4.3 XRD analysis

XRD analysis was carried out on the raw cement and ground samples of Cheddar limestone aggregate and ISF slag. Additionally, results are included here for cement hydration over time and CRT glass mortar hydration over time. The legends on the figures indicate the compounds that best fit the traces obtained. The numbers in square brackets refer to the compound's index card number in the Powder Diffraction File database.

4.3.1 Raw cement

The XRD trace obtained from raw cement was essentially identical to that obtained after a hydrating cement sample was quenched in acetone after 2 hours from mixing, as shown in Figure 4.3. It is therefore not duplicated here.

4.3.2 Cheddar limestone control aggregate

The trace obtained for the Cheddar limestone control aggregate was a good match for calcium carbonate. The trace is shown in Figure 4.1. Only two small peaks at 26.6 and 44.8° 2θ could not be identified. The calcium carbonate peaks are so intense it is suspected that they may be masking other peaks that would give an indication of any other compounds present.

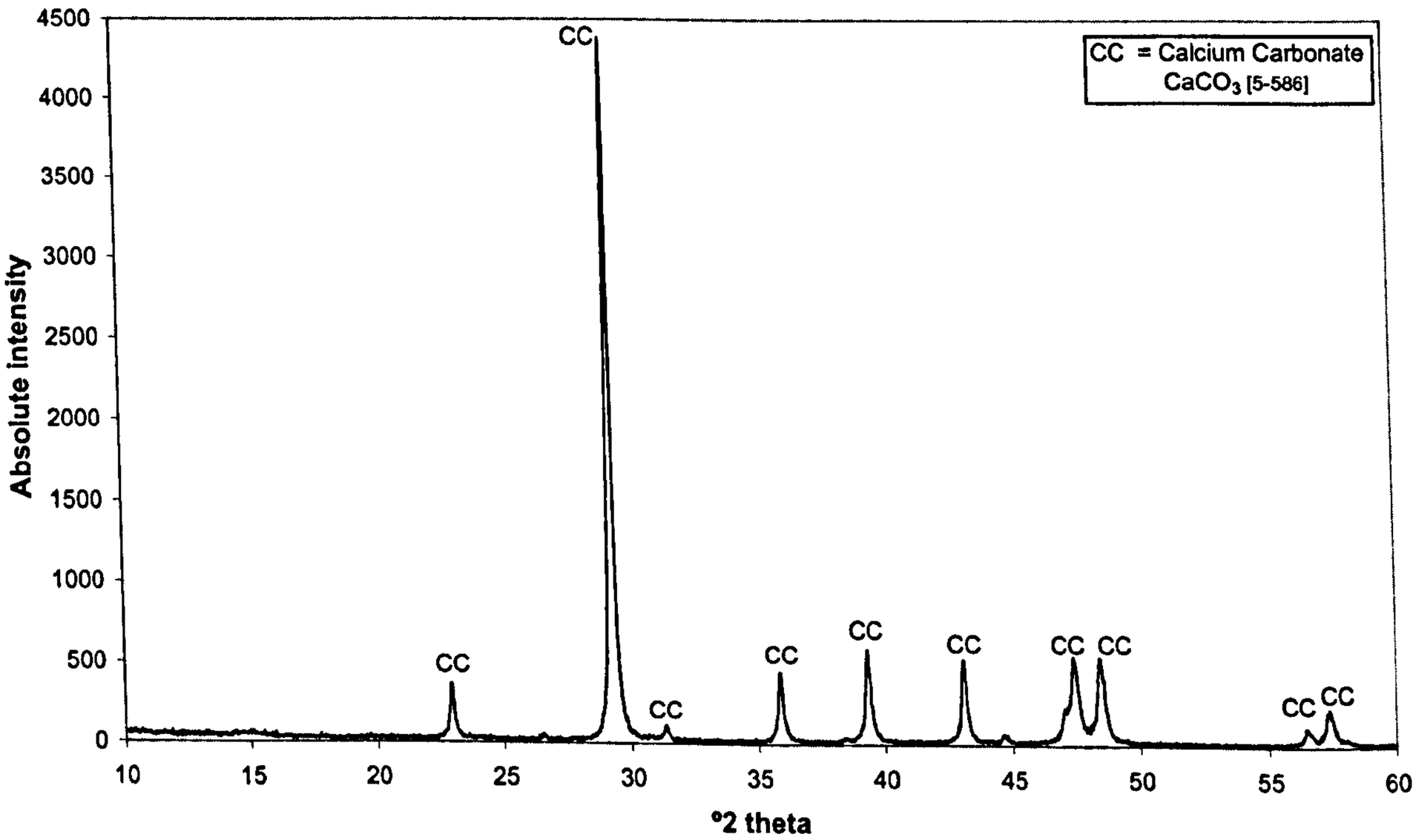

Figure 4.1: XRD trace of Cheddar limestone control aggregate

4.3.3 ISF slag

It was more difficult to identify the peaks from the ISF slag sample than any others, as the trace had an amorphous background hump which may have masked some of the peaks. In particular, there was uncertainty as to whether lead could be identified on the

trace. Possible lead peaks coincided with other compounds that appeared to be present, thus no definitive identification for lead could be made. However, as lead was known to be present in the ISF slag, it seemed reasonable to include the possible peak positions for lead on the XRD trace in Figure 4.2.

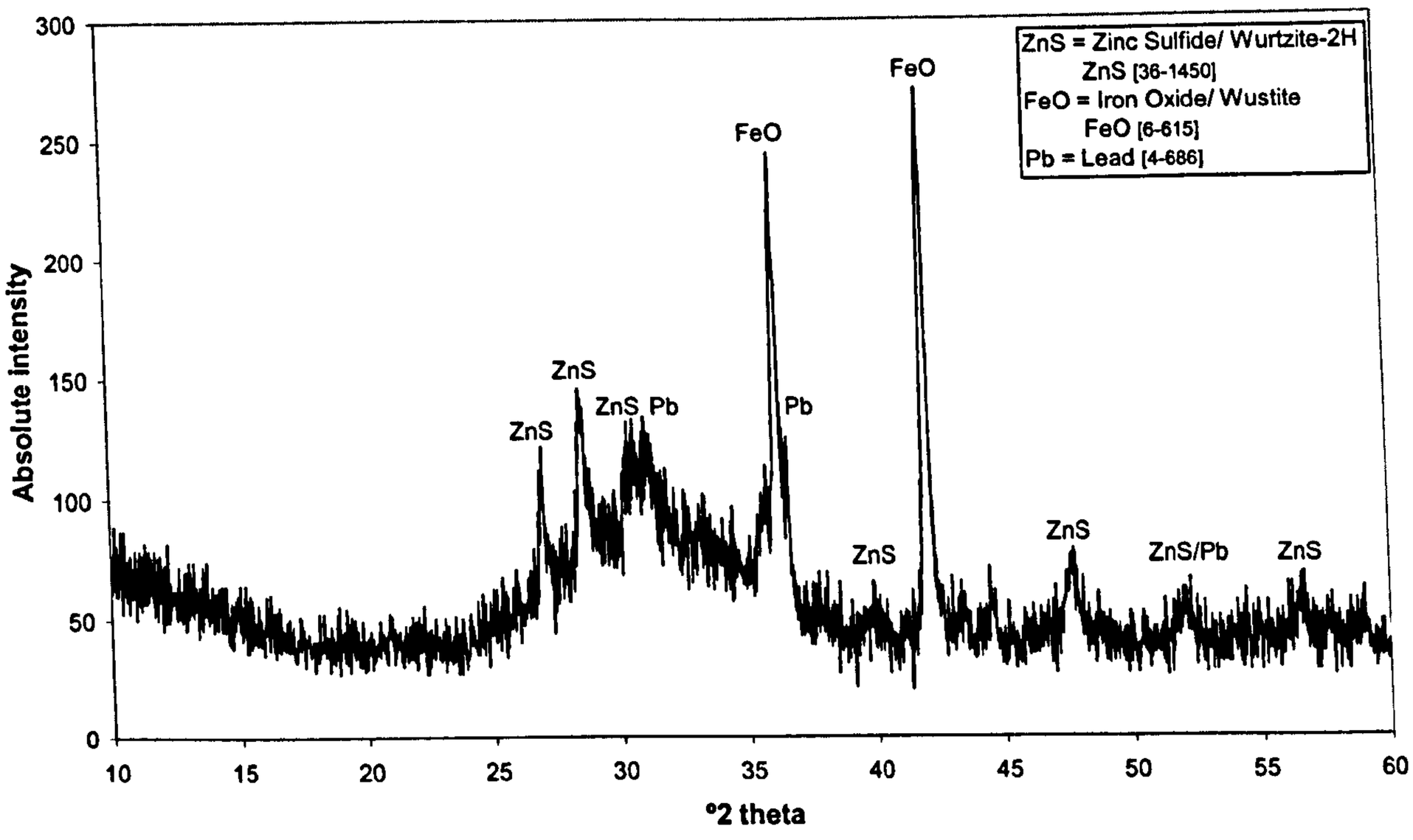

Figure 4.2: XRD trace of ISF slag

4.3.4 Hydrated cement

A sample of hydrating cement was quenched in acetone at 2, 4, 6 and 24 hours after mixing, as well as at 7 and 28 days of age. Figure 4.3 shows the XRD trace obtained from the sample quenched at 2 hours and Figure 4.4 shows the trace obtained after quenching at 28 days. The compounds identified in the cement samples include calcium silicate from the raw cement (C3S – Ca_3SiO_5) and calcium hydroxide/ Portlandite (CH – $Ca(OH)_2$), which is a cement hydration product. The 2 hour sample shows small peaks at locations where CH peaks would be (18.0 and 50.8° 2θ). This is possibly due to some localised crystallisation of CH during the early stages of hydration. However, large peaks attributable to CH were not apparent until after 24 hours, suggesting that cement hydration was well underway by this time. The intensity of the CH peaks increased up to 28 days of age. The C3S intensity gradually decreased over time, suggesting that it was being converted to CH and other hydration products, such as calcium silicate hydrate (CSH – not detected by XRD as non-crystalline), during the hydration reaction.

After 24 hours, as witnessed in the 28 day sample, calcium carbonate (CC – $CaCO_3$) was also apparent. CH in the hydrating samples had apparently become carbonated when exposed to carbon dioxide in the atmosphere during sample preparation. Peaks that have not been labelled in the figures could not be matched with confidence. Their intensities were evidently insufficient, relative to the larger peaks present, for them to be identified using the compound-matching software.

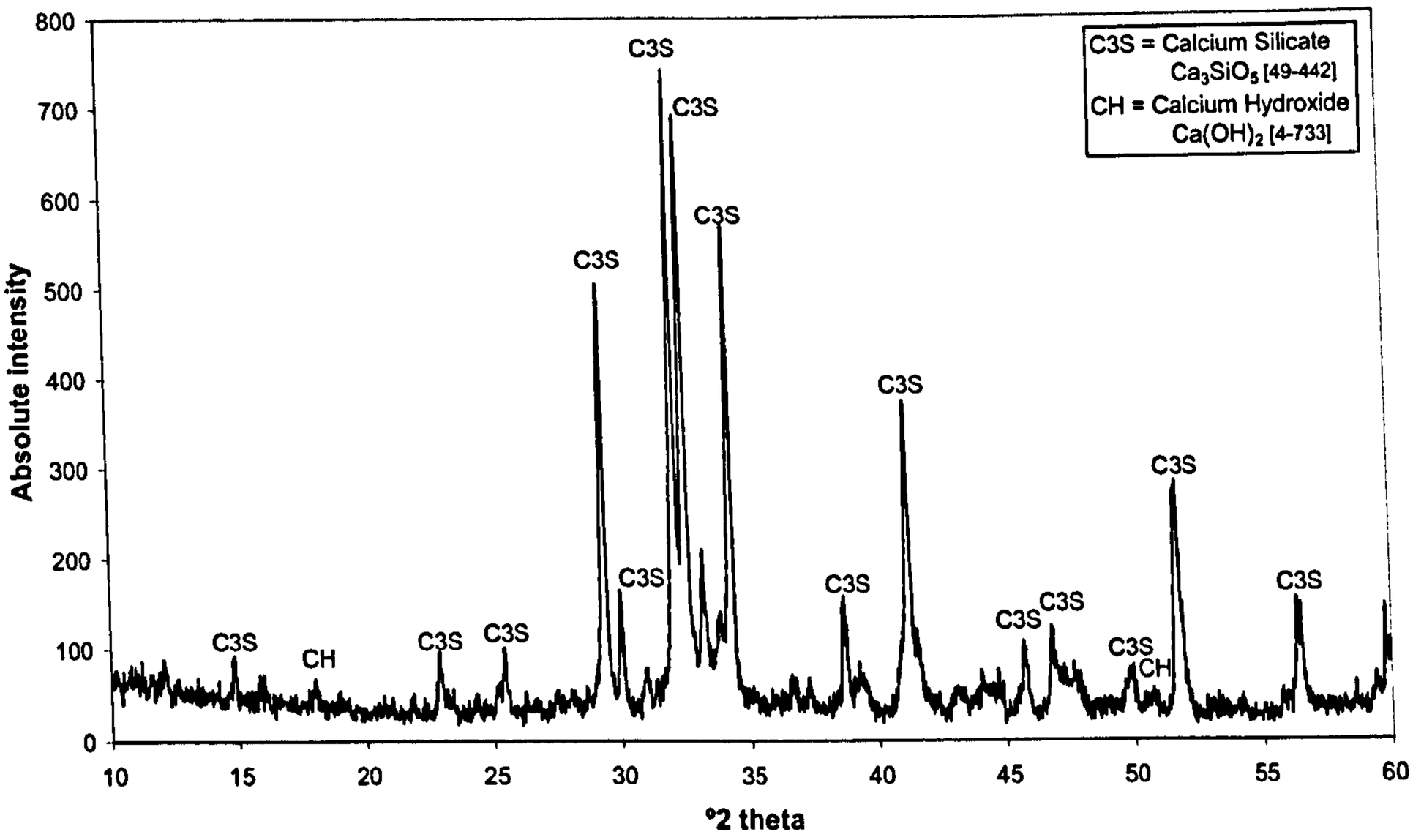

Figure 4.3: Hydrated cement, quenched after 2 hours

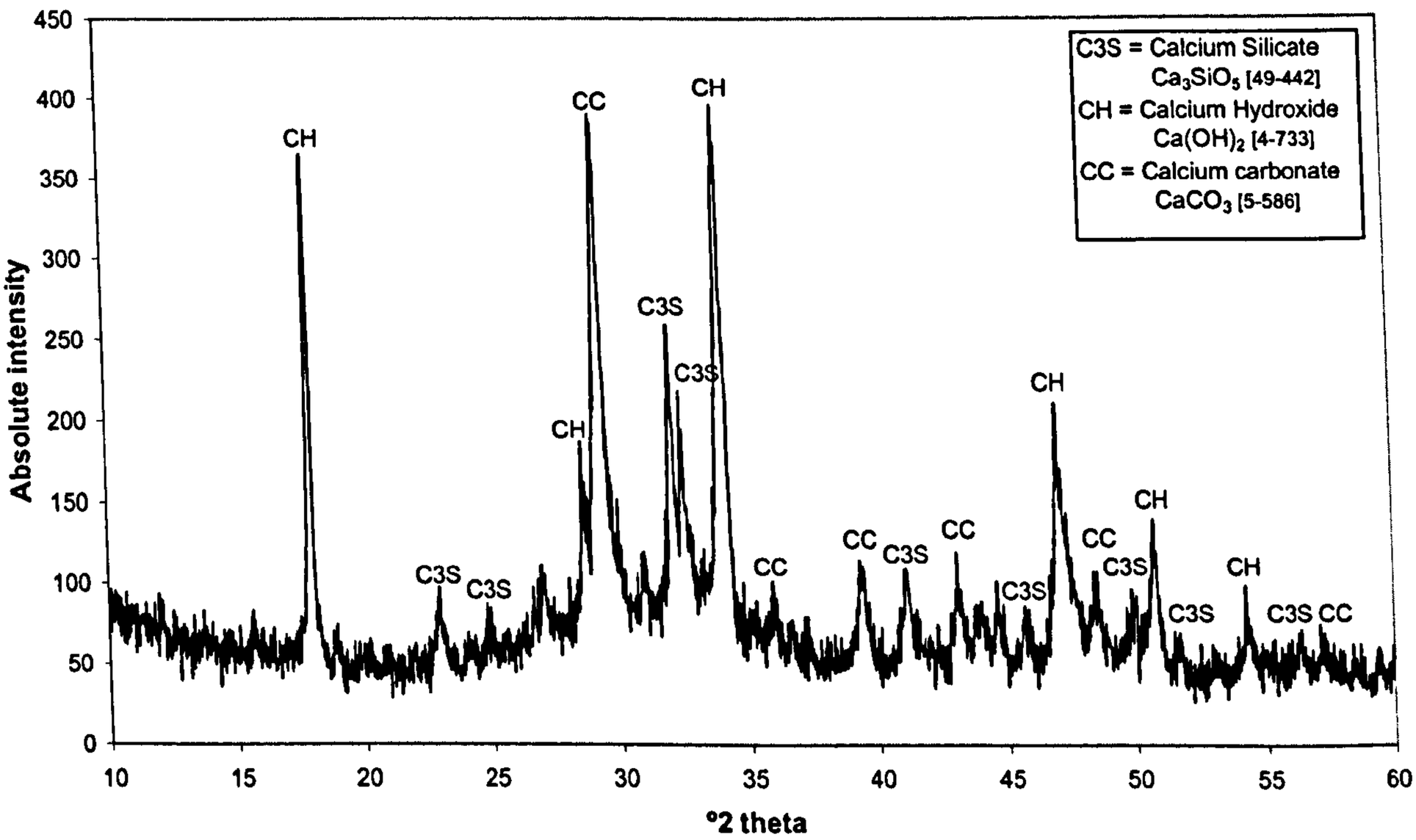

Figure 4.4: Hydrated cement, quenched after 28 days

4.3.5 CRT and bottle glass in hydrating mortars

XRD traces were not carried out on the CRT or bottle glass alone, as they are amorphous and would not be expected to produce any distinguishable peaks from XRD. However, XRD was carried out on crushed mortar samples containing the CRT and

bottle glass. Both produced a large amorphous background hump, with the only identifiable peaks corresponding to those present in the cement. The presence of the glass did not appear to cause a variation in the behaviour of the cement and the traces were comparable to those obtained from cement hydration, apart from some obvious distortion and masking of peaks by the amorphous background hump. As an example, the 28 day quenched data for the CRT glass/ cement sample is shown in Figure 4.5.

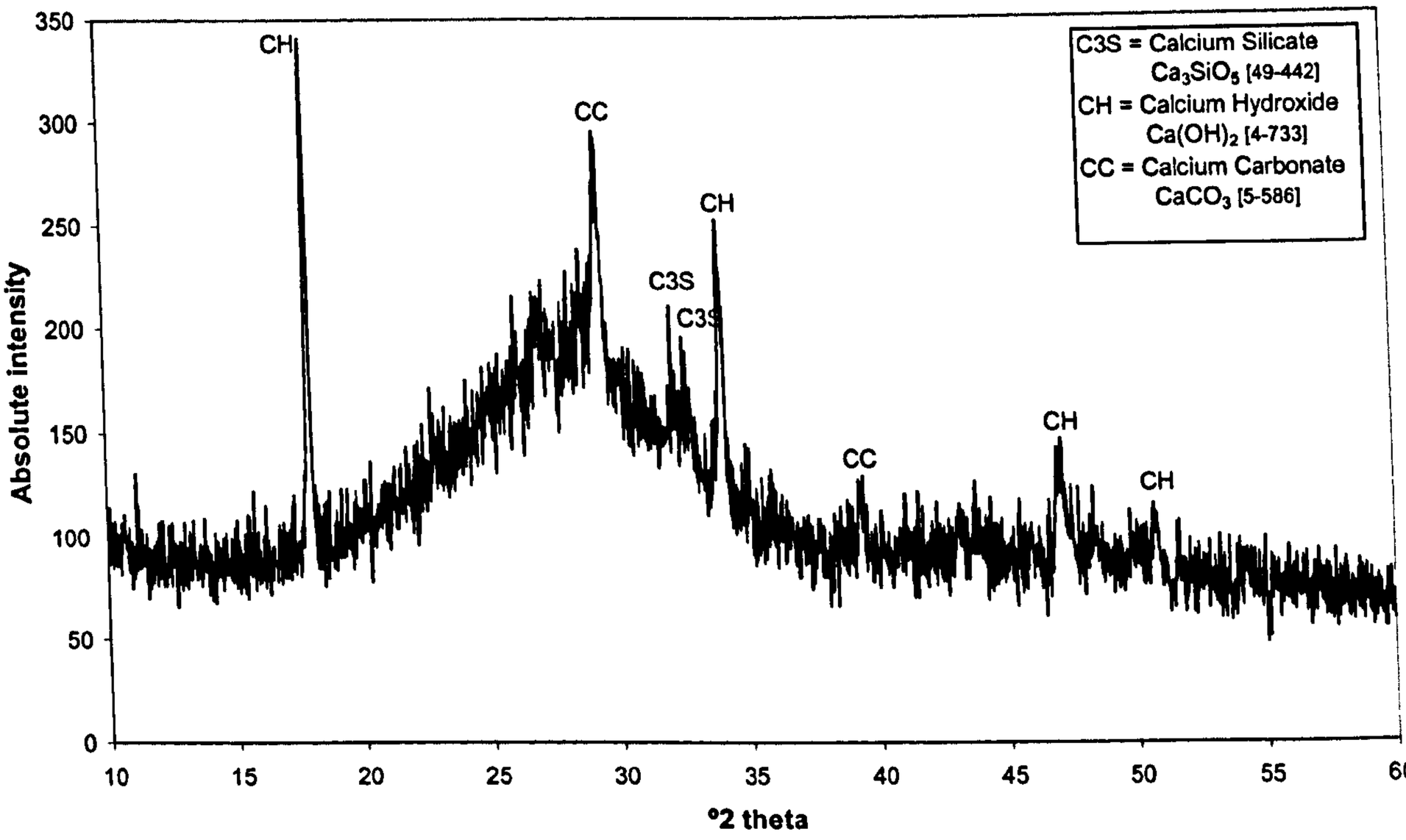

Figure 4.5: CRT glass mortar hydration, quenched after 28 days

4.4 SEM analysis of the aggregates

4.4.1 ISF slag

The ISF slag was mounted in resin and observed by SEM. The images reported here were obtained using the Jeol microscope using a windowless EDS detector. Figure 4.6 shows a backscattered electron image of a slag particle containing bright, spherical inclusions. Figure 4.7 is a general EDS analysis of the particle showing it largely to consist of silicon, calcium, iron and zinc, with traces of lead. The brightest regions (indicated by A) are shown by EDS (Figure 4.8) to consist of lead with no other elements in appreciable amounts, suggesting that these are metallic lead inclusions. Lead only appeared to be present in such inclusions, rather than being distributed throughout the bulk of the material. Smaller inclusions were also less frequently detected (indicated by B). When magnified (Figure 4.10), it could be seen that this too contained brighter regions of lead. However, the remainder of the inclusion was shown by EDS (Figure 4.9) to be iron with minor counts from other elements, suggesting such regions to be metallic iron inclusions.

On closer inspection it was apparent that the bulk of the material consisted of two main phases, as seen in Figure 4.11. (Increased magnification of region X in Figure 4.6) The darker regions of the bulk aggregate contained mainly silicon, calcium and iron (Figure 4.12), while the brighter areas were high in sulfur, zinc and iron (Figure 4.13). The brighter regions could therefore potentially be zinc sulfide, which would correspond to the results obtained from XRD analysis of the ISF slag (section 4.3.3).

4.4.2 CRT glass

The images reported here were obtained using the Camscan microscope, fitted with an EDS detector. Figure 4.14 shows a general backscattered electron image of the CRT glass mounted in resin. Some particles appear darker in colour than others, suggesting that different types of glass are present. From EDS analysis, it was apparent that the lighter particles, indicated by C, were lead-containing glass (Figure 4.15) while the darker particles, indicated by D, were barium containing (Figure 4.16). This is not particularly surprising, since the sample of glass used for this study comprised of crushed, mixed glass from all parts of a CRT. Lead is often found in the neck and funnel glass of a CRT, while barium and strontium tend to be used instead of lead in the plate/ screen glass of newer CRTs. The ions present seem to be uniformly distributed throughout their respective particles and individual glass particles do not contain any concentrated inclusions of any particular ion.

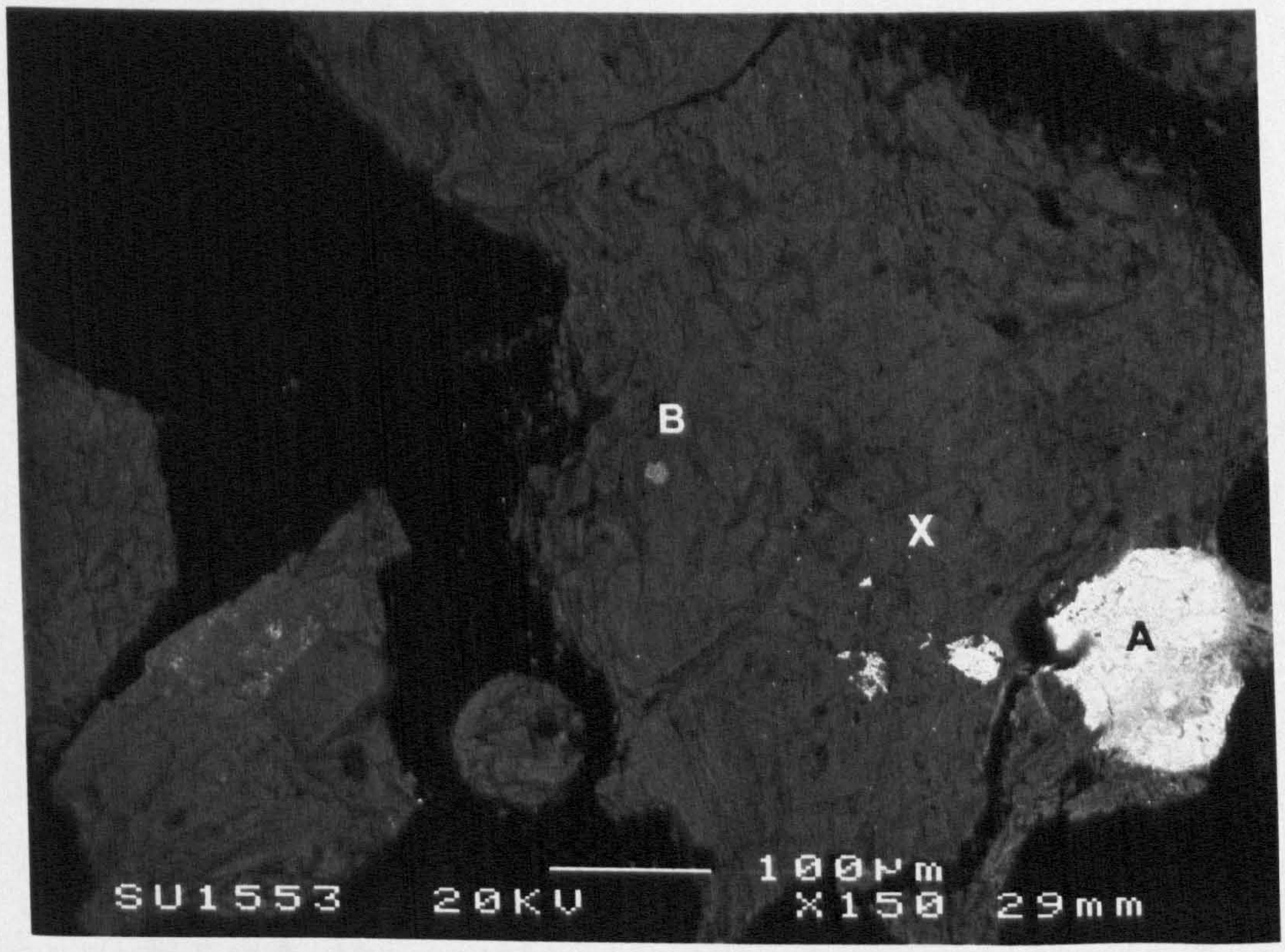

Figure 4.6: Backscattered electron image of ISF slag in resin, showing bright inclusions

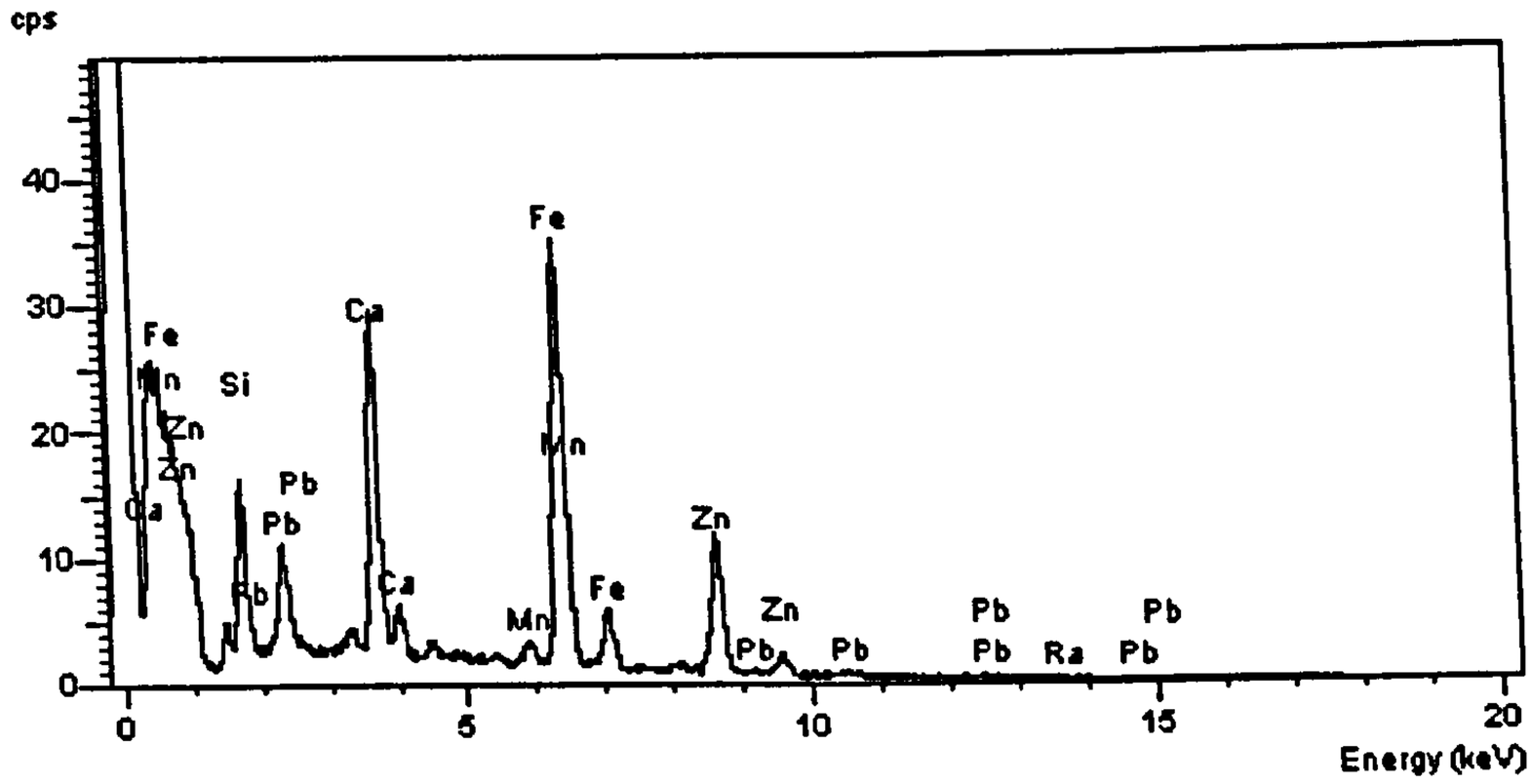

Figure 4.7: General EDS analysis of ISF slag particle (whole area of image shown in Figure 4.6)

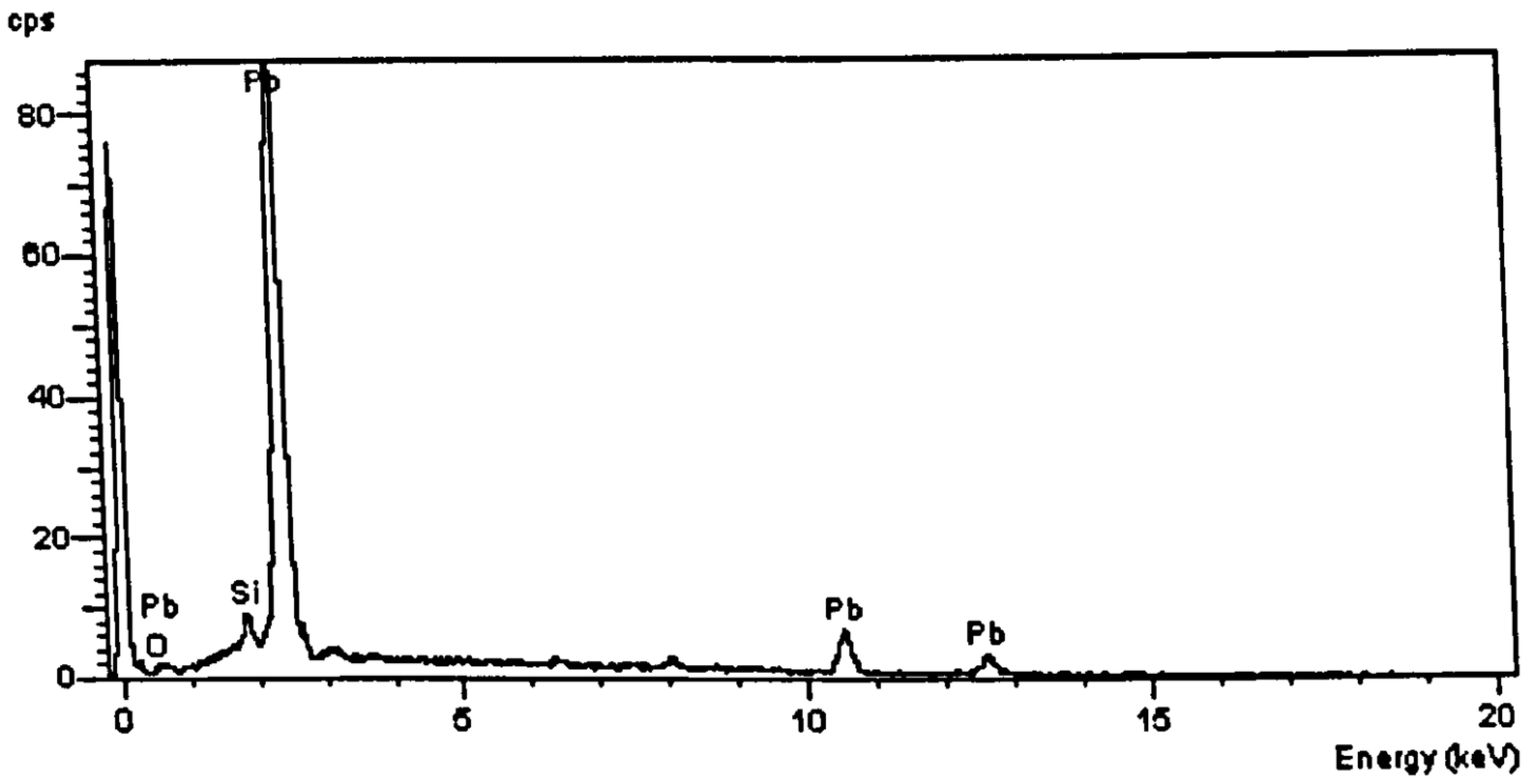

Figure 4.8: EDS analysis of bright inclusion (A) within ISF slag particle

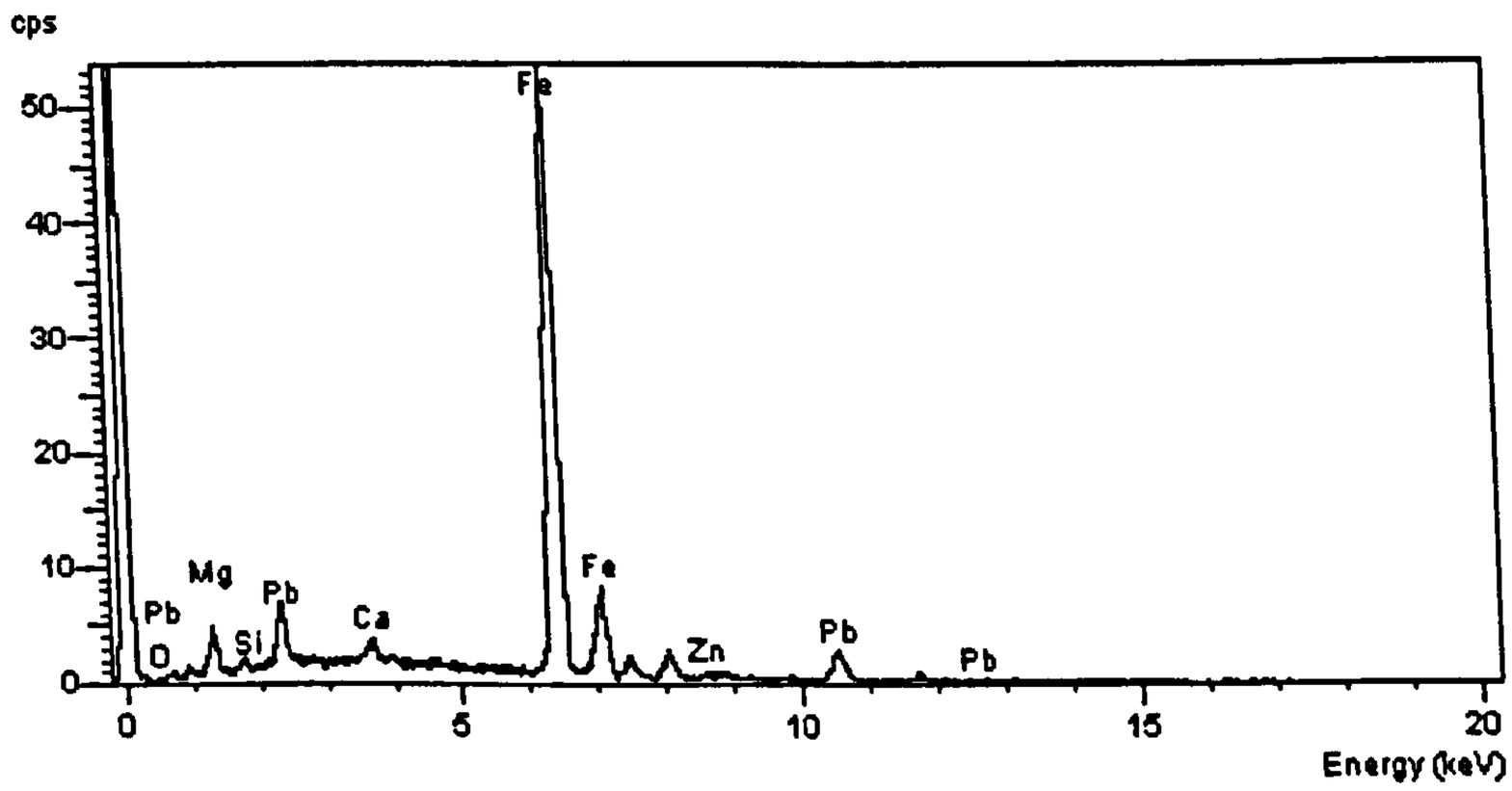

Figure 4.9: EDS analysis of bright inclusion (B) in ISF slag particle

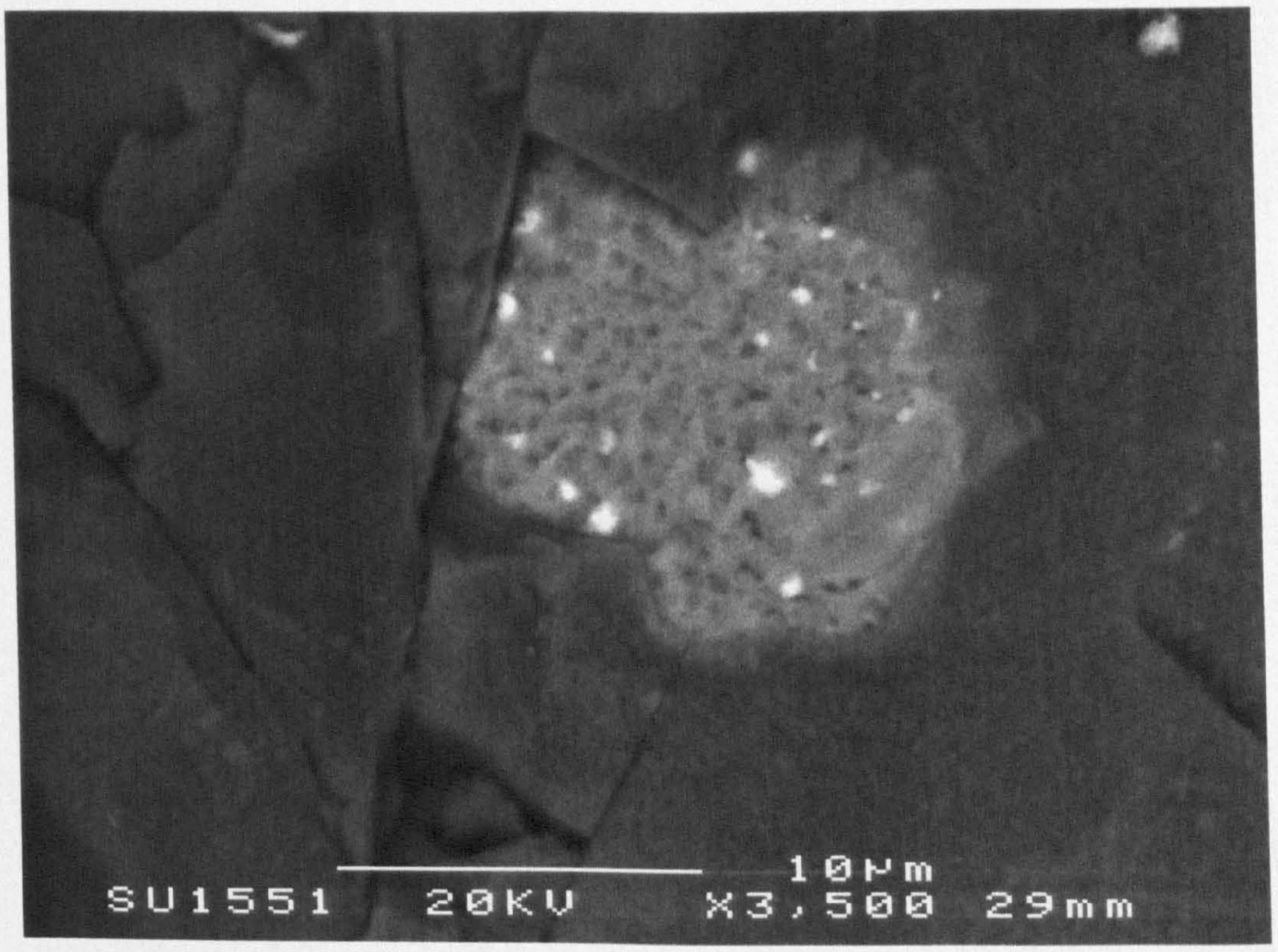

Figure 4.10: Backscattered electron image enlargement of Fe-rich inclusion (B) in ISF slag

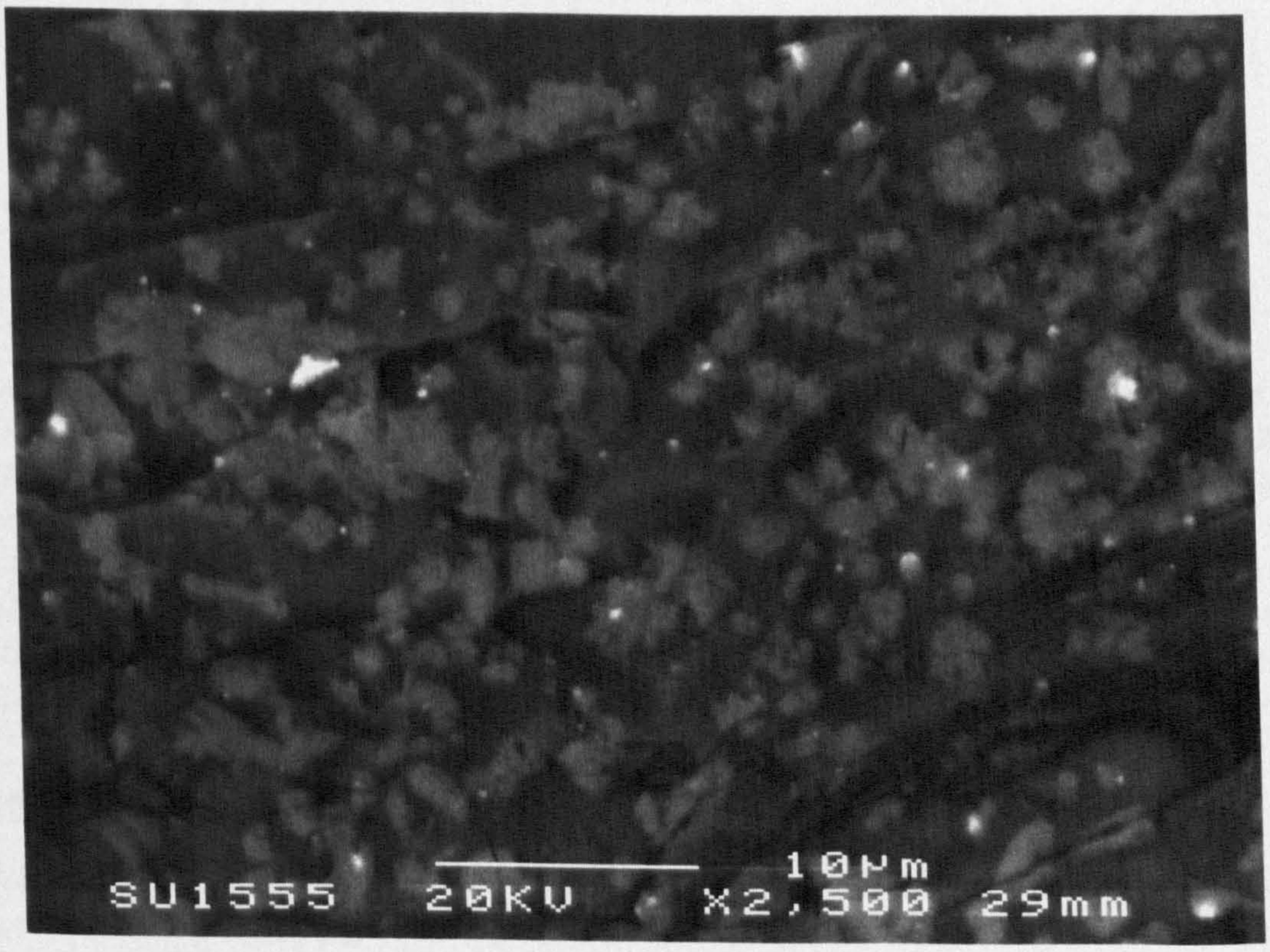

Figure 4.11: Magnified backscattered electron image of bulk of ISF slag particle

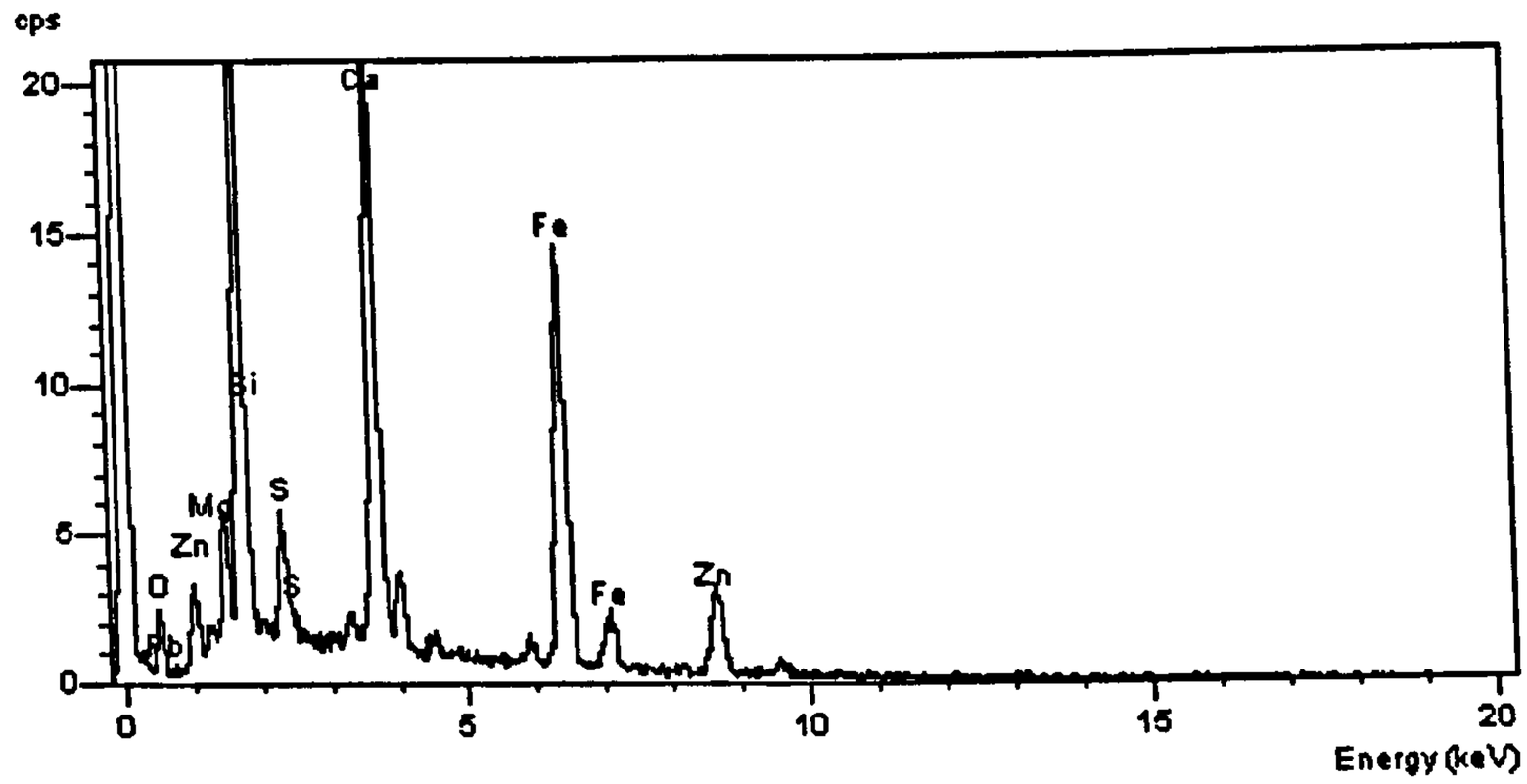

Figure 4.12: EDS analysis of darker regions in the bulk of the ISF slag

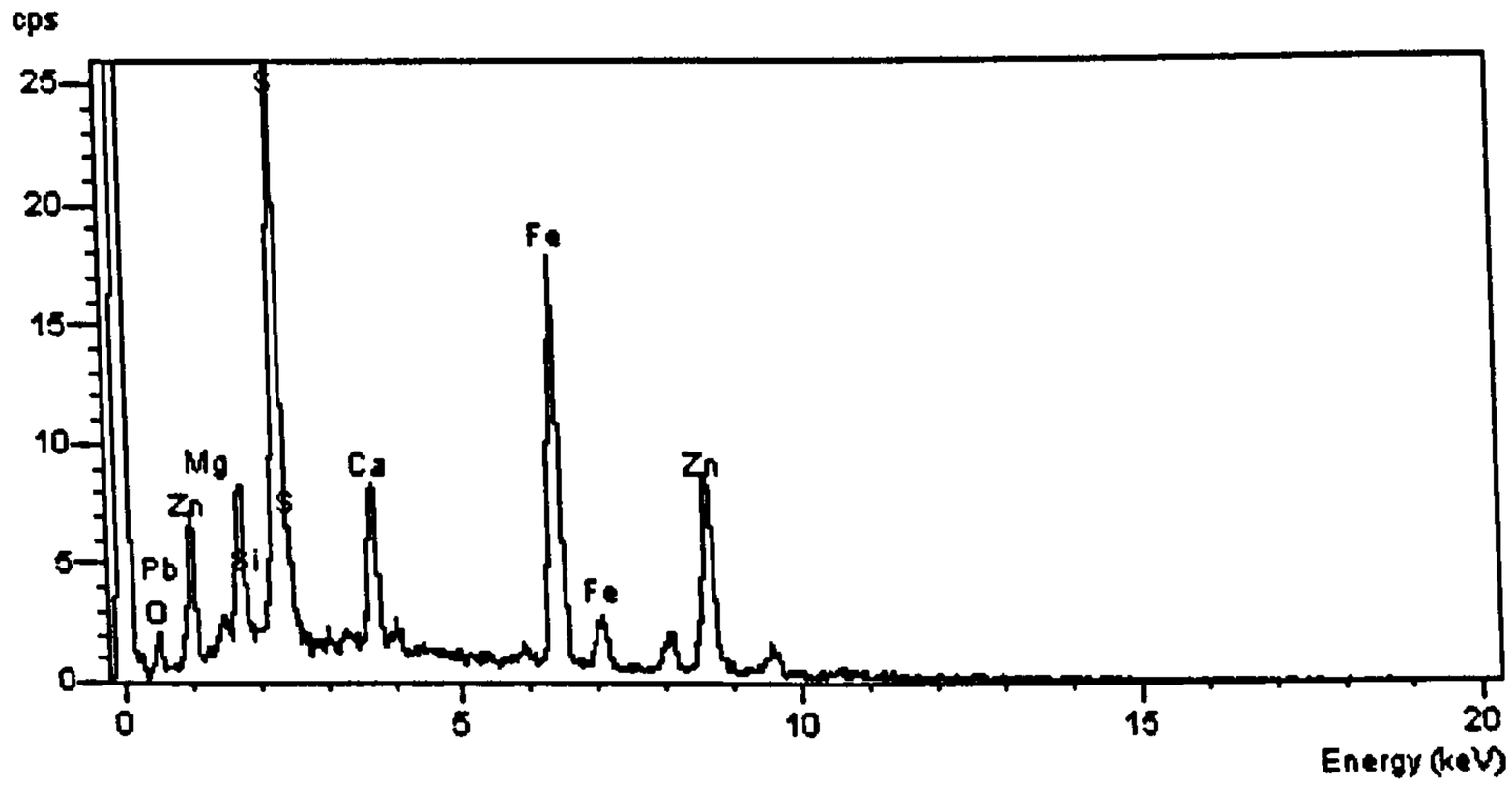

Figure 4.13: EDS analysis of the brighter regions in the bulk of the ISF slag

However, it can be seen (indicated by E) that there is a distinctly bright particle that, from EDS analysis, was apparently a shard of aluminium (Figure 4.17). On further examination of the sample, zinc metal shards were also observed (though much less frequently than aluminium). However, the EDS scan was not recorded so cannot be included here. The CRT glass that had been supplied from the processor had apparently been contaminated with shards of these metals as a result of a newly adopted processing method. The implications of this contamination are included in a later section (5.2).

4.5 TEM analysis of the ISF slag

Since TEM was to be carried out on crushed, quenched mortars containing the ISF slag to see if there were any gel coatings present around the cement grains, it was necessary to characterise the relevant materials using this technique. The cement, the limestone control aggregate and the ISF slag were all examined by TEM with EDS analysis and selected area diffraction patterns taken, to identify whether regions were crystalline (with

diffraction spot patterns) or amorphous (with ring patterns). All scale indicators used are approximate.

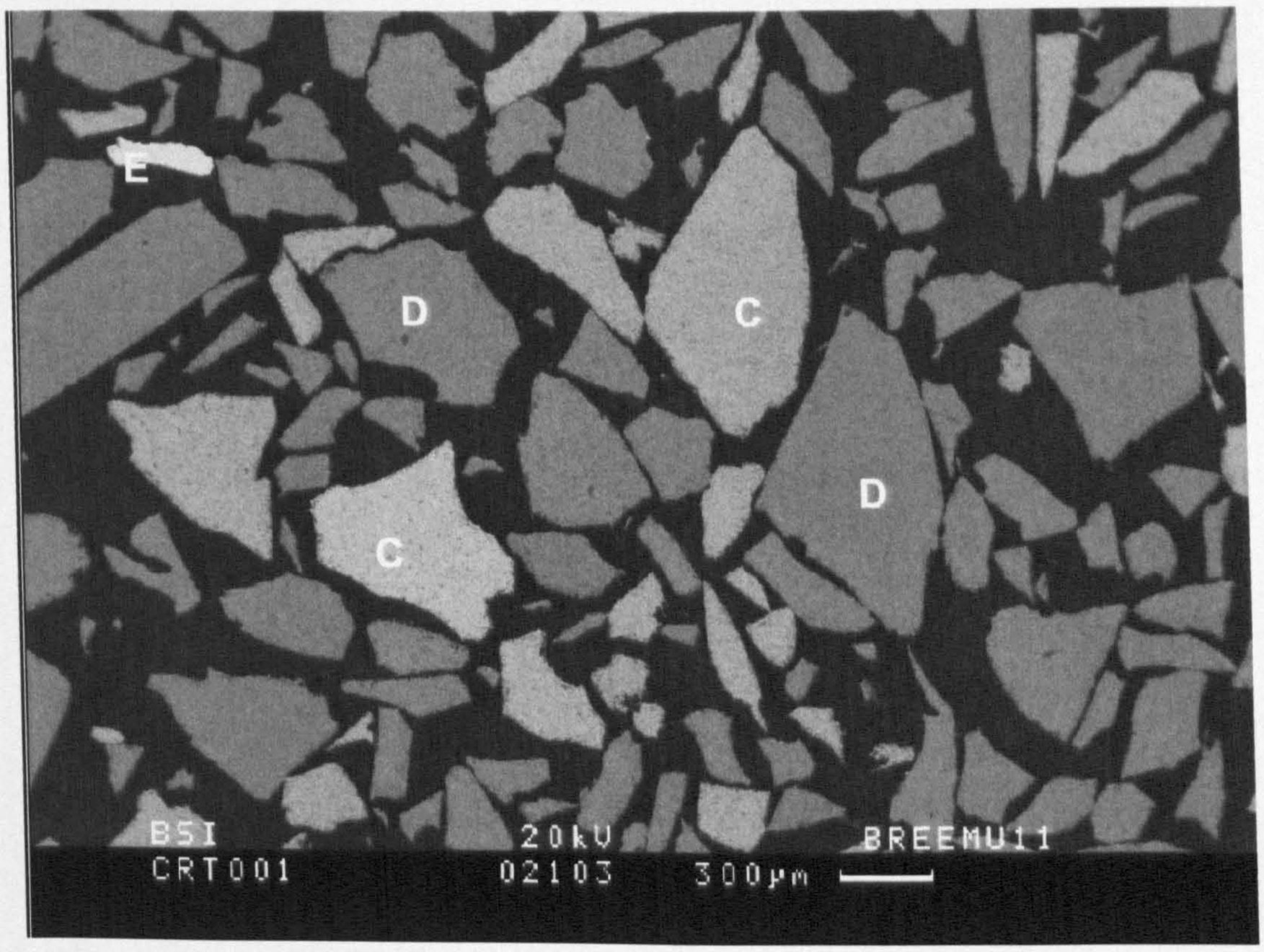

Figure 4.14: Backscattered electron image of CRT glass in resin

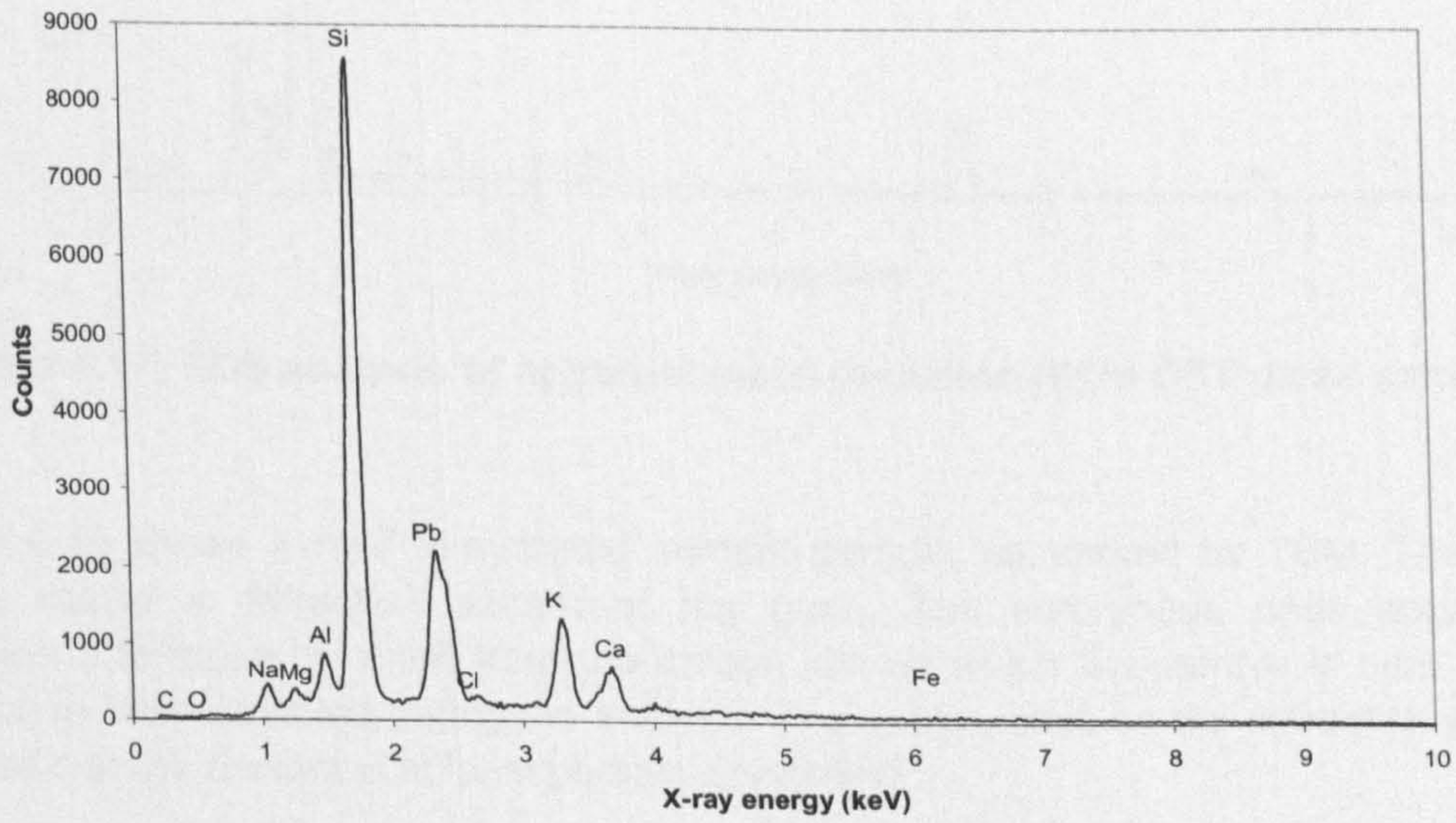

Figure 4.15: EDS analysis of brighter particles (C) in CRT glass sample

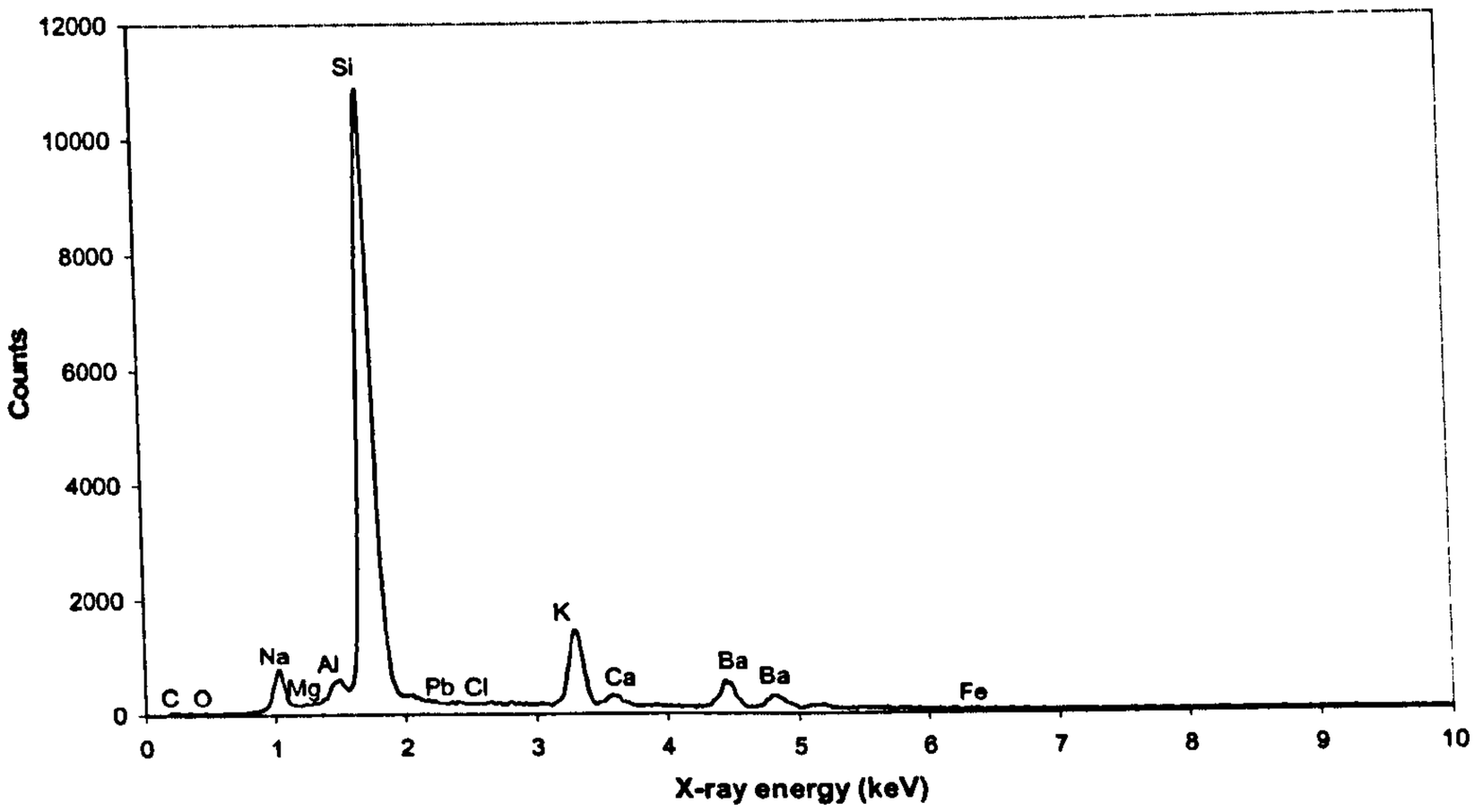

Figure 4.16: EDS analysis of darker particles (D) in CRT glass sample

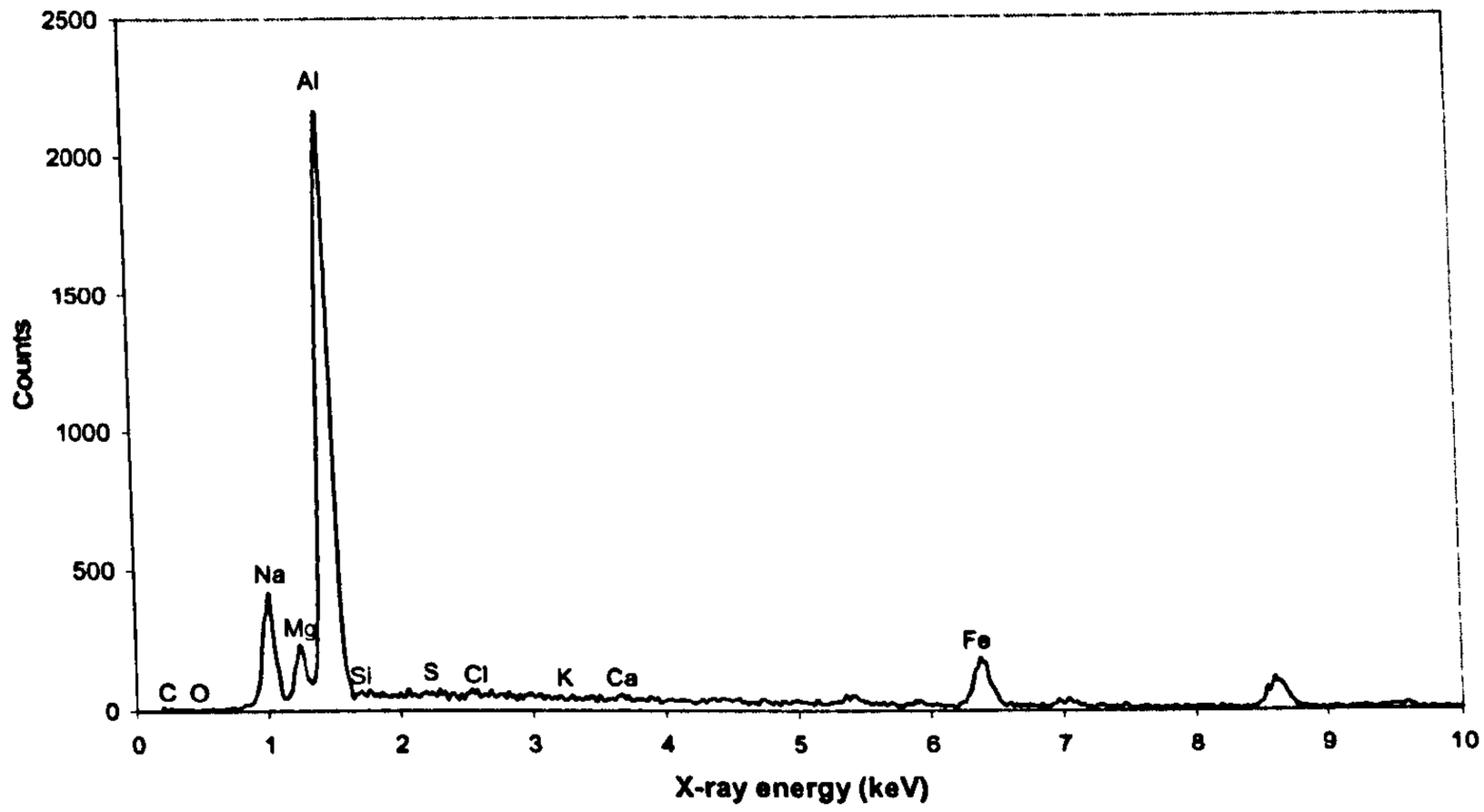

Figure 4.17: EDS analysis of apparent metal inclusion (E) in CRT glass sample

Figure 4.18 shows a raw/ unhydrated cement particle, as viewed by TEM. The inset image shows a diffraction pattern of the grain. The amorphous rings appear to correspond to those obtained from the carbon film on which the sample is held, which must have been detected during the analysis. The spots visible on the diffraction pattern indicate that the cement is at least partially crystalline.

Figure 4.19 shows crushed limestone aggregate particles, as viewed by TEM. The inset image is the diffraction pattern of the grain. Unlike the pattern from the raw cement, there are no amorphous rings apparent, suggesting from the spot pattern obtained that the aggregate is crystalline.

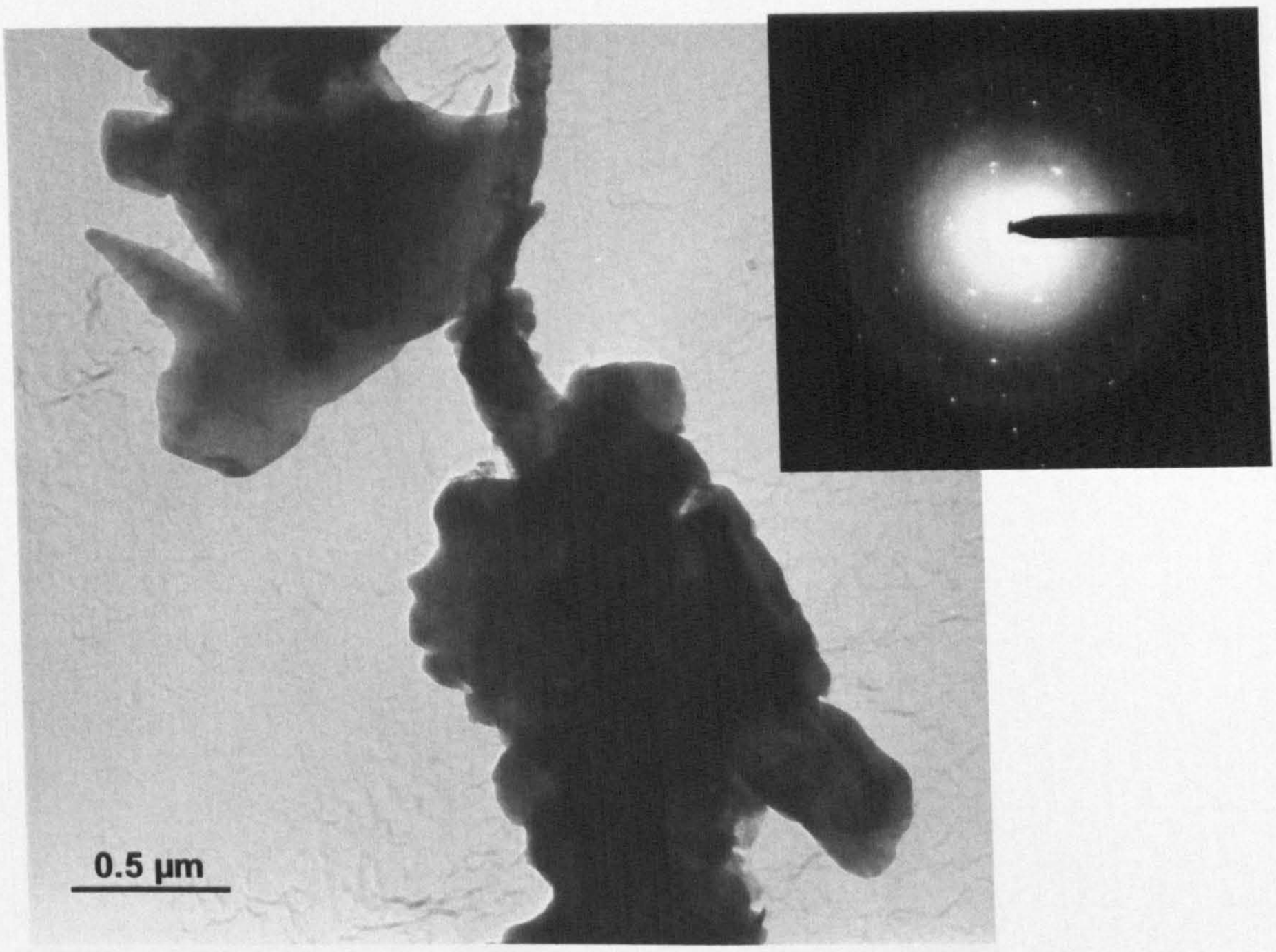

Figure 4.18: TEM image and diffraction pattern from cement particle

Due to the samples being finely ground before examination by TEM, the observed cement and aggregate particles did not show any distinguishing features with which they could be identified from each other when mixed as mortars. It was therefore necessary to carry out EDS analysis on particles to determine what was being viewed. Figure 4.20 shows that the raw cement particles comprise mainly of calcium and silicon at a ratio of approximately 3:1. The scan from the limestone control aggregate (Figure 4.21) shows mainly calcium to be present. When the ISF slag was analysed by EDS, different scans were obtained depending on which particles/ regions were examined, suggesting that the material is not homogenous in composition. This supports the observations made during SEM analysis (section 4.4.1). For example, one trace showed peaks of silicon, calcium and iron to be approximately equal, with lower peaks indicating the presence of zinc and aluminium (Figure 4.22A). Another trace showed large zinc, iron and copper peaks, although the copper was most likely to have been detected from the copper grid on which the sample was supported, rather than from the ISF slag itself (Figure 4.22B).

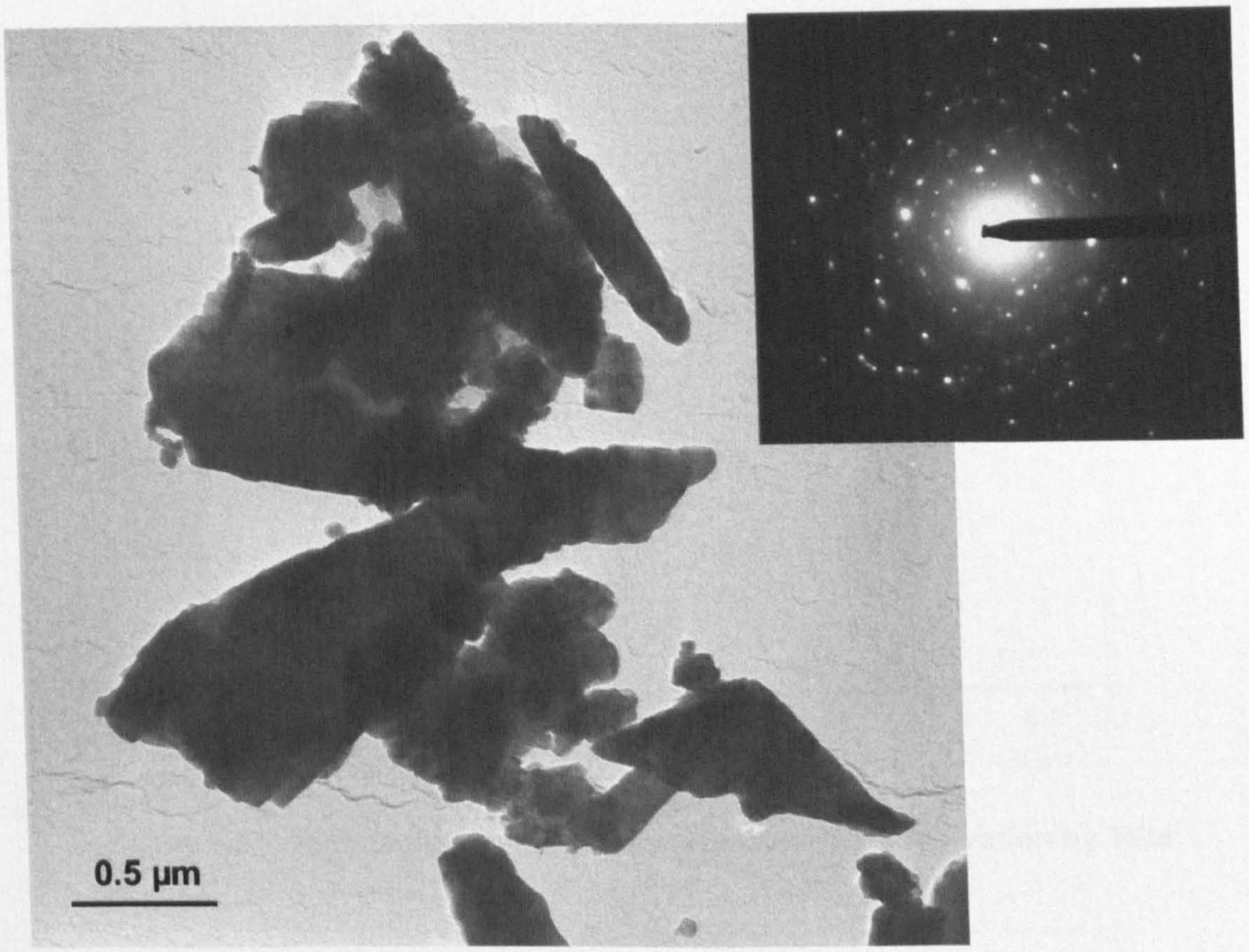

Figure 4.19: TEM image and diffraction pattern from limestone control aggregate

The diffraction pattern obtained from an ISF particle viewed by TEM (Figure 4.23) shows distorted spots and amorphous rings, suggesting that there are both amorphous and crystalline components present. However, when the sample holder was tilted on its axis, definite crystalline patterns were found, represented by the diffraction spot patterns in Figure 4.24. It was expected that diffraction patterns from the ISF slag would correspond to the crystalline phases that had been identified by XRD analysis (FeO, ZnS or Pb). Therefore, indexing these patterns was not seen to be useful in the context of the current work. They would, however, serve as a useful reference when carrying out further TEM analysis on the ISF slag.

Ultimately, this study confirmed that the ISF slag is a complex, inhomogeneous material, consisting of both crystalline and amorphous phases. Although the cement appeared to have some crystalline character in its raw state, on hydration it would be expected to form non-crystalline reaction products. This would make it very difficult to identify the formation of any amorphous compounds that may be present on the surface of the cement or the ISF slag particles during cement hydration, as suggested by Thomas *et al*[111] (see also section 2.4.6).

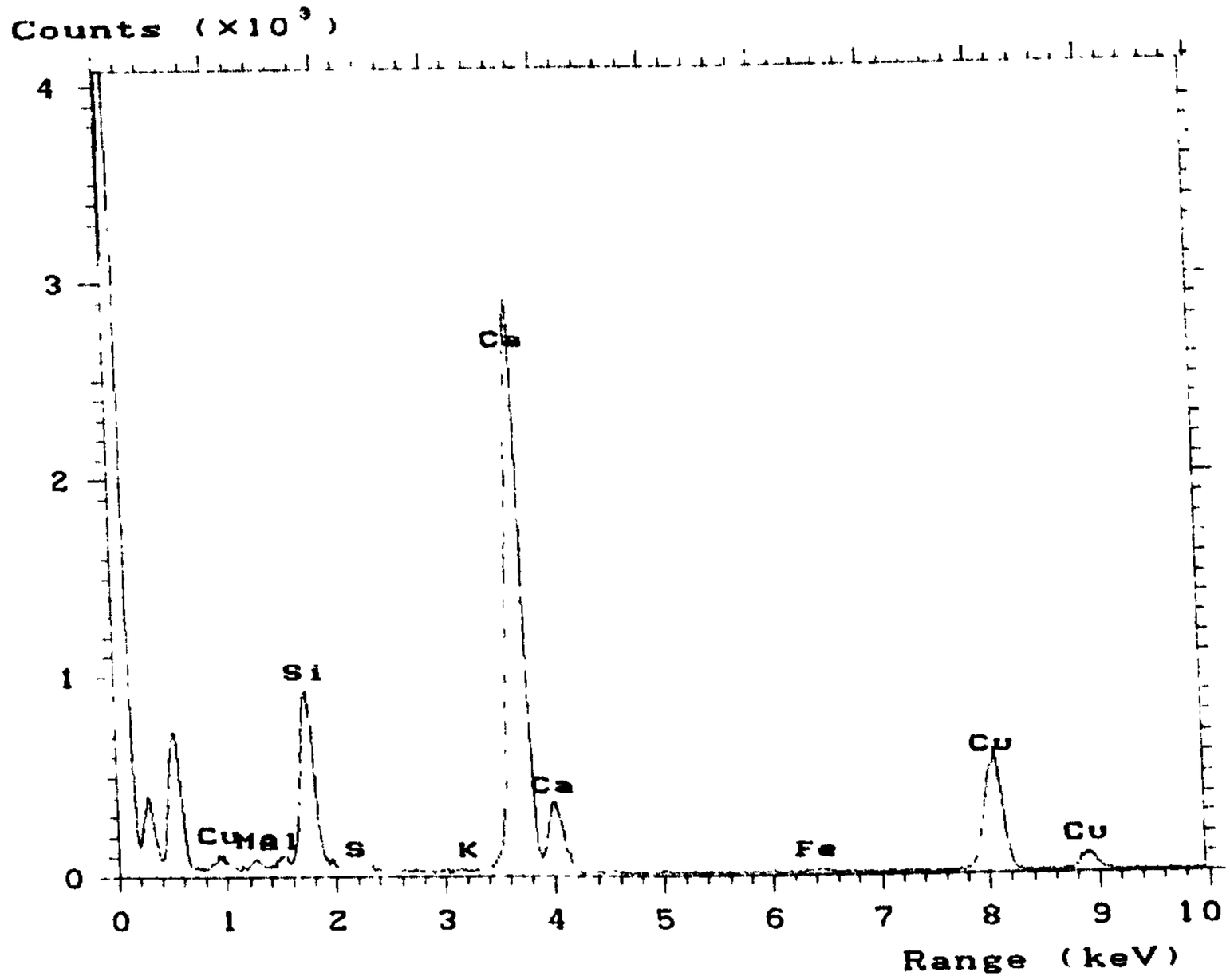

Figure 4.20: EDS analysis of cement particle during observation by TEM

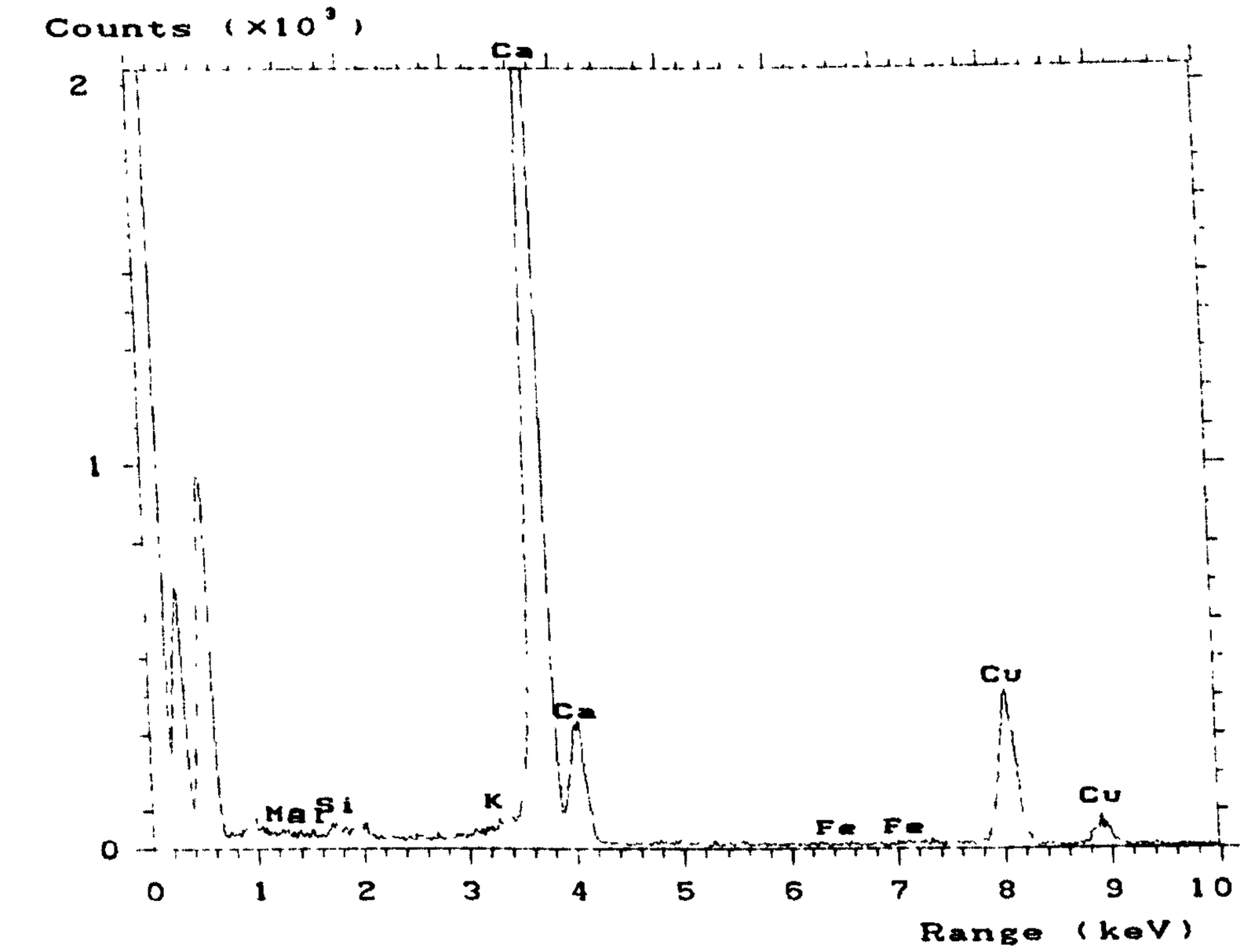

Figure 4.21: EDS analysis of limestone aggregate particle during observation by TEM

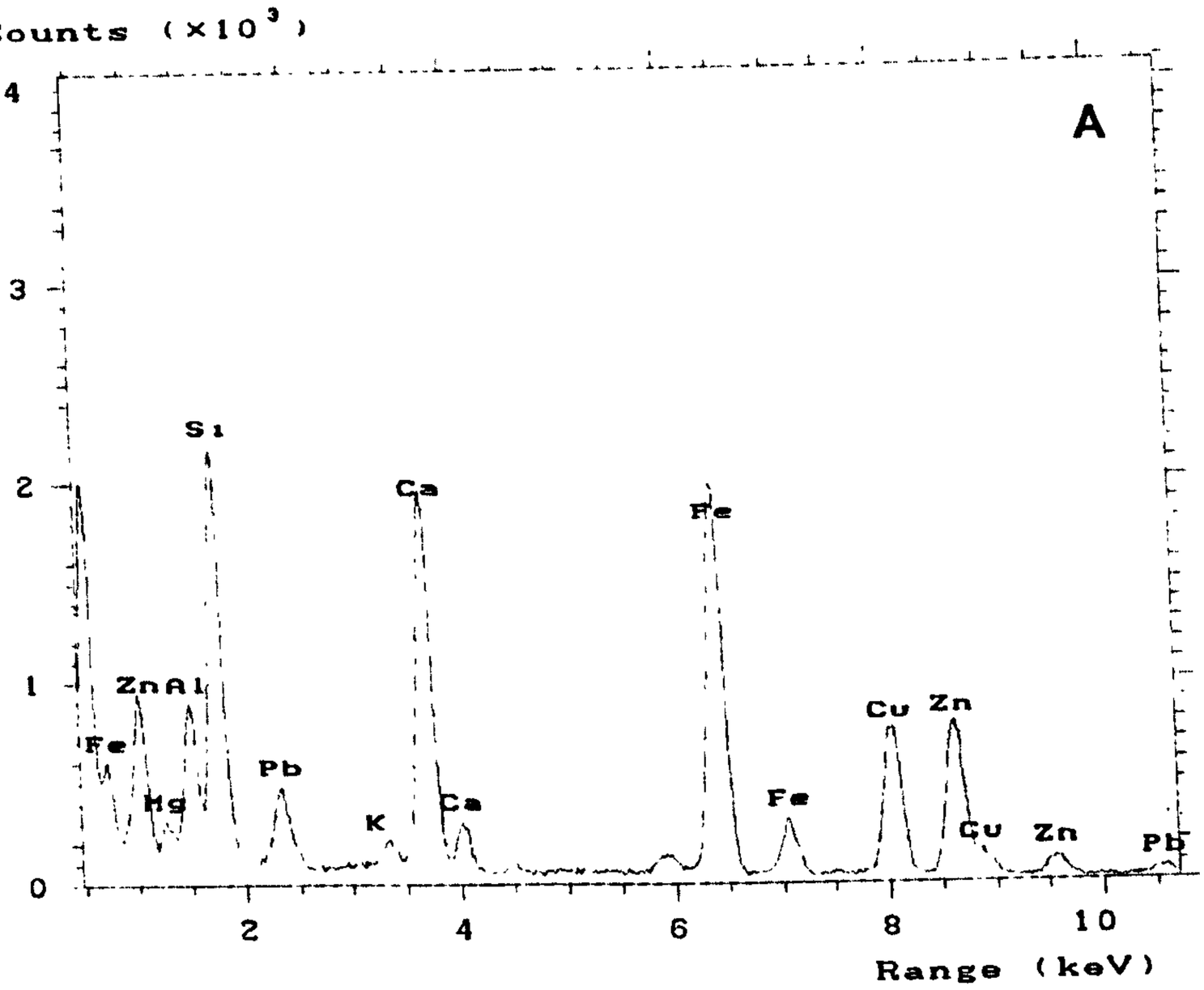

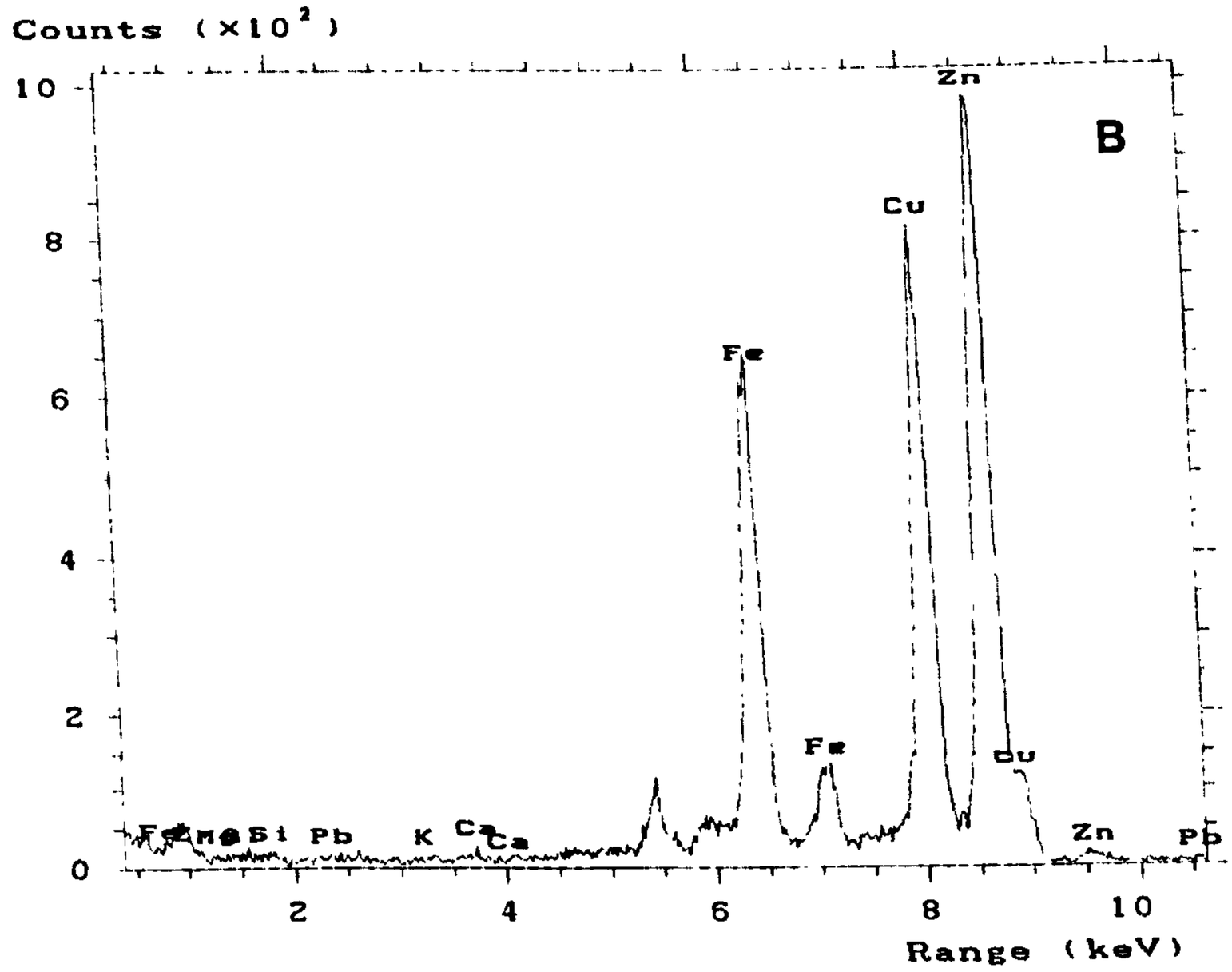

Figure 4.22: EDS analysis of ISF slag particles during observation by TEM

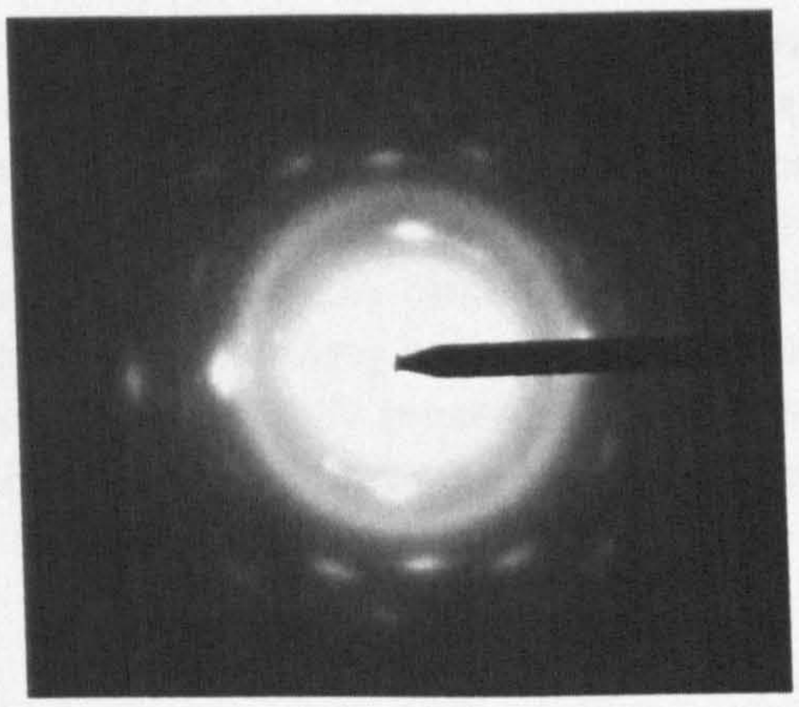

Figure 4.23: Diffraction pattern obtained from ISF slag particle showing amorphous rings and distorted spots

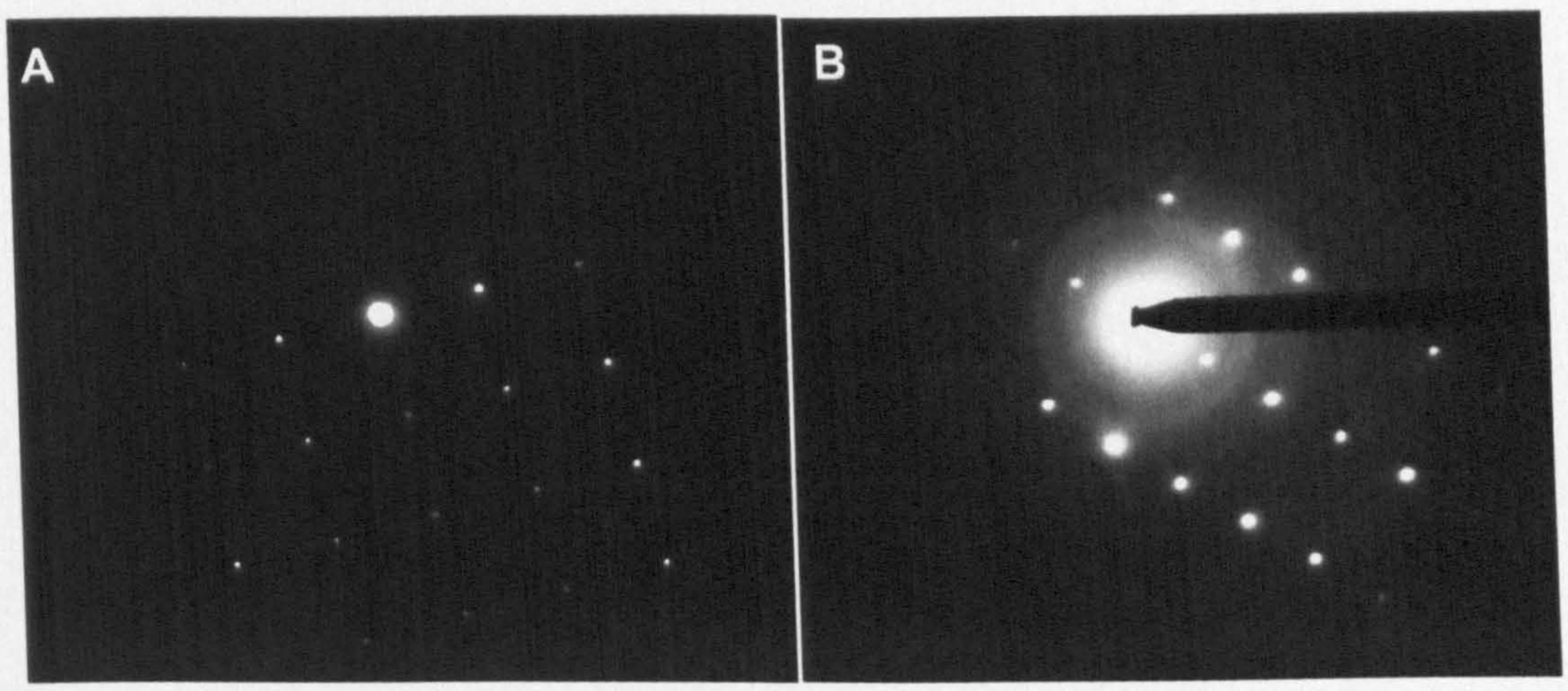

Figure 4.24: Diffraction patterns obtained from ISF slag particle on tilting sample holder

4.6 Characterisation summary

All the necessary physical property measurements that are needed when designing concrete mixes by the proposed method have been established. The components present in the cement before and after hydration have been identified as best as possible by XRD, which will be a useful reference for the following work. The grading of the secondary aggregate materials makes them suitable for use as fine aggregate (5-0mm grading) in concrete.

The CRT glass and bottle glass (BGL) samples unsurprisingly have a high silica content. The higher CaO content in the BGL suggests that it might be more durable than the CRT glass when subjected to a high alkali environment, such as that of a concrete mix. CRT glass is therefore anticipated to be susceptible to ASR. The CRT glass contains both lead and barium-containing glasses. The metal ions appear to be evenly distributed throughout individual glass particles, as would be expected in glass structures, rather than being present as concentrations.

The ISF slag contains many metallic elements and considerably less silica than the glasses analysed. However, it is still essentially amorphous, although some crystalline phases are present. The crystalline components appear to be mainly FeO and ZnS. Lead seems to be present in the slag mainly as metallic inclusions, as EDS analysis does not show it to be associated with any other ions. There is also evidence of fewer, smaller inclusions of iron. The surrounding bulk of the material consists of silicon, iron, calcium and zinc, with the zinc apparently present as finely dispersed zinc sulfide. TEM analysis of the ISF slag suggests that it may be difficult to identify potential amorphous gels at the surface of the slag or cement particles.

5 Concrete mixes containing the aggregates

Table 5.1 gives details of the control mixes that were used for this work. Table 5.2 gives details of mixes containing the ISF slag, Table 5.3 shows the concentration of additives that were used to overcome the retardation caused by the ISF slag in concrete and Table 5.4 gives details of mixes containing CRT glass. The majority of mixes used a cement content of 300 kg/m^3, with a water/ cement ratio (w/c) of 0.60. The coarse aggregate used (20-5mm) was crushed Cheddar limestone in all instances. The fine aggregate used in the TVS control mix (5-0mm) was a Thames Valley natural sand. Mixes were also made using crushed bottle glass (BGL) as fine aggregate for ASR testing purposes, to act as a relative comparison to the CRT glass mixes.

The following tables also show the measured slump of each mix (as a measure of workability, accurate to the nearest 5mm), the wet density (accurate to the nearest 10 kg/m^3), the demouldable age of concrete samples (accurate to the nearest whole day) and the compressive strength at 28 days of age (and 7 days of age where available) of hardened concrete cubes. The compressive strength is an average from either 2 or 3 samples, with the standard deviation between readings shown in brackets in the tables. The minimum target compressive strength for all mixes was 30 MPa at 28 days.

Table 5.1: Concrete mixes containing Thames Valley Sand or crushed bottle glass as fine aggregate

Mix name	Control (TVS)	Bottle glass
Relative density of replacement aggregate (Mg/m^3)	2.6	2.9
Cement content (kg/m^3)	300	300
Cement replacement materials (kg/m^3) **or** other additives	0	0
Coarse aggregate: 20-5mm (SSD weight, kg/m^3)	1135	1150
Replacement fine aggregate: 5-0mm (SSD weight, kg/m^3)	757	770
Free water/ cement ratio	0.6	0.6
Wet density of mix (kg/m^3)	2410	2360
Measured slump of mix (mm)	95	10
Demouldable age (days)	1	1
Average 7 day compressive strength (MPa)	n/a	n/a
Average 28 day compressive strength (MPa)	41.5 (±0.1)	37.5 (±1.3)

5.1 ISF slag concrete mixes

The standard ISF slag mix that was designed for this work used a cement content of 300 kg/m^3, with a w/c of 0.60. This is shown in the first column of Table 5.2, denoted by the heading 'ISF slag, 300/ 0.6'. Unless otherwise stated in the heading, all other ISF slag mixes were of the same overall cementitious material content and w/c ratio. Other mixes were trialled, utilising a higher cement content of 400 kg/m^3 and a w/c ratio of 0.45, in order to assess the factors that influence the delay in concrete setting when ISF slag is present in a mix. These details are given in the relevant headings in Table 5.2. Increasing the cement content of the ISF slag mix reduced the demouldable age of samples from 3 days (at 300 kg/m^3) to 2 days (at 400 kg/m^3). A detailed discussion of the factors effecting the retardation of ISF slag-concrete is given in section 8. Only the demouldable age of the various mixes will be highlighted here.

Table 5.2: Concrete mixes containing ISF slag as fine aggregate

Mix name	ISF slag 300/ 0.60	ISF + PFA	ISF + GGBS	ISF + NaOH	ISF + KNO_3	ISF slag 400/ 0.60	ISF slag 400/ 0.45
Relative density of replacement aggregate (Mg/m^3)	3.9	3.9	3.9	3.9	3.9	3.9	3.9
Cement content (kg/m^3)	300	195	195	300	300	300	300
Cement replacement materials (kg/m^3) **or** other additives	-	105 PFA	105 GGBS	37.50 g/l NaOH	94.78 g/l KNO_3	-	-
Coarse aggregate: 20-5mm (SSD weight, kg/m^3)	1135	1135	1135	1135	1135	1135	1135
Replacement fine aggregate: 5-0mm (SSD weight, kg/m^3)	1135	1135	1135	1135	1135	1135	1135
Free water/ cement ratio	0.6	0.6	0.6	0.6	0.6	0.6	0.45
Wet density of mix (kg/m^3)	2750	2750	2750	2730	2770	2700	2760
Measured slump of mix (mm)	20	45	5	10	15	collapse	20
Demouldable age (days)	3	4	4	1	4	2	2
Average 7 day compressive strength (MPa)	35.3 (±1.2)	n/a	n/a	n/a	n/a	n/a	n/a
Average 28 day compressive strength (MPa)	49.0 (±0.5)	40.5 (±2.6)	49.8 (±1.0)	39.3 (±1.3)	46.5 (±2.8)	54.3 (±3.9)	69.5 (±0.7)

Additives that were tested include the cement replacement materials, pulverised fuel ash (PFA) and ground granulated blast furnace slag (GGBS) at replacement levels of 35% (by weight). The same replacement level was chosen for both so that a direct comparison could be made between each when assessing their potential to reduce the leaching of metal ions from the ISF slag and their effect on the delay in the concrete setting process. The presence of these cement replacement materials appeared to worsen rather than improve the set retardation experienced with the ISF slag.

Other additives utilised included sodium hydroxide (NaOH) and potassium nitrate (KNO_3), which were used to increase the alkali content of mixes to 7.0 kg/m^3 Na_2O_{eq}, from the 1.8 kg/m^3 Na_2O_{eq} provided by the cement, during ASR testing. NaOH reduced the demouldable age to 1 day, while KNO_3 prolonged the retardation to 4 days. Further testing to investigate this phenomenon was carried out on a smaller scale using ICC, which is discussed in section 8.5.

Relatively small (4.5 litre) concrete mixes were also made that incorporated various additives that had been shown by ICC to be useful in overcoming the retardation in set caused by the ISF slag. No strength or workability measurements were taken for these mixes. They were solely used for temperature monitoring the concrete in insulated cube moulds. These mixes were of the same design as that given in the first data column of Table 5.2, with the additive quantities shown in Table 5.3. The 'high' and 'low' addition levels refer to those described in an earlier section (3.6.4), for the isothermal conduction calorimetry work.

Table 5.3: Additives used in concrete for temperature monitoring experiments

Additive	Low addition (g/l)	High addition (g/l)
$CaCl_2$		110.53
$CaNO_3.4H_2O$	73.03	232.89
$BaCl_2.2H_2O$	76.32	
$MgCl_2.6H_2O$		201.32
$MgNO_3.6H_2O$		253.95
KOH		55.26

Despite the delay in setting that was experienced with mixes containing the ISF slag, they gave compressive strength results approximately equivalent to, if not greater than those of a comparable control mix, shown in Table 5.1. Only the mixes containing PFA and NaOH give lower compressive strength results than the control at 28 days of age, which gave an average result of 41.5 MPa (±0.1). PFA is known to provide improved late strength at the expense of early strength, which may account for the decrease witnessed here[14,15]. It has been shown that NaOH, although it can accelerate the concrete setting reaction, may cause a reduction in strength development in concrete, which appears to be confirmed by these results[142].

A significant point to note regarding the 28 day strength of the ISF slag mixes is that the hydration reaction must effectively 'catch up' with the point at which the majority of the compressive strength is achieved in the control concrete, despite the delay experienced with the ISF slag mixes over the first few days. There is uncertainty as to why the ISF slag mixes provide additional concrete strength. It is possible that it is a result of pozzolanic activity due to the glassy nature of the aggregate.

As would be expected, mixes containing the ISF slag had a higher wet density than those that did not. This is because the slag itself is a more dense material than traditional

aggregates used in concrete. This property may be useful in some concrete applications, such as noise barriers for instance.

The slump measurement of the majority of mixes containing the ISF slag falls outside the specified target range of 30-60mm. From observations made when working with these mixes, it is apparent that they have a very fine tolerance for water – mixes often appear quite dry, however any excess water will bleed from the mix if too much is present. ISF slag mixes therefore often lacked the cohesion that would normally be expected from a mix designed with a 30-60mm target slump. Despite this, adequate samples could be cast with the assistance of a vibration table to achieve good compaction of the concrete. Improved workability was achieved when PFA was used as a cement replacement material in ISF slag concrete. The spherical particle shape and fineness of PFA improves the particle packing of the materials in the mix and it is often used to improve mix workability in applications where the water content must remain low to assure high concrete strength[14,15].

5.2 CRT glass concrete mixes

The standard CRT glass mix that was designed for this work used a cement content of 300 kg/m^3, with a w/c of 0.60. All CRT glass mixes, irrespective of any additives they contained, were of the same overall cementitious material content and w/c ratio. Details of these mixes are given in Table 5.4.

Table 5.4: Concrete mixes containing CRT glass as fine aggregate

Mix name	CRT glass	CRT + $LiOH.H_2O$	CRT + $LiNO_3$	CRT + PFA (high)	CRT + PFA (normal)	CRT + GGBS (high)	CRT + GGBS (normal)
Relative density of replacement aggregate (Mg/m^3)	2.9	2.9	2.9	2.9	2.9	2.9	2.9
Cement content (kg/m^3)	300	300	300	195	225	150	180
Cement replacement materials **or** other additives (kg/m^3)	-	2 $LiOH.H_2O$	11 $LiNO_3$	105 PFA	75 PFA	150 GGBS	120 GGBS
Coarse aggregate: 20-5mm (SSD weight, kg/m^3)	1150	1150	1150	1150	1150	1150	1150
Replacement fine aggregate: 5-0mm (SSD weight, kg/m^3)	770	770	770	770	770	770	770
Free water/ cement ratio	0.6	0.6	0.6	0.6	0.6	0.6	0.6
Wet density of mix (kg/m^3)	2460	2430	2440	2460	2450	2430	2450
Measured slump of mix (mm)	25	35	50	60	35	40	30
Demouldable age (days)	1	1	1	1	1	1	1
Average 7 day compressive strength (MPa)	37.7 (±1.3)	42.7 (±1.1)	45.2 (±0.6)	31.5 (±0.9)	n/a	32.3 (±1.0)	n/a
Average 28 day compressive strength (MPa)	48.8 (±0.8)	53.5 (±2.6)	54.7 (±1.4)	41.7 (±0.6)	43.8 (±2.0)	47.0 (±0.9)	45.8 (±0.6)

PFA and GGBS were again used in mixes with the CRT glass. These were included at addition levels specified in BRE Digest 330[51] for the minimisation of ASR with both 'normal' and 'high' reactivity aggregates. The 'normal' replacement levels were 25% PFA and 40% GGBS, while the 'high' replacement levels were 35% PFA and 50% GGBS. The lithium compounds, lithium hydroxide monohydrate ($LiOH.H_2O$) and lithium nitrate ($LiNO_3$) were also used as additives to minimise ASR with CRT glass, according to the BRE Information paper, IP1/02[72]. The levels chosen were those to mitigate ASR with 'high' reactivity UK aggregate materials. The hydroxide was added to the mix water at 1.30 kg per kg of Na_2O_{eq} provided by the cement, while the nitrate was added as a 30% solution at 5.95 kg per kg Na_2O_{eq} provided by the cement. (4.15 kg mix water was removed per kg Na_2O_{eq} of nitrate solution added to compensate for the nitrate being a 30% solution). The Na_2O_{eq} provided by the cement in these mixes was calculated to be 1.8 kg/m^3.

The CRT glass mixes also show increased compressive strength results after 28 days when compared to the control. Again, concrete mixes containing PFA show little evidence of the improvement, though the strength might be expected to improve relative to the control at later ages. The CRT glass is finer in grading than the TVS control aggregate that it replaces. This could potentially lead to better particle packing and therefore improved strength characteristics when the CRT glass concrete is compared to the control.

The slump measurements generally fall within the target range of 30-60mm, apart from the CRT glass mix with no additives, which had a slump of just 25mm. Overall, the strength and workability characteristics for concrete mixes containing the CRT glass were satisfactory and in accordance with the targets set.

5.2.1 Contamination of CRT glass with Al and Zn and its implications

After initial work was carried out on the CRT glass in the early stages of this project, the supplier changed their process for reclaiming materials from CRTs, resulting in a finer grading of glass. Although this finer grading appeared to offer improved concrete workability characteristics compared to the original, slightly coarser grade of glass, problems were experienced due to additional contamination of the glass with aluminium and zinc metal. This had apparently occurred during the new processing/ crushing technique. An SEM image showing the presence of a shard of aluminium was shown earlier in Figure 4.14.

Powdered aluminium metal (and sometimes powdered zinc) are utilised as gas forming admixtures in the production of aerated concrete. For example, aluminium reacts with the calcium hydroxide that forms during cement hydration, producing tricalcium aluminate hydrate (hydrogarnet) (and other calcium aluminate hydrates) and hydrogen gas, according to the following equation:

$$2Al + 3Ca(OH)_2 + 6H_2O \rightarrow 3CaO.Al_2O_3.6H_2O + 3H_2$$

When zinc is used, calcium zincate and hydrogen are formed. The hydrogen produced in each case is quickly replaced by air[11,143,144]. The aluminates formed from this kind of reaction should be equivalent to those formed during the cement hydration process, thus are assumed to contribute to the concrete strength and hardening in the same way.

Due to the presence of aluminium and zinc in the CRT glass, this gas expulsion phenomenon caused concrete samples containing the new grade of CRT glass to rise out of their moulds slightly as hydrogen gas tried to escape from the concrete. Attempts were made to remove the metal shards by passing the glass through a 2.36mm sieve. However, smaller fragments of the metals must still have remained, as the same observations were made, but to a lesser extent. Previous studies[145] on the use of incinerator bottom ash in concrete report a similar phenomenon, caused by the presence of metallic aluminium. The ash was treated by immersing it in a solution of sodium hydroxide for 15 days until all hydrogen had been produced and expelled. Such a treatment was not chosen for the CRT glass used for this project as there was concern that the hydroxide solution would degrade the glass prior to testing.

The main concern with respect to this testing was that an unreasonable reduction in compressive strength would be brought about by the presence of additional porosity in the concrete/ mortar, as a result of the escaping gas. Consequently, in order for acceptable samples to be cast to test the general suitability of the CRT glass as aggregate, the casting process was altered slightly. Samples were shaken on a vibrating table for approximately 1 minute, every 30 minutes, for 2 hours, in an attempt to expel any gas that was evolved within the wet concrete due to the reaction of the aluminium and zinc. During this time, the samples were topped up with further concrete as the gas was displaced, so that the sample moulds could be levelled.

CRT concrete samples that had undergone this additional treatment did not expand in the same way as previously seen and the compressive strength results were improved. It is accepted that this method would not completely overcome the problems experienced and that some additional porosity would remain in the structure of the hardened concrete due to the reaction gases. However, the samples were seen to be adequate to test the glass for its ASR susceptibility and leaching behaviour.

5.3 Concrete mixes summary

The ISF slag and CRT glass have been successfully incorporated into concrete mixes as 100% fine aggregate, providing strength and workability characteristics comparable to a control concrete mix. A new batch of CRT glass from the supplier was found to be contaminated with shards of aluminium and zinc metal, which caused the concrete to rise from its moulds due to gas expulsion from the mix. This problem was overcome by slightly amending the mix method used. There has been no evidence to suggest that the presence of any residual aluminium metal in the mix would directly affect the durability of the concrete, particularly with respect to ASR. Various additives have also been incorporated into concrete mixes containing the secondary aggregate materials in an attempt to overcome the anticipated problems of ASR with the aggregates and delayed setting with the ISF slag.

6 Alkali-silica reaction

6.1 80°C testing of aggregates

Expansion measurements were taken from mortar prisms containing the secondary aggregate materials at set intervals over a 14 day period. Only the 14 day results are quoted in Figure 6.1. Two grades of CRT glass were tested. Both were classed as 5-0mm aggregate, although one was towards the finer end of this limit (F) and the other towards the coarser boundary (C). The actual grading results were given in Table 4.1. The behaviour of the two grades is compared on the graph below. A bottle glass sample (BGL) of the same grading as the finer CRT glass was tested using the same cement as the CRT samples (alkali content = 0.59% Na_2O_{eq}) as well as a cement with a higher alkali content of 1.43% Na_2O_{eq}. Only the results of the latter are included in Figure 6.1 for clarity.

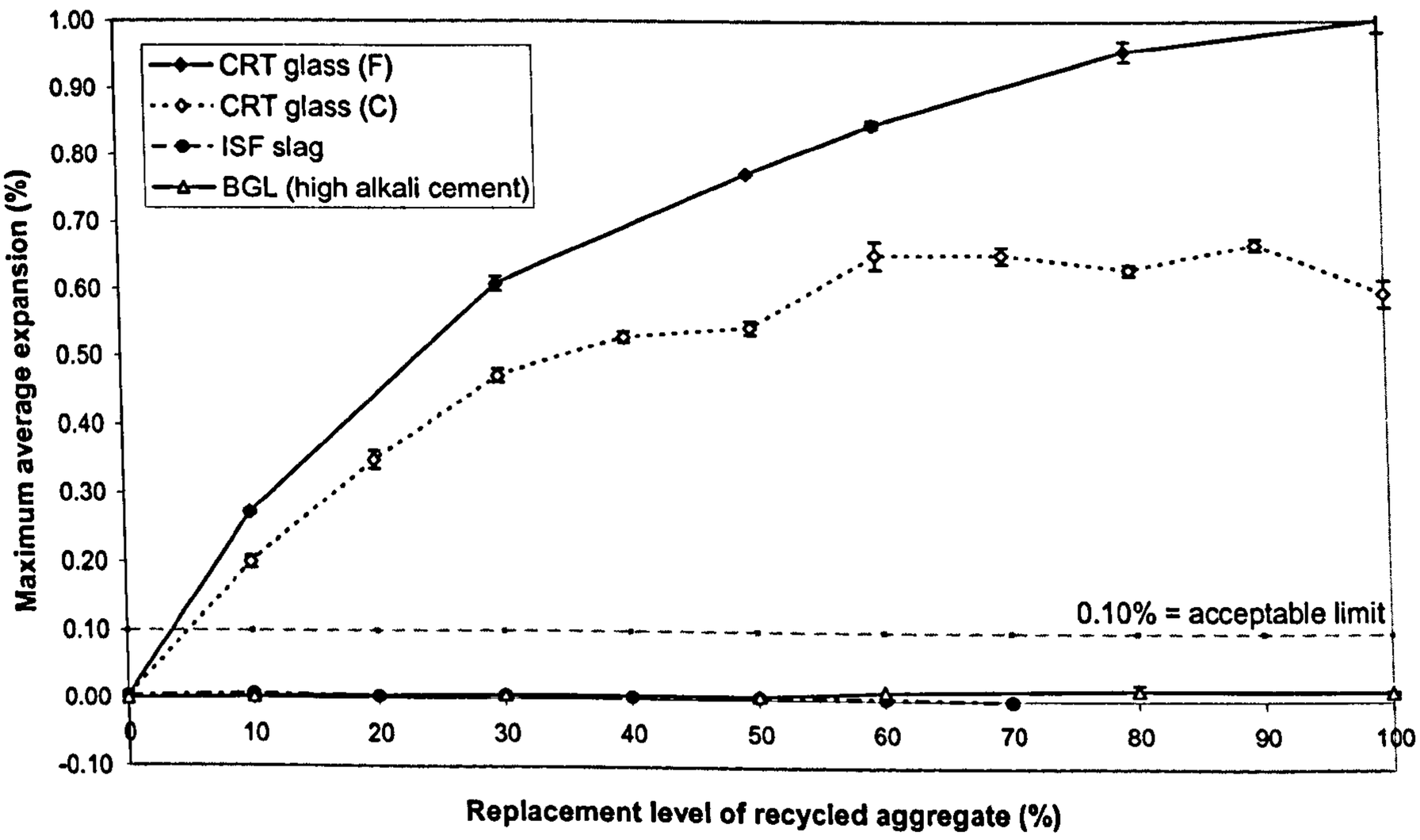

Figure 6.1: Accelerated ASR mortar bar testing at 80°C over a range of replacement levels

In Figure 6.1, the ISF slag shows virtually no expansion over the course of the experiment, suggesting that it is not susceptible to ASR. It has been established that 0.10% expansion in this test represents the maximum acceptable expansion for an aggregate to be considered non-reactive with respect to ASR[86]. The CRT glass exceeds this value even at replacement levels of only 10%, with the extent of the expansion increasing up to 100%. This indicates that there is no pessimum replacement level for

the CRT glass and that the extent of the reaction is proportional to the level of replacement. Although these observations indicate that the CRT glass undergoes an expansive reaction in the presence of alkali solutions, a petrographic examination was necessary to confirm that the expansion witnessed was truly a result of ASR.

In light of the high expansion results witnessed with the CRT glass, the lack of expansion seen with crushed bottle glass of the same grading was surprising. Use of the higher alkali cement with the bottle glass only caused a minor increase in expansion compared to the cement used in the other tests. Other workers have shown expansion of bottle glass caused by ASR when tested by this 80°C test and other various expansion techniques[63]. However, samples were tested for 140 days instead of the 14 days usual to this method. Expansion of bottle glass samples were less than the recommended limits (and of a similar order to the results of this work) up to 14 days, so it would appear to pass the limiting criteria. When tested for longer, samples expanded significantly after approximately 28 days up to ~1.7%, or ~2.3%, depending on the exact sample used. The same glass also showed minimal expansion in 38°C tests. The authors concluded that this 80°C test may not be suitable to assess ASR with glass aggregates[146].

6.1.1 Microscopy on thin sections from 80°C ASR testing

Optical microscopic examination of thin sections of mortar samples from this testing confirmed that no ASR gel was present in samples containing the ISF slag. In Figure 6.2, the ISF slag appears as black inclusions throughout the surrounding cement paste. The figure also shows a relatively large limestone particle with many inclusions to the bottom right of the image (highlighted with a dotted line). There is no evidence of cracking and no areas that have been filled with fluorescent yellow resin during the thin section preparation method, suggesting that the mortar is intact and has not suffered any degradation from ASR.

However, the degree of internal cracking within the CRT glass-containing mortar samples increased as the percentage replacement of CRT glass increased. In the most severe case, at replacement levels of 100%, cracks were observed to run across the entire cross-section of the sample.

There were many sites from which expansive cracks appeared to originate. These sites were generally found to be in smaller glass aggregate particles as opposed to the larger particles, suggesting that ASR occurs preferentially in particles with a larger surface area to volume ratio. This was confirmed by the finer grade of CRT glass resulting in higher mortar bar expansions than the coarser grade of glass. Similar conclusions have been drawn by other workers[147]. Finer particles react more quickly than coarser particles, thus below a certain particle size a point is reached where they are so fine that their reaction occurs and is completed before the concrete/ mortar is able to harden, thus behaving as a pozzolan and contributing to the strength of the set product, as described earlier in section 2.4.2.

The petrographic image given in Figure 6.3 shows the presence of desiccated ASR gel (A) lining the cracks that have formed within a single CRT glass particle (B) from the 'coarse' 100% CRT glass mortar sample (C). In places, the surrounding regions are also stained with gel, which masks the colouring normally seen in the cement matrix. These

observations were common throughout the CRT glass mortar samples and have led to the conclusion that the CRT glass is susceptible to ASR. This supports the expansion results that were obtained from the accelerated testing of mortar bars.

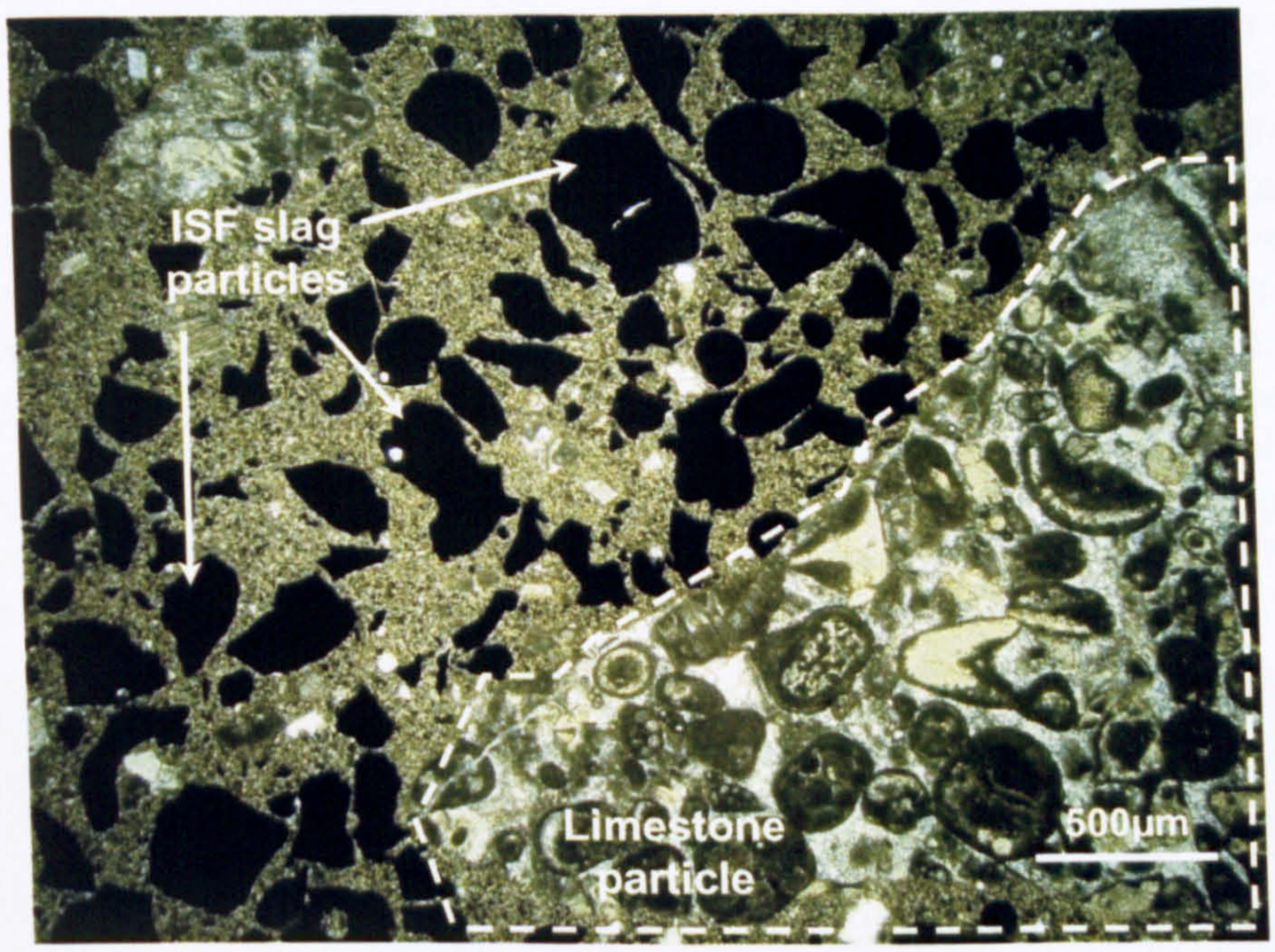

Figure 6.2: 70%(vol) ISF slag mortar sample viewed using plain polarised light

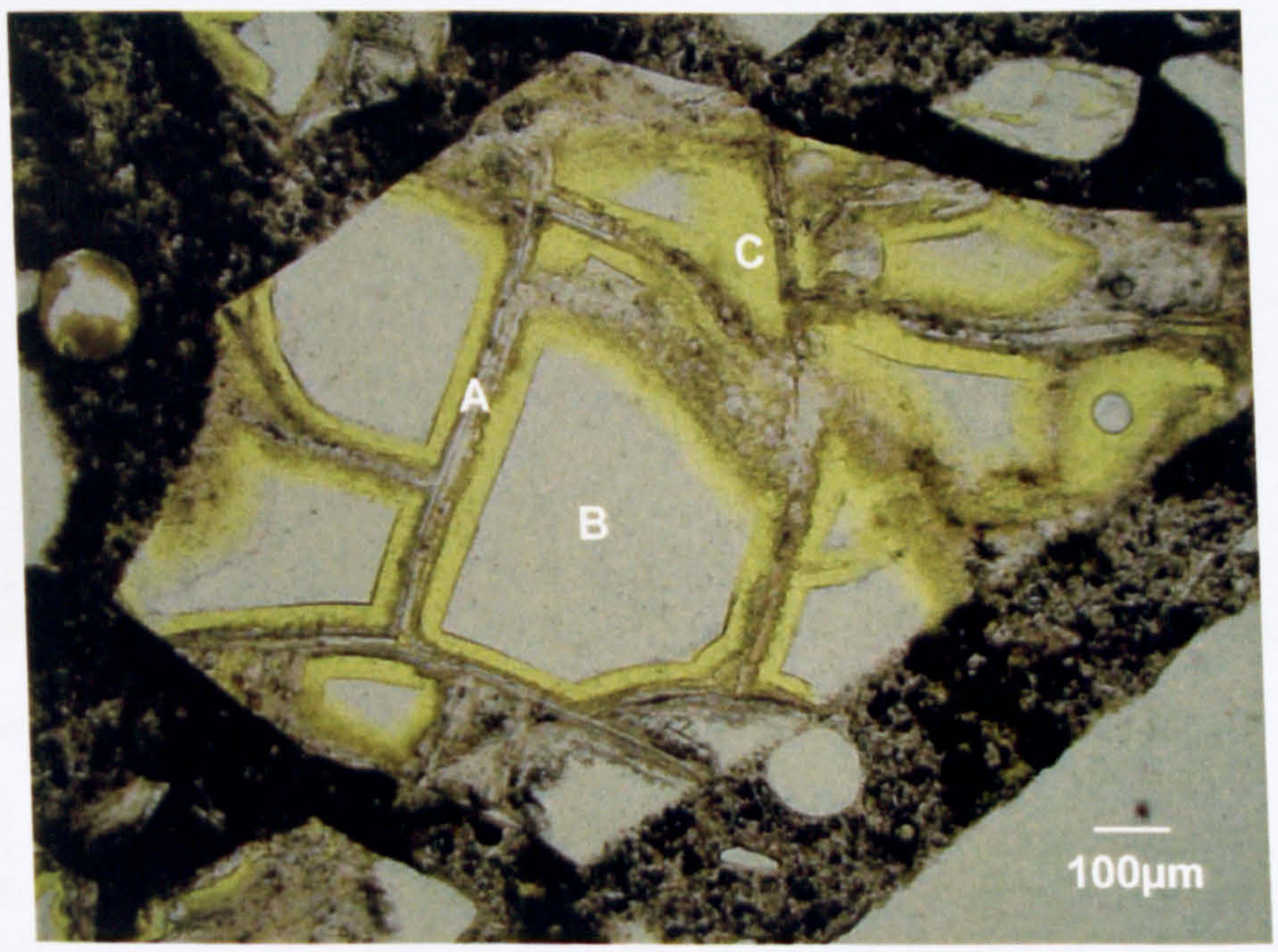

Figure 6.3: Section through 100% CRT glass mortar sample, showing expansive cracks lined with ASR gel, viewed with plain polarised light.
Key: A = ASR gel, B = CRT glass particle, C = fluorescent resin

Further analysis was carried out on mortar samples containing the replacement aggregate materials using SEM and EDS analysis. This provided additional information to that obtained during petrographic analysis. As mentioned in an earlier section (4.4.2), it was apparent that two different types of glass were present within the CRT glass aggregate. These appeared as different coloured fractions when examined using a backscattered electron image, which can be seen in Figure 6.4. EDS analysis showed that the fractions that appeared lighter in colour (D) contained lead, whereas those that appeared greyer in colour (E) contained barium. Lead has a higher average atomic number than barium, so appears brighter and lighter in colour when viewed using backscattered electrons. The evidence of two distinctly different types of glass was not particularly surprising, since lead is often found in the tube of a CRT and barium or strontium containing glass tends to be more recently used for the plate/ screen of the CRT[26,27]. This glass sample apparently contained glass from all sections of a CRT. Interconnected cracking was observed to run throughout the sample, passing through both leaded glass and barium glass fractions. These cracks were generally filled with desiccated ASR gel and occasionally the impregnating resin.

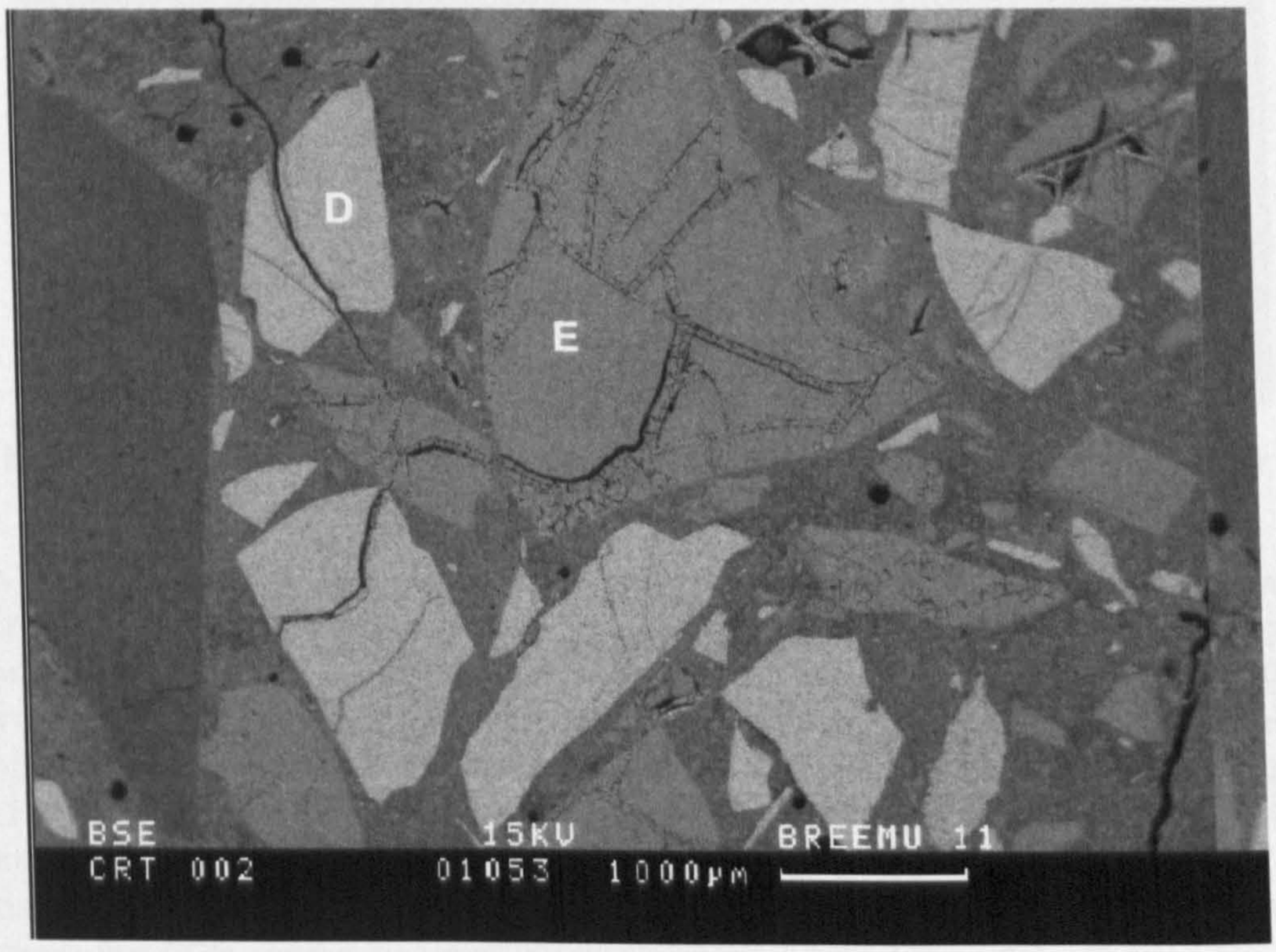

Figure 6.4: Backscattered electron image of section through 100% CRT glass mortar sample, showing the presence of two different types of glass. D = lead glass, E = barium glass

When a 100% BGL mortar sample was analysed microscopically for comparison with the CRT glass samples, very little evidence of cracking or areas that had filled with the fluorescent resin were observed. Areas of possible ASR attack were mainly located at the edges of the mortar sample, suggesting that the direct exposure to the surrounding NaOH solution during the 80°C test had made the edge regions most susceptible to attack. For this reason, further BGL mortar samples were cast using a cement of a higher total alkali content, to see if this increased the extent of the ASR damage within

the bulk of the sample. Although the increased alkali content did cause a higher average expansion of the BGL mortar samples overall, the expansion was still significantly less than that witnessed with the CRT glass in Figure 6.1 and the regions of ASR attack were still near the edge of the samples, as shown by the SEM image in Figure 6.5.

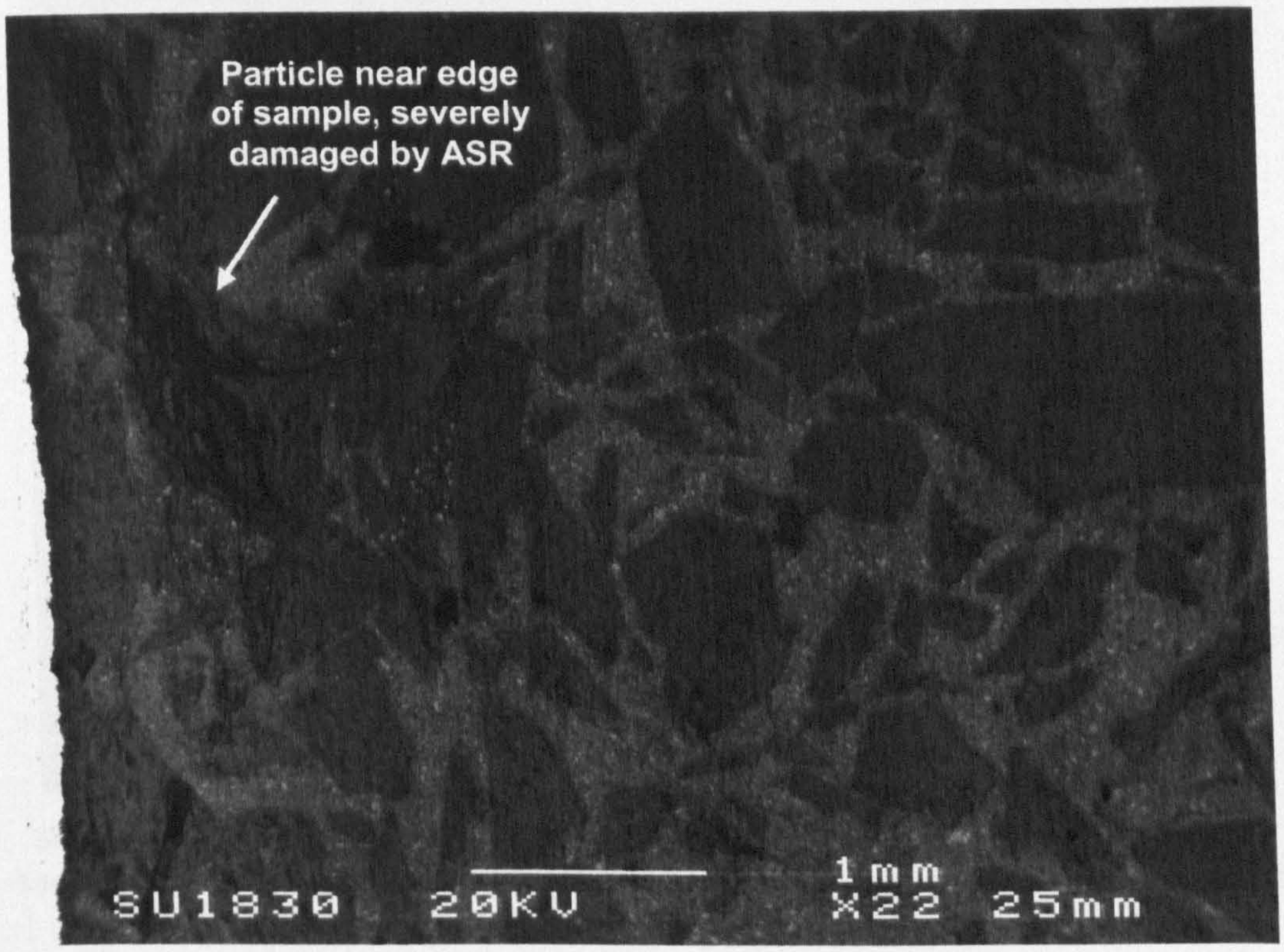

Figure 6.5: Secondary electron image of section through 100% BGL mortar sample, showing ASR damaged particles near sample edges

With closer inspection, ASR gel could be detected within the cracked regions, shown in Figure 6.6 as the brighter, flecked regions (F), surrounding the smoother glass particles (G). EDS analysis showed the gel to contain silicon and calcium in a ratio of approximately 0.8:1 (Figure 6.7) whereas EDS on gels within an equivalent CRT mortar sample contained relatively less calcium than silicon, at a Si:Ca ratio of approximately 1.6:1 (Figure 6.8). As mentioned in section 2.4.3, the presence of calcium in ASR gel makes it harder and less likely to take in water and expand, thus making it less damaging to the surrounding concrete. The EDS results presented here suggest that the gel from the BGL sample contains relatively more calcium than the gel from the CRT glass, which may account for the bottle glass samples being less expansive during ASR testing.

It was interesting to note that the gel within the CRT glass particles, when analysed by EDS, often showed the presence of lead. This must have been released when the leaded glass particles were attacked as a result of ASR, as no lead was otherwise apparent in the surrounding hardened concrete. Lead was also detected in the gel present within fractions of the barium glass, suggesting that it was mobile in the gel phase and capable of movement throughout the structure. Leach testing was therefore carried out on ASR damaged CRT-concrete samples to assess whether ASR was likely to compound any leaching issues. This is reported in a later section (7.6).

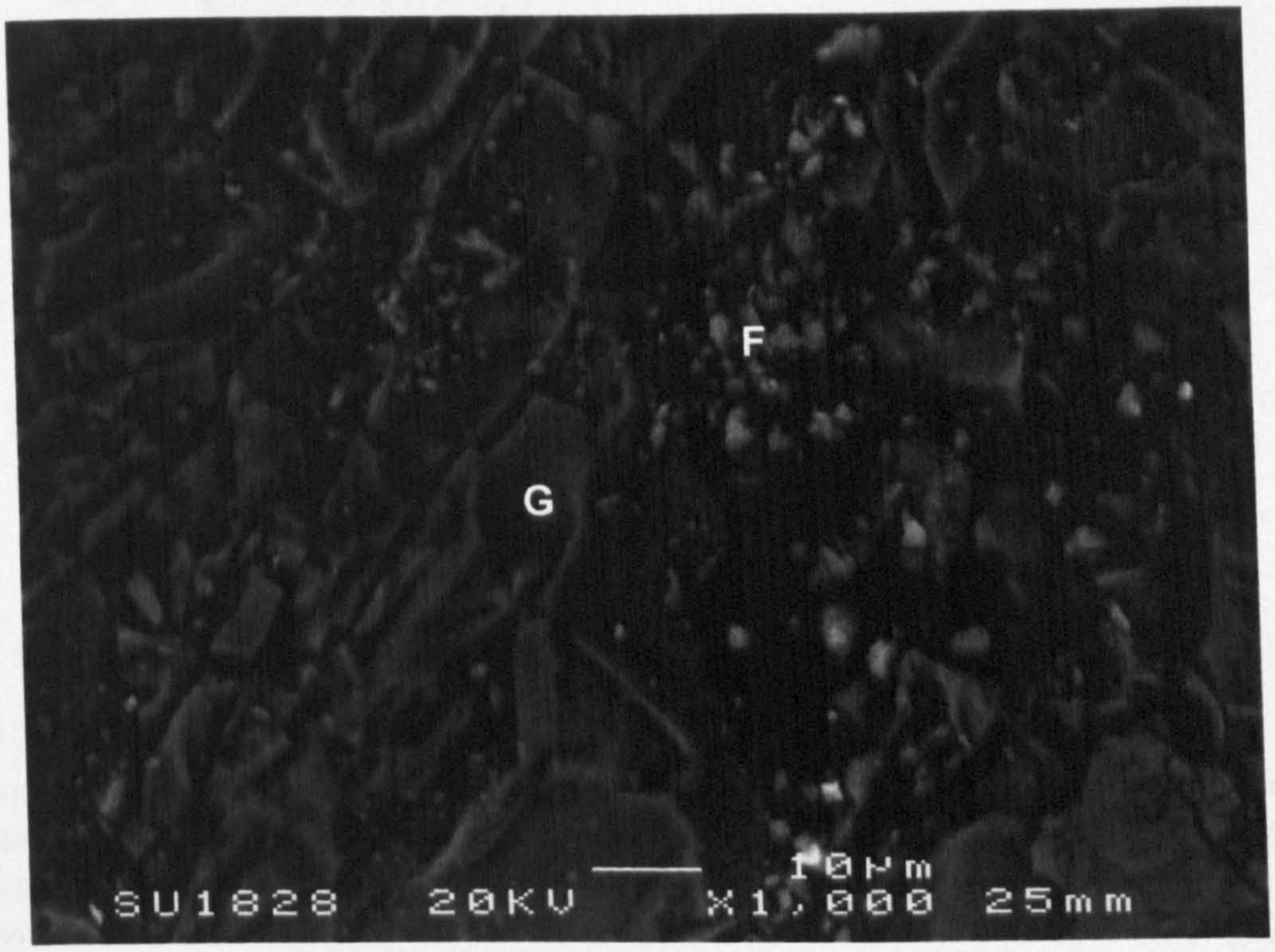

Figure 6.6: Secondary electron image of section through 100% BGL mortar sample, showing ASR gel as bright flecks (F) within cracked glass particle (G)

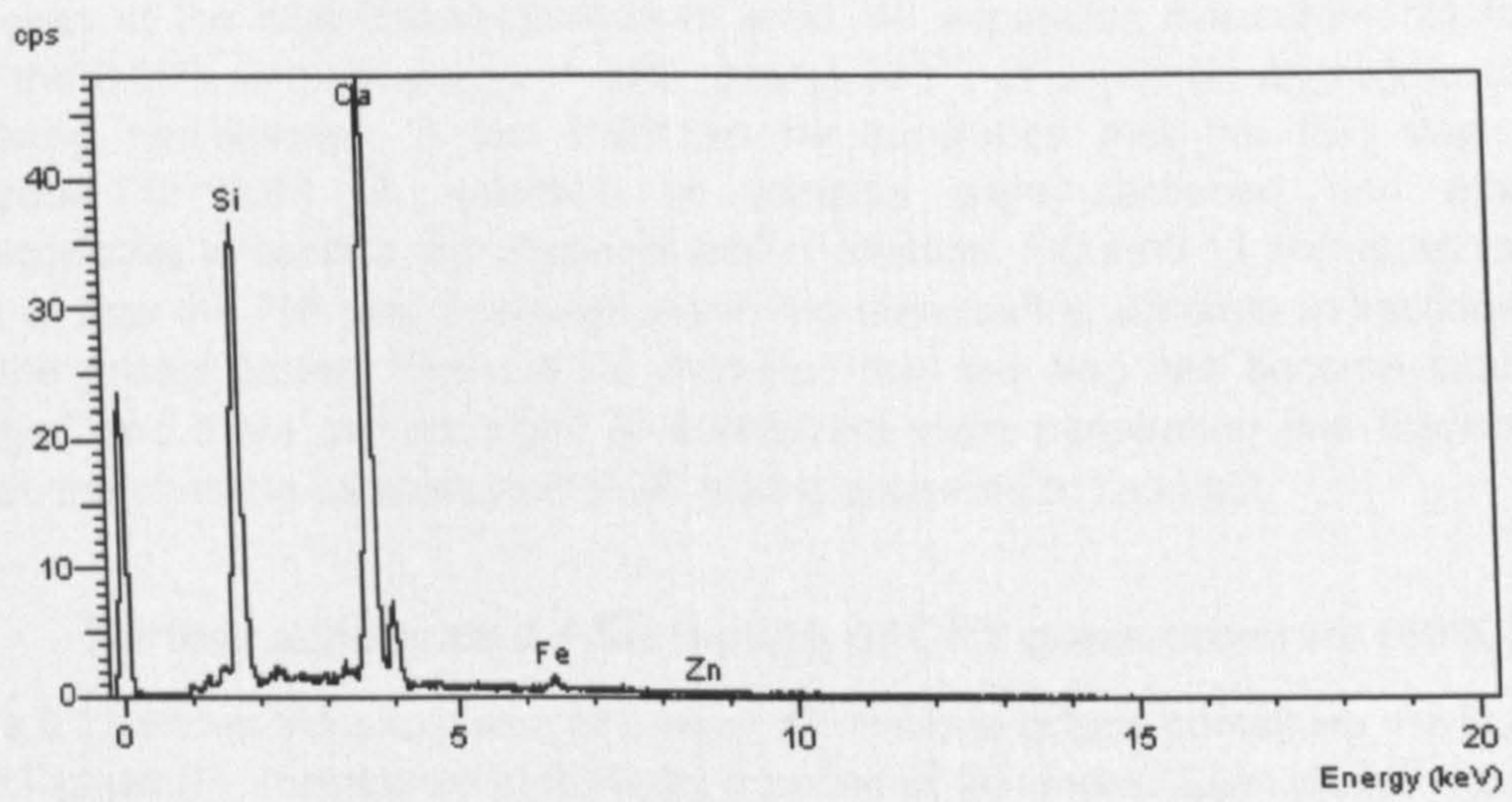

Figure 6.7: EDS analysis of ASR gel within 100% BGL mortar sample

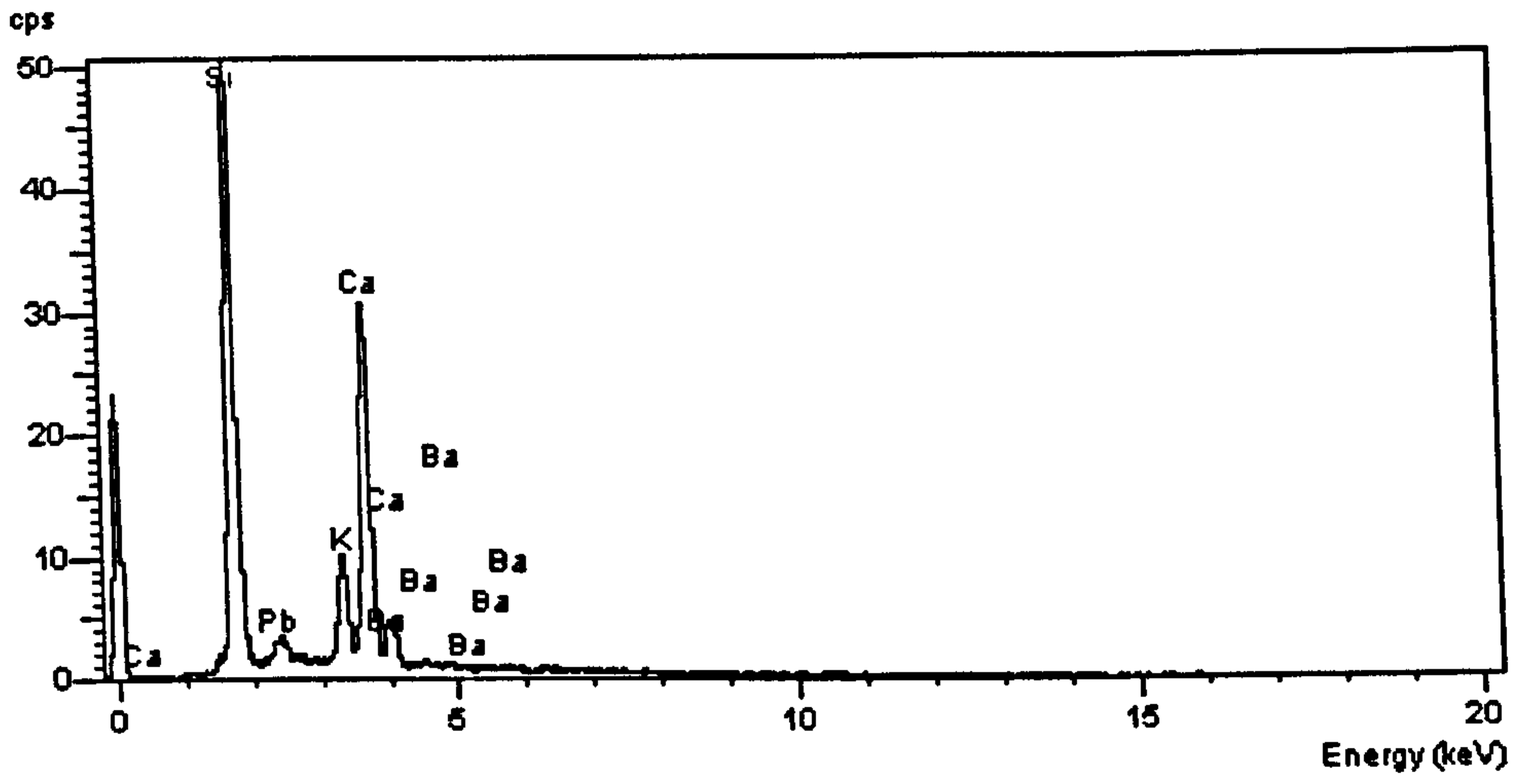

Figure 6.8: EDS analysis of ASR gel within 100% CRT mortar sample

6.2 Further accelerated ASR testing of ISF slag concrete

Figure 6.9 shows the expansion behaviour of concrete prisms containing ISF slag, maintained at 60°C for a period of 20 weeks, while Figure 6.10 shows the equivalent results from ISF slag prisms stored at 38°C for 78 weeks (1.5 years). Each plotted value is an average of measurements taken from 3 samples, with error bars showing the standard deviation between readings.

In both cases, there do not appear to be signs of any deleterious expansion caused by ASR, even at the high spiked-alkali level used. All expansion measurements fall well below the 0.05% limit proposed in BRE Digest 330[51], at which an aggregate may be considered non-reactive. It can therefore be concluded that the ISF slag is not susceptible to ASR. A selection of samples were sectioned and examined microscopically to confirm this apparent lack of reaction. Figure 6.11 shows an example image of how the ISF slag appeared within the surrounding concrete in sections taken from the prisms tested. There is no evidence that the slag has become cracked or damaged and there are no signs of fluorescent resin penetrating into the concrete. Overall, the concrete samples from ASR testing appeared to be intact.

6.3 Further accelerated ASR testing of CRT glass concrete (60°C)

Figure 6.12 shows the expansion behaviour of concrete prisms containing the fine grade of CRT glass (F), maintained at 60°C for a period of 20 weeks. Each plotted value is an average of measurements taken from 3 samples, with error bars showing the standard deviation between readings. The 60°C results from CRT glass alone are compared with those using mitigation techniques at 'high' reactivity addition levels, as specified in BRE Digest 330[51] and the BRE Information Paper, IP1/02[72]. It can be seen that the concrete mix containing no ASR mitigation additives expanded significantly, compared to those that did. Figure 6.13 shows the same results displayed with a different scale, to better compare the differences in expansion measurements of mixes containing the various mitigation techniques. Also included is a comparable BGL sample.

All additives used at doses recommended for mitigation of ASR with high reactivity UK aggregate materials successfully reduce expansion below the limit of 0.05% given in BRE Digest 330[51] for 38°C testing and used here for guidance. The BGL sample again shows negligible expansion at 60°C. The reasons for this were discussed earlier (6.1).

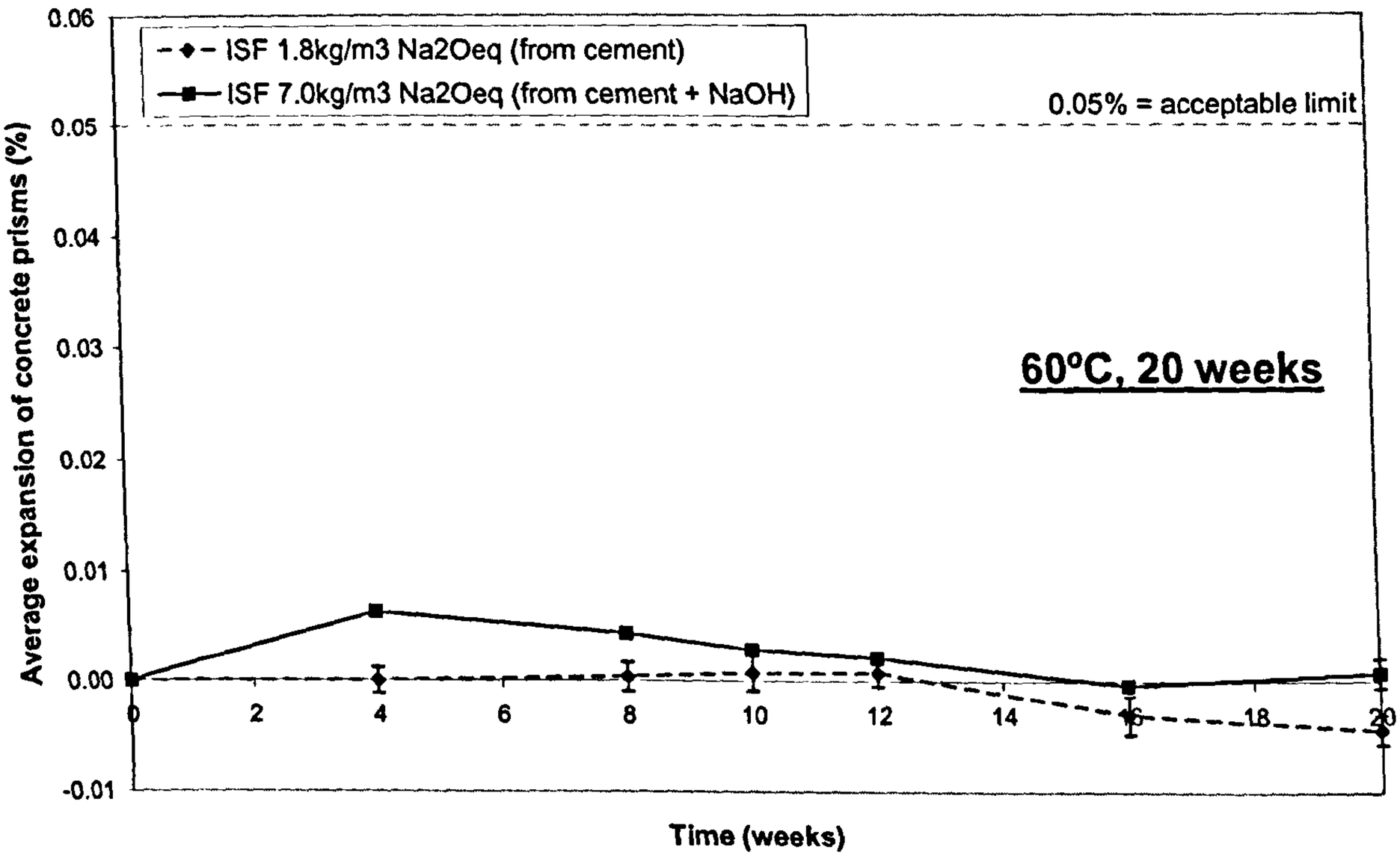

Figure 6.9: Accelerated ASR testing of ISF slag prisms at 60°C for 20 weeks

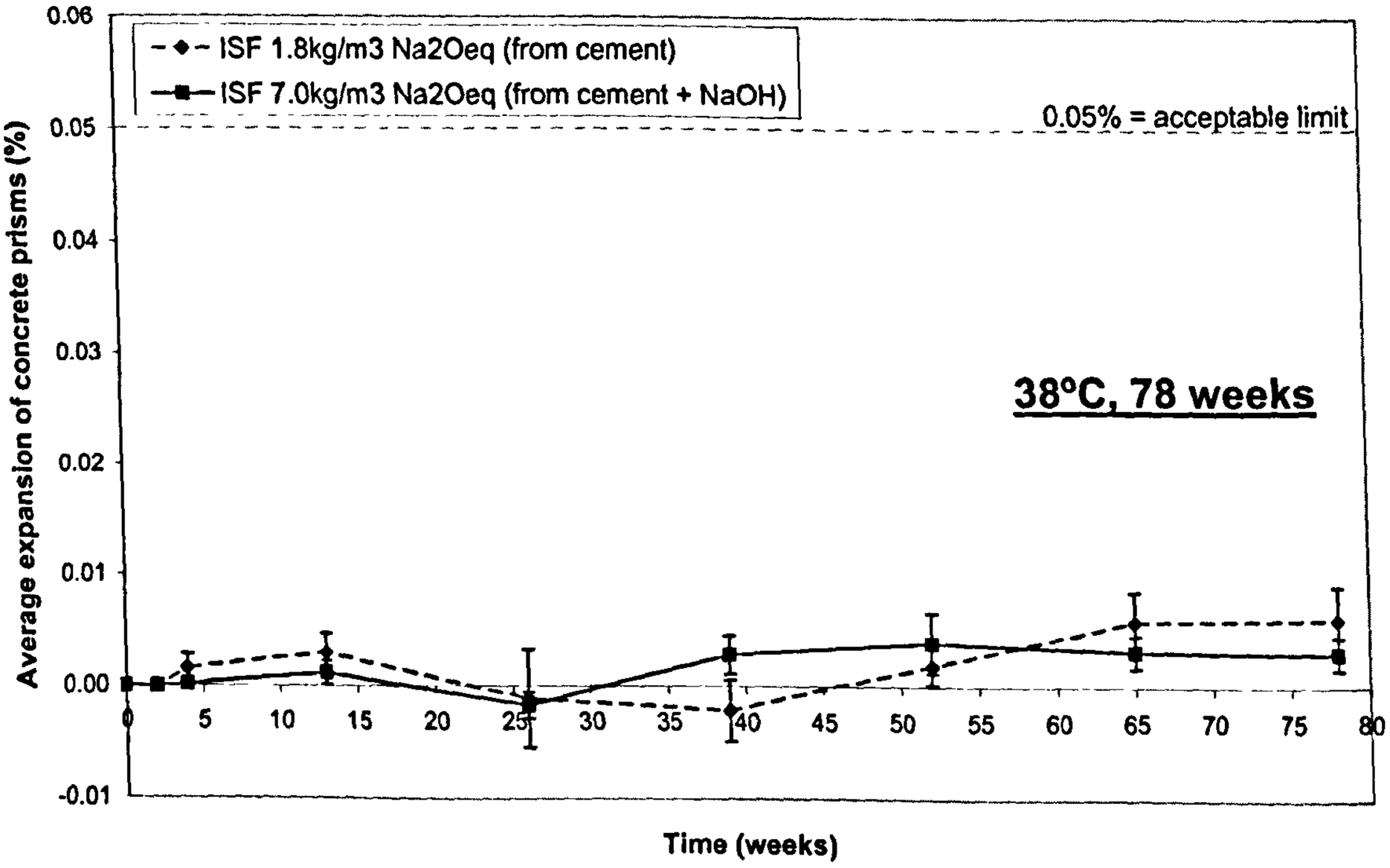

Figure 6.10: Accelerated ASR testing of ISF slag prisms at 38°C for 78 weeks

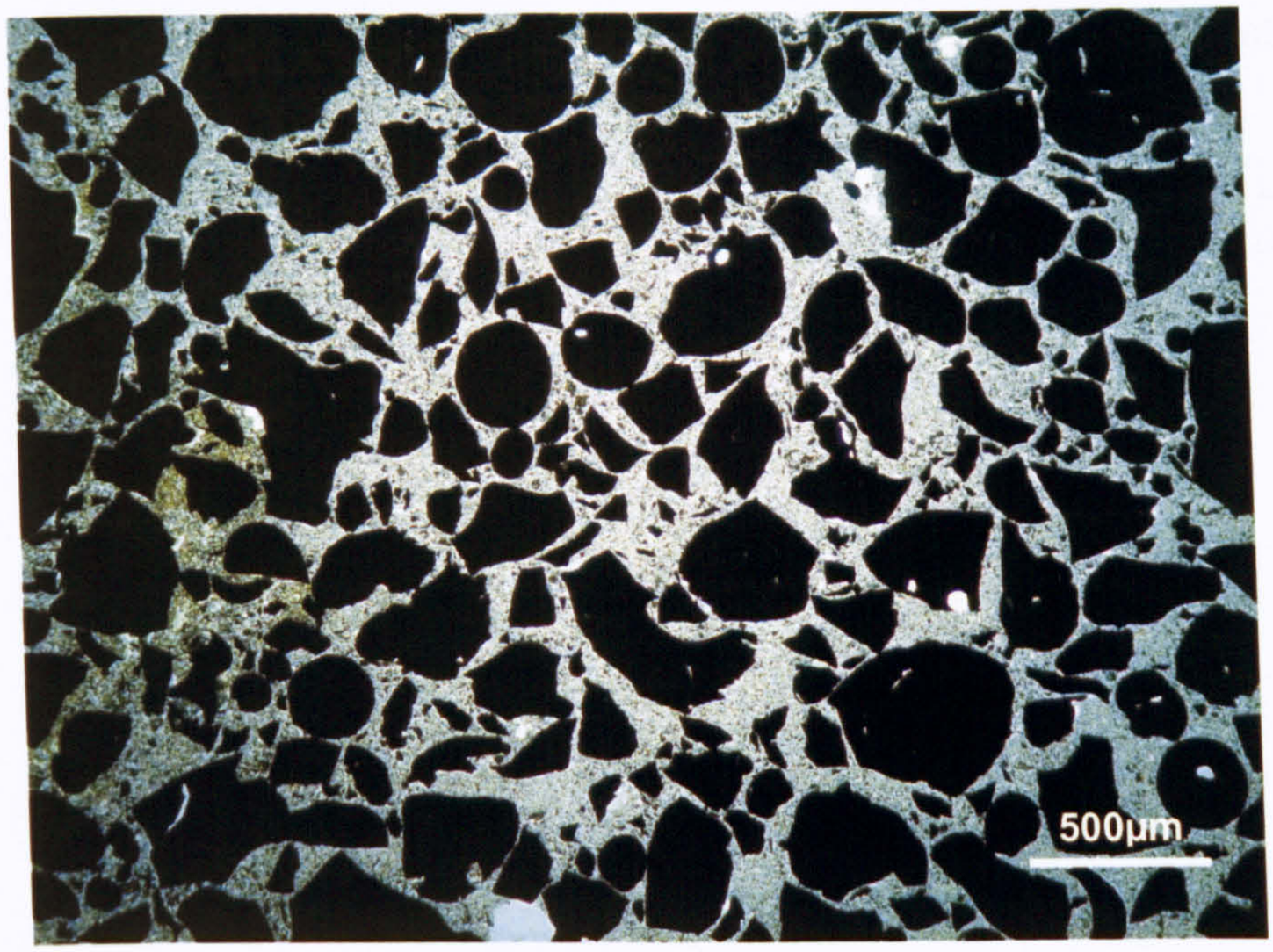

Figure 6.11: ISF slag concrete sample (1.8 kg/m^3 Na_2O_{eq}, from 60ºC testing) viewed using plain polarised light. Image shows no cracking or degradation of the ISF aggregate

However, samples containing PFA additions were showing signs of a possible slow reaction and those containing GGBS appeared to be approaching the limit, particularly when the error bars showing the standard deviation between results were considered. The large standard deviation shown on the last value for GGBS was caused by one of the three expansion results being notably lower than the other two. If this result were not considered, the average would actually equal the limit of 0.05%.

Microscopic examination of the samples showed evidence of ASR damage, confirming that the expansion seen was indeed a result of ASR. Figure 6.14 shows a section through a CRT glass-concrete prism containing a high level PFA addition as an example. Several glass particles show signs of cracking (H), although the cracks are quite fine and the glass has generally not become so damaged that the fluorescent resin has been able to fill many of the cracks. The image also shows several air voids that have become filled with resin (J). These residual voids remain within the concrete from the gas expulsion caused by contamination of the CRT glass sample with shards of aluminium and zinc metal, as discussed in section 5.2.1. Concrete sections containing the CRT glass with GGBS were observed to be similar, with occasional evidence of finely cracked glass particles.

Further samples were cast using 'normal' rather than 'high' PFA and GGBS addition levels in association with the CRT glass. Figure 6.15 compares these results to the high levels shown in the previous figures. It can be seen that CRT mixes using normal addition levels of PFA and GGBS have clearly exceeded the limit value used – GGBS more so than PFA. This indicates that the results seen late in the testing with the high addition levels are likely to be a result of the early stages of ASR, suggesting that the

use of PFA and GGBS to control ASR with this aggregate would not be satisfactory under the current UK guidance for high reactivity aggregates.

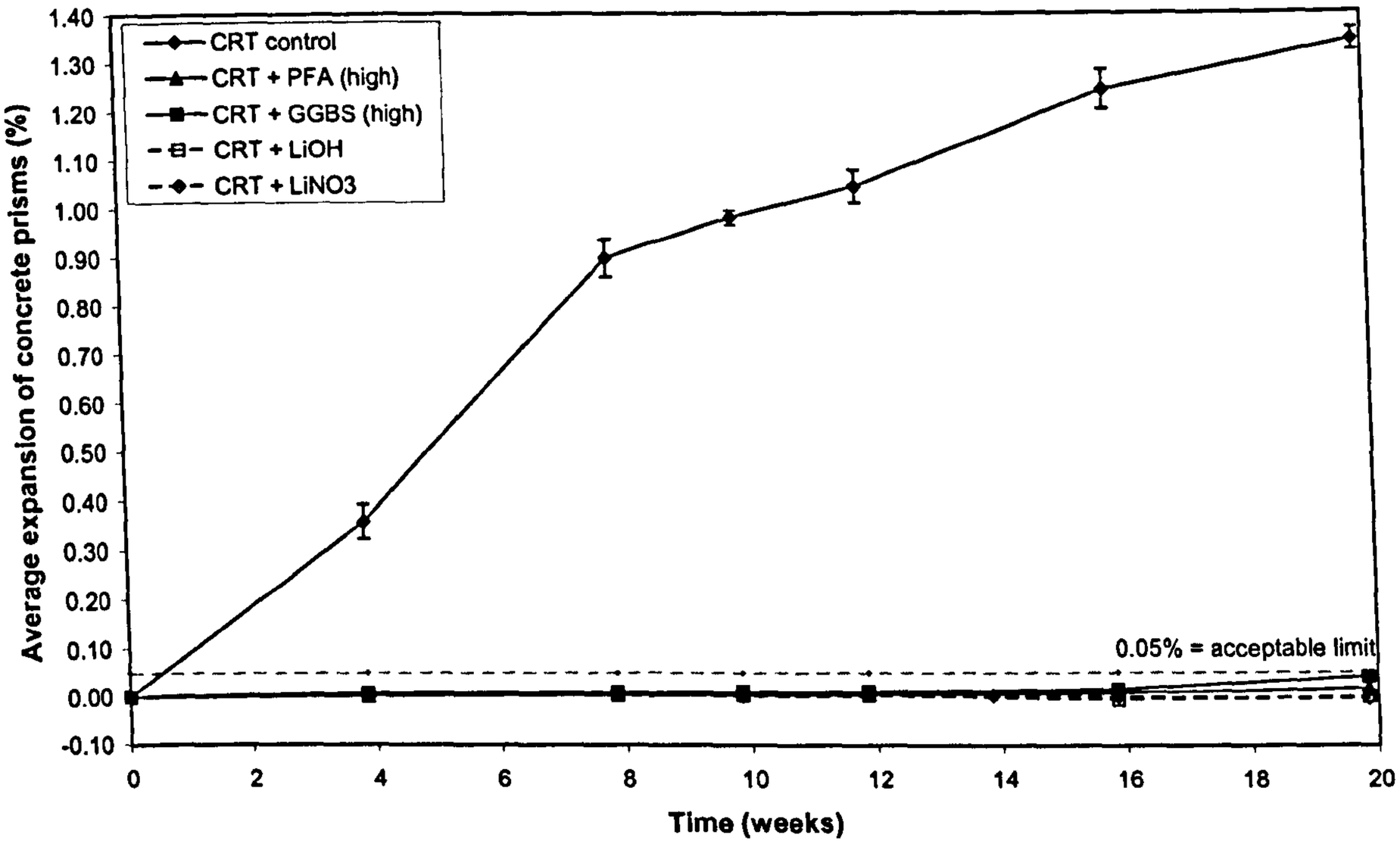

Figure 6.12: Accelerated ASR testing of CRT glass prisms at 60°C

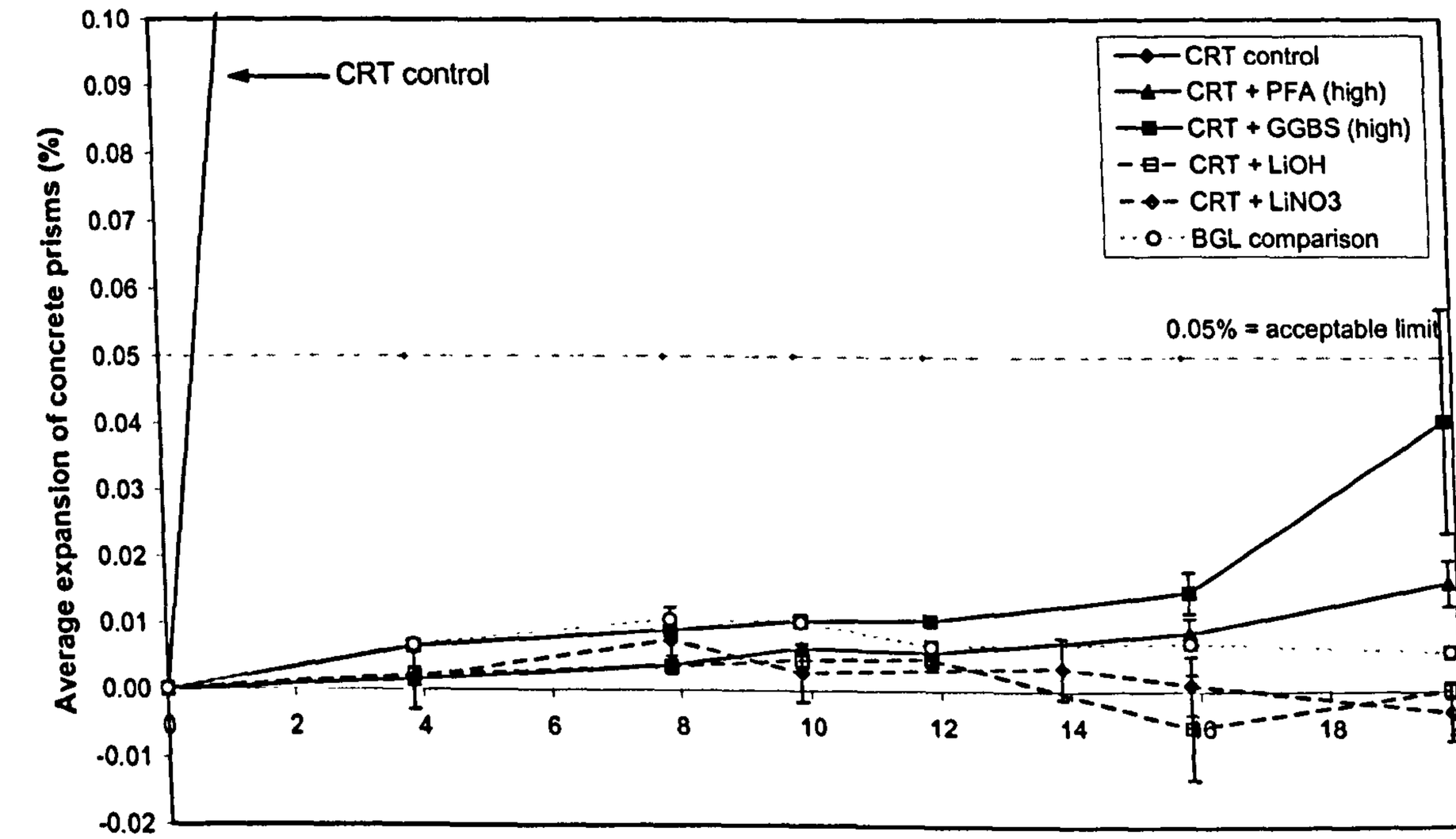

Figure 6.13: Accelerated ASR testing of CRT glass prisms at 60°C (increased scale)

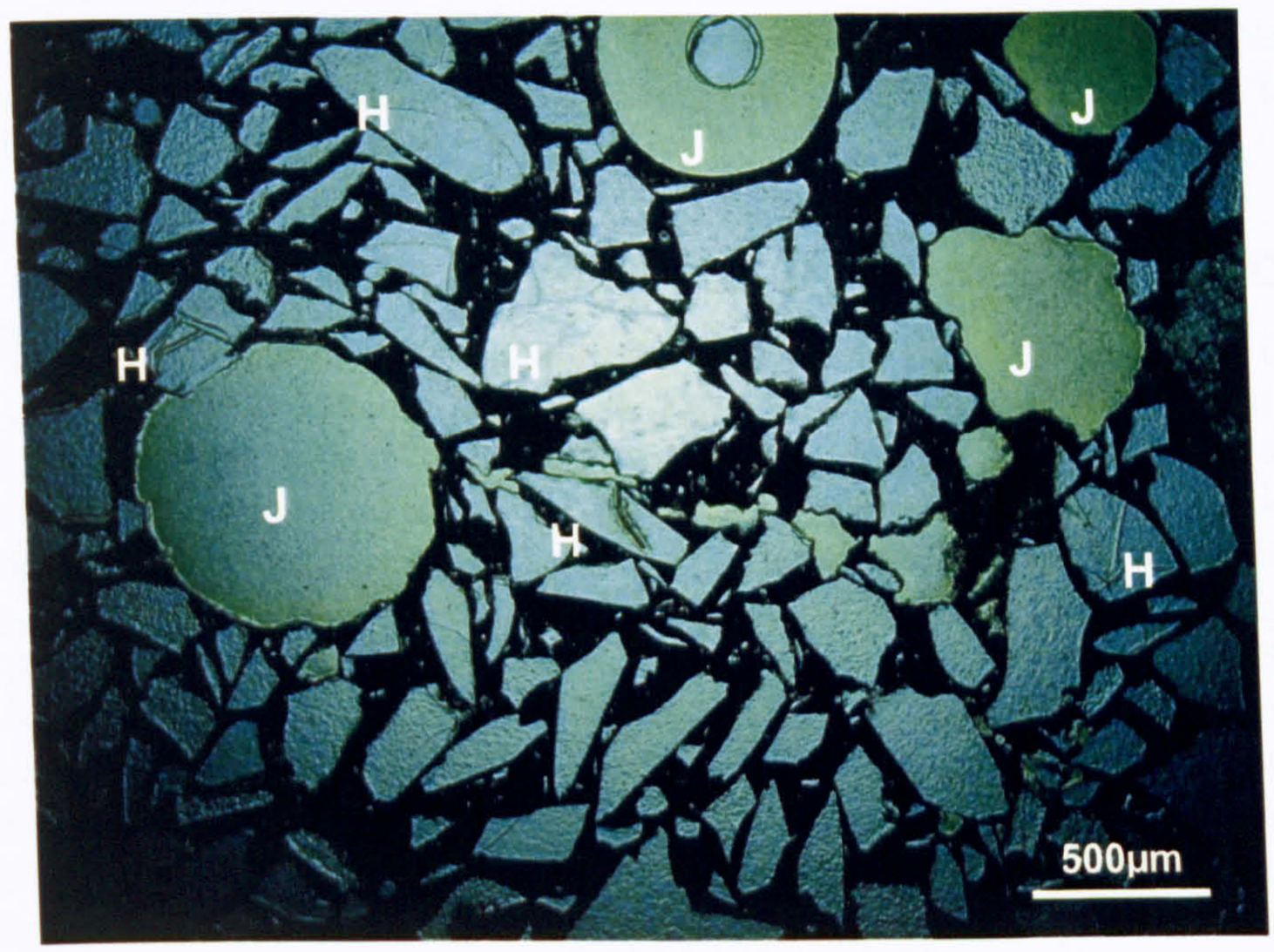

Figure 6.14: CRT glass-concrete sample with PFA (high) from 60°C testing, viewed using plain polarised light. Image shows occasional particles with cracking (H) and resin filled air voids remaining from reaction of contaminant metals (J)

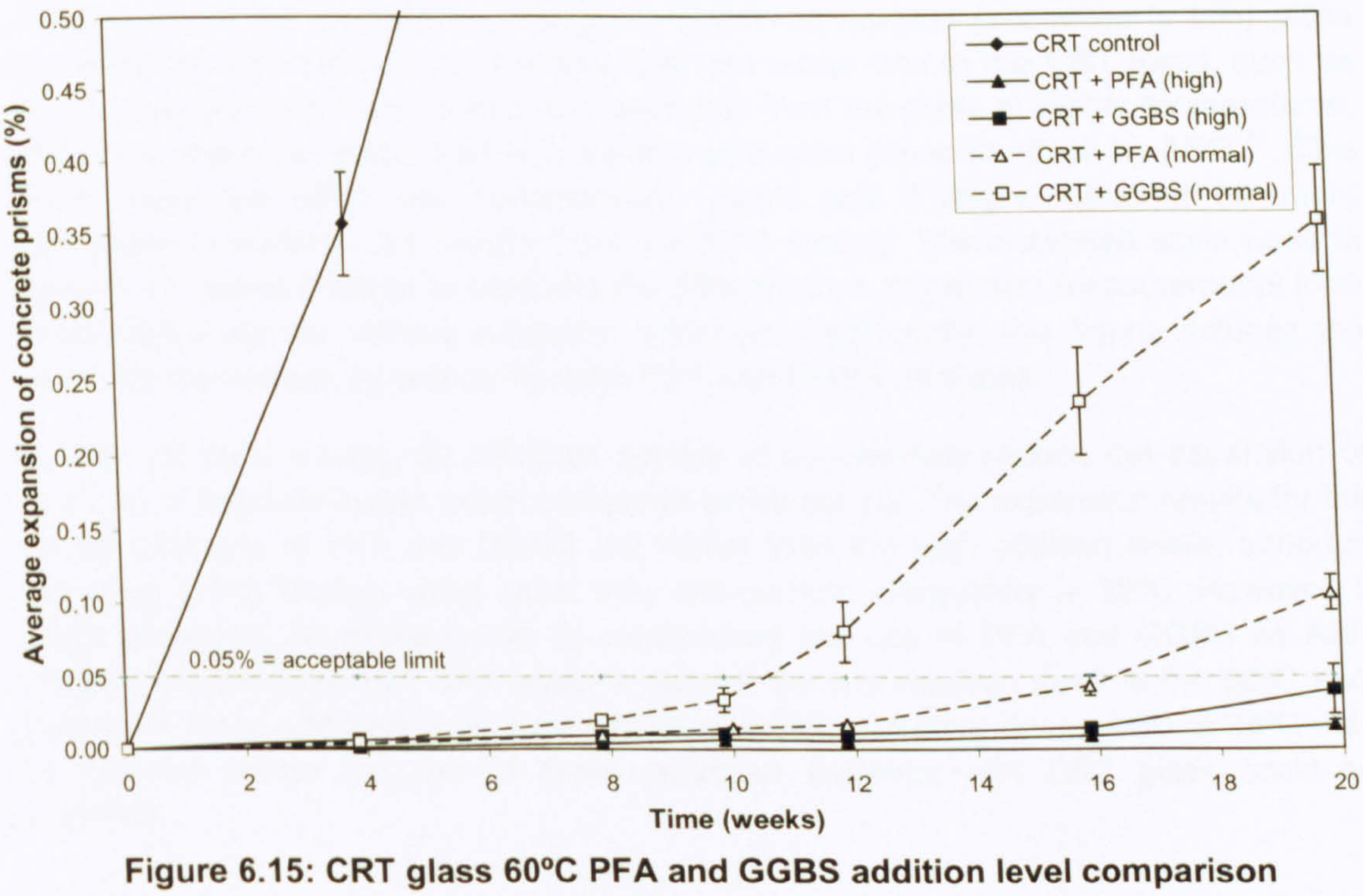

Figure 6.15: CRT glass 60°C PFA and GGBS addition level comparison

The lithium compounds tested seem to be most suitable at minimising the potential expansion caused by ASR with CRT glass. Both the nitrate and the hydroxide appear to provide similar protection to the concrete over the course of the 60°C testing. Assuming the effectiveness of the two chemicals is equivalent, it may be seen as preferable to use the nitrate rather than the hydroxide in practice, as it is less caustic than the hydroxide and so has fewer handling issues associated with it[72]. Also, the addition of further

hydroxide to the concrete is likely to cause an increase in the pH of the concrete's pore water, which may in turn lead to increased leaching of lead and barium ions from the glass, which would be undesirable. (See section 7.4).

6.4 Further accelerated ASR testing of CRT glass concrete (38°C)

Figure 6.16 shows the expansion behaviour of concrete prisms containing the fine CRT glass (F), maintained at 38°C for a period of 78 weeks (1.5 years). Each plotted value is an average of measurements taken from 3 samples, with error bars showing the standard deviation between readings. Since many of the lines appear to overlap, the data is also displayed using an increased scale in Figure 6.17. Although the concrete mix containing CRT glass with no mitigation additives expands significantly, it does not do so to the same extent as equivalent samples that were subject to 60°C testing. Since the degree of expansion does not appear to be levelling off at all after 1.5 years, but instead increasing at a relatively consistent rate up to ~0.60% expansion, it is apparent that this test at 38°C is not as severe, even over the longer time period, as the 60°C test. In time, the samples stored at 38°C may reach similar expansion levels to those that were attained in the 60°C test in just 20 weeks (approximately 1.35% expansion). If that were the case, it could potentially be concluded that the 60°C test is ultra-accelerated compared to more realistic, lower temperature conditions.

However, there is concern that increasing the temperature to as high as 60°C might provide enough thermodynamic energy for additional reaction processes to take place that might not otherwise occur. For example, the metal ions in the CRT glass, such as barium, may become more mobile and leachable from the glass at higher temperatures, which may make the glass itself less durable and more prone to attack by ASR[141]. This would make the 60°C test unrealistically harsh and it might therefore be more appropriate to consider the results from the 38°C testing. The increased scale used in Figure 6.17 makes it easier to compare the differences in expansion measurements from mixes containing the various mitigation additives. Additionally, this figure includes the results for the normal, as well as the high PFA and GGBS additions.

As with the 60°C testing, all additives appear to successfully reduce the expansion of prisms to acceptable levels, when compared to the control. The expansion results for the normal additions of PFA and GGBS are higher than the high addition levels, although according to the limiting value used, they still perform adequately at 38°C. However, it would potentially be irresponsible to recommend the use of PFA and GGBS as ASR mitigation techniques with CRT glass in light of the late reaction seen in the 60°C test. Testing of these additives over a (potentially significant) further time period at 38°C may be required before the use of these particular additives with CRT glass could be specified.

6.5 ASR summary

The ISF slag did not suffer damage as a result of ASR during accelerated testing, even when elevated alkali levels were used. This was confirmed by microscopic examination. This would suggest that ISF slag is not susceptible to ASR. However, the CRT glass

appears to be highly susceptible to ASR, increasing in the severity of attack as glass replacement levels reach 100%. Surprisingly, the BGL did not suffer such expansion.

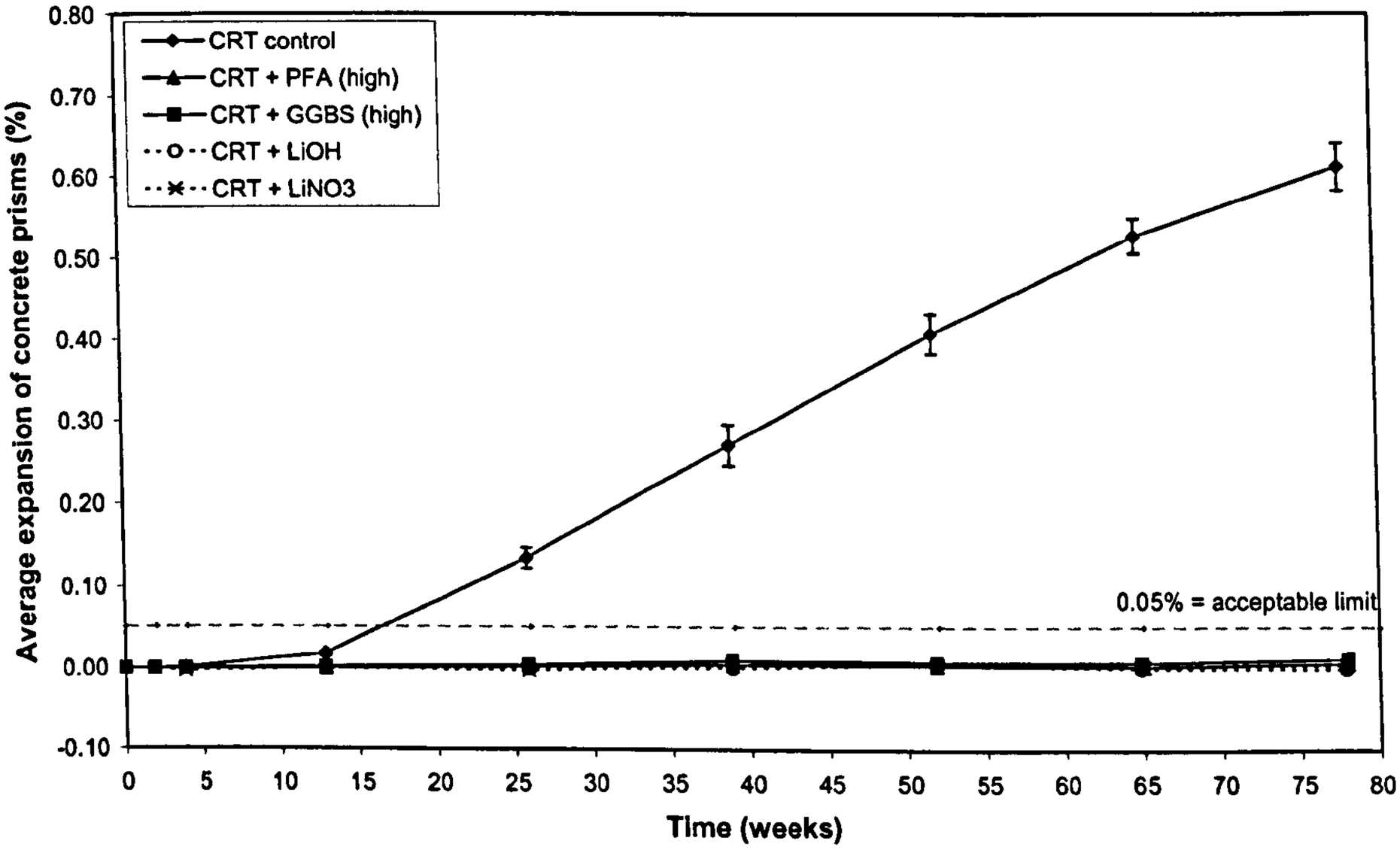

Figure 6.16: Accelerated ASR testing of CRT glass prisms at 38°C

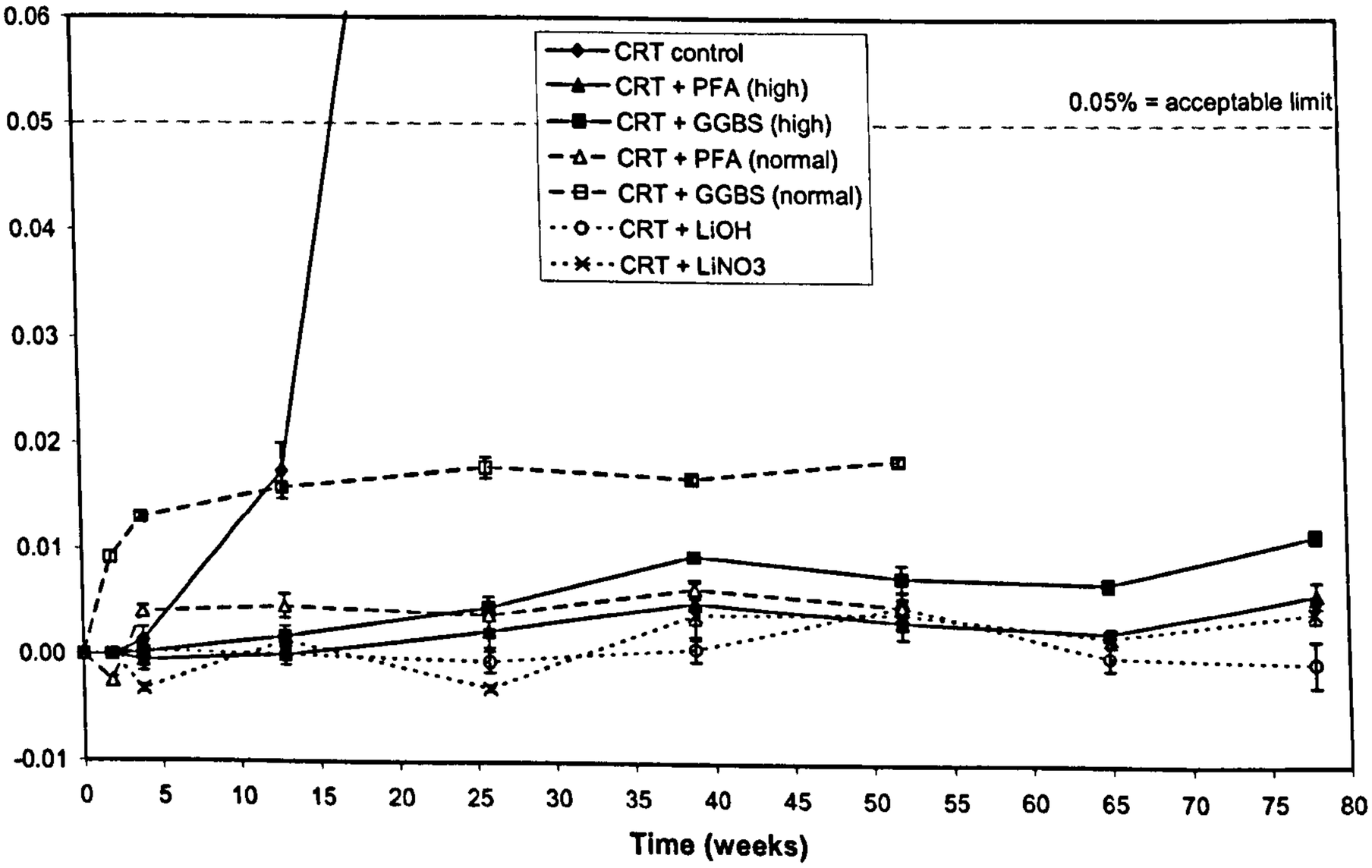

Figure 6.17: Accelerated ASR testing of CRT glass prisms at 38°C (increased scale)

Other studies suggest that the BGL may have shown increased reaction if tested over a longer period of time. The CaO content of the BGL, as mentioned earlier, may have improved the durability of the glass in the short term, making it less susceptible to ASR than CRT.

Despite the CRT being highly reactive, the expansion can be controlled/ minimised by the inclusion of various established mitigation additives. The lithium compounds, lithium hydroxide monohydrate and lithium nitrate, used at levels recommended for high reactivity aggregates, seem to be most effective at minimising ASR with the CRT glass. This work has also shown that accelerated ASR testing at 60°C may be proportionally more severe than the equivalent 38°C testing that is carried out over a longer time period.

7 Leaching of metal ions

7.1 Tank-style monolithic leach test

100mm concrete cubes, containing either ISF slag or CRT glass, that were subject to mild agitation in the tank leaching test showed no evidence of leaching of lead, zinc or barium. All results fell below the detection limit of 0.1 mg/l, suggesting that neither material poses any risk if the concrete in which it is contained remains intact. However, consideration must be given to the leaching behaviour if the concrete were damaged, leaving exposed ISF slag or CRT glass surfaces, or if the material were to be crushed and reused in another application.

7.2 Tumble-style leach testing

As well as the tank-style leaching that was carried out on concrete cubes containing the ISF slag and CRT glass, additional tumble-style leach testing was carried out on both the aggregate materials alone and crushed concrete containing the replacement aggregates. The aggregates themselves were tested using both deionised water and a pH 13 buffer solution as the leachate, whereas the crushed concrete samples were leached only in deionised water, allowing them to dictate their own pH.

The average pH of the various test solutions and the standard deviation of the results obtained are summarised in Table 7.1. The deionised water (DI) used for the testing initially had an average pH of 6.5. The final pH of the water increased when the aggregates were leached. However, the pH of the samples leached in the pH 13 buffer solution were largely unaffected, due to the buffering action. When PFA and GGBS were tested with the aggregates, they appeared to further influence the resultant pH of the solution. Since the average pH of the PFA samples in deionised water was between that of the ISF slag and CRT glass without PFA, the resulting pH must be dictated by the PFA itself. Similarly, the GGBS must dictate the pH in deionised water. In the pH buffer solution, the PFA and GGBS marginally reduce the average pH of the buffer. This apparently contradictory behaviour in deionised water and the high alkali buffer solution suggests the PFA and GGBS must have some buffering capacity of their own – releasing alkali at low pH but adsorbing it at high pH. The average pH of the solutions obtained from the crushed concrete samples in deionised water was 12.3. The pH must have been elevated by alkali ions contributed from the cement.

Although the pH of the solution will obviously influence the leaching characteristics of the materials being tested, the action of the high alkali buffer was a useful means of standardising the leaching that would be expected in a concrete environment. In the results that follow, unless otherwise noted, any other variations in pH that were experienced have been thought not to significantly influence the leaching trends witnessed.

	Average pH	Standard Deviation
Deionised water control	6.5	0.20
ISF slag in DI	9.1	0.45
CRT glass in DI	7.0	0.86
BGL in DI	9.8	0.46
ISF/CRT + PFA in DI	8.6	0.39
ISF/CRT + GGBS in DI	10.3	0.13
pH 13 buffer solutions	13.0	0.18
ISF/CRT + PFA in buffer	12.7	0.05
ISF/CRT + GGBS in buffer	12.8	0.11
Crushed concrete samples in DI	12.3	0.34

Table 7.1: Summary of the resultant pH from the various leach test solutions

Leaching results are often expressed according to the surface area over which the ions have been released, e.g. mg/cm^2. This is practical when a regular shape with measurable surface dimensions is tested, such as a cube or cylinder of material. However, when a material is crushed or granular in nature, the absolute surface area is not easily calculated. In such circumstances, it is necessary to express the leaching of ions according to the mass of sample from which they are released, e.g. mg/kg. In order to provide a degree of standardisation to such results, the material must be of a specific grading before it can be tested.

In this study, granular materials (the secondary aggregates) were sieved to pass a 4mm sieve and crushed concrete was graded between >5<10mm, in accordance with the standard test method used[106]. Consequently, leach testing of the aggregates alone may be more severe than the testing of crushed concrete, as a larger surface area will have been available for leaching. However, the presence of cement around the aggregate in the crushed concrete samples would obviously influence the available aggregate surface area for leaching – this is one of the main advantages of encapsulation in concrete.

Since the effectiveness of the encapsulation methods was one of the primary interests of this leaching study, variations in the surface area of the test samples has not been considered of primary importance here. It is acknowledged that the surface area of a material would have an influence on leaching and the compromises made here highlight the difficulties faced when comparing materials by current leaching standards.

All leach testing results discussed in the following sections were obtained from tumble-style leach testing. Leaching of minor ions and those that were found not to be of great influence during the study have been qualitatively summarised here.

7.2.1 Leaching of arsenic

A selection of both aggregate alone and concrete samples were analysed for arsenic. In all cases results obtained fell below the detection limits of the equipment (<0.1 mg/l)[l]. Given that CRT glass does not appear to contain arsenic (see Table 4.5), this is as

[l] **NB:** The actual minimum detection limit of the equipment was 0.1 mg/l. The calculation made on the results to give units of mg/kg of sample mean that the minimum leaching result obtainable is 1.0 mg/kg

expected. It was anticipated that arsenic leaching may have been an issue with the ISF slag, however it can be concluded from the results obtained that the ISF slag is not likely to pose an environmental risk as a result of arsenic leaching.

7.2.2 Leaching of sodium and potassium

Many of the leaching results obtained from the aggregates for sodium and potassium were of a similar order and the leaching of these ions does not appear to have been very influential in the behaviour of any of the other metals. There did not appear to be notable differences between the sodium and potassium leaching from CRT and BGL, so the differences in their ASR behaviour could not be attributed to the leachability of these ions. Consequently, only a qualitative discussion of the results for sodium and potassium is given here.

Leaching of sodium from the ISF slag, the CRT glass and the BGL were all of a similar order (~80 mg/kg). Potassium leaching for the ISF slag and the CRT glass were similar (~20 mg/kg), although higher than the potassium leaching from BGL (~5 mg/kg). When PFA was included in leach tests on the aggregates, the sodium and potassium leaching were notably increased (Na: ~145 mg/kg, K: ~70 mg/kg), suggesting the additional ions were contributed from the PFA itself. There was no equivalent increase when GGBS was tested in association with the aggregates.

Leaching of sodium from concrete containing the CRT glass was higher than from ISF slag concrete (CRT: ~170 mg/kg, ISF: ~80 mg/kg), although potassium leaching was approximately equivalent (~300 mg/kg). However, all levels were slightly increased compared to a control concrete containing TVS aggregate (Na: ~60 mg/kg, K: ~135 mg/kg) suggesting that some additional alkali was being contributed to the concrete from these replacement aggregate materials. When a CRT concrete prism that had been subjected to ASR testing was crushed and leached, significant quantities of sodium and potassium were released (Na: ~1200 mg/kg, K: ~1000 mg/kg). This is not particularly surprising, since the ASR process will have degraded the glass structure and the ions would instead be present within the gel product formed from the reaction. No additional patterns could be identified between the release of these ions and the leaching of the other ions from this study.

7.2.3 Leaching of strontium

Since leaching of strontium is not regulated in the same way as other metal ions such as lead and barium, only a brief summary of the leaching results obtained are included here.

Leaching of strontium from BGL in deionised water and a pH 13 buffer solution consistently fell below the detection limit of the equipment (<0.1 mg/l). This is as expected since the BGL did not appear to contain any strontium (see Table 4.5). Leaching from the ISF slag also usually fell below the detection limit or was occasionally just on the detection limit, giving a result of ~1 mg/kg. Leaching from the CRT glass was approximately the same in both deionised water and in the pH 13 buffer solution, at ~2 mg/kg. PFA and GGBS in solution with the CRT glass did not influence the leaching results obtained for strontium.

Strontium leaching from concrete containing the ISF slag was ~10 mg/kg in most tests. This was reduced to ~2 mg/kg when PFA was included as a cement replacement material and to ~5 mg/kg when GGBS was used. Leaching from concrete containing the CRT glass was ~30 mg/kg in most tests. This was again reduced to ~10 mg/kg when PFA was used and to ~15 mg/kg with GGBS.

If strontium leaching from the aggregates were ever considered an issue, it appears that the cement replacement materials tested would be useful in reducing the leaching levels from concrete (PFA more so than GGBS). However, it would obviously depend on what limiting criteria were set as to whether these additives would be sufficient or not.

7.3 Leaching of calcium and silicon

It was hoped that the leaching results for silicon and calcium would give an insight into the alkali-silica reactivity displayed by the replacement aggregate materials and the inherent durability of the glasses. The calcium leaching results from the ISF slag, the CRT glass and the bottle glass (BGL) at a liquid to solid ratio (L/S) = 10 are given in Figure 7.1, while the silicon leaching results are shown in Figure 7.2. The results shown are an average of two measurements, with error bars showing the standard deviation between them. For some of the calcium results, the associated errors are negligible and are not apparent due to the scale of the graph.

The ISF slag and CRT glass show a significant reduction in leached calcium at high pH (in the pH 13 buffer) compared to the deionised water. However the calcium leaching from the BGL sample is similar in both deionised water and the pH 13 buffer solution. The reasons for this are unclear but it implies that calcium leaching from the BGL is not particularly pH dependent. Silica dissolution from glass at high pH would be expected and this is apparent in the results from all the samples tested. Silicon leaching in the pH 13 buffer is consistently higher than in the deionised water.

More calcium and silicon are leached from the BGL at high pH than from the CRT glass. This is perhaps not surprising, since XRF analysis of the materials (Table 4.5) showed the BGL to contain a higher percentage of both these ions than the CRT. However, the ratio in which these ions are leached at high pH does not directly correspond to the ratio of their compositions, so it is not clear exactly how the leaching patterns of these ions are related, if at all. The silicon and calcium contents of the ISF slag indicate that it is not a true silicate glass in the way the CRT and BGL are, so it would not necessarily be expected to show the same patterns in leaching as the glasses. However, the ISF slag leaching closely resembles the trends seen with the CRT glass, despite the calcium and silicon contents being very different in each.

The leaching of calcium and silicon from the ISF slag and the CRT glass are little effected by the aggregate type. This is true for both the deionised water and the pH 13 buffer solution. There are no apparent differences that would account for the variations seen in the leaching characteristics of the heavy metal ions lead, zinc and barium, from these aggregates. The leaching of these ions is therefore assumed to be unrelated to the leaching of calcium and silicon.

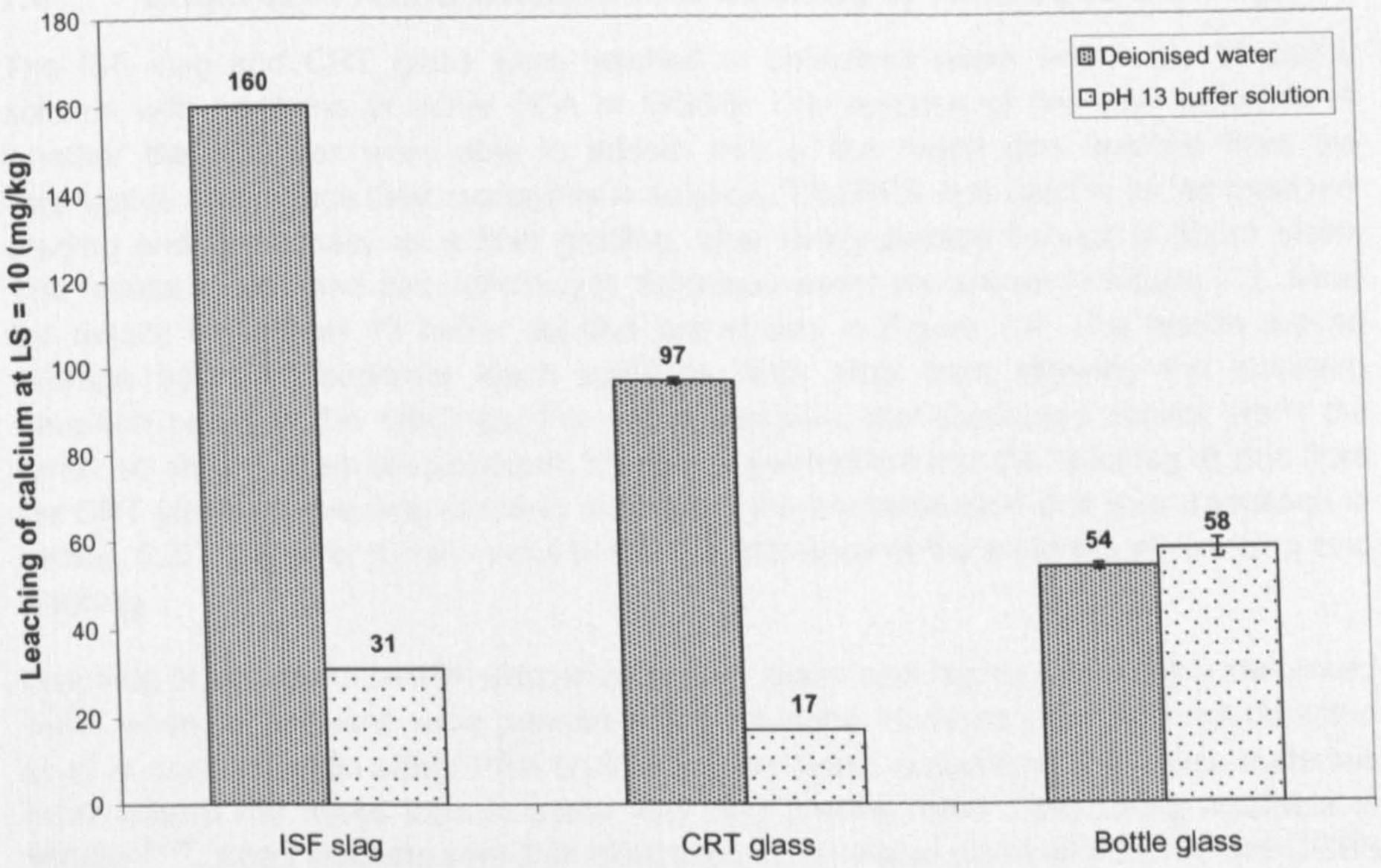

Figure 7.1: Leaching of calcium from the replacement aggregates

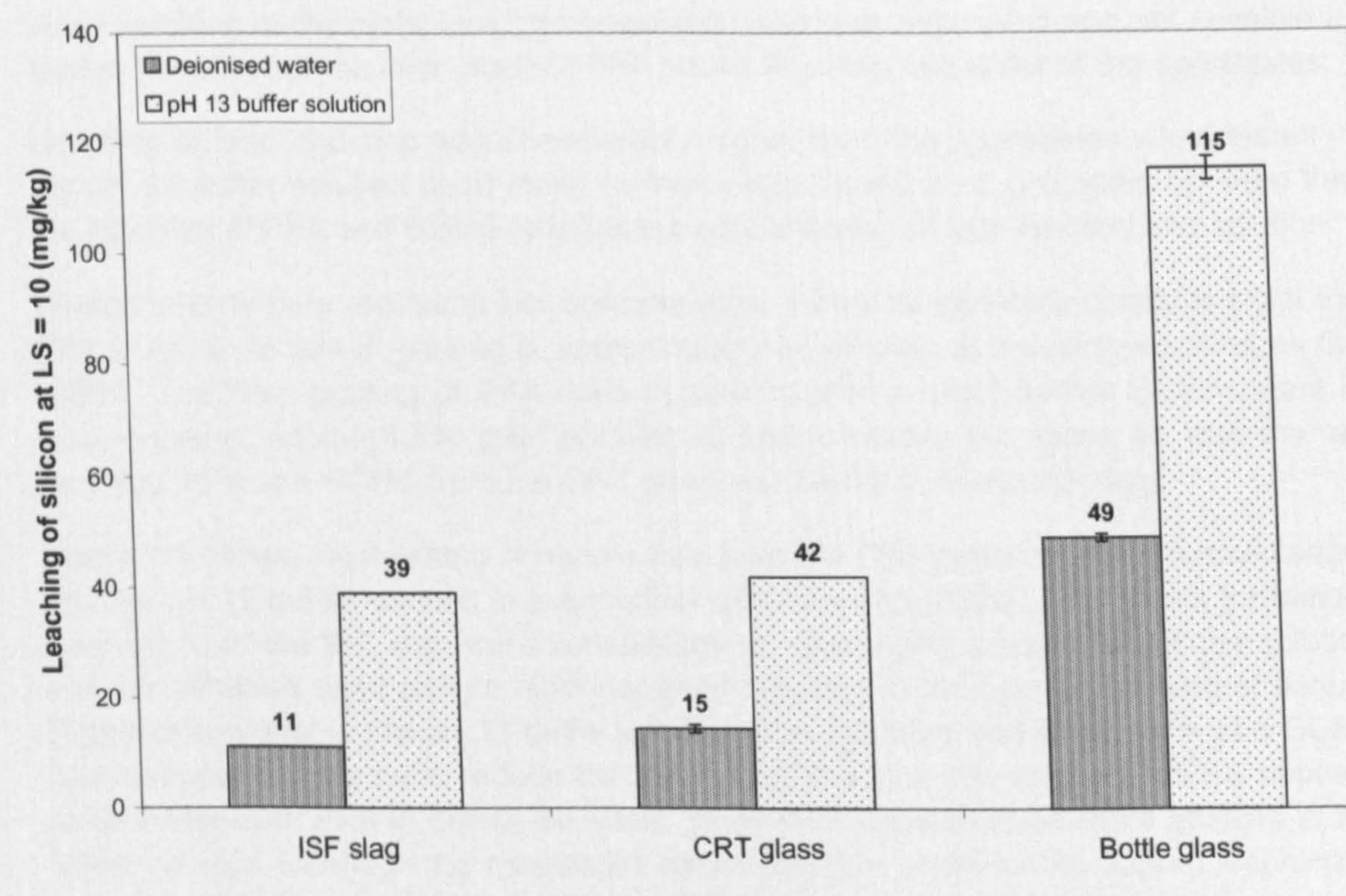

Figure 7.2: Leaching of silicon from the replacement aggregates

7.4 Effect of PFA and GGBS on the leaching of ISF slag and CRT glass

The ISF slag and CRT glass were leached in deionised water and a pH 13 buffer solution with additions of either PFA or GGBS. The purpose of this was to establish whether the additives were able to adsorb any of the metal ions leached from the aggregates and reduce their availability in solution. The PFA was used in its 'as received' grading and additionally as a finer grading, after being passed through a 63μm sieve. The results of lead and zinc leaching in deionised water are shown in Figure 7.3, while the results for the pH 13 buffer solution are shown in Figure 7.4. The results are an average from two separate leach solutions, with error bars showing the standard deviation between the readings. For some samples, the duplicated results were the same, so no error bars are apparent. It must be pointed out that the leaching of zinc from the CRT glass sample was primarily a result of the contamination that was discussed in section 5.2.1, however it was useful to test the efficiency of the additives at reducing zinc leaching.

Leaching of zinc from the ISF slag and the CRT glass was higher than lead in deionised water when no additions were present in the solutions. However, zinc was not detected at all in solution when either PFA or GGBS were used, suggesting that these materials must adsorb the metal ions in some way and prevent them from being available in solution[97,98]. Lead leaching was also minimised in deionised water when PFA and GGBS were used with the CRT glass and when GGBS was used with the ISF slag. However, minimal lead leaching of 1 mg/kg was detected when PFA was used with the ISF slag. Since leaching of the metal ions into deionised water was minimal, it was not possible to assess the effect of the finer grade of PFA on the leaching behaviour of the aggregates.

Leaching of lead and zinc was considerably higher from the aggregates when tested in the pH 13 buffer solution (lead more so than zinc). However, it can again be seen that the inclusion of PFA and GGBS reduces the concentration of ions leached into solution.

When the error bars are taken into consideration, it may be generally concluded that the PFA in its 'as received' grading is approximately as efficient at reducing leaching as the GGBS. The finer grading of PFA does appear to offer a slight further improvement in lead leaching, although the zinc leaching is approximately the same as with the 'as received' PFA and GGBS from the CRT glass and higher from the ISF slag.

Figure 7.5 shows the leaching of barium ions from the CRT glass in both deionised water and the pH 13 buffer solution in association with PFA and GGBS. The results for barium leaching from the ISF slag were consistently at ~2.0 mg/kg irrespective of the solution and the additives used and so have not been included in the figure. Leaching of barium is generally higher in the pH 13 buffer solution than the deionised water. PFA and GGBS again appear to be able to reduce the leaching of the ions into solution. GGBS appears to be better than PFA in deionised water, while PFA appears to be more efficient in the buffer solution, although the associated errors are quite large for the barium leaching at high pH. The finer grading of PFA actually increases the leaching compared to the coarser grading in both solutions and the reasons for this are not clear.

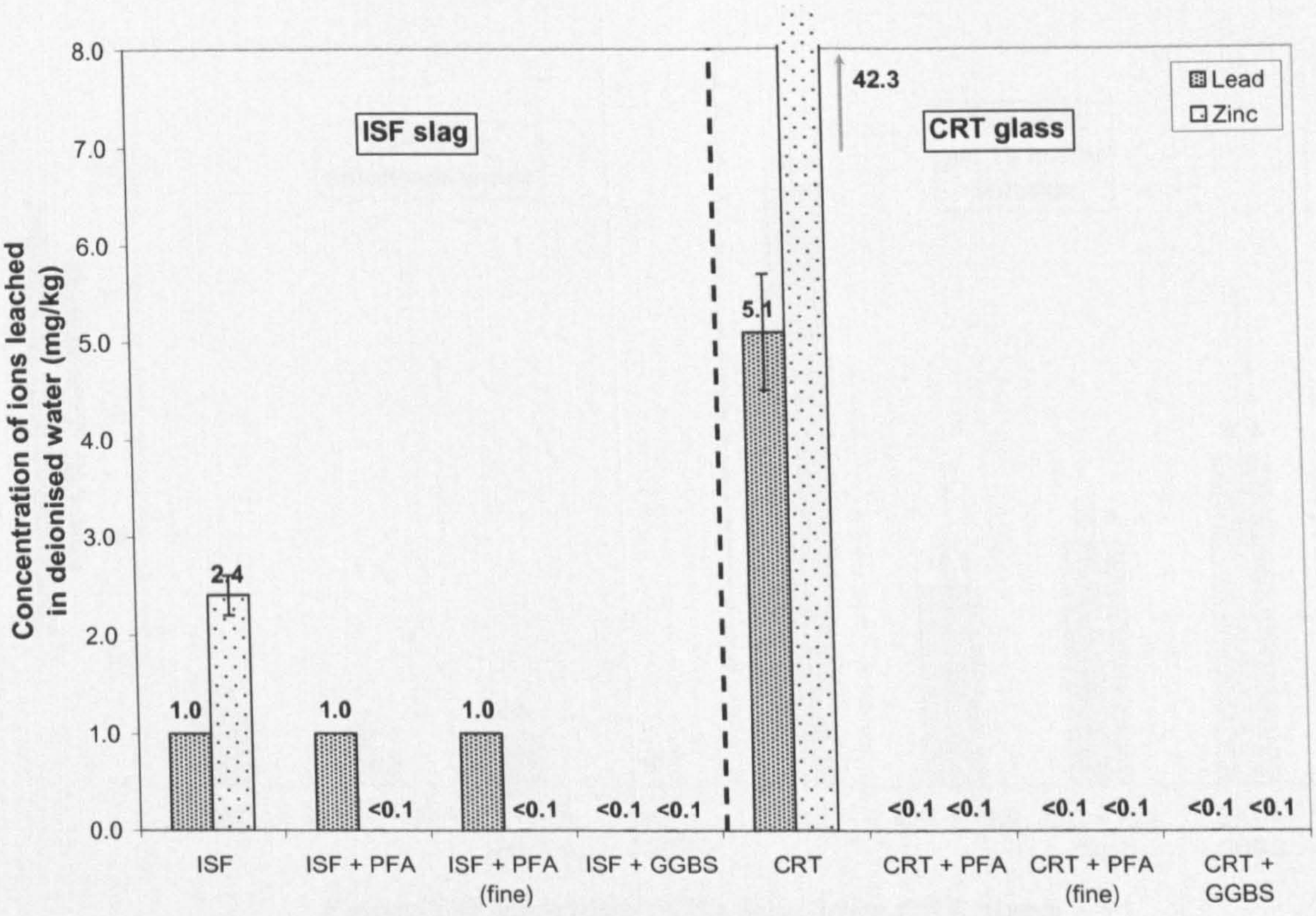

Figure 7.3: Leaching of Pb and Zn ions in the presence of PFA and GGBS in deionised water

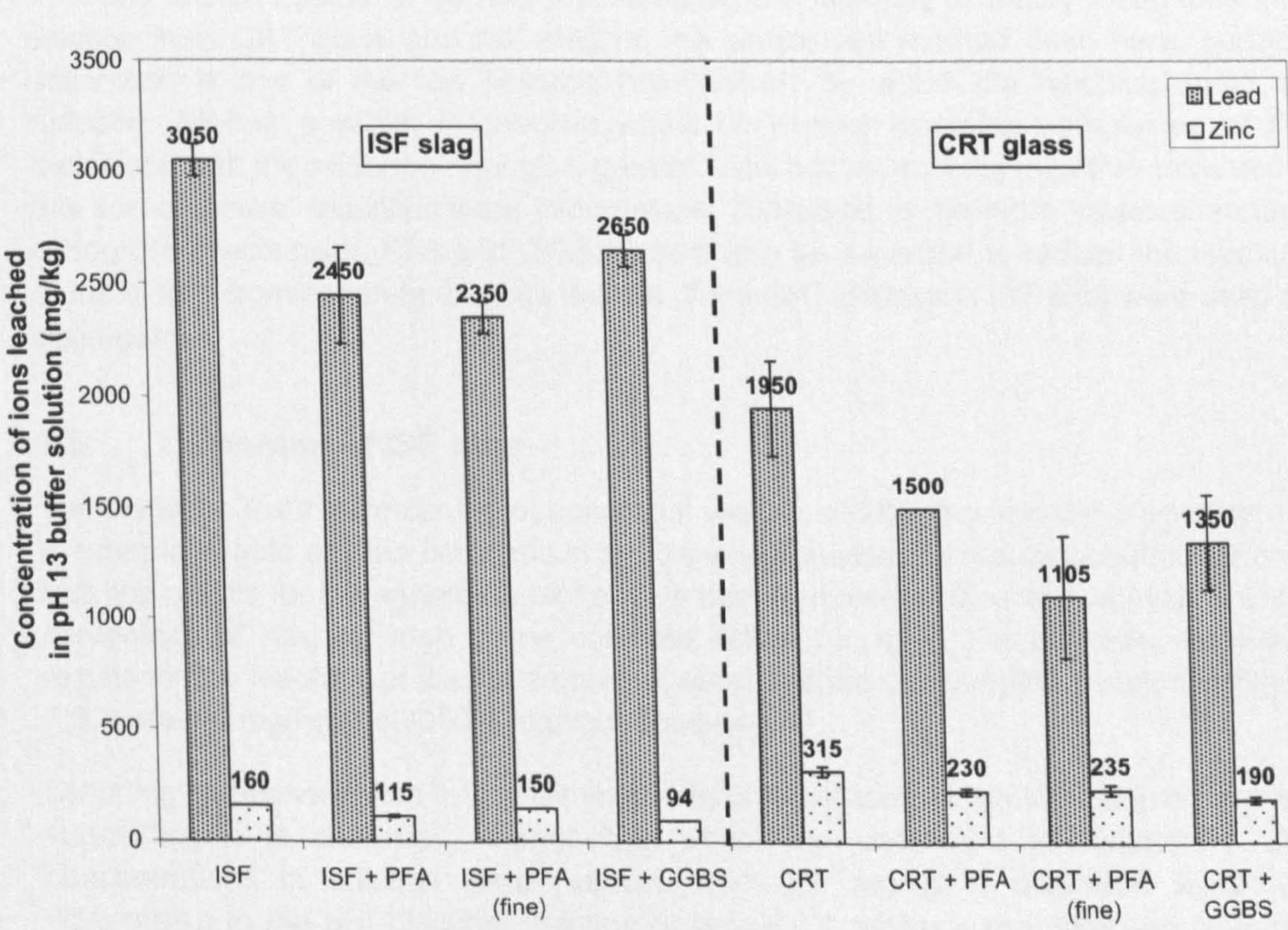

Figure 7.4: Leaching of Pb and Zn ions in the presence of PFA and GGBS in a pH13 buffer solution

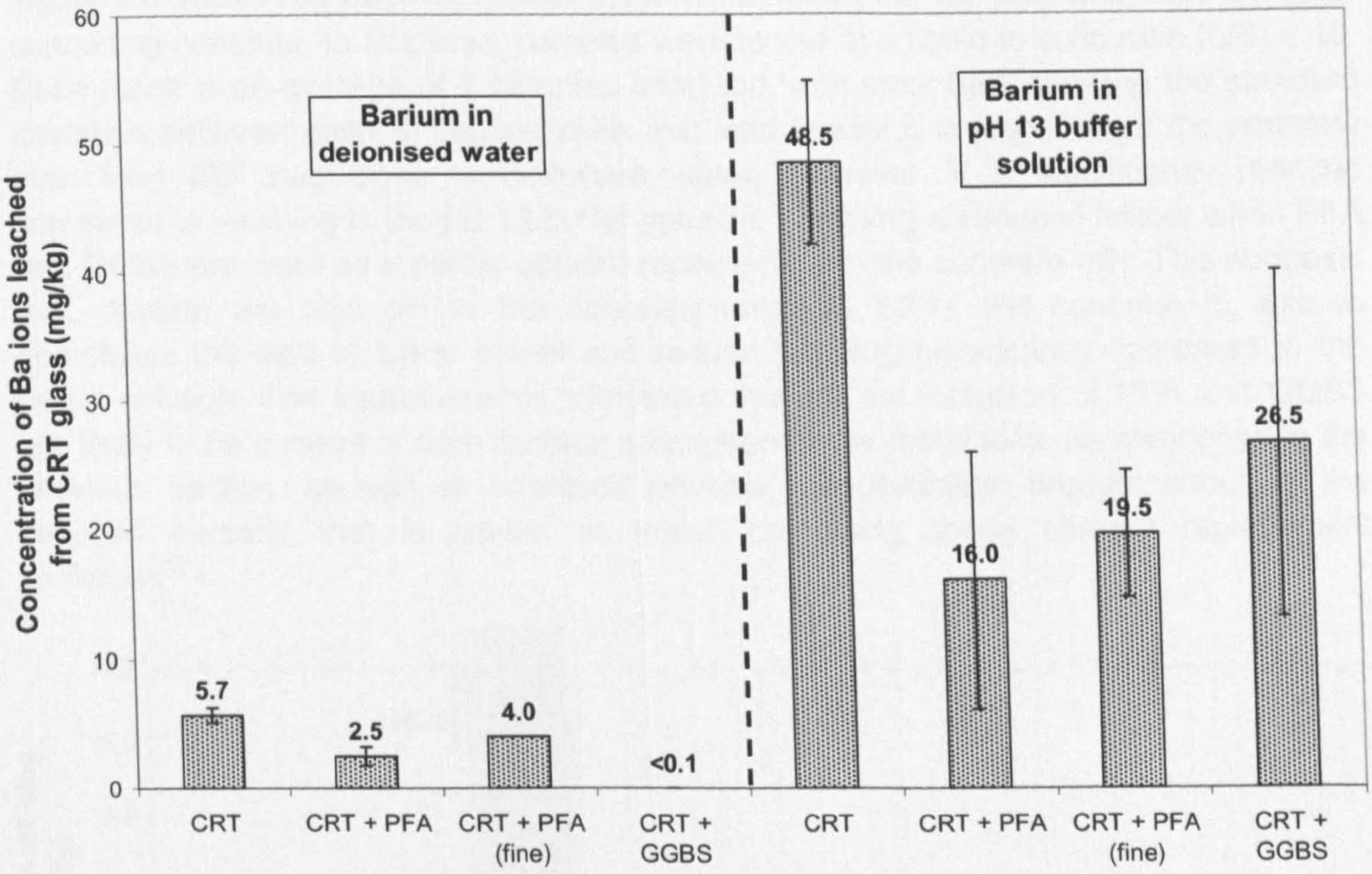

Figure 7.5: Leaching of Ba ions from CRT glass in the presence of PFA and GGBS

PFA and GGBS appear to be useful at reducing the leaching of heavy metal ions into solution from CRT glass and ISF slag. In the simple test method used here, surface adsorption is one of the few possible mechanisms by which the leaching could be reduced. Another possible mechanism would be through chemical complexing of the metal ions with the additives, though a greater reduction in leaching might be expected if this sort of 'active' reduction were taking place, compared to the more 'passive' surface adsorption mechanism. PFA and GGBS would also be expected to reduce the leaching of metal ions from concrete to some degree, if the CRT glass and ISF slag were used as aggregates.

7.5 Leaching of ISF slag

Tumble leach tests were carried out on equal weights of ISF slag and ISF slag-concrete. In order to enable a direct comparison to be made between the results obtained for each test, the results for the aggregate alone have been reduced so they are equivalent to the percentage of slag included in the concrete mixes, i.e. 41%. For example, the actual results for the leaching of lead in deionised water and the pH 13 buffer solution in Figure 7.6, were 1.0 mg/kg and 3050.0 mg/kg respectively.

Leaching of zinc ions was totally eliminated by the inclusion of the ISF slag in concrete, suggesting it is chemically immobilised within the concrete's microstructure. Zinc concentrations in solution were reduced from 1.0 mg/kg in deionised water and 65.6 mg/kg in the pH 13 buffer solution to below 0.1 mg/kg – the detection limits set, when the crushed concrete samples were tested.

Figure 7.6 shows the leaching results obtained for lead from ISF slag and from ISF slag-containing concrete. In all cases, samples were tested at a liquid to solid ratio (L/S) = 10. Each result is an average of 2 samples analysed, with error bars showing the standard deviation between each. It can be seen that lead leaching is higher from the concrete than from ISF slag alone in deionised water. However, it is significantly reduced compared to leaching in the pH 13 buffer solution. Leaching is reduced further when PFA and GGBS are used as a partial cement replacement in the concrete mix. This suggests that, despite the high pH in the concrete (average 12.1), the concrete is able to immobilise the lead to some extent and reduce leaching significantly compared to the buffer solution. The improvements witnessed through the inclusion of PFA and GGBS are likely to be a result of both surface adsorption of the metal ions, as mentioned in the previous section, as well as improved physical immobilisation brought about by the reduced porosity that is typical of mixes containing these cement replacement materials[99].

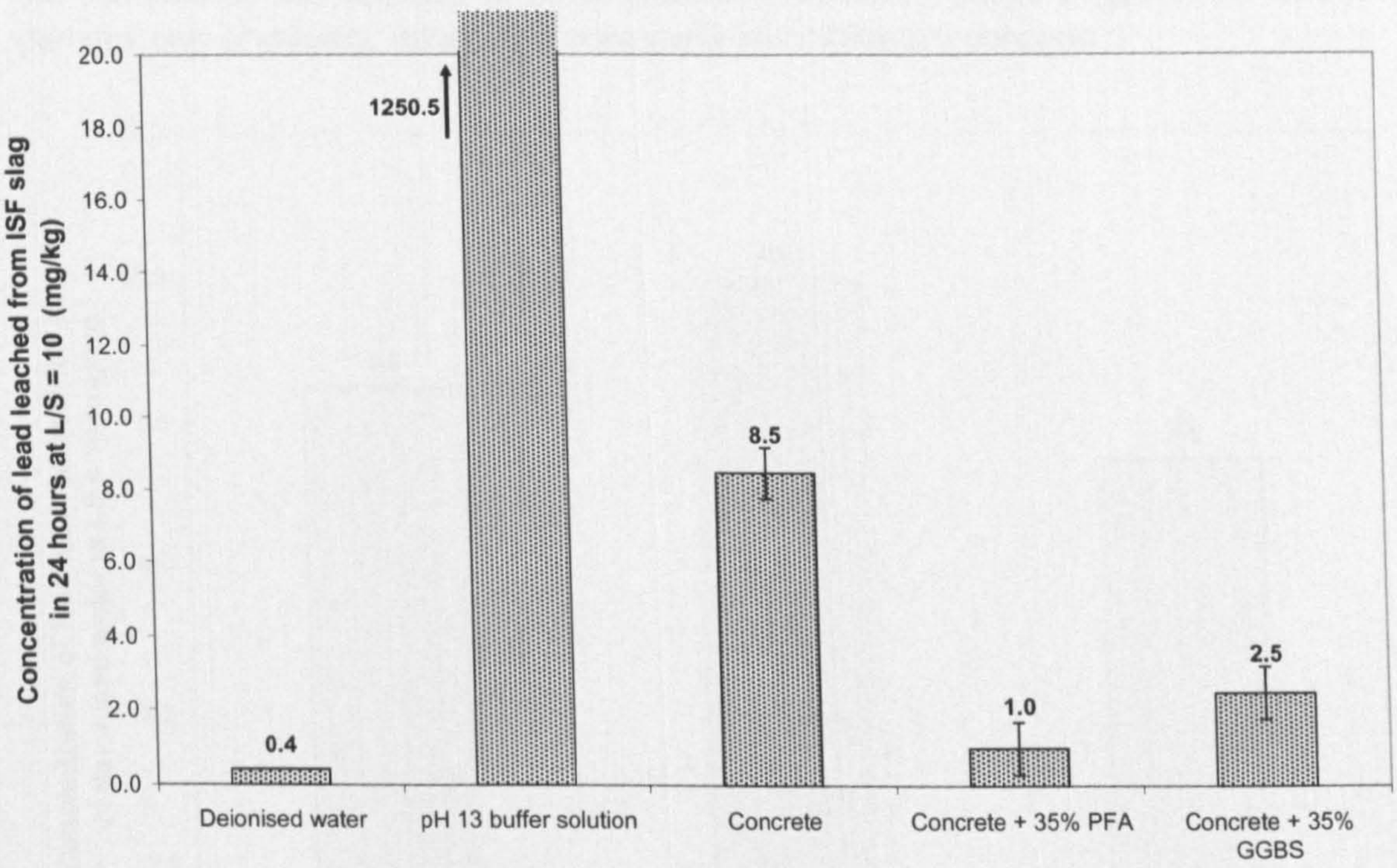

Figure 7.6: Leaching of lead from ISF slag and ISF slag-concrete

The UK Environment Agency gives guidance limits for this test for a material to be considered acceptable for disposal as inert/ non-hazardous landfill. The limit set for lead is 0.5 mg/kg[107]. This level is exceeded in all cases apart from the ISF slag aggregate leached in deionised water. However it must be remembered that the results for the aggregate alone have been normalised to be equivalent to the level of aggregate present in the concrete and would otherwise exceed the regulatory limit. The elevated pH of approximately 12 experienced within a concrete mix appears to exacerbate the leaching. Results would therefore need to be improved before ISF slag could be safely included in concrete as a 100% replacement for natural fine aggregate. However, if the replacement level was reduced to 50% for example, the lead leaching would be expected to drop to at least half the values shown here, which would suggest that additions of 35% PFA, as

used for this testing, would sufficiently reduce the leaching of lead from concrete containing the ISF slag.

Figure 7.7 shows the leaching of lead from ISF slag-concrete mixes of varying cement content and water/ cement ratio. When the cement content of the mix is increased from 300 kg/m^3 to 400 kg/m^3, there is no improvement in lead leaching. However, the density of this mix was actually lower, at 2700 kg/m^3 compared to 2750 kg/m^3. This would suggest that the increased density provides improved physical immobilisation to the leached lead ions. When the cement content is increased to 400 kg/m^3 and the water/ cement ratio decreased from 0.6 to 0.45, a slight improvement is seen in the lead leaching behaviour. The density of this mix was again higher, at 2760 kg/m^3. This suggests that a decreased water/ cement ratio, which would be expected to bring about a corresponding increase in concrete density, does appear to reduce lead leaching from the ISF slag in concrete. Since all results obtained here are only marginally different and the concrete density appears to be of greatest influence, it would suggest that lead is perhaps only physically, rather than chemically immobilised in concrete.

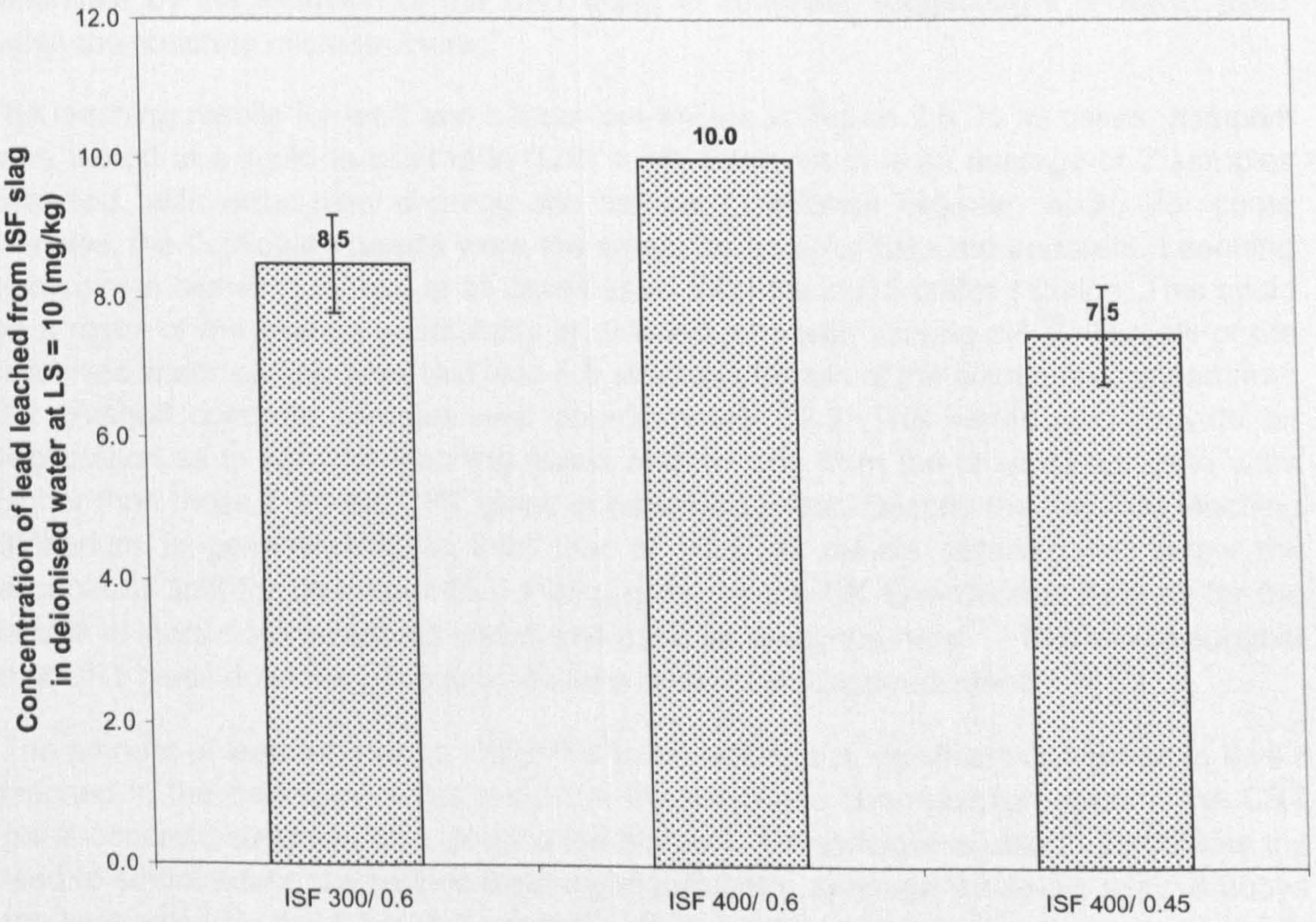

Figure 7.7: Leaching of lead from ISF slag-concrete of varying cement content and water/cement ratio

7.6 Leaching of CRT glass

The main metal ions of concern from CRT glass are lead and barium. Since strontium limits are not specified by the UK Environment Agency and other sources suggest a high human tolerance for strontium[31], it was decided that the leaching behaviour of strontium

was not of high priority. Although not thought to be of great concern with this aggregate, zinc leaching was also measured.

Tumble leach tests were carried out on equal weights of CRT glass and CRT glass-concrete. In order to enable a direct comparison to be made between the results obtained for each test, the results for the aggregate alone have been reduced so they are equivalent to the percentage of glass included in the concrete mixes, i.e. 32%. For example, the actual results for the leaching of lead in deionised water and the pH 13 buffer solution in Figure 7.8, were 5.1 mg/kg and 1950.0 mg/kg respectively.

As shown in Figure 7.3, surprising quantities of zinc were leached from the CRT glass aggregate. Although no EDS images were taken to confirm zinc contamination, the high levels of zinc leached from the CRT glass here and throughout this leach testing is supporting evidence that additional zinc was present as a contaminant in the glass, as detailed in section 5.2.1. The zinc leaching is consistently higher than from the ISF slag, even though XRF analysis shows the slag to contain significantly more zinc than the CRT (ISF = 13.95%, CRT = 0.21%, see Table 4.5). Despite this, zinc leaching was again eliminated by the inclusion of the CRT glass in concrete, suggesting it is immobilised within the concrete microstructure.

The leaching results for lead and barium are shown in Figure 7.8. In all cases, samples were tested at a liquid to solid ratio (L/S) = 10. Each result is an average of 2 samples analysed, with error bars showing the standard deviation between each. For some samples, the duplicated results were the same, so no error bars are apparent. Leaching of barium is higher than lead in all cases apart from the pH13 buffer solution. This could be a result of the change in solubility of different ions with varying pH[100]. The pH of the deionised water sample after test was 6.5, whereas the pH of the solutions obtained from the crushed concrete samples was approximately 12.3. This would also provide an explanation as to why the leaching levels of both ions from the crushed concrete were higher than those from the CRT glass in deionised water. Despite the fact that leaching of barium is generally higher than that of lead, all results obtained fall below the acceptable limit for barium of 20.0 mg/kg given by the UK Environment Agency for the landfill of inert/ non-hazardous waste and used for guidance here[107]. This would suggest that CRT glass does not pose any risk as a result of its barium content.

The amount of lead leached in the pH13 buffer solution is significant compared to levels leached in the deionised water and from the concrete. The reduction seen in the CRT glass-concrete suggests that, despite the high pH, the concrete is able to immobilise the lead to some extent and reduce leaching significantly, although the levels are still above the limit given by the EA of 0.5 mg/kg[107]. This suggests that encapsulation in concrete alone is insufficient to prevent lead leaching from CRT glass when used at a 100% replacement level.

However, when GGBS and PFA are used as a replacement for a percentage of the Portland cement in concrete containing the glass, lead leaching is reduced to below the detection limits of the equipment (0.1 mg/l). A reduction is also witnessed with barium. The improvements witnessed through the inclusion of PFA and GGBS are likely to be a result of both surface adsorption of the metal ions, as discussed in section 7.4, as well as

improved physical immobilisation brought about by the reduced porosity that is typical of mixes containing these cement replacement materials[99].

The addition levels of PFA and GGBS shown in Figure 7.8 were those specified for the minimisation of ASR with high reactivity aggregates (35% PFA and 50% GGBS). It is interesting to note that PFA reduces the leaching of barium more than GGBS, yet it was used at a lower replacement level. This would suggest that PFA is more efficient at reducing leaching than GGBS. Figure 7.9 compares the leaching of barium ions from CRT glass-concrete containing PFA and GGBS at levels specified for ASR mitigation with both high and normal reactivity aggregates. As would be expected, the results from the high addition level mixes are lower than those with normal addition levels. Results from PFA mixes are consistently lower than those from mixes with GGBS, despite the PFA replacement actually being lower.

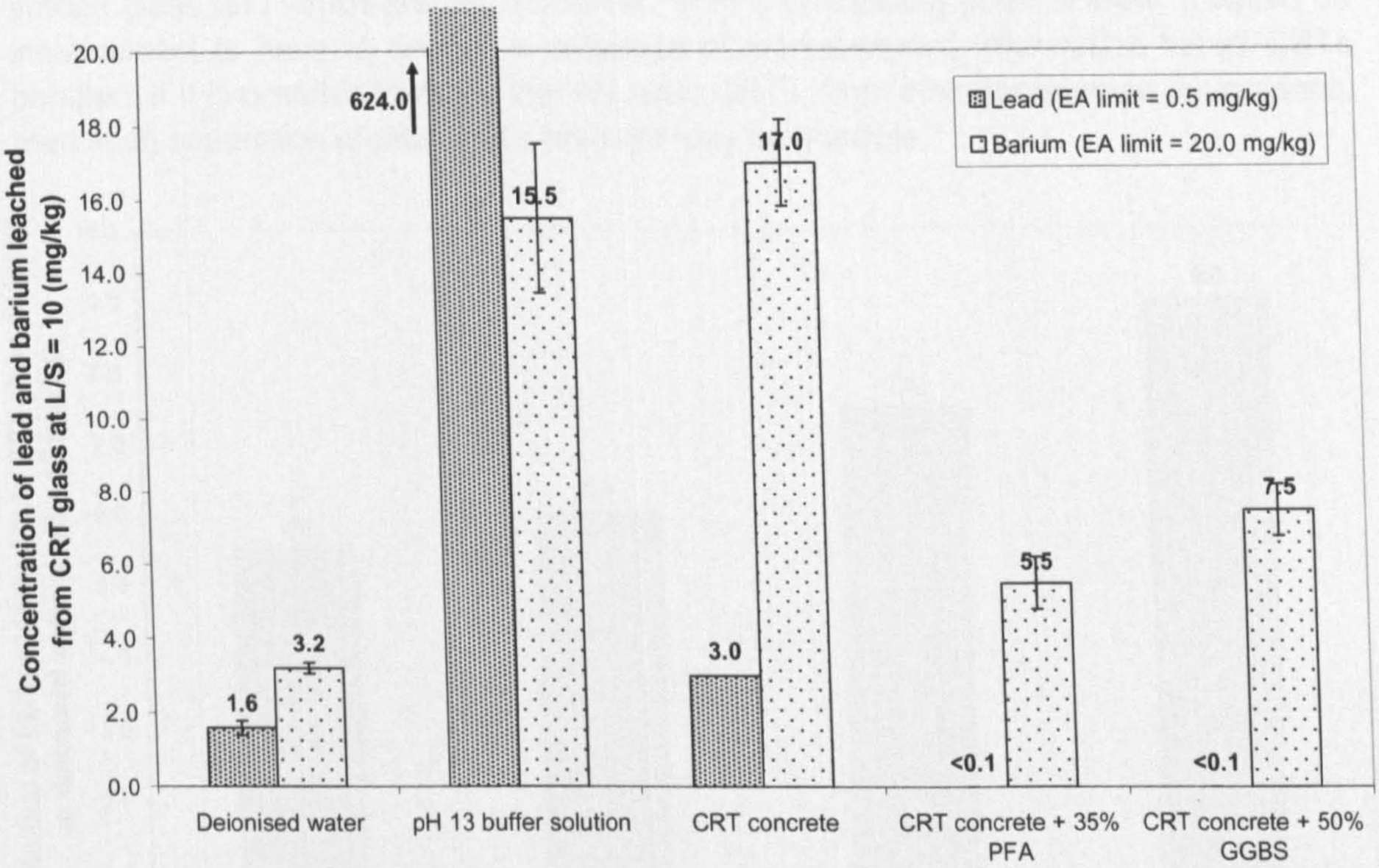

Figure 7.8: Leaching of lead and barium from CRT glass and CRT glass-concrete

It was shown in section 6 that CRT glass is highly susceptible to ASR. It might be anticipated that if concrete containing the CRT glass were to be damaged by ASR, the lead and barium ions within the glass may be more prone to leaching. Leach testing was therefore carried out on crushed concrete prisms that had been subject to accelerated ASR testing at 60 degrees. The prisms had been severely damaged as a result of ASR. However, leaching results for lead and barium were actually lower than those obtained from an equivalent aged sample that had not undergone ASR testing (lead = <1.0 mg/kg, barium = 13.5 mg/kg after ASR testing, compared to lead = 2.0 mg/kg, barium = 15.0 mg/kg after testing a sample of equivalent age without ASR testing).

Although lead and barium were shown to be present in the ASR gel in samples that had been subject to accelerated testing at 80 degrees (section 6.1.1), they do not appear to be more readily leachable from concrete that has suffered from ASR compared to

concrete that has not. The reasons for this are not clear, unless the ions are simply not readily leachable from the ASR gel once it has formed. This particular area has not been pursued further as it was not the main focus of this study.

Since all barium leaching levels have fallen below regulatory limits, this would suggest that if it were possible to separate the lead-containing glass from the barium-containing glass in a CRT prior to its use as aggregate in concrete, it would pose no environmental risk from the leaching of metal ions. However, it is appreciated that perfect separation would be difficult, due to the lead frit that is used to weld the different glass sections together. It was also noted earlier (section 2.3.1) that the plate/ screen glass of older CRTs would be likely to contain lead as radiation shielding, rather than just barium and strontium. It would no doubt be possible to obtain historical data from major CRT manufacturers that would indicate which monitors are likely to contain lead in their screen glass and which are not. However, from a processing point of view, it would be inconvenient to have to consult a database of manufacturing information for all CRTs handled. If it is possible to easily identify older CRTs, from their appearance for instance, then such separation of new CRTs from old may be possible.

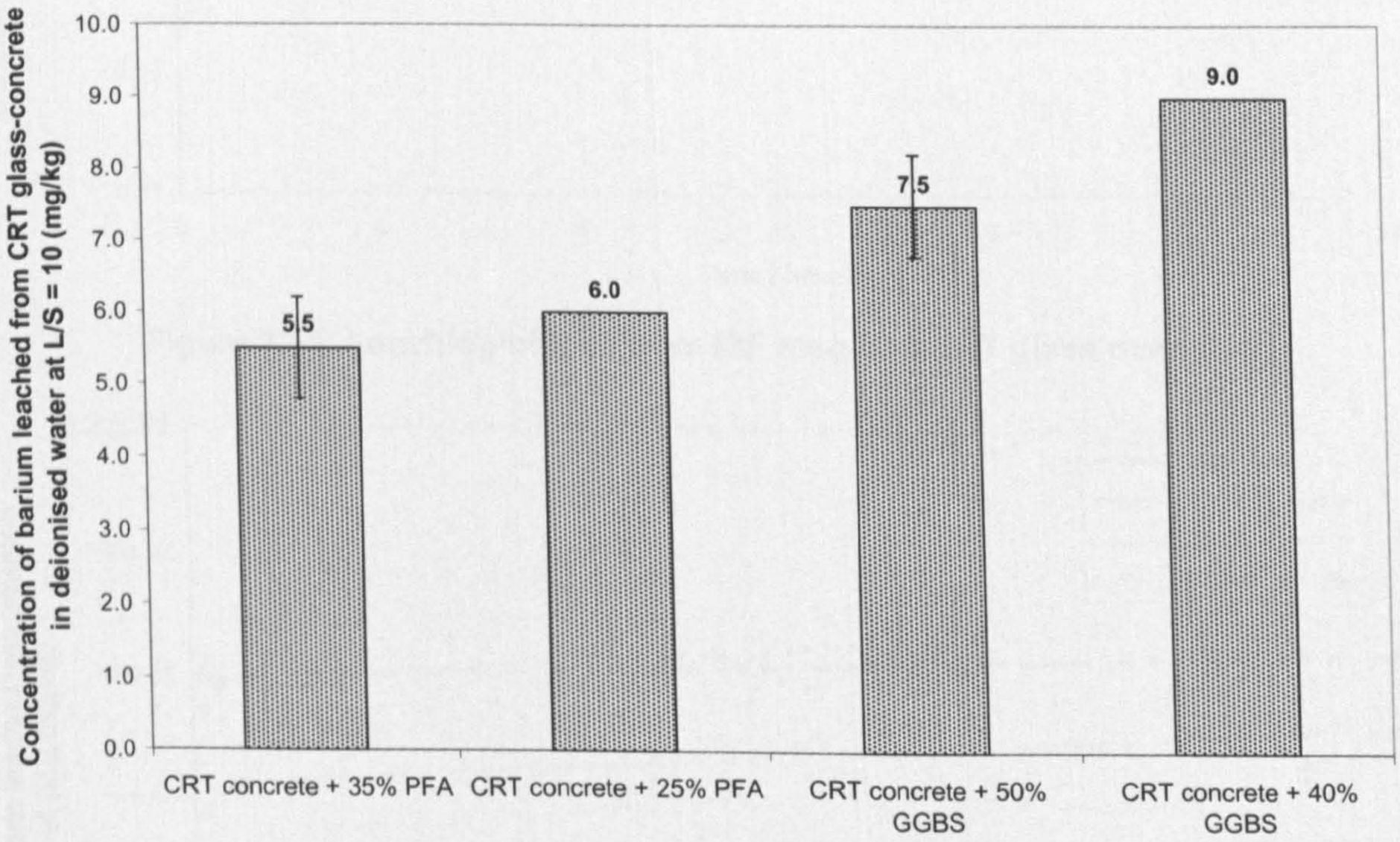

Figure 7.9: Leaching of barium from CRT glass-concrete with additions of PFA and GGBS

7.7 Rapid, short-term leach testing

The purpose of this rapid test was to see how much lead and zinc was released from the aggregates over a short period of time and assess the possible causes of the retardation witnessed with the ISF slag. This test compared the leaching behaviour over the first hour in solution to the 24 hour results. Lead leaching results are given in Figure 7.10 and those for zinc in Figure 7.11. In all cases, samples were tested at a liquid to solid ratio (L/S) = 10. Each result is an average of 2 samples analysed, with error bars showing the

standard deviation between each. It is assumed that the zinc leaching from the CRT glass is a result of zinc metal contamination, rather than from the glass itself. However, the zinc would still be present in a concrete mix containing this glass and so the CRT zinc leaching results serve as a useful comparison to the ISF slag.

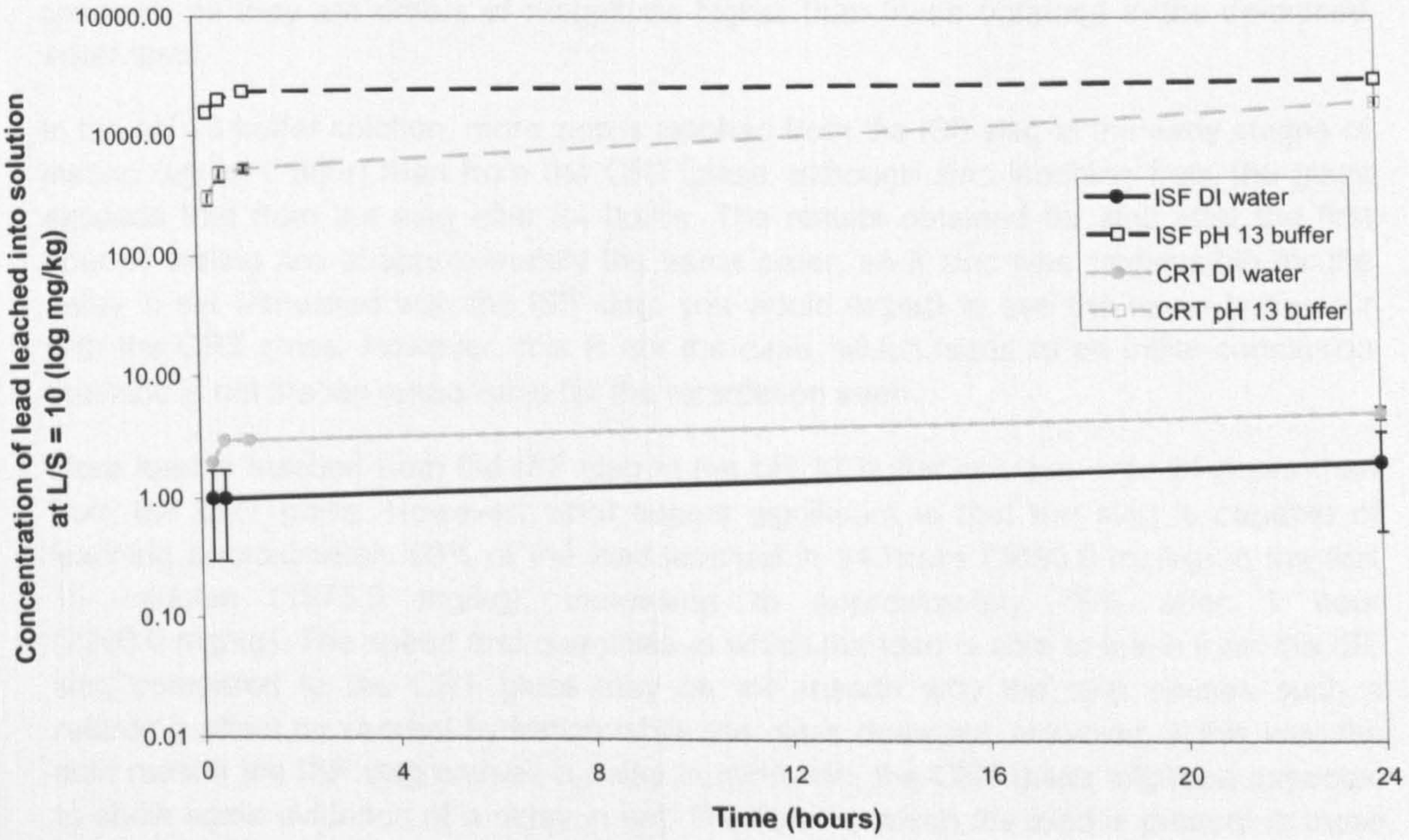

Figure 7.10: Leaching of lead from ISF slag and CRT glass over time

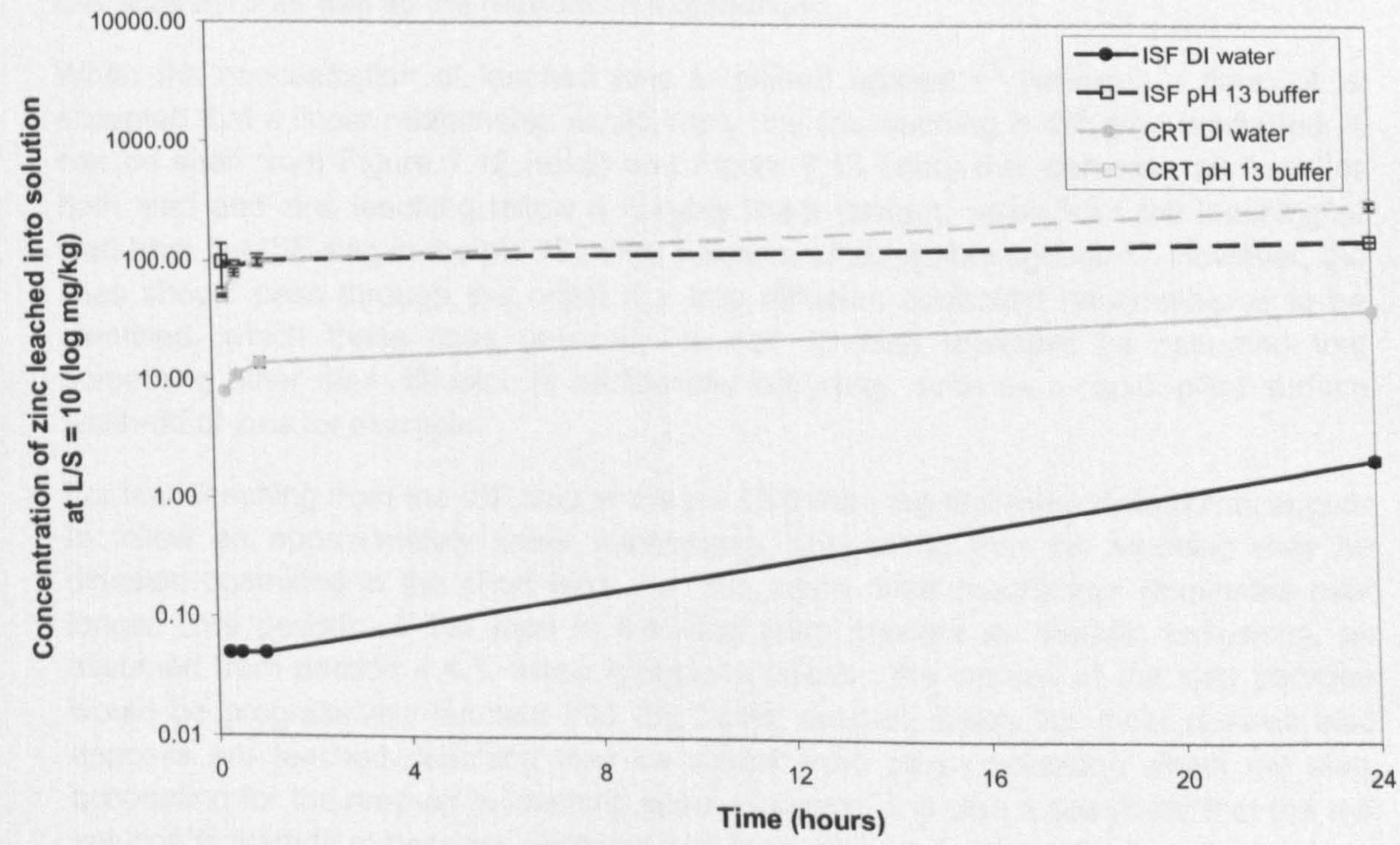

Figure 7.11: Leaching of zinc from ISF slag and CRT glass over time

Generally, relatively little lead and zinc are leached from the ISF slag in deionised water up to 24 hours of testing. Higher concentrations of both are actually leached from the CRT glass, which does not show any delay in the setting process when included in a concrete mix. These results seem to indicate that the increased level of leaching experienced in the pH 13 buffer solution is more likely to influence the setting of concrete, as they are orders of magnitude higher than those obtained in the deionised water tests.

In the pH 13 buffer solution, more zinc is leached from the ISF slag in the early stages of testing (up to 1 hour) than from the CRT glass, although zinc leaching from the glass exceeds that from the slag after 24 hours. The results obtained for zinc after the first hour of testing are of approximately the same order, so if zinc was responsible for the delay in set witnessed with the ISF slag, you would expect to see the same behaviour with the CRT glass. However, this is not the case, which leads to an initial conclusion that zinc is not the ion responsible for the retardation seen.

More lead is leached from the ISF slag in the pH 13 buffer solution over 24 hours than from the CRT glass. However, what seems significant is that the slag is capable of leaching approximately 50% of the lead leached in 24 hours (3050.0 mg/kg) in the first 15 minutes (1575.0 mg/kg), increasing to approximately 75% after 1 hour (2360.0 mg/kg). The speed and quantities at which the lead is able to leach from the ISF slag compared to the CRT glass may be the reason why the slag causes such a retarding affect on cement hydration while the glass does not. However, if this was the sole reason the ISF slag caused a delay in hydration, the CRT glass might be expected to show some evidence of a delay in set. The form in which the lead is present in these aggregate materials – as metallic inclusions in the ISF slag but distributed throughout the glass structure in the CRT glass, as shown in section 4.4, must influence the leaching characteristics as well as the retardation experienced.

When the concentration of leached ions is plotted against $t^{½}$ (where t = time), it is accepted that a linear relationship would imply that the leaching is diffusion controlled. It can be seen from Figure 7.12 (lead) and Figure 7.13 (zinc) that generally all lines for both lead and zinc leaching follow a roughly linear pattern, apart from the leaching of lead from the ISF slag in the pH 13 buffer solution, when plotted against $t^{½}$. However, the lines should pass through the origin if a true diffusion controlled relationship is to be identified, which these lines generally do not. It must therefore be assumed that something other than diffusion is additionally occurring, such as a rapid initial surface wash-off of ions for example.

For lead leaching from the ISF slag in the pH 13 buffer, the first three data points appear to follow an approximately linear relationship, suggesting that the leaching may be diffusion controlled in the short term, but that some other mechanism dominates over longer time periods. If the lead in the slag were present as metallic inclusions, as assumed from section 4.4.1, those inclusions nearest the surface of the slag particles would be progressively leached into the buffer solution. Once the most obvious lead deposits are leached, leaching may be slower from other inclusions within the slag, accounting for the drop off in leaching seen. However, it is also a possibility that the test solution is starting to become saturated with lead after 24 hours under test. Testing over a range of liquid:solid ratios would be required to eliminate or confirm this possibility.

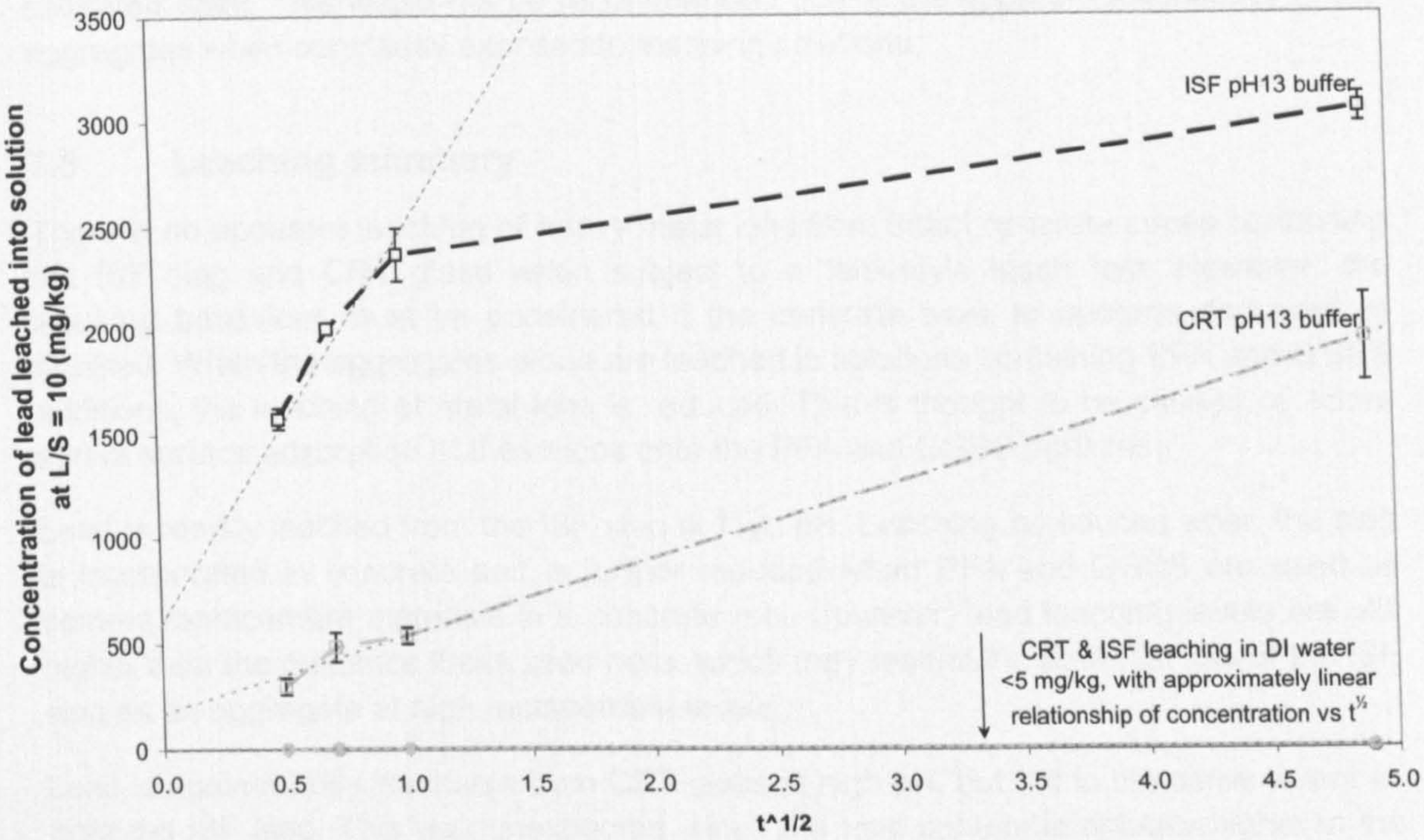

Figure 7.12: Concentration of lead leached from ISF slag and CRT glass vs $t^{½}$

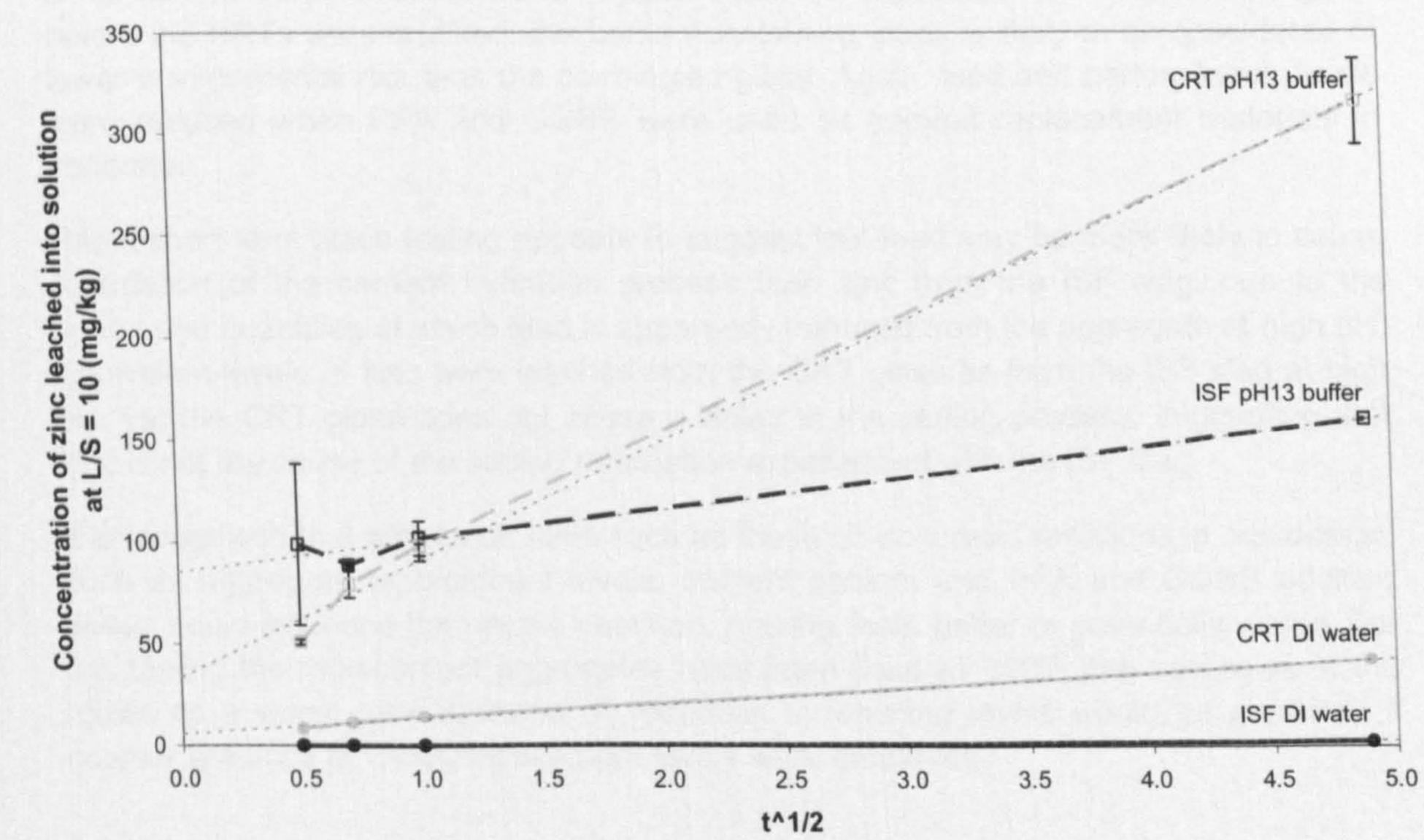

Figure 7.13: Concentration of zinc leached from ISF slag and CRT glass vs $t^{½}$

Once concrete containing the aggregates had set and hardened, there would probably be an insufficient liquid:solid ratio within the pore water of the concrete for diffusion controlled leaching of the aggregates to occur, unless the concrete were maintained in a

saturated state. This would not be recommended due to the apparent leachability of the aggregates when constantly exposed to leaching solutions.

7.8 Leaching summary

There is no apparent leaching of heavy metal ions from intact concrete cubes containing the ISF slag and CRT glass when subject to a tank-style leach test. However, the leaching behaviour must be considered if the concrete were to become damaged or crushed. When the aggregates alone are leached in solutions containing PFA and GGBS additions, the leaching of metal ions is reduced. This is thought to be caused by some sort of surface adsorption of these ions onto the PFA and GGBS particles.

Lead is readily leached from the ISF slag at high pH. Leaching is reduced when the slag is incorporated in concrete and is further reduced when PFA and GGBS are used as cement replacement materials in a concrete mix. However, lead leaching levels are still higher than the guidance limits used here, which may restrict the potential use of the ISF slag as an aggregate at high replacement levels.

Lead is again readily leachable from CRT glass at high pH, but not to the same extent as from the ISF slag. This was unexpected, since the lead content is actually higher in the CRT glass. Barium leaching from the CRT glass was below the guidance limits used in all cases, suggesting that the CRT glass does not pose an environmental risk as a result of its barium content. If the barium glass could be separated from the leaded glass before the CRTs were crushed, the barium containing glass is likely to be considered of lower environmental risk than the co-mingled glass. Again, lead and barium leach levels were reduced when PFA and GGBS were used as cement replacement materials in concrete.

Rapid short-term leach testing appears to suggest that lead may be more likely to cause retardation of the cement hydration process than zinc from the ISF slag, due to the speed and quantities at which lead is apparently released from the aggregate at high pH. Equivalent levels of zinc were leached from the CRT glass as from the ISF slag at high pH, yet the CRT glass does not cause a delay in the setting process, suggesting that zinc is not the cause of the setting retardation experienced with the ISF slag.

It is recognised that with leach tests such as these on concrete, variations in mix design, such as aggregate replacement levels, cement content and PFA and GGBS addition levels, could influence the results obtained, making them better or potentially worse. For this testing the replacement aggregates have been used as 100% fine aggregate in the mixes as a worst case scenario. A reduction in leaching levels would be expected if coarser gradings or lower replacement levels were employed.

8 Retardation of concrete set

Although concrete containing the ISF slag experienced a delay in set, that containing CRT glass did not. This was unexpected, since the CRT glass actually contained more lead than the ISF slag, according to the XRF analysis given earlier (section 3.2.4) and lead has previously been identified as causing a delay in concrete set (section 2.4.6). This initially led to the conclusion that zinc must be the species within the ISF slag that was responsible for the delay.

However, the concrete containing CRT glass still did not suffer from a delay when it was apparent that it had been contaminated with shards of zinc metal. The leaching results presented in section 7.7 showed that zinc leached as rapidly into solution from the CRT glass as it did from the ISF slag in a high alkaline environment and notably faster in deionised water. This would appear to suggest that zinc is not the species that is responsible for the retardation caused and it is more likely to be lead, due to its rapid release into solution from the ISF slag. There has been no evidence to directly confirm this so the effect of both ions has still been considered here. Due to the lack of retardation experienced with the CRT glass, this section is primarily concerned with identifying the cause of the delay with the ISF slag and possible methods to overcome it.

8.1 Microscopic (SEM) analysis of retarding ISF mortar

SEM studies were carried out to see if there was any evidence of zinc or lead-containing compounds coating the surface of the cement grains and preventing hydration from occurring, based on observations made in a previous study[112].

Hardened ISF slag mortar samples, when examined by SEM and EDS, only showed the presence of the metal ions zinc and lead within the aggregate particles themselves. These ions were not detected in any other regions within the cement matrix. Even though these metal ions will only be detected by EDS analysis at concentrations above approximately 1%, these findings potentially suggest that zinc and lead ions do not migrate from the slag in appreciable quantities.

Further SEM analysis was carried out on a mortar sample in which hydration was being delayed, by utilising the cryo-stage on the SEM. It was hoped that examination of a mortar mix containing the ISF slag during its retardation period would give a better indication as to what was causing the delay in set. Once the moisture was evaporated from the surface of the sample, secondary electron images of the mortar showed spherical ISF slag particles protruding from regions of cement, as shown in Figure 8.1. The slag particles did not appear to have been attacked or degraded in any way.

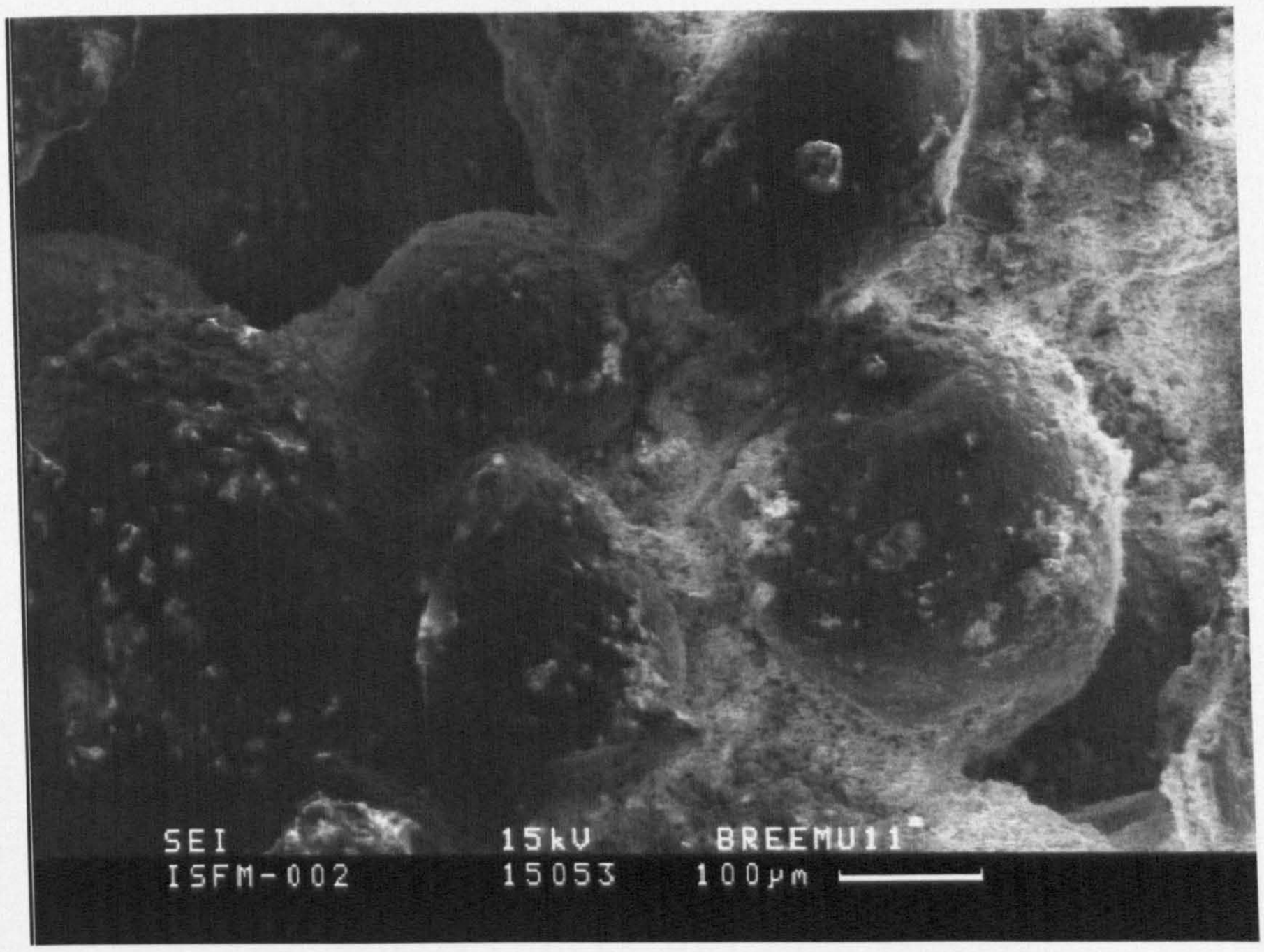

Figure 8.1: Secondary electron image of ISF slag particles within a mortar mix that is suffering from a delay in the hydration process

Closer examination of the cement grains showed that they did not appear to have hydrated particularly, even after a period of 18 hours. In Figure 8.2, distinct cement particles can still be distinguished (e.g. A and B). EDS analysis showed no presence of any metal ions on the surface of these cement grains implying that they were not necessarily being coated by layers of gelatinous lead or zinc compounds. It was thought possible that this was due to limitations of the equipment and that an examination at higher magnification and resolution might give more information. However, there was no evidence from SEM examination that suggested what was causing the delay in hydration that was being experienced.

8.2 Microscopic (TEM) analysis of retarding ISF mortar

It was hoped that the higher resolution of TEM would show evidence of any coatings that may have been present on the surface of cement grains within a mortar containing the ISF slag. It was apparent from the characterisation studies carried out for this work (section 4.5) that it was not always easy to distinguish what exactly was being observed using the microscope, as the particles being analysed were usually similar in appearance. Also, due to the high magnification used for TEM and the finely ground nature of the samples being analysed, it was not obviously apparent whether a particular area or particle being examined was truly representative of the sample as a whole. However, the observations reported here are the conclusions drawn after examination of several particles/ regions and are believed to be typical of the sample being analysed.

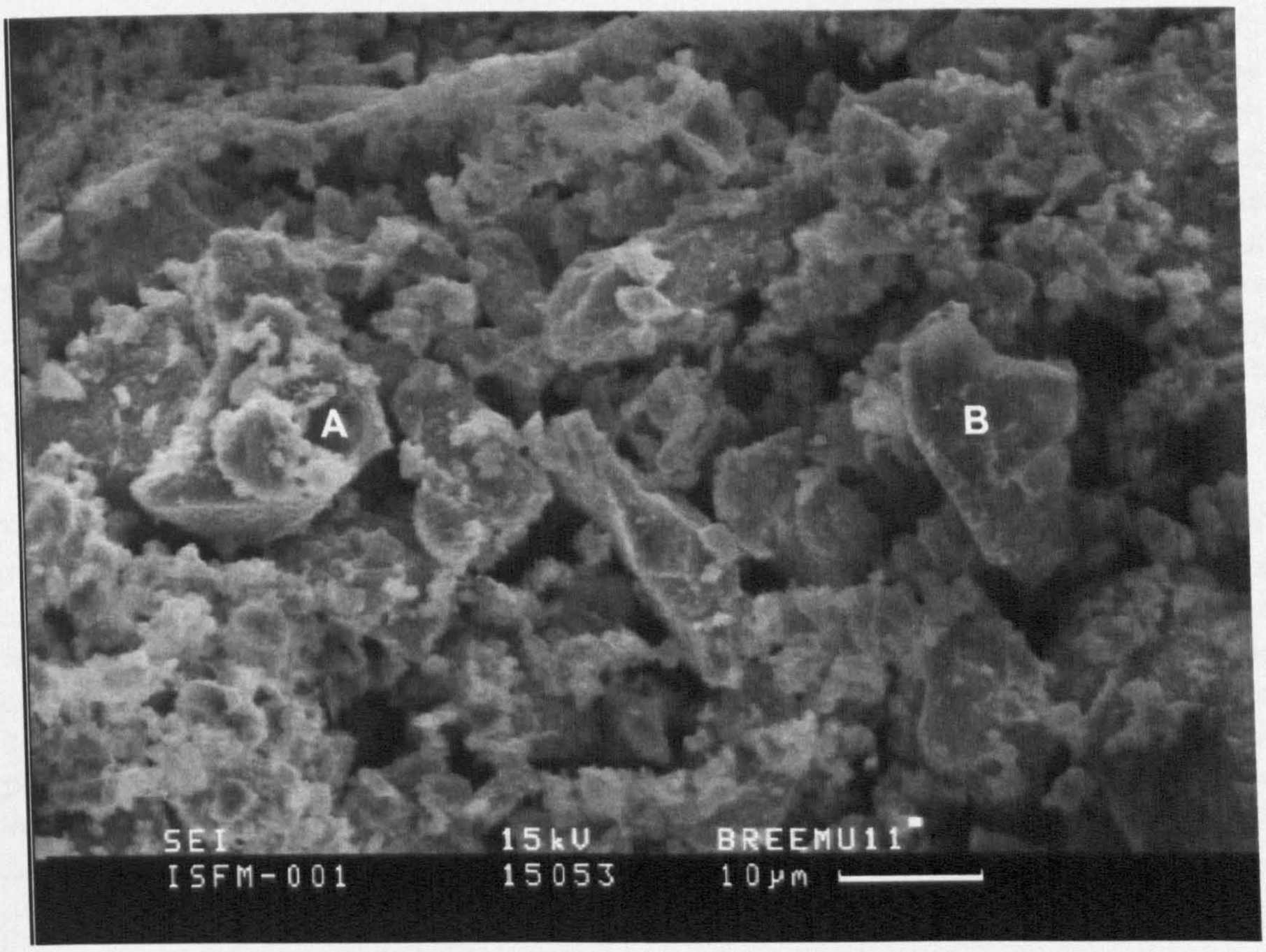

Figure 8.2: Secondary electron image of cement grains within a mortar mix containing ISF slag

8.2.1 Comparison with previous TEM studies on retarding mortars

Previous studies have suggested that it was possible to see evidence of lead-containing gel layers coating cement grains using TEM[111]. It was argued that these layers were responsible for the delay in setting witnessed. Attempts were made to replicate this study in the hope of making similar observations, however several difficulties were experienced.

In the study mentioned, the lead was added as a soluble nitrate solution rather than being contained in an aggregate as in the case of the ISF slag. It was therefore not possible to precisely control the lead (or zinc) addition levels in the mortar to be examined in the same way.

The TEM used by Thomas *et al* for their observations was an AEI EM7 high voltage electron microscope, which allowed the samples to be prepared in a way that was not reproducible with the equipment used for this work (a Philips EM420 TEM) as the vacuum was not sufficient and it would be likely to damage the microscope. (It is assumed from the experimental description in reference [111] that the samples were placed directly into the vacuum chamber of the TEM to remove the remaining water from the sample, effectively quenching it before observation). For this work, samples instead had to be quenched in acetone and dried before being ground and mounted for observation.

The original study used a separate machine to that used for the imaging (a JEM 100C electron microscope) to carry out EDS elemental analysis on the samples. An advantage of the present study is that the TEM used for the observation and imaging was fitted with an integrated EDS system. It is suspected that it would have been difficult, if not impossible, to establish which areas were of a particular elemental composition when the imaging was carried out on a high resolution TEM and the EDS analysis was carried out on a different machine. This raises questions as to the conclusiveness of the outcomes of the previous study. This seems important, since few authors provide direct evidence for a 'coating mechanism' as the cause of the retardation by metal ions, but many others quote this work and imply an coating mechanism is responsible for their own observations. (See for example, references [116-118] & [120])

The sample preparation method adopted for this TEM study was very different to that used in the SEM work with the cryo-stage. It would therefore not be as likely that a cohesive coating would be witnessed around the cement grains during the analysis. It was appreciated that, at best, incoherent fragments of any remaining gel might be detectable on the surface of cement grains when observed by TEM. Unfortunately, since it was established that the ISF slag showed evidence of both amorphous and crystalline phases when diffraction patterns were obtained in the TEM (section 4.5), this feature would not necessarily be useful to help identify amorphous gels from the diffraction patterns of the cement or aggregate particles.

8.2.2 Observations from TEM

Detailed characterisation of the raw materials used in the mortars for TEM observation was given in section 4.5. Further to this, additional cement and ISF mortar samples were examined that were allowed to hydrate and harden. Figure 8.3 shows TEM images and diffraction patterns from the hardened ISF mortar (A), the hardened cement sample (B), the quenched ISF mortar sample (C) and a quenched cement sample for comparison (D).

Although the spot patterns of the hardened samples are different (A & B), they both show the presence of undefined amorphous rings, suggesting that the hardened product in each case was at least partially non-crystalline. When cement and ISF mortar samples were quenched during their hydration period and examined by TEM, no evidence of anything apparently coating the cement grains was observed around the particles. Although the diffraction patterns from the quenched samples (C & D) are ultimately different from the patterns obtained from the raw materials and the hardened cement and mortar samples, the amorphous ring patterns from both quenched samples are very similar, suggesting that the rings must be contributed by the cement. No lead or zinc could be detected around the cement particles by EDS analysis. There was therefore no evidence to suggest that any lead or zinc-containing amorphous coating was present around the cement grains to prevent them from hydrating.

If lead or zinc precipitates were to form in the alkaline environment of a cement mix, you would perhaps expect them to accumulate around the lead or zinc-rich areas from which the ions originated (i.e. the ISF aggregate particles), rather than favouring coating the cement grains. However this was also not witnessed in these samples.

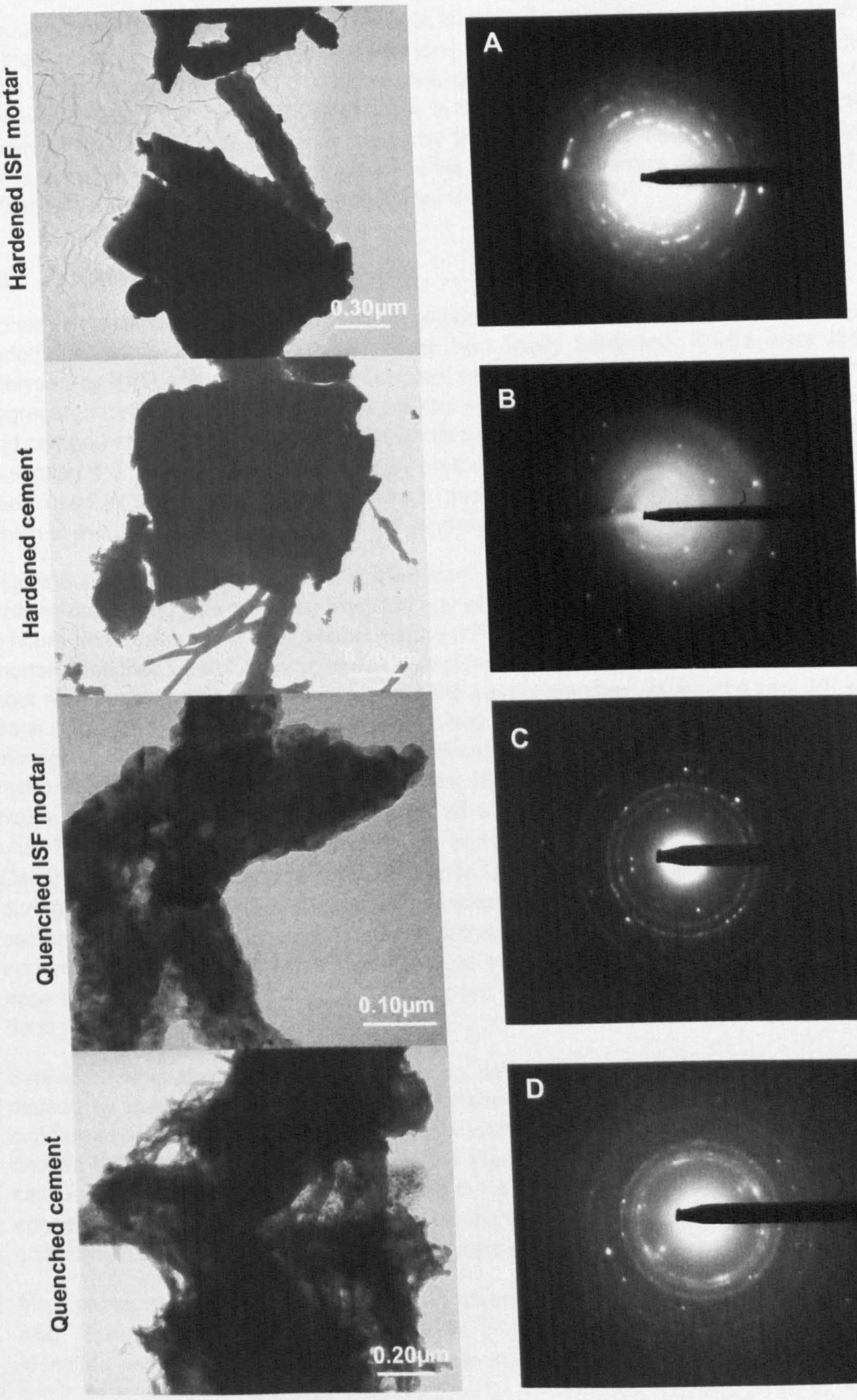

Figure 8.3: TEM images and diffraction patterns from ISF mortars and cement

Although these observations do not appear to support the idea of a coating mechanism for the retardation of set in cement by metal ions, many variations and compromises had to be imposed in an attempt to replicate the original study that was being followed. However, the fact that these difficulties arose in the first place raises questions as to the validity of the conclusions that were drawn by the initial studies. The work that follows tracks the attempts to further prove/ disprove the coating mechanism theory and provide further evidence for an alternative theory about the retardation.

8.3 XRD analysis

Mortar samples containing the ISF slag were quenched over time during the retardation period and up to 28 days after the mortar had finally hardened. These were then analysed by XRD and compared to equivalent samples of hydrated cement and control aggregate mortars. The XRD traces for the raw materials (ISF slag, limestone aggregate and cement) and for hydrating cement quenched over time were analysed and discussed in section 4.3. The peaks that were seen on the XRD patterns of those samples have been used in this section to identify which peaks are attributable to the cement and which to the ISF slag in the quenched ISF mortars.

Figure 8.4 shows the XRD trace obtained from an ISF mortar quenched after 2 hours from mixing, along with the trace from the raw ISF slag and the cement, quenched after 2 hours from mixing as a comparison. Figure 8.5 shows the trace obtained from the ISF mortar quenched after 72 hours, which proved to be approximately equivalent to the 24 hour results obtained from the cement and the control samples. Again, the raw ISF slag trace is included, plus the trace from cement that had been quenched after 28 days from mixing, showing the hardened cement products. The peaks corresponding to calcium hydroxide (CH) only began to appear on the ISF slag traces as small peaks after 48 hours, while the peak at approximately 18° 2θ was not predominant on the XRD traces until 72 hours, by which time the mortar had finally hardened. This confirmed that $Ca(OH)_2$ (CH - Portlandite), which corresponds to the peak at 18° 2θ, was not produced during the retardation period caused by the inclusion of the ISF slag. As witnessed in the cement sample quenched after 28 days, calcium carbonate (CC – $CaCO_3$) was also apparent in the 72 hour quenched ISF sample. Again, CH in the hydrating samples had apparently become carbonated when exposed to carbon dioxide in the atmosphere during sample preparation

Similar observations, of $Ca(OH)_2$ not being detected by XRD during the retardation caused by lead and zinc ions have been made by Lieber[120]. It would appear that the crystallisation of $Ca(OH)_2$ is in some way involved in the mechanism of retardation caused by the ISF slag. This ties in with the theory put forward in section 2.4.6 that the calcium and hydroxide ions may be utilised in the conversion of a lead or zinc hydroxide species into a hydroxy-compound, thus delaying the super-saturation and precipitation of crystalline $Ca(OH)_2$ and so delaying cement hardening.

Most peaks in the XRD traces have been attributed either to the cement or to the ISF slag. Some additional XRD peaks present in the ISF mortar samples could not be identified with confidence (e.g. the peak at 44.6° 2θ, labelled X), but these did not

change appreciably during the retardation period to suggest that they might correspond to a species that was responsible for the delay.

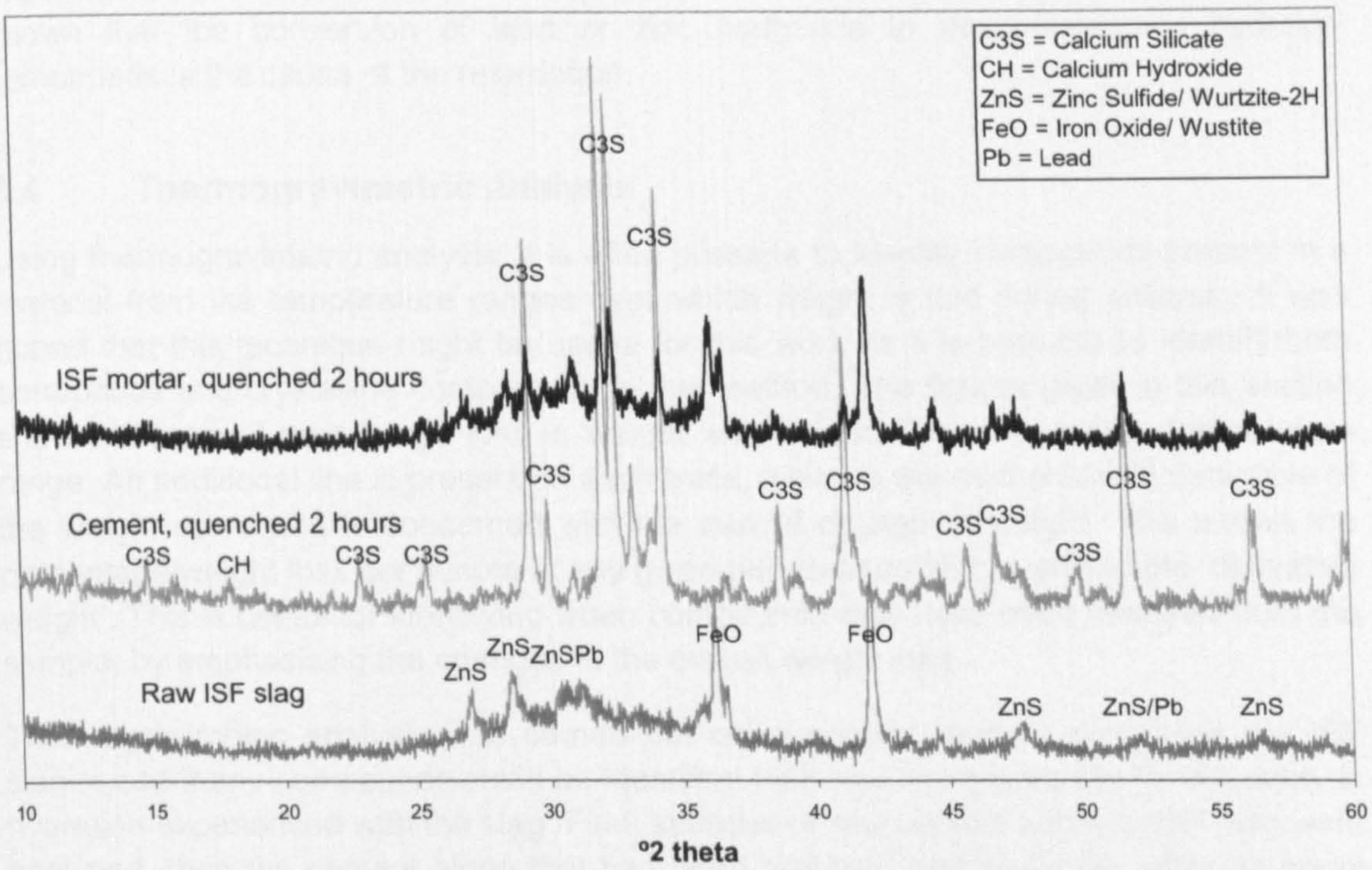

Figure 8.4: XRD trace of hydrating ISF slag mortar, quenched after 2 hours (plus controls)

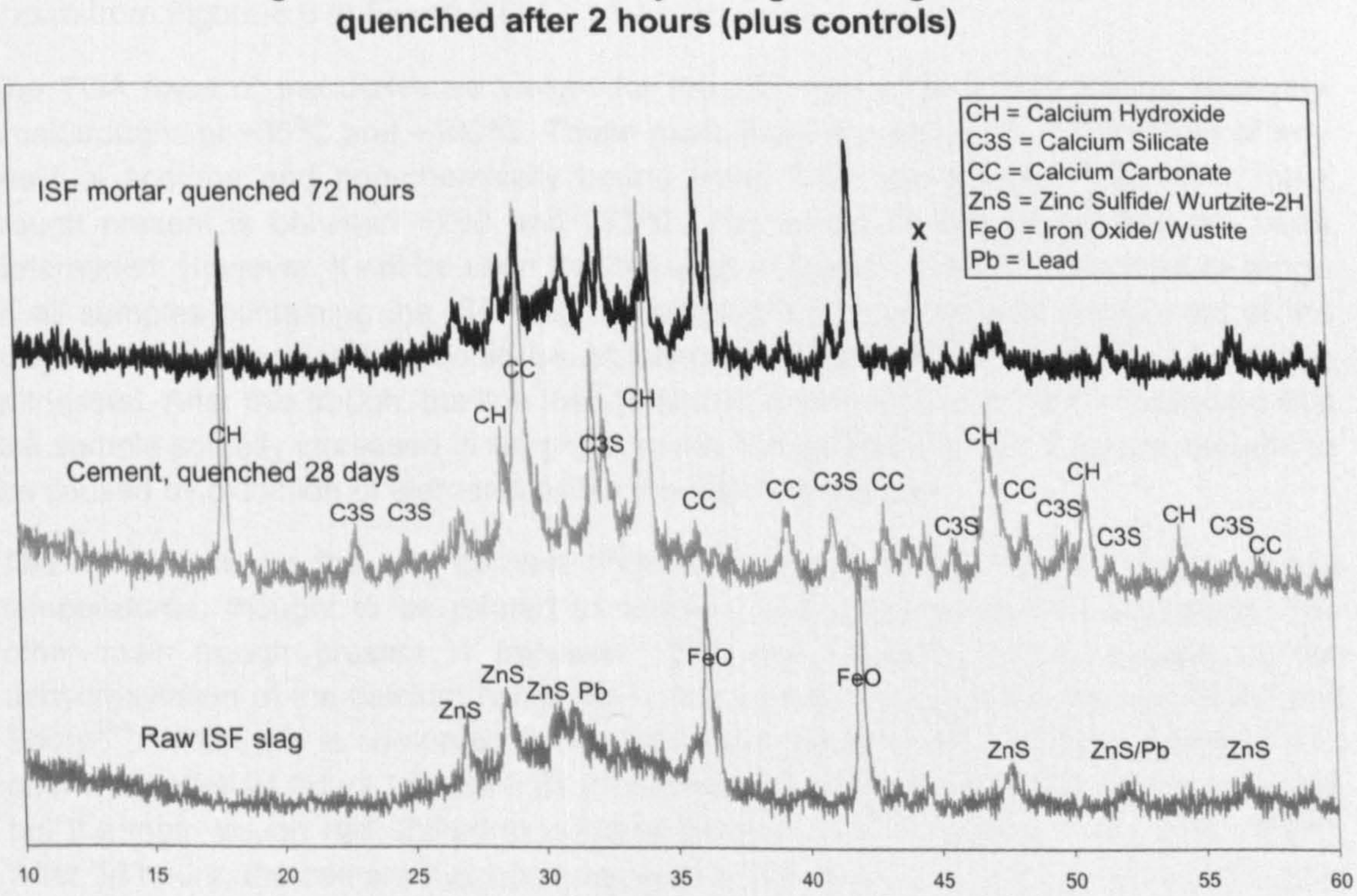

Figure 8.5: XRD trace of hydrating ISF slag mortar, quenched after 72 hours (equivalent to 24 hours with no retardation) (plus controls)

Unfortunately, the hydroxy-zincate species that has been previously reported during cement retardation by zinc[120,123] (or an equivalent hydroxy-plumbate species from lead) could not be identified in the ISF slag samples. Therefore, it cannot be conclusively shown that the conversion of lead or zinc hydroxide to their respective hydroxy-compounds is the cause of the retardation.

8.4 Thermogravimetric analysis

Using thermogravimetric analysis, it is often possible to identify compounds present in a material from the temperature ranges over which weight is lost during analysis. It was hoped that this technique might be useful for this work as it is possible to identify both amorphous and crystalline compounds by this method. The figures given in this section show the gradual percentage loss in weight with time over an increasing temperature range. An additional line is present on each trace, which is the mathematical derivative of the weight curve and is concerned with the rate of change of weight. This shows the percentage weight loss per minute at any given temperature and is termed the 'derivative weight'. This is useful for identifying when compounds may have been released from the sample, by emphasising the changes in the overall weight loss.

Thermogravimetric analysis was carried out on quenched mortars containing the ISF slag to see if any compounds could be identified that may be responsible for the delay in hydration experienced with the slag. First, samples of raw cement and raw ISF slag were analysed, then the cement alone that had been hydrated and quenched after 24 hours as a comparison to the hydrated ISF slag mortar mixes. The results from these runs are shown from Figure 8.6 to Figure 8.8.

The TGA trace of the derivative weight for the ISF slag (Figure 8.6) shows relatively small troughs at ~35°C and ~100°C. These most likely correspond to evaporation of any residual acetone and non-chemically bound water from the sample. The other main trough present is between ~200 and 275°C. The cause of this trough has not been determined. However, it will be seen that a trough is evident over this temperature range in all samples containing the ISF slag, suggesting it is a permanent component of the slag and not a species that could be attributed as responsible for the delay in setting witnessed. After this trough, the line then peaks between ~275 and 340°C, indicating that the sample actually increased in weight over this temperature range. This was thought to be caused by oxidation of elements within the ISF slag sample.

The TGA trace for the raw cement (Figure 8.7) again shows small troughs at low temperatures, thought to be related to acetone and unbound water evaporation. The other main trough present is between ~375 and ~430°C. This is caused by the dehydroxylation of the calcium hydroxide in the cement, as demonstrated by Bland and Sharp[148]. When this is compared to the trace from cement that had been hydrated and quenched after 24 hours (Figure 8.8), it can be seen that generally they are very similar, but the main trough has shifted to a higher temperature of between ~390 and ~470°C. After 24 hours, the cement hydration reaction would have been well underway and more hydration compounds (including calcium hydroxide) will have formed. It would therefore take longer to decompose the calcium hydroxide present in the hydrated cement than it would in the anhydrous cement, hence the peak and final temperatures would be displaced to higher temperatures, as observed.

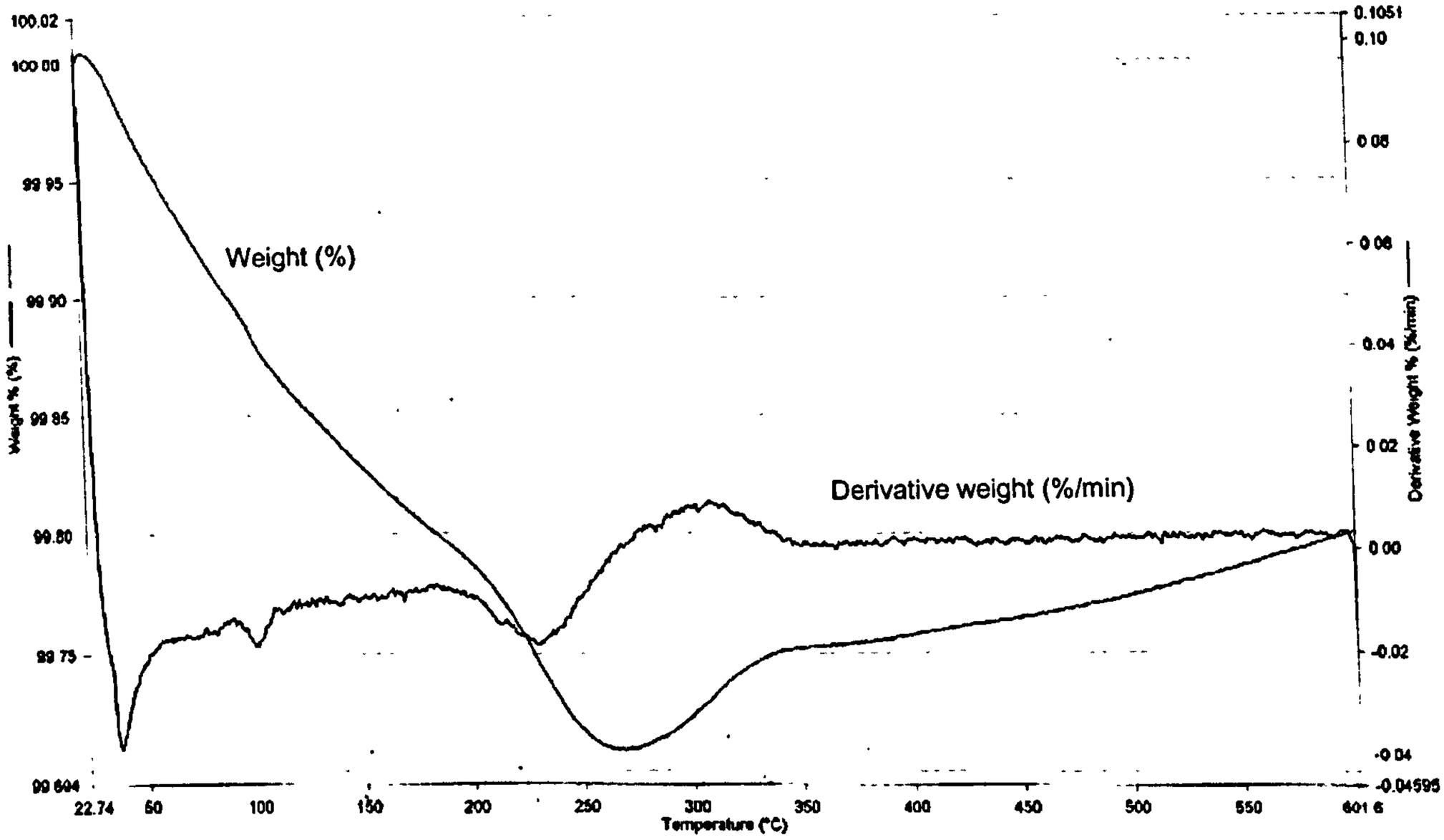

Figure 8.6: TGA data for ISF slag alone

From these curves, it is also possible to quantitatively determine the amount of CH present in the sample, by measuring the step in the curve associated with the breakdown of the phase. The sloping lines either side of the step region mean that the measurement of the step must be approximated by using the points at which tangents from each of the lines cross[148]. The raw cement sample in Figure 8.7 shows a change of ~0.3%, attributable the CH present initially in the cement, while the cement that has been quenched after 24 hours in Figure 8.8 shows a change of ~1.7%. As the cement has hydrated, more CH has been produced as a hydration product.

These TGA runs act as a useful control to which the results from quenched mortars containing the ISF slag could be compared. TGA traces from these mortars quenched at various times from 2 hours up to 72 hours are shown in Figure 8.9 to Figure 8.12. Initially, it would appear that one of the TGA traces is out of sequence. The 24 hour quenched sample shows a trough between ~400 and ~470°C, while those either side of it at 2 hours and 48 hours do not. However, the trough reappears and is larger after 72 hours. Re-running the samples confirmed that they had not been mixed up.

The trough at this point corresponds to that on the hydrated cement sample quenched after 24 hours, as shown in Figure 8.8, suggesting that it is attributable to CH in hydrated cement. The sample had visibly not hydrated by this time and it is thought that the presence of this trough after 24 hours comes as a result of inadequate quenching of the mortar sample. The samples were quenched in acetone, which was replaced at intervals in an attempt to remove all the unbound water present in the mortar samples. However, if not all of the water was driven off, the sample will have continued to react with any remaining water and hydrate over time, which would account for the observation seen here.

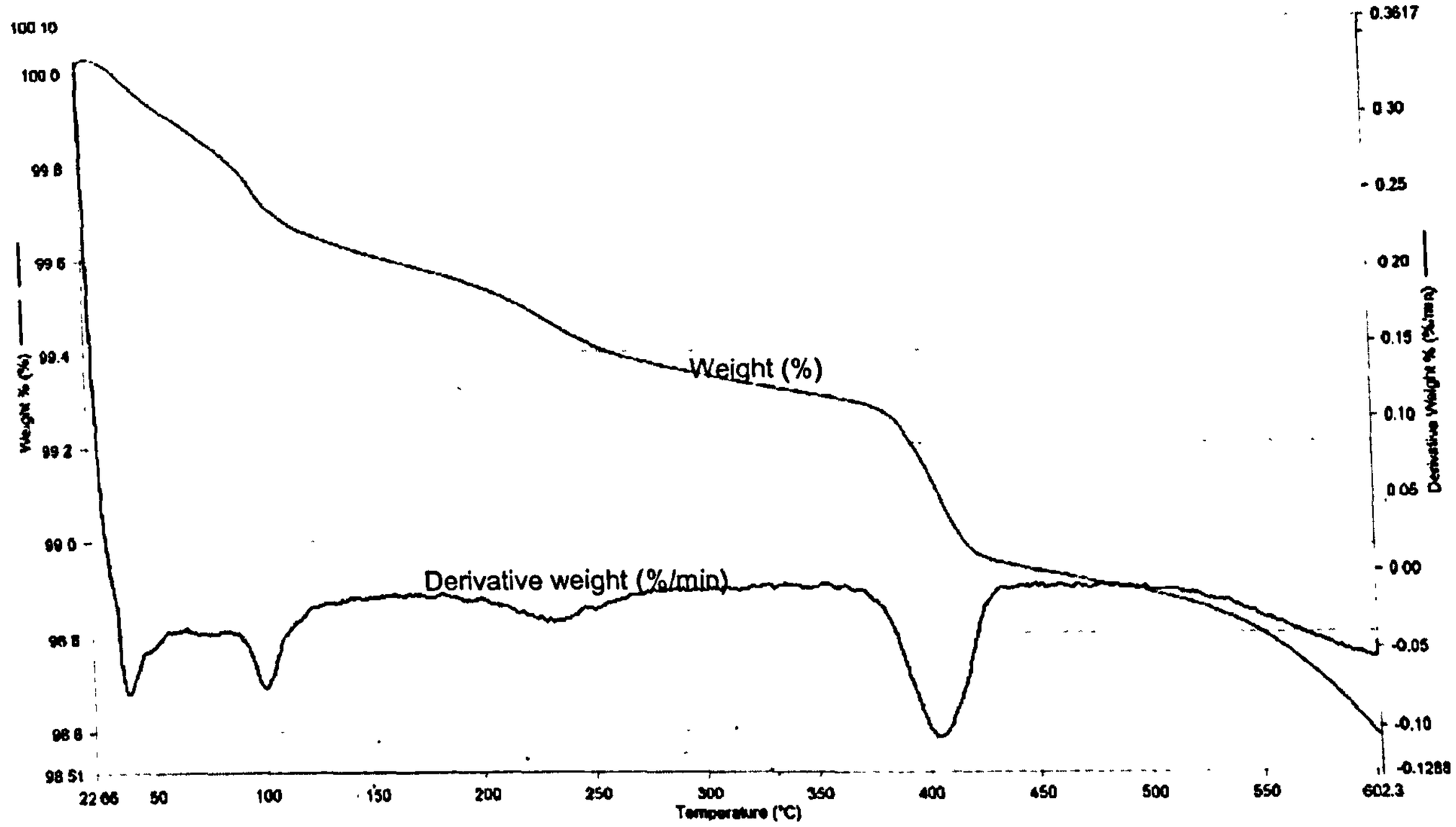

Figure 8.7: TGA data raw cement

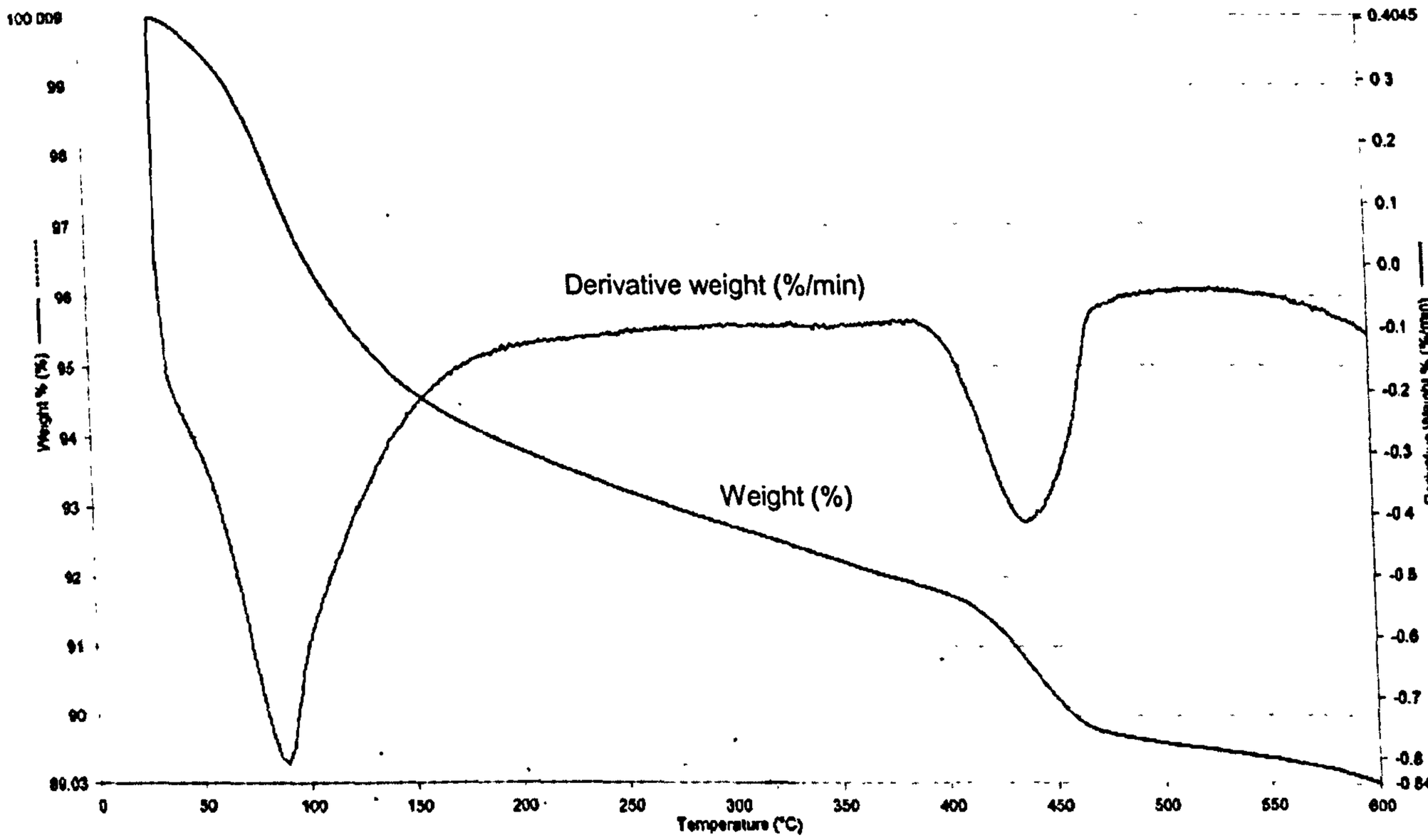

Figure 8.8: TGA data for cement that had been hydrated and quenched after 24 hours

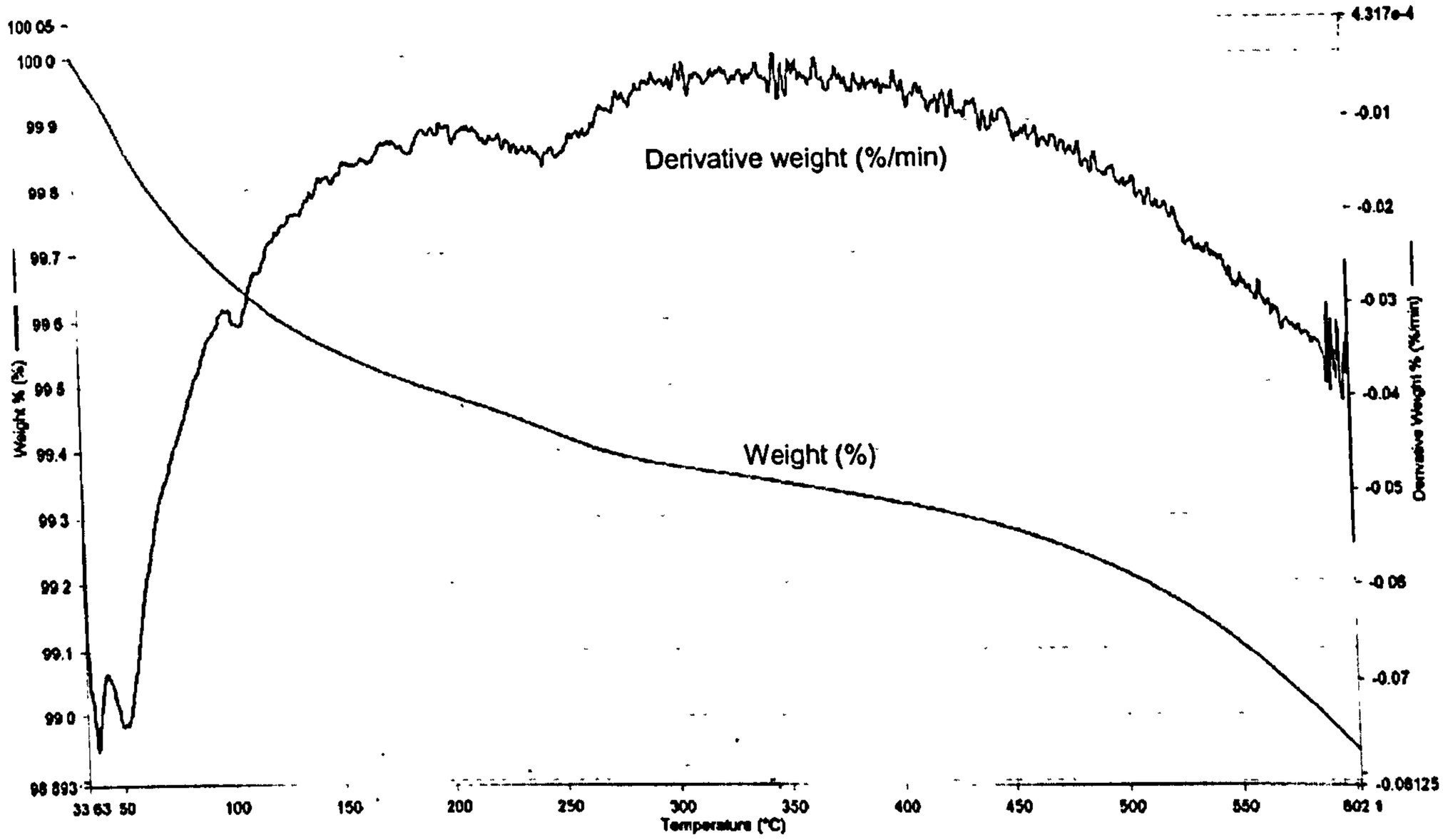

Figure 8.9: TGA data for ISF slag mortar that had been hydrated and quenched after 2 hours

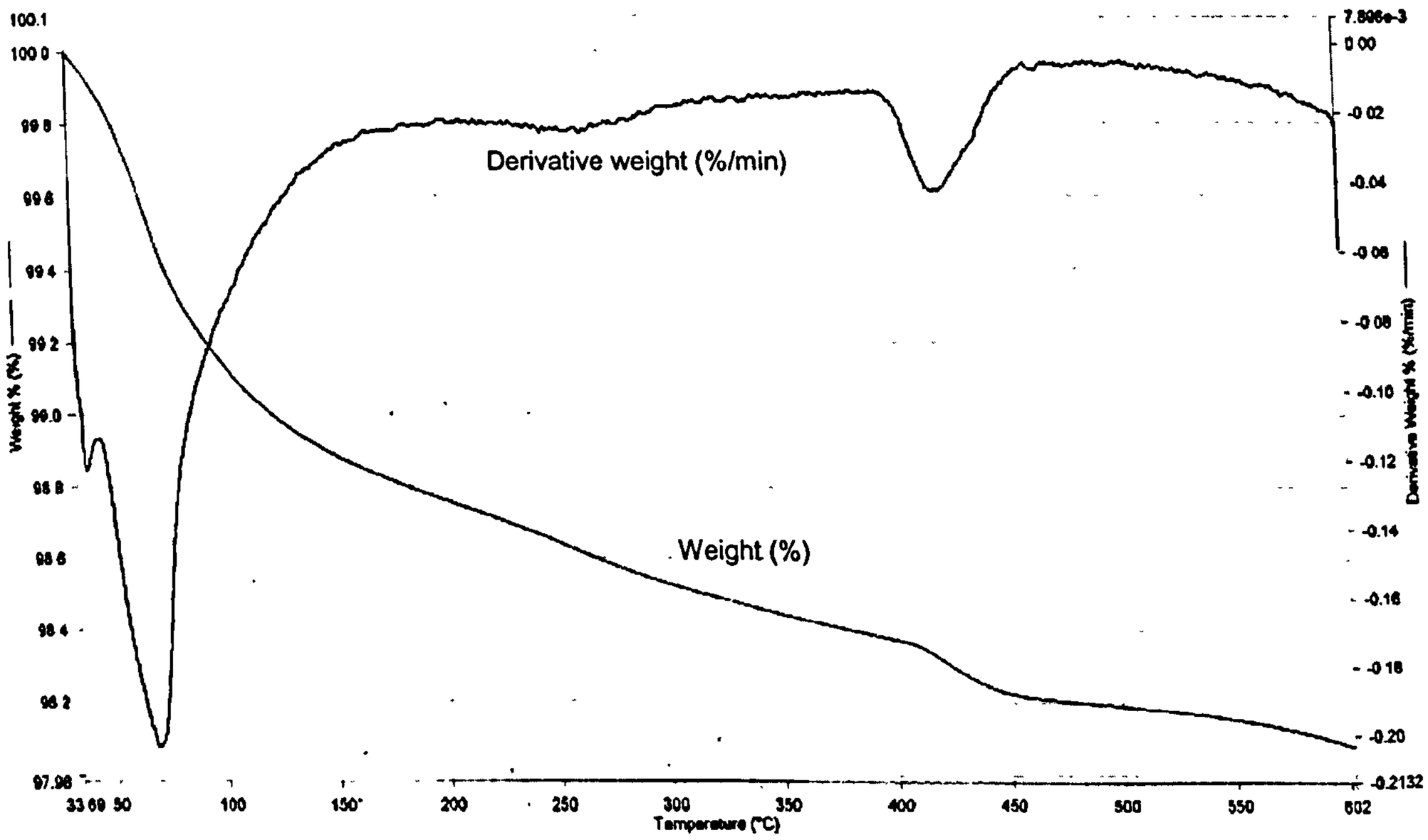

Figure 8.10: TGA data for ISF slag mortar that had been hydrated and quenched after 24 hours

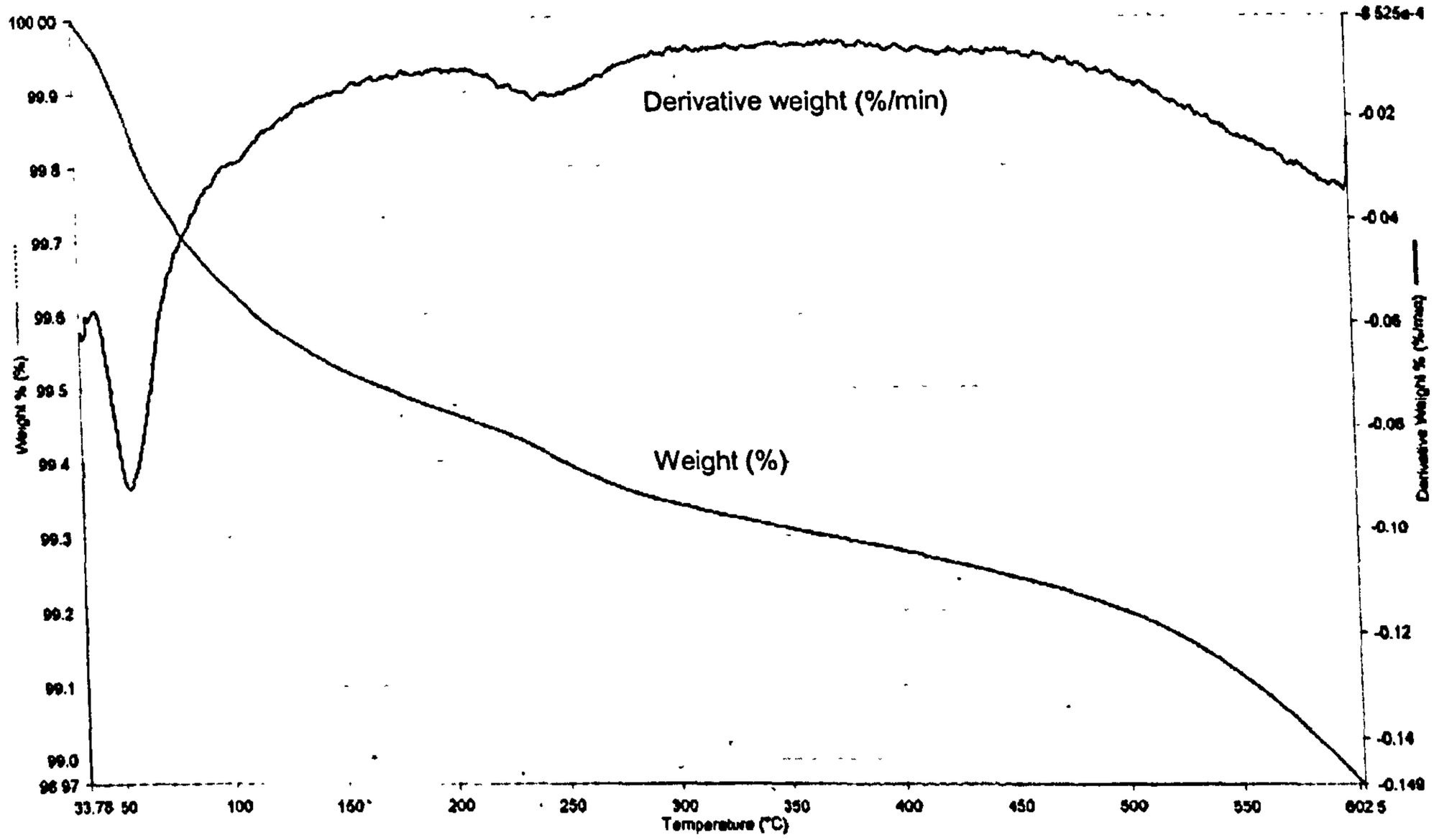

Figure 8.11: TGA data for ISF slag mortar that had been hydrated and quenched after 48 hours

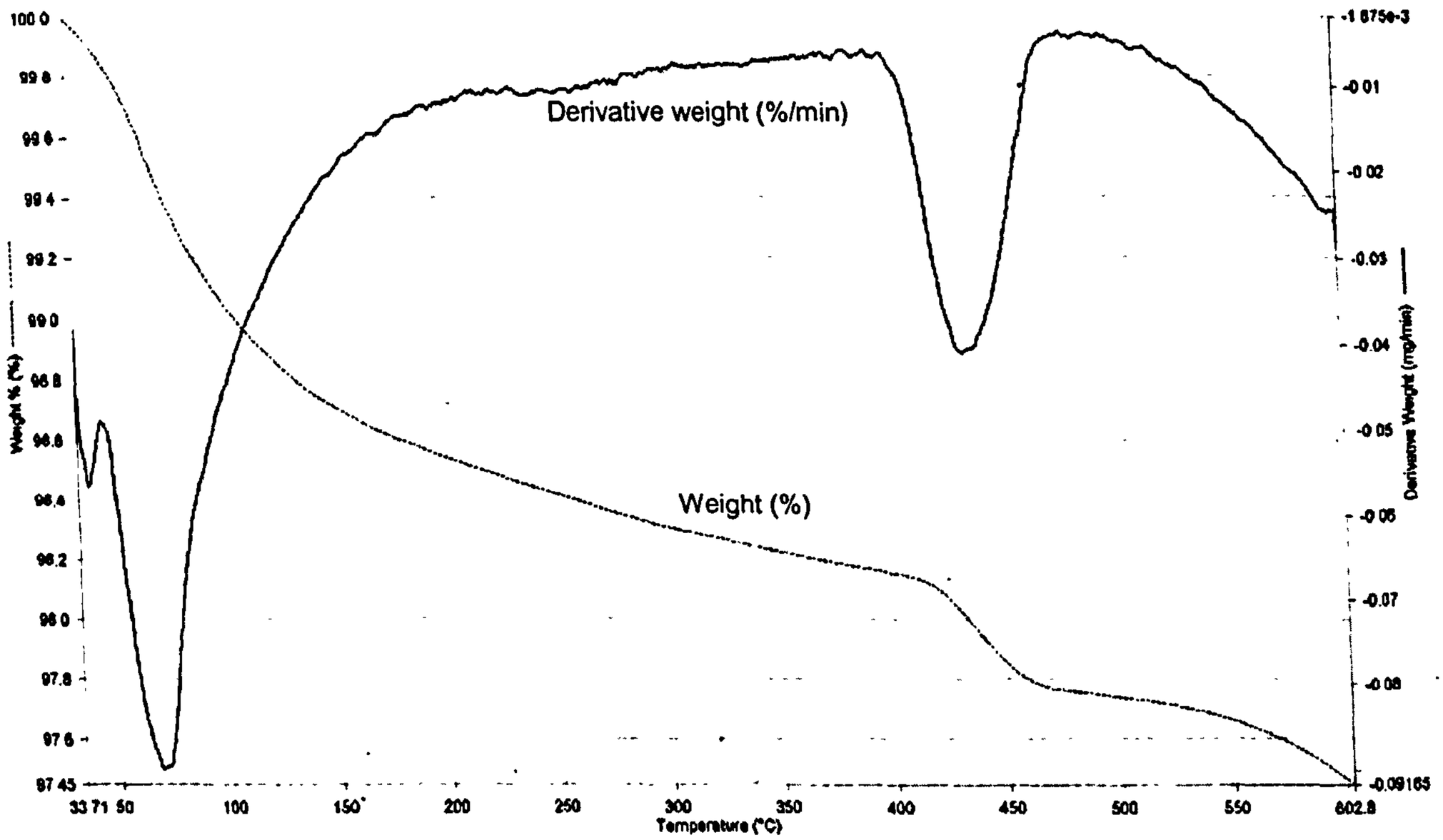

Figure 8.12: TGA data for ISF slag mortar that had been hydrated and quenched after 72 hours

After 72 hours the CH trough between ~400 and 470°C reappeared and by this time the ISF mortar sample had hardened, so it is thought to be a genuine effect. It was not thought practical to attempt to calculate the percentage of CH present in the hydrated ISF slag sample. The analysis of the ISF slag sample alone (Figure 8.6) shows a gain in weight over this temperature range, which would obviously conflict with the loss experienced by the dehydroxylation of CH.

In addition to this trough, the trough between ~200 and ~275°C that was evident in the raw ISF slag sample can also be detected at various intensities in the mortars quenched over time. No additional troughs were detected, other than these, that could potentially have been attributed to the retarding species present in the ISF slag mortars.

8.5 Isothermal conduction calorimetry

Isothermal conduction calorimetry (ICC) provided a small scale method of assessing the delayed hydration period when ISF slag was included in mortar samples. It was also a convenient method to test various additives in association with the slag to see if the retardation could be overcome. All additives were tested at 'high' and 'low' addition levels. Any that were found to be useful in reducing the retardation experienced were used in full-scale concrete mixes and tested using internal temperature monitors and logging equipment (section 8.6). The aggregates were ground to pass a 150µm sieve before being used in the mortars for this testing, so the heat generated by the cement hydration reaction would transfer evenly throughout the sample to the detectors.

It is appreciated that grinding the samples in this way may have increased the surface availability of the metal ions (lead and zinc) that were suspected to be responsible for the delay in set experienced. These retardation results were therefore anticipated to be more severe than would be expected from a regular concrete or mortar mix.

Due to the number of additives tested, it was not possible to carry out duplicate runs in order to obtain an average of the results. Even if time had been available for this to be done, due to the nature of the testing it would probably not have been a particularly useful indication of the associated errors. Although samples were all mixed in the same way, there will have been inevitable time differences incurred when setting up the mortar samples in the calorimeter. All sample profiles will be accurate to within approximately 10 minutes and the maximum heat energy generated will be accurate to approximately ±0.05 W/kg, when the variation in the output is assessed. Since the reaction that is being considered takes place over days rather than hours, these errors were not seen to be significant to this testing.

8.5.1 Influence of zinc and lead doping on control aggregate mortars

Figure 8.13 shows the calorimetry results obtained from testing a control aggregate mortar that had been doped with 0.2g of either PbO or ZnO. The rise in energy observed, generated by the hydration of the mortar mix and calculated here as W/kg, shows the time over which hydration took place for each of the mixes.

It can be seen that both lead and zinc cause a delay in hydration, when compared to the control. The lead addition delays hydration for approximately 24 hours, while the zinc

addition causes a delay of approximately 120 hours. 0.2g of the metal oxide was added in each case, so they were not equivalent on a molar basis. Equivalent molar additions would be expected to show a less dramatic variation in the time to hydration. However, these results confirm that lead and zinc ions do cause a delay in the hydration of cement.

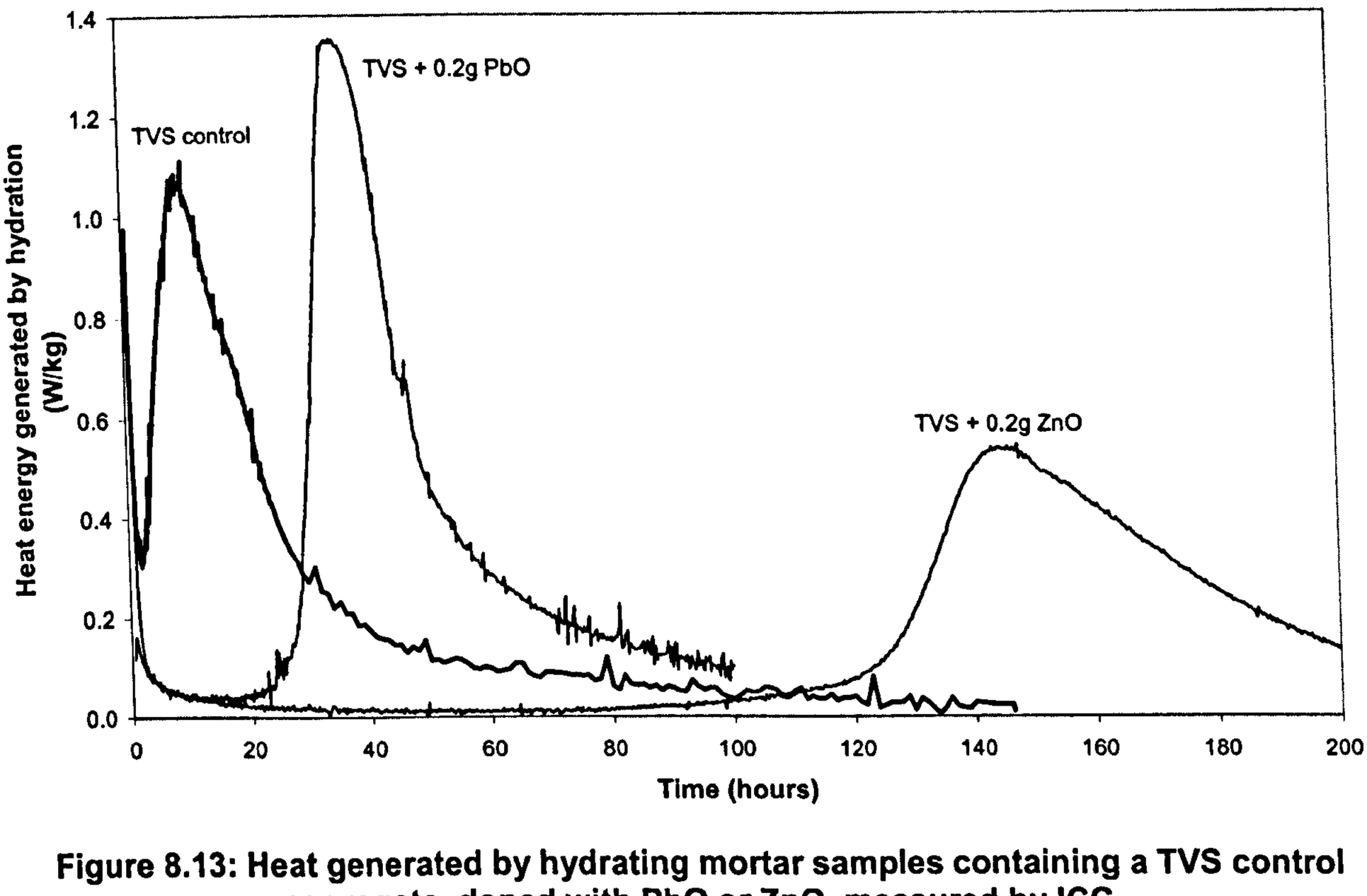

Figure 8.13: Heat generated by hydrating mortar samples containing a TVS control aggregate, doped with PbO or ZnO, measured by ICC

8.5.2 Influence of ISF slag replacement level on retardation of mortar samples

To establish a manageable delay period that could be used as a benchmark to assess the effect of any additives tested, the ISF slag was used at various replacement levels in the mortars, from 20% up to 100%. The calorimeter results for this are shown in Figure 8.14. As the ISF slag replacement level is increased, the onset of hydration is delayed and the maximum hydration energy observed is reduced. Figure 8.15 shows the total energy output for each of the samples over time, once hydration had commenced. Apart from the 20% ISF sample, which shows a slightly different shaped profile in Figure 8.14, the total heat output of all the other samples are close to that of the control (0% ISF) and lie between ~100-120kJ/kg, suggesting that cement hydration has occurred to approximately the same extent in all samples, once the delay has passed.

When the time to hydration is plotted against the percentage ISF slag replacement, as shown in Figure 8.16, it can be seen that the relationship is non-linear. A proportionally longer delay is experienced as the ISF slag replacement level is increased. The reason for this is not clear. If the variation was related to the increased ISF slag surface area available from which the metal ions could leach, a linear trend would be expected. The curve in the data line is more closely fitted to a 'squared' relationship (as shown by the dotted line on the graph), perhaps suggesting that more than one factor is influencing the resulting behaviour.

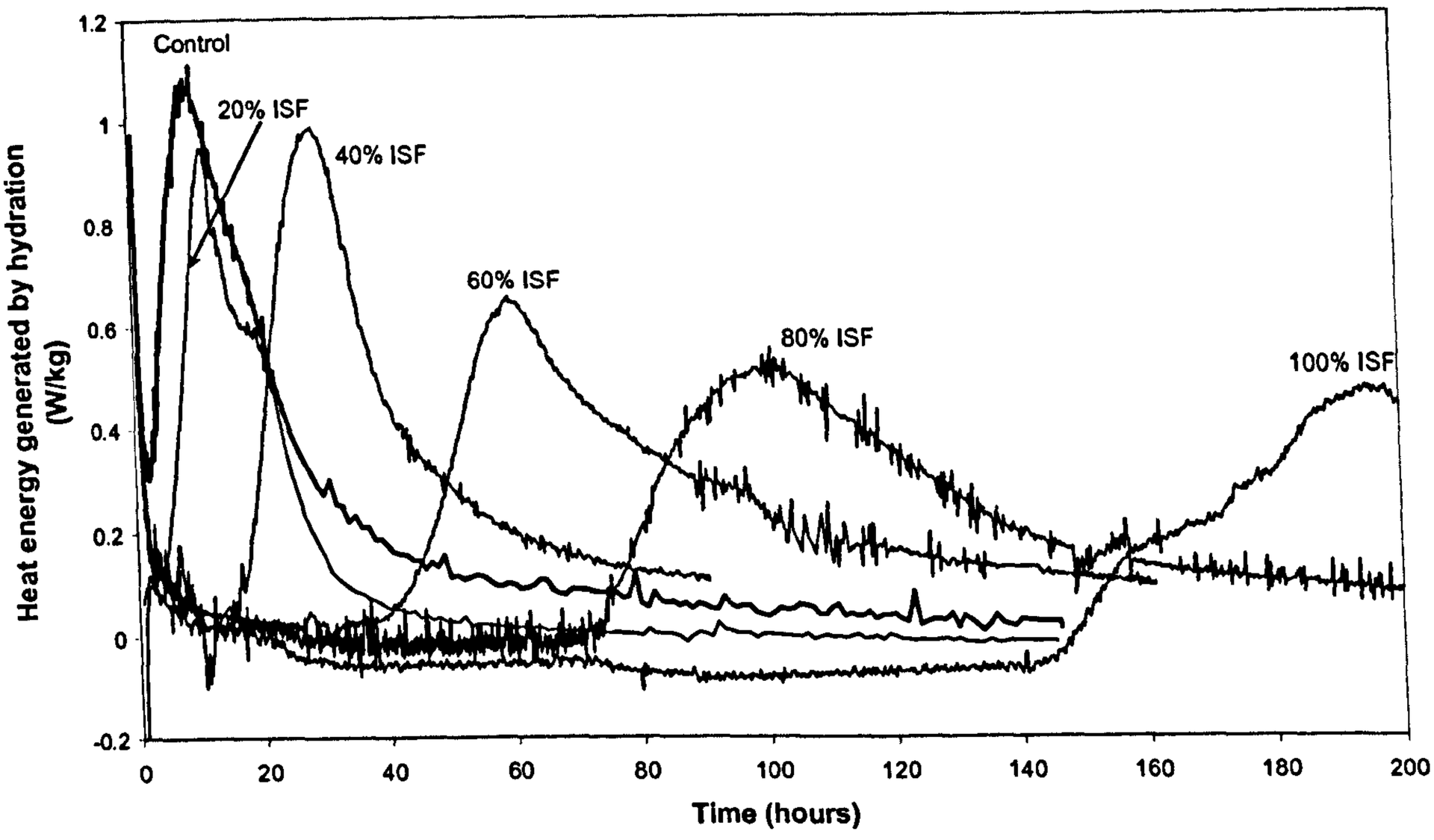

Figure 8.14: Heat generated by hydrating mortar samples containing ISF slag, measured by ICC

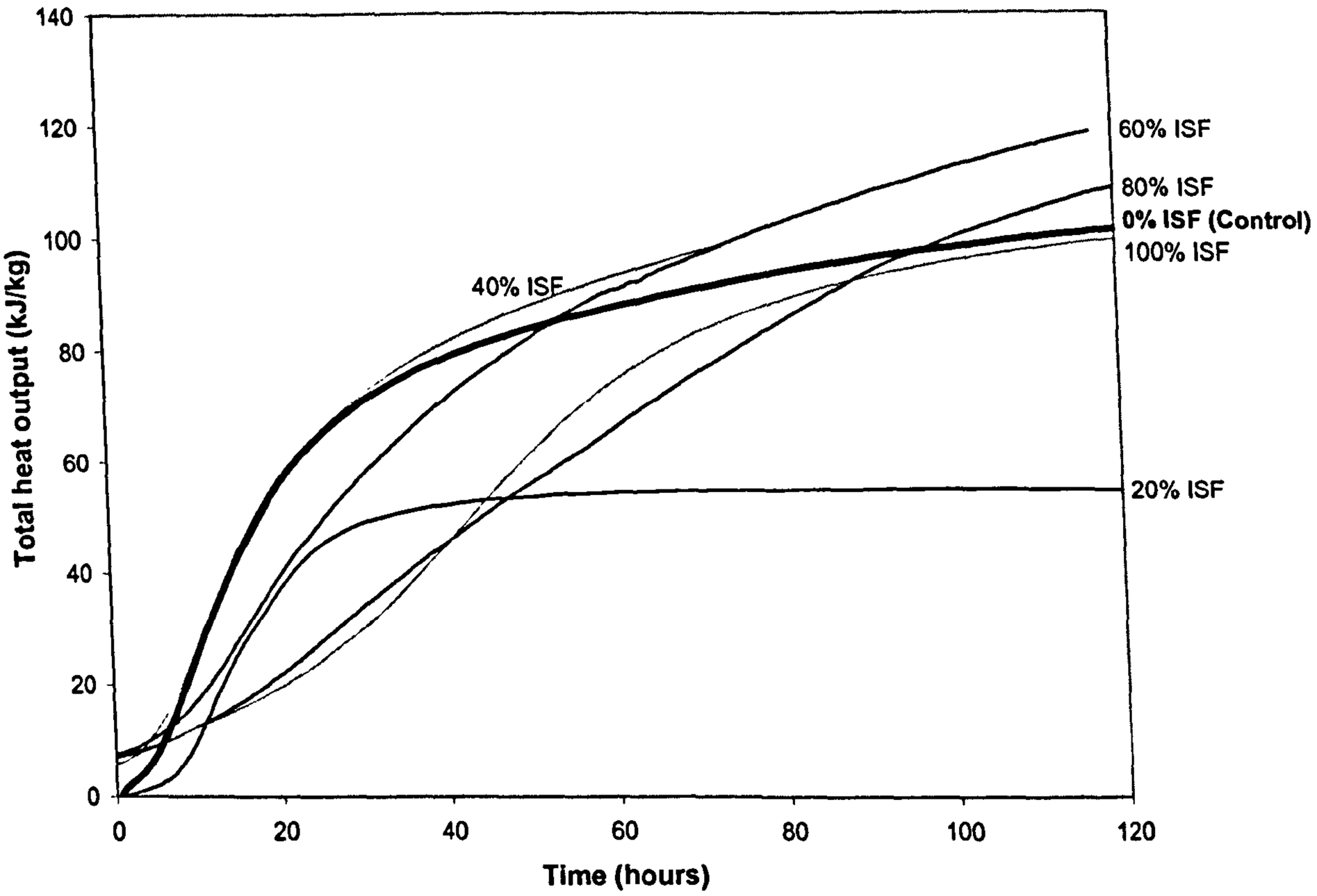

Figure 8.15: Total heat output of samples shown in previous figure, once hydration has commenced

If this relationship between the percentage ISF slag replacement and the time to hydration were true for full scale concrete mixes as well as the mortars made with ground aggregate, it would be possible to approximate the delay that would be experienced for any given replacement level. However, due to the variables that are introduced by grinding the aggregate, this data would not be directly transferable to a full scale concrete mix. Varying replacement levels were not tested in concrete, since the main focus of the work was to investigate additives that may be able to overcome the delay if high ISF replacement levels were used.

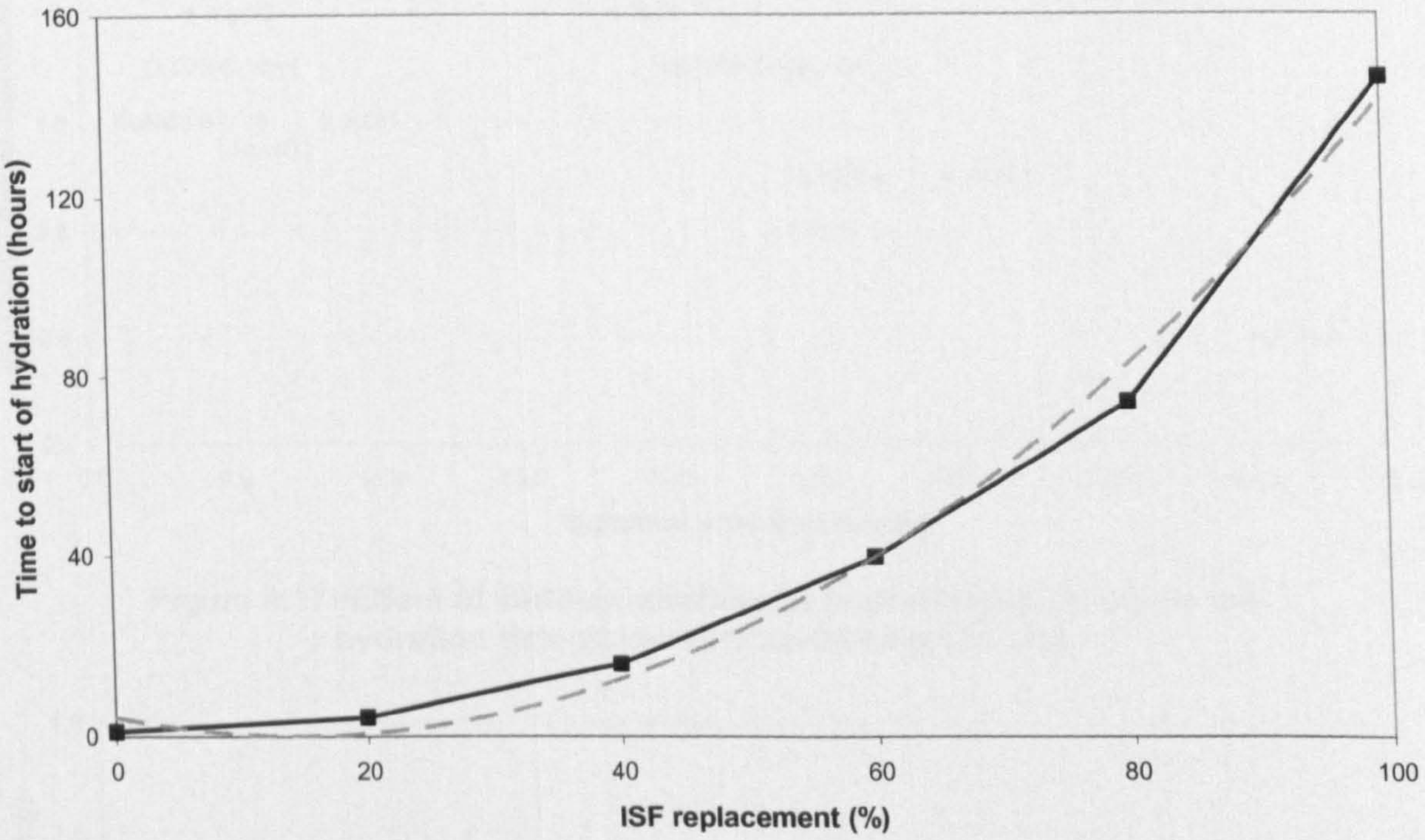

Figure 8.16: Variation in time to hydration with % ISF slag replacement

It was known by this time that concrete samples containing ISF slag as a 100% replacement for the sand normally present in a mix were demouldable 3 days after mixing. It was therefore decided that 60% replacement would provide a suitable delay from which the effect of the various additives could be distinguished.

8.5.3 Influence of chemical additives on retardation

Once the ISF replacement level of 60% had been established, various additives were tested. Results for the additives have been presented as the maximum hydration energy against the time to hydration in the following figures, so their effects can be clearly distinguished. Figure 8.17 shows the results from the 'high' addition levels, while Figure 8.18 shows the results from the 'low' addition levels (as discussed in section 3.6.4). The closer the results are to the TVS control aggregate sample, the more useful the additive is seen to be at overcoming the retardation caused by the ISF slag. The higher the reaction energy, the more vigorous the reaction had apparently been once hydration had commenced.

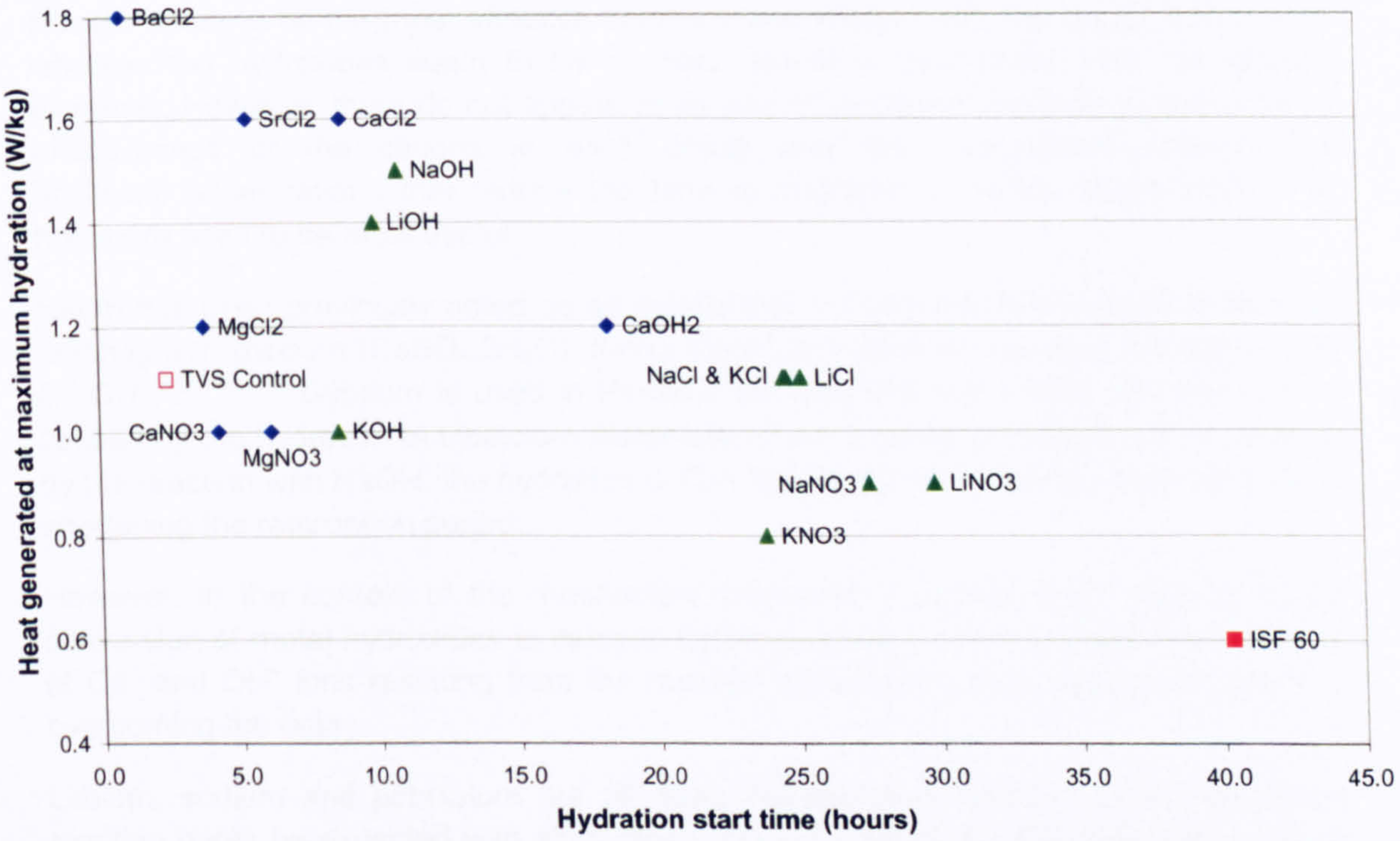

Figure 8.17: Effect of various additives at high addition levels on the hydration time of mortars containing ISF slag

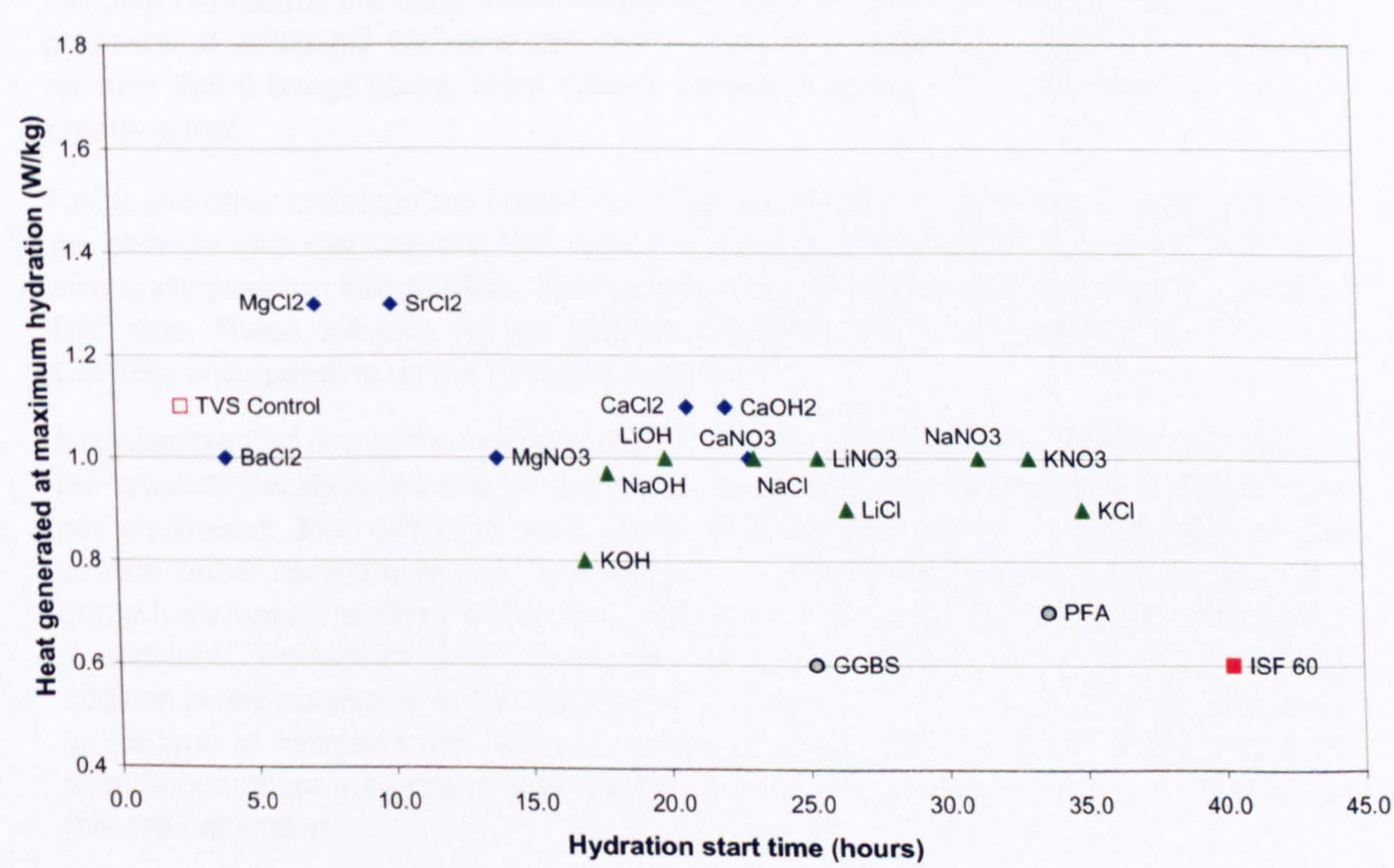

Figure 8.18: Effect of various additives at low addition levels on the hydration time of mortars containing ISF slag

In both figures, additives based on group II elements (♦) appear to be generally better at overcoming the retardation than those based on group I elements (▲). The chlorides and nitrates seem to be the most effective anions in association with the group II elements, whereas the hydroxides seem to be of most benefit in association with the group I elements. However, there do not appear to be any other definite patterns in the order of effectiveness of the cations in each group and their associated anions. The additives/concentrations that reduce the time to hydration to within approximately 16 hours are seen to be most useful.

NaOH has been previously noted as an accelerator in concrete. It is thought to work by reacting with gypsum ($CaSO_4.2H_2O$) during the initial hydration, resulting in Na_2SO_4 and $Ca(OH)_2$[142,149,150]. Gypsum is used in Portland cement to prevent flash set that can be caused by the hydration of tricalcium aluminate (C_3A). If some of the gypsum is used up by the reaction with NaOH, the hydration of C_3A may occur more quickly than usual, thus shortening the retardation period.

However, in the context of the mechanism proposed in section 2.4.6 relating to the conversion of metal hydroxides to calcium hydroxy-species, the increased concentration of Ca^+ and OH^- ions resulting from the reaction with $CaSO_4$ may also be beneficial in overcoming the delay.

Lithium, sodium and potassium are all more reactive than calcium, so an equivalent reaction might be expected with all of these group I hydroxides. The calorimetry results for the group I hydroxides seem to support this. The only group II hydroxide tested was $Ca(OH)_2$, which will obviously not react in the same way with $CaSO_4$ as NaOH. Although $Ca(OH)_2$ did reduce the delay experienced with the ISF slag, this may just be due to the presence of additional Ca^+ and OH^- ions in the mix, rather than from any additional reaction that it brings about. More soluble calcium species (Cl^-, NO_3^-) seem to have a greater effect.

$CaCl_2$ and other chlorides are known to act as accelerators in concrete. It is thought that the chloride ions displace the OH^- ions in tricalcium silicate (C_3S) that would normally eventually pass out into solution. This causes a premature saturation of the solution with OH^- ions. These will pick up any calcium ions that are in the solution, thus forming $Ca(OH)_2$ and speeding up the hydration reaction[151].

It is possible that one of the reasons why the group I chlorides did not perform as well as the group II chlorides is because the molar concentrations of the chlorides added were not equivalent. The additions were made at equivalent molar concentrations of the cations rather than the anions, to compare the relative behaviour of the group I and group II elements, so there will be twice the molar concentration of chloride in the group II additions. Potassium and lithium chlorides show moderate improvement at high addition levels compared to the low additions. However, there is relatively little difference in the time to hydration with NaCl at the two concentrations. In fact, the lower addition level brings about a slightly shorter delay than the higher concentration. The reasons for this are not known.

Also, the chlorides of the other group II metals tested appeared to be more effective than $CaCl_2$. This may be related to their respective solubilities. At room temperature, the order

of solubility of the group II ions is Ba<Sr<Mg<Ca[152]. Although the order of efficiency of the ions as accelerators does not exactly follow this pattern, barium is certainly the most effective and calcium the least effective at both addition levels. The reason why the least soluble ions are most effective is again unclear. It is suspected that the nitrates may undergo a similar type of reaction, since the results of the nitrates, when compared to their equivalent chlorides, are often of a similar order. However, a reliable pattern is again not apparent.

In general, the common influence of all of these proposed additives seems to be to increase the concentration of hydroxide ions in solution. Calcium ions will be provided by the cement as it hydrates (or other group II ions may reduce the need for calcium by reacting with the retarding species in its place), which would allow the super-saturation and precipitation of $Ca(OH)_2$ to occur more quickly and so reduce the retardation experienced. More details about this proposed mechanism are given in section 8.7.

Barium and strontium additions have been shown to be useful in overcoming the retardation experienced with the ISF slag. Since the CRT glass contains these ions, it is possible that they may play some part in preventing a delay with the CRT glass. However, as mentioned earlier, from the leaching results it is thought that it is more likely to be a result of the relative speed at which lead is able to leach from the two aggregate materials.

8.5.4 Influence of PFA, GGBS on retardation

Figure 8.18 also included the results from calorimetry experiments using additions of PFA and GGBS in association with the ISF slag. These additives appear to offer a slight improvement in the delay experienced, but are not as effective as many of the additives already discussed. The results that were obtained from temperature monitoring of concrete containing the additives show a different trend and are discussed in the next section (8.6).

8.6 Temperature monitoring of setting concrete

Temperature monitoring was carried out on various concrete mixes containing the ISF slag as a replacement for the fine aggregate normally in the mix. The loggers used were programmed to take readings every 15 minutes to the nearest 0.5°C. Details of the mixes tested were given in Table 5.2.

8.6.1 Effect of cement content and w/c ratio on the retardation period

Figure 8.19 shows the temperature profiles obtained from ISF-concrete mixes of varying cement content and water/ cement ratio, compared to a control mix using Thames Valley Sand aggregate. It can be seen that the ISF slag mixes show a characteristic delay in set, similar to that experienced during the calorimetry analysis. The TVS control mix shows an increase in temperature over the first few hours after casting. The maximum temperature reached is similar to that obtained with the ISF slag mixes of the same w/c ratio. The temperature profiles for the control mix are identical to the ISF slag mixes apart from the delay in set, which suggests that the extent of hydration, although delayed, is the same.

The graph also shows that increasing the cement content, regardless of the corresponding w/c ratio, reduces the retardation period experienced with the ISF slag. Reducing the w/c ratio only influences the maximum temperature reached, rather than the delay. This implies that the most important relationship to dictate the retardation behaviour of concrete mixes containing the ISF slag is the cement/ ISF aggregate ratio. Therefore, if the ISF slag replacement level in the mix was reduced, a proportionally shorter delay period would be experienced, as witnessed in previous studies[40].

The delay caused by the presence of heavy metal ions in concrete has previously been attributed to the presence of gelatinous metal hydroxide layers coating the cement grains and preventing hydration, as mentioned in section 2.4.6. If this were the case, the heat generated by the reaction may be expected to increase more gradually, as hydration would likely be dependent on the diffusion of water through this layer to the cement. However, this is not the case and the reaction profiles that eventually occur with the ISF slag are essentially identical to that of the control.

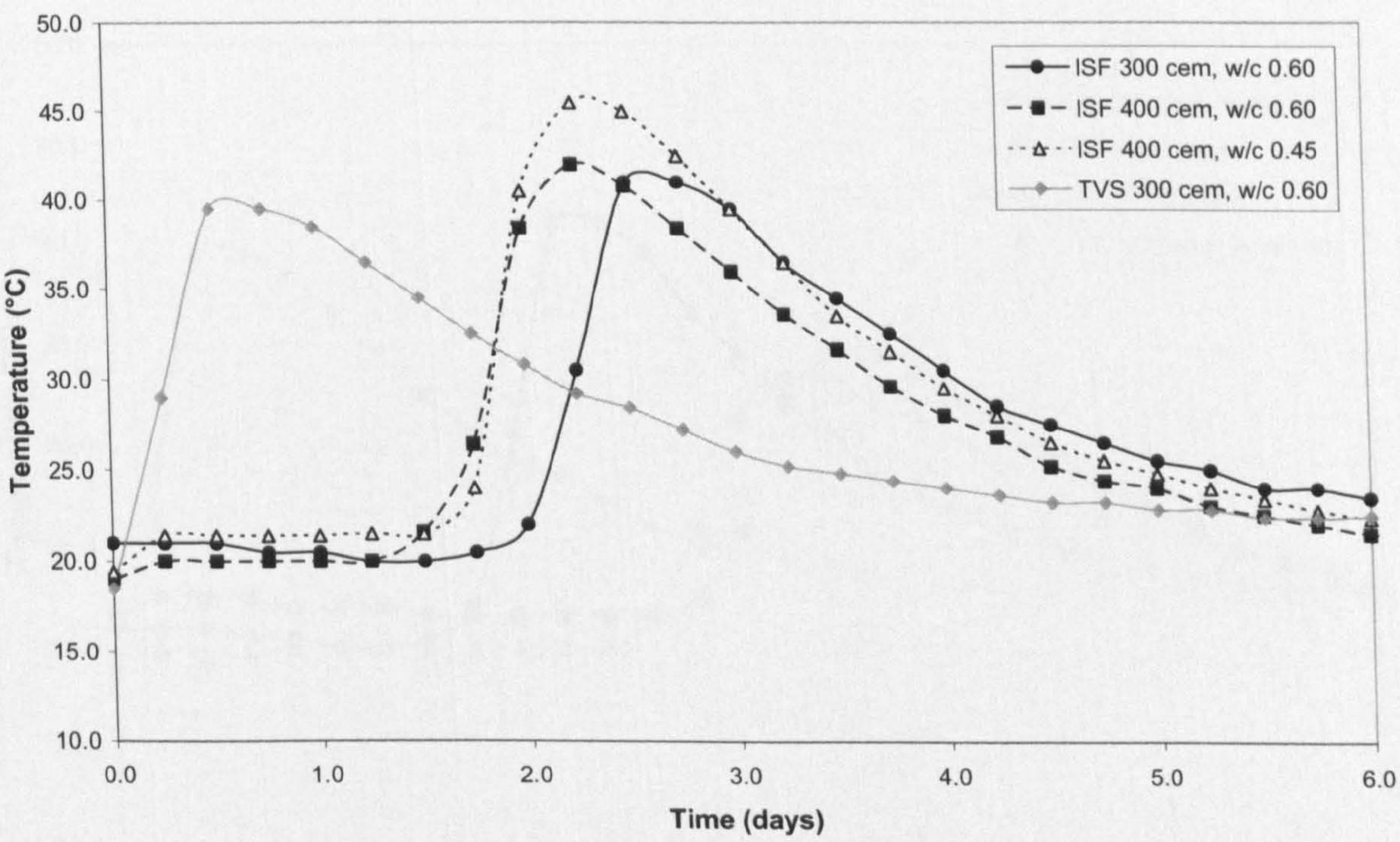

Figure 8.19: Influence of cement content and water/ cement ratio on setting behaviour of ISF slag concrete

8.6.2 Effect of PFA and GGBS on the retardation period

The results from isothermal conduction calorimetry and from leach testing suggested that the inclusion of PFA and GGBS in a concrete mix with ISF slag might reduce the delay experienced by making the metal ions suspected of causing the retardation unavailable in the mix. It can be seen in Figure 8.20 that the inclusion of these cement replacement materials did not prevent the delay in set, but instead caused a longer delay and a lower heat of hydration, assumed to be a result of the reduction in Portland cement used.

PFA and GGBS are known to develop their strength more slowly than Ordinary Portland Cement, as they do not produce as much heat during their hydration reaction[138]. Although it would obviously depend on their specific replacement levels, concrete mixes containing PFA and GGBS would normally be expected to be demouldable within the same time-scale as Portland cement mixes, though their early compressive strengths would be lower.

PFA and GGBS rely on the presence of calcium hydroxide in a mix to trigger their pozzolanic reaction (as discussed in section 2.4.2). If the calcium and hydroxide ions were being used up during the retardation period to convert the retarding species into a metal hydroxy-compound, the pozzolanic action of these materials may not be triggered in the usual way. It would therefore be expected that an even further delay in setting would be experienced, as seen in Figure 8.20. These results therefore indirectly support the theory that competition for the calcium and hydroxide ions in the mix is responsible for the delay in set.

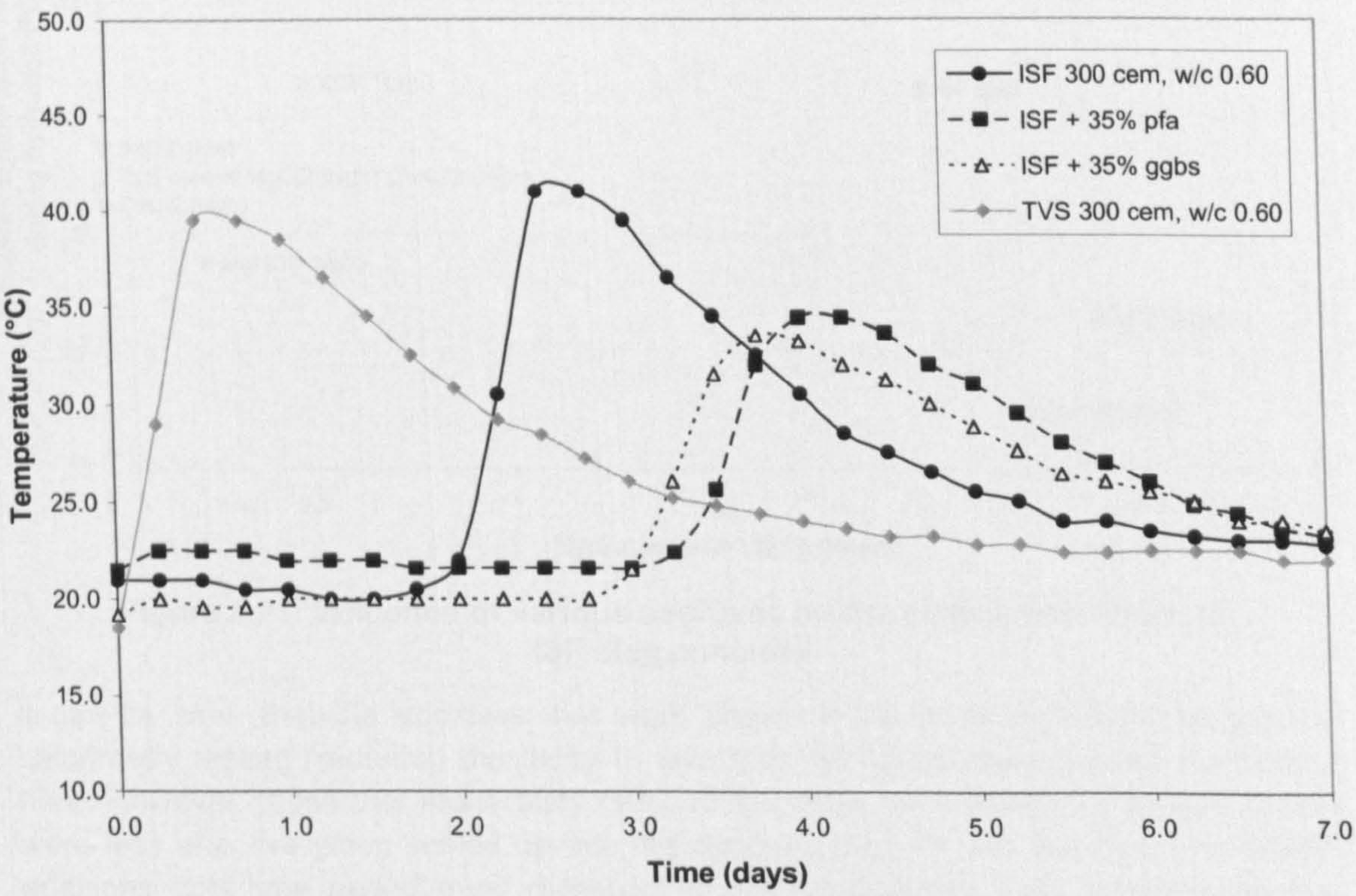

Figure 8.20: Influence of PFA and GGBS on the setting behaviour of ISF slag concrete

This difference between the results obtained from isothermal conduction calorimetry and the temperature monitoring of concrete highlights the problems that arise when trying to directly compare the two techniques. The samples being tested were quite different – small scale mortar samples with ground aggregates compared to full scale concrete mixes. These particular additives must react over a range that is critical between the two techniques and the effectiveness of any additives that appear to improve the retardation by such a small amount during the calorimetry testing would not necessarily be reliable

in concrete. However, more positive results were obtained when further additives that were shown by calorimetry to be successful at overcoming the delay were tested in concrete mixes.

8.6.3 Effect of various chemical additives on the retardation period

Figure 8.21 shows the effect of several chemical additions (at either high or low addition levels) on the retardation of ISF concrete. For simplicity, the results are presented as the peak hydration temperature plotted against the time to the start of hydration, although all profiles were essentially the same as those given in the previous figures.

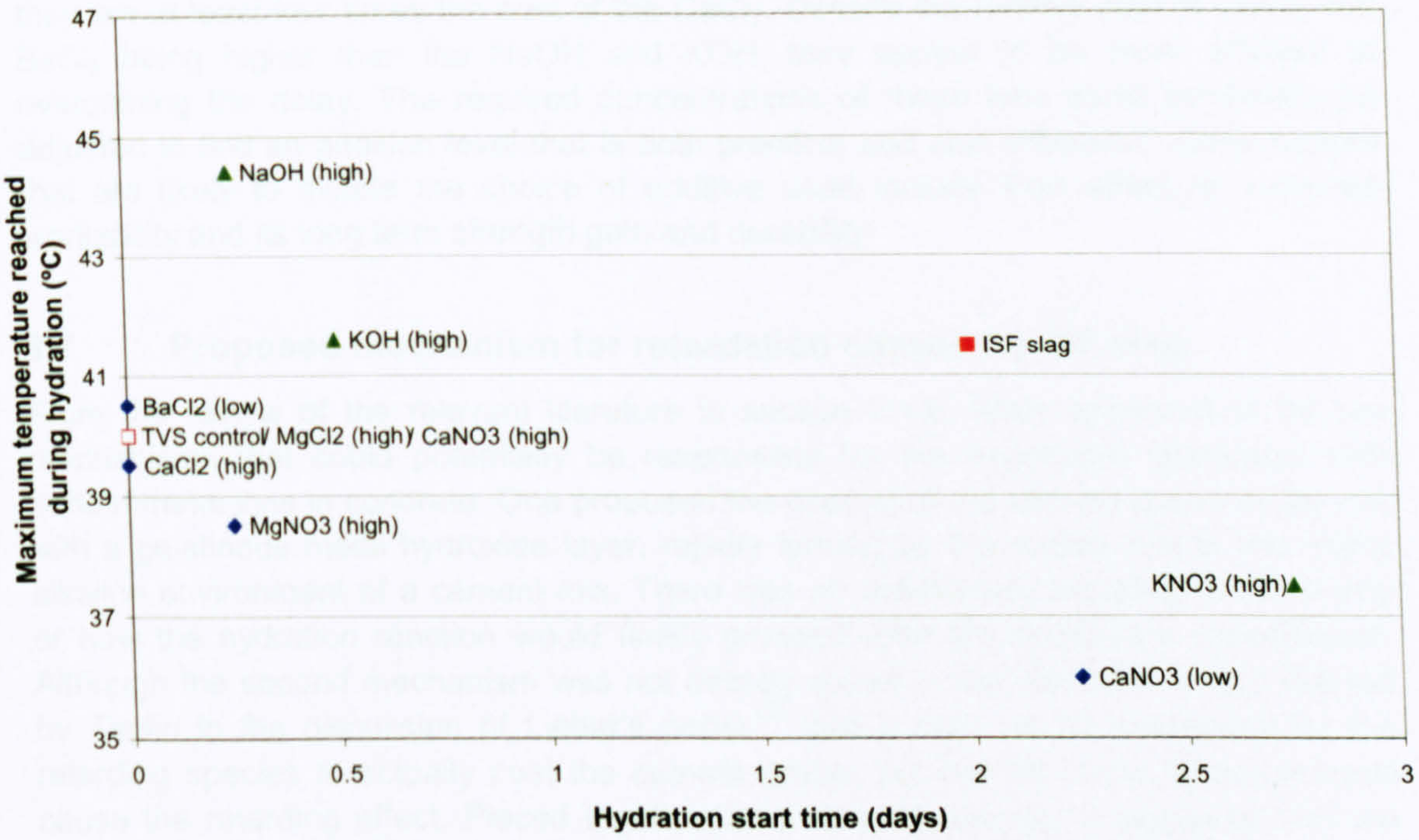

Figure 8.21: Influence of various additives on the setting behaviour of ISF slag concrete

It can be seen that the additives that were shown to be most successful during the calorimetry testing (reducing the delay to less than 16 hours) were equally successful here. However, those that moderately reduced the delay (to between 16 and 24 hours) were less effective when scaled up into the concrete mix. As with the PFA and GGBS additions, this time period must represent a critical crossover area between the two techniques used. Additives that reduce the delay to within 16 hours in the calorimetry testing are still equally as successful in concrete, while anything that experiences a longer delay does not appear to be sufficient to overcome the retardation caused by the ISF slag in concrete within a manageable timeframe. Variations in the concentrations used may be able to overcome this, but this effect emphasises the need for representative testing of materials in general, rather than relying on potentially more practical small-scale testing.

Of all the successful chemical additives tested in concrete, $BaCl_2$ is the only one that was able to be used at the 'low' addition level. From the calorimetry results, low additions of

$MgCl_2$, $SrCl_2$ and $MgNO_3$ also reduced the retardation to within 16 hours, so would be expected to work as efficiently in concrete with ISF slag.

Although these additives appear to be almost equally as efficient at minimising the delay, the relative cost of some of them, when their required dosage is considered, may preclude their use. Although the effective NaOH and KOH additions were of high concentration, due to their low molecular weight and relatively low cost anyway, they are actually the cheapest additives of those tested, NaOH being the cheapest of the two. The cost of the high concentration of $CaCl_2$ and the low concentration of $BaCl_2$ would be nearly equal, although they are approximately twice the price of the required dose of KOH. The use of the other additives tested at high doses would likely be non-viable, as they are at least four times the cost of the $CaCl_2$. Despite the relative cost of $CaCl_2$ and $BaCl_2$ being higher than the NaOH and KOH, they appear to be more efficient at overcoming the delay. The required concentrations of these ions could potentially be adjusted to find an addition level that is both practical and cost effective[m]. Other factors that are likely to dictate the choice of additive used include their effect on concrete workability and its long term strength gain and durability.

8.7 Proposed mechanism for retardation caused by ISF slag

From the review of the relevant literature in section 2.4.6, there appeared to be two mechanisms that could potentially be responsible for the retardation witnessed with certain metal ions in concrete. One proposed the coating of the cement grains in the mix with a gelatinous metal hydroxide layer, rapidly formed by the metals due to the highly alkaline environment of a cement mix. There was no satisfactory explanation as to why or how the hydration reaction would finally proceed after the retardation experienced. Although the second mechanism was not directly stated in the literature, it was inferred by Taplin in the discussion of Lieber's paper[120] that it may not be necessary for the retarding species to actually coat the cement grains, but that its mere presence could cause the retarding effect. Pieced together from several sources, it appeared that the second possible mechanism would be as follows. It is this mechanism that seems to be best supported by the results obtained from this study.

It is agreed that metal hydroxide precipitates would quickly form in the high alkaline environment of a cement mix. However, there does not appear to be any reason why they should preferentially coat the cement grains. Zinc and lead ions are amphoteric and the hydroxide precipitates would re-dissolve in an excess of hydroxide ions to form soluble zincates (ZnO_2^{2-}) and plumbates (PbO_2^{2-})[117]. Lieber[120] noted the apparent conversion of ZnOH to a calcium zincate compound ($CaZn_2(OH)_6.2H_2O$) during the retardation period. This would require the availability of both calcium and hydroxide ions in the solution, which there would be during the normal cement hydration process. The calcium and hydroxide ions gradually saturate the mix water until super-saturation is reached and solid $Ca(OH)_2$ (Portlandite) is precipitated out, marking the start of the cement hydration/ hardening process. A generalised equation for the conversion of the retarding species, M, would therefore be:

---

[m] Relative prices, used for guidance, were obtained from VWR International's laboratory supplies catalogue, 2003 edition

$$M \xrightarrow{\text{in the presence of OH- ions}} MOH \xrightarrow{\text{in the presence of excess OH- and Ca+ ions}} CaM_2(OH)_x.yH_2O$$

However, if the retarding species (zinc or lead hydroxide) was to use up the calcium and hydroxide ions from the surrounding solution to convert to the hydroxy-species, it would appear reasonable to anticipate that the solution would not become saturated with calcium and hydroxide ions until all of the retarding species had converted to this form. This would obviously prolong the time required before the calcium hydroxide would precipitate out, but the eventual reaction of the cement would be expected to be largely unaffected by the delay. If this is assumed to be the case, it follows that an increase in the concentration of available hydroxide ions present will shorten the retardation period experienced and that the total heat of hydration for the reactions should be largely unchanged.

This appeared to be the mode of action of the additives that were tested by isothermal conduction calorimetry and temperature monitoring of concrete cubes. There also appears to be more circumstantial evidence to support this mechanism: the reaction profiles from the temperature testing were virtually the same as the control mix; calcium hydroxide was not detected in the XRD samples until after the retardation period had ceased; the aggregate/ cement ratio is critical to the delay in set rather than any other factor (if diffusion of water through a gelatinous layer was suspected to cause the eventual hydration of the cement, the water/ cement ratio of the mix would be expected to influence the delay); and no evidence of any gel or coatings of any sort were observed by microscopy.

It is unfortunate that neither a lead nor zinc hydroxy-species was detected during the course of this testing, as that would have provided more conclusive evidence that this proposed reaction mechanism was correct. It would also have indicated whether lead, zinc or a combination of both of these ions was in fact responsible for the retardation experienced with the ISF slag.

If zinc was the cause of the delay and insoluble calcium hydroxy-zincate was formed as a result, the zinc would then be chemically bound up, making it less likely to leach from the hardened concrete that eventually formed, as seen in the leach testing in section 7 and leaching studies by previous authors[95]. Even if the zinc was not the primary cause of the retardation, it is still possible that this reaction would have taken place with any zinc that leached into solution, making the zinc unavailable for leaching once the concrete had hardened. Lead leaching is still relatively high from concrete containing the ISF slag. It is therefore proposed that if a hydroxy-plumbate species is formed it may be soluble, allowing it to be more readily leachable from the concrete. However, no literature has been identified to support or disprove this suggestion.

There are still questions as to why the CRT glass did not suffer from the same sort of retardation as the slag. Possible reasons include: the lead being present as an integral component of the glass, rather than as metallic inclusions; the lead not leaching so rapidly from the CRT glass as from the slag in high alkali solutions; the presence of barium and strontium in the CRT glass, since group II additions appeared to overcome the retardation experienced with the ISF slag.

8.8 Retardation summary

Microscopy studies have shown no evidence of any observable coatings that could be responsible for the delay in set experienced with the ISF slag. This is in contradiction with previous studies, but careful consideration of their methodology as well as the results obtained here throws doubt on the validity of their analysis. TGA and XRD analysis did not indicate the presence of any new species that may be responsible for the delay, although XRD confirmed that $Ca(OH)_2$ (Portlandite) was not formed until after the retardation period had ended.

Isothermal conduction calorimetry was used to test a range of additives on the cement hydration process, to see if any could overcome the problems caused by the inclusions of ISF slag in cement and mortars. It was apparent that the most successful additions for overcoming the delay in setting were those containing group II cations and/or those that in some way promoted an increase in the concentration of hydroxide ions in the mix. Internal temperature monitoring of setting concrete confirmed these findings and showed that the aggregate/ cement ratio was critical to the delay experienced, while the water/ cement ratio was not.

This evidence has led to the proposal of a detailed mechanism for the retardation, involving the conversion of a metal hydroxide to a metal hydroxy-species. This conversion reaction would use up calcium and hydroxide ions from the surrounding solution and delay the super-saturation and precipitation of $Ca(OH)_2$, which marks the start of the hydration/ hardening process. Unfortunately, such compounds have not been detected directly in this study, suggesting that they are either amorphous or not present in sufficient quantities to be detected by XRD. Thus the mechanism is not definitively proven.

The exact metal responsible for the delay caused by the ISF slag (assumed to be either zinc or lead) has not been identified, but the mechanism should be applicable to both ions. Additives to overcome the delay experienced have also been suggested, which should be transferable, perhaps at different concentrations, to other metal-retarded systems.

9 Conclusions and suggestions for further work

9.1 Conclusions

Both ISF slag and CRT glass are physically suitable for use as aggregate in concrete, giving good strength and workability characteristics.

CRT glass has been shown to be highly susceptible to ASR, but this detrimental reaction can be controlled through the use of lithium compounds, $LiOH.H_2O$ and $LiNO_3$. The ISF slag does not appear to be susceptible to ASR.

Barium does not leach from the CRT glass at levels above the guidance limits that were used for this work, so it may be considered of minimal environmental concern with respect to barium. However, lead has been shown to leach from the aggregates, even when encapsulated in concrete. This leaching is reduced when PFA and GGBS are used as cement replacement materials in the concrete. However, with ISF slag, levels still exceed the guidance limits used. This would suggest that, as a result of its leaching behaviour, the ISF slag may not be suitable for use as aggregate under the conditions tested (i.e. 100% fine aggregate). Although the leaching of lead is sufficiently reduced when these additives are used in concrete, CRT glass could potentially be used without additions of PFA or GGBS if the barium glass components could be separated from the lead containing components.

The ISF slag leads to an appreciable delay in setting when used as 100% fine aggregate. Various additives have been shown to reduce this delay to more manageable levels, though it could be further reduced by limiting the percentage replacement of ISF slag. The most promising additives from those tested, when costs are considered, are $BaCl_2$, $CaCl_2$, NaOH and KOH. CRT glass does not cause any delay in cement hydration, despite it containing lead. This may be due to the rate at which lead is released from the glass in a highly alkaline environment. However it may be possible that the barium and/or strontium in the glass may help to prevent the retardation, since these ions were shown to overcome the delay experienced with the ISF slag.

The proposed mechanism for this delay (that is best supported by this work, though conclusive evidence was not obtained) involves the conversion of a metal hydroxide to a metal hydroxy-species ($M \rightarrow MOH \rightarrow CaM_2(OH)_x.yH_2O$). This conversion reaction uses up calcium and hydroxide ions from the surrounding solution and delays the super-saturation and precipitation of $Ca(OH)_2$, which marks the start of the hydration/ hardening process. Although lead has been suspected as the delaying species from this study, this mechanism could also apply to zinc, as it too is amphoteric and forms a hydroxide at high pH, which would tend to be converted to an insoluble hydroxy-zincate in the presence of calcium ions.

9.2 Guidance for the use of CRT glass and ISF slag

It is hoped that both the ISF slag and CRT glass will eventually find a use in concrete applications, although it is clear from this study that certain precautions would be necessary to reduce or overcome the issues highlighted by this work.

The CRT glass is highly susceptible to ASR, even at relatively low replacement levels. If it was suspected that the conditions under which ASR occurs were likely to be met (i.e. sufficiently high relative humidity environment – silica and alkali ions would be provided from the CRT glass and the cement) then suitable mitigation techniques would need to be employed to minimise the risk of ASR damage. The use of the lithium compounds – lithium hydroxide and nitrate – have been shown to be most successful at preventing expansion of CRT glass-concrete samples caused by ASR.

However, if there was concern about the possibility of lead leaching from concrete into surrounding groundwater supplies, the use of PFA and GGBS as cement replacement materials would be preferred to minimise leaching. The use of PFA in association with lithium additions has previously been successfully trialled[78]. However, this would obviously result in increased costs, compared to just using one additive. Possible ways of overcoming this would be to either reduce the CRT glass replacement level to a point at which PFA and/ or GGBS are able to prevent the leaching as well as minimise ASR, or to use barium containing glass that had been separated from the leaded glass of a CRT, since the barium leaching levels are not of major concern.

The retardation of concrete setting, caused by the inclusion of ISF slag as fine aggregate in concrete, can be overcome by the use of various additives. The most successful and financially viable of these are barium chloride, calcium chloride, sodium hydroxide and potassium hydroxide. Although the use of these hydroxide additives would elevate the alkali content of the concrete, there should still be no risk of ASR with the ISF slag aggregate. The use of chloride additives may not be possible if steel reinforcements were present in the concrete, as chloride ions can increase the risk of steel corrosion[11]. The exact concentration of these additives necessary to prevent retardation will depend on the ISF slag replacement level in the concrete and would likely require further investigation. However, it is anticipated from this work that replacement levels below approximately 50% would experience an acceptable delay without the use of these additives.

Leaching results have suggested that the use of ISF slag as 100% fine aggregate in concrete may result in unacceptable levels of lead release if the concrete were to become damaged and the aggregate exposed. Use of a lower ISF slag replacement level would obviously improve the leaching behaviour, as would the inclusion of PFA and GGBS. Further investigation would be required to establish the optimum replacement level, with or without other additions, that would be most viable with respect to leaching, retardation and costs. Other possibilities would be to investigate the use of ISF slag in applications that would restrict its contact with water, such as bitumen-bound pavement construction.

9.3 Recommendations for further work

In light of the work that has been carried out for this study, there are a number of recommendations for further testing which would add weight to the findings of this research.

It was unfortunate that a hydroxy-zincate or hydroxy-plumbate species were not detected during the XRD analysis of retarding mortar samples, since this would have provided more conclusive proof that the proposed mechanism for the retardation of cement hydration with ISF slag was correct. It would be of benefit to repeat the XRD testing on quenched ISF mortars as a second attempt to identify these compounds. Another possible test would be to look for these species in control samples that have been doped with known concentrations of zinc and/ or lead compounds, rather than the ISF slag, to see if they can be detected in such an instance. The analysis is complicated somewhat by the relatively complex nature of the ISF slag. The mechanism might be proved more easily in a simpler system.

It would be interesting to carry out ASR testing and, in particular, leach testing on separated samples of lead and barium-containing glass from CRTs. Due to the apparently acceptable barium leaching that was demonstrated during this study, the barium-containing glass components may find applications for their use more readily if there was no concern about lead leaching. Also, ASR testing on the separate glass fractions would indicate whether either glass was more or less susceptible to this type of reaction.

There is some uncertainty as to the suitability of PFA and GGBS at minimising ASR with the CRT glass over time, due to the apparent reaction experienced, despite these additions, during 60°C testing. Testing at 38°C over a longer time period would give a better indication of the expected behaviour of all of the mitigation additives. Additionally, testing of CRT glass with the additives under real, outdoor exposure conditions would probably provide the best assessment of their suitability. However, it is accepted that the time periods required for this sort of testing would be lengthy (possibly up to 5 years).

It would be interesting to further investigate the non-linear relationship between the time to hydration and the percentage ISF slag replacement that was witnessed during the isothermal conduction calorimetry testing. It would be useful to carry out equivalent testing on concrete mixes containing the slag, to see if the non-linear trend was still apparent. This would also give an indication of the percentage ISF slag replacement that would result in an acceptable hydration period in concrete, without the use of additional additives.

The concentrations of the additives tested in association with the ISF slag were standardised for this work, so the effect of equivalent molar concentrations of the cations could be compared. However, it would be useful to carry out a more comprehensive analysis of the additive concentrations required to overcome the retardation caused by the ISF slag at various slag replacement levels, to find the most economical additions.

10 References

1 HM Customs and Excise, Notice LFT1: A general guide to landfill tax, May 2004

2 WEEE Directive, 'Directive 2002/96/EC of the European Parliament and of the Council of 27 January 2003 on Waste Electrical and Electronic Equipment (WEEE), Official Journal of the European Union, 13.02.2003, pp. L 37/24-L 37/38

3 RoHS Directive, 'Directive 2002/95/EC of the European Parliament and of the Council of 27 January 2003 on the Restriction of the use of Certain Hazardous Substances in Electrical and Electronic Equipment, Official Journal of the European Union, 13.02.2003, pp. L 37/19-L 37/23

4 HM Customs and Excise, Notice AGL1: Aggregates Levy, August 2004

5 Quarry Products Association website: www.qpa.org, last checked July 2005

6 British Aggregates Association website: www.british-aggregates.com/aggtax01, last checked July 2005

7 London Remade Newsletter, Issue 3, Winter 2001: http://www.londonremade.com/html_newsletters/newsletter.htm, last checked July 2005

8 CSIRO, 'Making concrete with glass - now possible', CSIRO (Australia's Commonwealth Scientific and Industrial Research Organisation) Manufacturing and Infrastructure Technology, Press release: 13/05/02, Ref: 2002/90

9 DeVries P, 'Concrete re-cycled: Crushed concrete as aggregate', 21st Annual Convention, Institute of Concrete Technology, Coventry, April 1993.

10 Desmyter J, Blockmans S, 'Evaluation of different measures to reduce the risk of alkali-silica reaction in recycled aggregate concrete', Proc. 11th International Conference on Alkali-Aggregate Reaction (ICAAR), Quebec, Canada, Eds. Berube MA, Fournier B, Durand B, ICON/CANMET, pp. 603-612, 2000

11 Ramachandran VS, 'Concrete admixtures handbook – Properties, science and technology', Noyes publications, New Jersey, USA, 1984

12 Lea FM, 'The chemistry of cement and concrete', 3rd Edition, Edward Arnold (Publishers) Ltd, 1970

13 Hobbs DW, 'Effect of mineral and chemical admixtures on alkali-aggregate reaction', Proc. 8th International Conference on Alkali-Aggregate Reaction (ICAAR), Kyoto, Japan, Eds. Okada K, Nishibayashi S, Kawamura M, Elsevier Applied Science Publishers Ltd, pp. 173-186, 1989

14 Technical data sheet – 'Pulverised fuel ash for concrete', UK Quality Ash Association, 2000

15 Malin N, 'The fly ash revolution: Making better concrete with less cement', Environmental Building News, Vol. 8, No. 6, pp. 1 & 8-13, June 1999

16 HM Government, 'Controlling the environmental effects of recycled and secondary aggregates production, Good practice Guidance', document produced by the office of the deputy prime minister, 22 March 2000

17 Emery JJ, Hooton RD, Gupta RP, 'Utilisation of blast furnace, nonferrous and boiler slags', Silicates Industriels, Vol. 42 (4-5), pp. 111-120, 1977

18 Sugiri SM, Khosama LK, Munaf DR, 'Mechanical behaviour of high performance nickel slag concrete', Proceedings of the 13th FIP Congress (International Federation for Prestressing), Amsterdam, AA Balkema Publishers, pp. 551-554, 1998

19 Sarkar SL, Bonen D, 'Non-ferrous lead-smelting slag waste as a potential constituent in the production of blended cement', 2nd Int. Symp. Blended Cements, Malaysia, Singapore np (Pub), pp. 108-113, 1994

20 Atkinson RJ, Hannaford AL, Harris L & Philip TP, 'Using smelter slag in mine backfill', Mining Magazine, pp. 118-123, August 1989

21 Barritt C, 'The future of recycled and secondary aggregates', Concrete in a changing world – New standards and conformity, ICT Convention, April 2001

22 Li Z, Li F, Li JSL, 'Properties of concrete incorporating rubber tyre particles', Magazine of Concrete Research, Vol. 50, No. 4, pp. 297-304, December 1998

23 Benazzouk A, Queneudec M, Doyen G, 'Physico-mechanical properties of rubber – cement composites', Proc. Int. Symp. Recycling and reuse of used tyres, Concrete Technology Unit, University of Dundee, Eds. Dhir RK, Limbachiya MC, Paine KA, Thomas Telford Publishing Ltd, pp. 237-249, 2001

24 El-Dieb AS, Abdel-Wahab MM, Abdel-Hameed ME, 'Concrete using rubber tyre particles as aggregate', Proc. Int. Symp. Recycling and reuse of used tyres, Concrete Technology Unit, University of Dundee, Eds. Dhir RK, Limbachiya MC, Paine KA, Thomas Telford Publishing Ltd, pp. 251-259, 2001

25 Kew HY, Cairns R, Kenny MJ, 'The use of recycled rubber tyres in concrete', Proc. Int. Conf. on Sustainable Waste Management and Recycling: Used Post-Consumer Tyres, Kingston University, London, Eds. Limbachiya MC, Roberts JJ, Thomas Telford Publishing Ltd, pp. 135-142, September 2004

26 Hreglich S, Falcone R, Vallotto M, 'The recycling of end of life panel glass from TV sets in glass fibres and ceramic productions', Proc. Int. Symp. Recycling & reuse of glass cullet, Dundee, Eds. Dhir RK, Limbachiya MC, Dyer TD, Thomas Telford Publishing Ltd, pp. 123-134, 2001

27 Siikamaki R, Hupa L, 'Utilisation of EOL CRT glass as a glaze raw material', Proc. Int. Symp. Recycling & reuse of glass cullet, Dundee, Eds. Dhir RK Limbachiya MC, Dyer TD, Thomas Telford Publishing Ltd, pp. 135-146, 2001

28 Marshall M, Henderson J, 'New approaches to the challenge of CRT recycling', Proc. Int. Symp. Recycling & reuse of glass cullet, Dundee, Eds. Dhir RK, Limbachiya MC, Dyer TD, Thomas Telford Publishing Ltd, pp. 75-84, 2001

29 Menad N, 'Cathode ray tube recycling', Resources, Conservation and Recycling, Vol. 26, pp. 143-154, 1999

30 Townsend TG, Musson S, Jang YC, Chung IH, 'Characterization of lead leachability from cathode ray tubes using the toxicity characteristic leaching procedure', Florida Center for Solid and Hazardous Waste Management, Report No. 99-5, December 1999

31 ATSDR (Agency for Toxic Substances and Disease Registry), 'Toxicological Profile for Strontium', US Department of Health and Human Services, April 2004

32 Amini M, Ahanj M, 'Leach of cesium and barium from Sol-Gel derived zincborosilicate and borosilicate glasses', Journal of Sol-Gel Science and Technology, Vol. 18, Part. 2, pp. 119-125, 2002

33 Luo W, Fu SS, 'The effect of barium, phosphorus and lead compositional variations on waste glass properties', Ceramic Transactions, Vol. 87, pp. 631-640, 1998

34 California electronic asset recovery inc. website: http://www.cearinc.com/CRTRecycling.htm, last checked July 2005

35 Bernardo E, Scarinci G, 'Foam glass as a way of recycling glasses from cathode ray tubes', Glass Science and Technology, Vol. 78, No. 1, pp. 7-11, 2005

36 Saterlay AJ, Wilkins SJ, Compton RG, 'Towards greener disposal of waste cathode ray tubes via ultrasonically enhanced lead leaching', Green Chemistry, The Royal Society of Chemistry, Vol. 3, pp. 149-155, 2001

37 Nash A, Britannia Zinc Ltd. Personal communication with R. Hooper, BRE, Watford, UK, 1999

38 Hooper R, McGrath C, Morrison C, Lardner K, 'Ferro-silicate slag from ISF zinc production as a sand replacement: A review', Proc. American Concrete Institute (ACI) 5th International Conference on Innovations in design with emphasis on seismic, wind and environmental loading, quality control and innovation in materials/ hot weather concreting, Cancun, Mexico, Ed. Malhotra VM, ACI Publications, pp. 811-838, 2002

39 Atzeni C, Massidda L, Sanna U, 'Use of granulated slag from lead and zinc processing in concrete technology', Cement and Concrete Research, Vol. 26, No. 9, pp. 1381-1388, 1996

40 Morrison C, Hooper R, Lardner K, 'Initial studies into the use of zinc slag as a concrete aggregate', BRE Client report no. 203 970, March 2001

41 Sugita S, Shoya M, Sugawara T, 'Studies on the properties of concrete with zinc slag as fine aggregate', CAJ Review, pp. 92-95, 1988

42 Mandin D, van der Sloot HA, Cervais C, Barna R, Mehu J, 'Valorization of lead-zinc primary smelters slags', Studies in Environmental Science, Waste materials in Construction: Putting theory into practice, Eds. Goumans JJJM, Senden GJ, Van der Sloot HA, Elsevier Science, pp. 617-630, 1997

43 Massidda L, Sanna U, Delpiano F, 'Possible uses of silicate slag from lead and zinc processing in the cement industry', Materials Engineering, Vol. 9, n. 3-4, pp. 237-252, 1998

44 Spina V, Chiappetta F, Niceforo D, Marasco A, Nastro A, 'Utilization proposal of slag from zinc production with mineral aggregate in the mix design of bituminous concrete', Materials Engineering, Vol. 13, No. 1, pp. 109-119, 2002

[45] Ito H, Nakamura T, Kawahara M, Morinaga K, 'Phase transformations and leaching characteristics of lead and zinc slag after heat treatment', Zinc and Lead '95, Proc. Int. Symp. Extraction and applications of zinc and lead, Sendai, Ed. Azakami T, Tohoku University (Pub), pp. 502-511, 1995

[46] Motz H, Geiseler J, 'Products of steel slags. An opportunity to save natural resources', WASCON 2000, Waste Materials in Construction, Proc. Int. Conf. Science and engineering of recycling for environmental protection, Harrogate, England, Eds. Woolley GR, Goumans JJJM, Wainwright PJ, Pergamon Oxford/ Amsterdam, pp. 207-218, 2000

[47] Hobbs DW, 'Alkali-silica reaction in concrete', Thomas Telford, London, 1988

[48] Gillott JE, Rogers CA, 'Alkali-aggregate reaction and internal release of alkalis', Magazine of Concrete Research, Vol. 46, No. 167, pp. 99-112, June 1994

[49] West G, 'Alkali-aggregate reaction in concrete roads and bridges', Thomas Telford Publishers Ltd, London, 1996

[50] Nixon PJ, Page CL, Hardcastle J, Canham I, Pettifer K, 'Chemical studies of alkali silica reaction in concrete with different flint contents', Proc. 8th International Conference on Alkali-Aggregate Reaction (ICAAR), Kyoto, Japan, Eds. Okada K, Nishibayashi S, Kawamura M, Elsevier Applied Science Publishers Ltd, pp. 129-134, 1989

[51] BRE, 'Alkali-silica reaction in concrete', Digest 330, Construction Research Communications, London, 1999

[52] French WJ, 'A review of some reactive aggregates from the United Kingdom with reference to the mechanism of reaction and deterioration', Proc. 7th International Conference on Alkali-Aggregate Reaction (ICAAR), Ottawa, Canada, Ed. Grattan-Bellew PE, Noyes Publications, pp. 226-230, 1986

[53] French WJ, Poole AB, 'Alkali-aggregate reactions and the Middle East', Concrete, January 1976, pp. 18-20

[54] Harrisson A, 'Deleterious processes in concrete', Concrete, pp. 13-14, Nov/Dec 1995

[55] Concrete Society Working party report, 'Alkali-silica reaction - minimising the risk to concrete. Guidance notes and model specification clauses', Technical report No.30, Concrete Society, 1995 revision.

[56] Matsuda T, Ishii K, Morino K, 'Effect of volcanic glass on alkali-aggregate reaction', CAJ Review, 1986

[57] Curtil L, Gielly J, Murat M, 'Chemical behaviour of natural opal and silica glass in basic solutions. Application to AAR', Proc. 9th International Conference on Alkali-Aggregate Reaction (ICAAR), London, England, Ed. Poole AB, Concrete Society Publications, pp. 217-223, 1992

[58] Dyer TD, Dhir RK, 'Use of glass cullet as a cement component in concrete', Proc. Int. Symp. Recycling and Reuse of Glass Cullet, Dundee, Eds. Dhir RK, Limbachiya MC, Dyer TD, Thomas Telford Publishing Ltd, pp. 157-166, 2001

[59] Shao Y, Lefort T, Moras S, Rodriguez D, 'Studies on concrete containing ground waste glass', Cement and Concrete Research, Vol. 30, pp. 91-100, 2000

[60] O'Rourke A, Clarke J, 'Social barriers to the recovery and reuse of recyclable construction waste materials', Proc. Int. Symp. Recycling and reuse of glass cullet, Dundee, Eds. Dhir RK, Limbachiya MC, Dyer TD, Thomas Telford Publishing Ltd, pp. 147-155, 2001

[61] Zhang X, Groves GW, 'The alkali-silica reaction in OPC/silica glass mortar with particular reference to pessimum effects', Advances in Cement Research, Vol. 3, No. 9, pp. 9-13, 1990

[62] Hobbs DW, Gutteridge WA, 'Particle size of aggregate and its influence upon the expansion caused by the alkali-silica reaction', Magazine of Concrete Research, Vol, 31, No. 109, pp. 235-242, December 1979

[63] Yamada K, Abe Y, Ishiyama S, 'ASR expansion caused by glass cullet under rapid test method', Proc. Int. Conf. on Sustainable Waste Management and Recycling: Glass Waste, Kingston University, London, Eds. Limbachiya MC, Roberts JJ, Thomas Telford Publishing Ltd, pp. 109-116, 2004

[64] Diamond S, Thaulow N, 'A study of expansion due to alkali-silica reaction as conditioned by the grain size of the reactive aggregate', Cement and Concrete Research, Vol. 4, pp. 591-607, 1974

[65] Jin W, Meyer C, Baxter S, '"Glascrete" – Concrete with glass aggregate', ACI Material Journal, pp. 208-213, March-April 2000

[66] Ridout G, 'The ASR cancer spreads but Hawkins offers four preventives', Surveyor, pp. 8-11, 21st November 1985

[67] Connell MD, Higgins DD, 'Effectiveness of granulated blastfurnace slag in preventing alkali-silica reaction', Proc. 10th International Conference on Alkali-Aggregate Reaction (ICAAR), Melbourne, Australia, Ed. Shayan A, pp. 530-537, 1996

[68] Duchesne J, Berube MA, 'The effectiveness of supplementary cementing materials in suppressing expansion due to ASR: Another look at the reaction mechanisms. Part 1: Concrete expansion and Portlandite depletion', Cement and Concrete Research, Vol. 24, No. 1, pp. 73-82, 1994

[69] Shayan A, Diggins R, Ivanusec I, 'Long-term effectiveness of fly ash in preventing deleterious expansion due to alkali-aggregate reaction in concrete', Proc. 10th International Conference on Alkali-Aggregate Reaction (ICAAR), Melbourne, Australia, Ed. Shayan A, pp. 538-545, 1996

[70] Institute of Structural Engineers, 'Structural effects of alkali-silica reaction - Technical guidance on the appraisal of existing structures', The Institute of Structural Engineers, July 1992

[71] Aitcin PC, Regourd M, 'The use of condensed silica fume to control alkali-silica reaction – a field case study', Cement and Concrete Research, Vol. 15, No. 4 pp. 711-719, 1985

[72] BRE, Information paper IP1/02, 'Minimising the risk of alkali-silica reaction: alternative methods', Construction Research Communications, London, 2002

[73] Sakaguchi Y, Takakura M, Kitagawa A, Hori T, Tomosawa F, Michihiko A, 'The inhibiting effect of lithium compounds on alkali-silica reaction', Proc. 8th International Conference on Alkali-Aggregate Reaction (ICAAR), Kyoto, Japan, Eds. Okada K, Nishibayashi S, Kawamura M, Elsevier Applied Science Publishers Ltd, pp. 229-234, 1989

[74] Diamond S, Ong S, 'The mechanisms of lithium effects on ASR', Proc. 9th International Conference on Alkali-Aggregate Reaction (ICAAR), London, England, Ed. Poole AB, Concrete Society Publications, pp. 269-278, 1992

[75] Stark DC, 'Lithium salt admixtures – an alternative method to prevent expansive alkali-silica reactivity', Proc. 9th International Conference on Alkali-Aggregate Reaction (ICAAR), London, England, Ed. Poole AB, Concrete Society Publications, pp. 1017-1025, 1992

[76] Baxter SZ, Stokes. DB, Manissero. CE, 'A lithium-based pozzolan for ASR control', Proc. 11th International Conference on Alkali-Aggregate Reaction (ICAAR), Quebec, Canada, Eds. Berube MA, Fournier B, Durand B, ICON/CANMET, pp. 573-582, 2000

[77] Stokes DB, 'Use of lithium to combat alkali silica reactivity', Proc. 10th International Conference on Alkali-Aggregate Reaction (ICAAR), Melbourne, Australia, Ed. Shayan A, pp. 862-867, 1996

[78] Wang HH, Stokes DB, Tang F, 'Compatibility of lithium-based admixture with other concrete admixtures', Proc. 10th International Conference on Alkali-Aggregate Reaction (ICAAR), Melbourne, Australia, Ed. Shayan A, pp. 884-891, 1996

[79] RMC Readymix datasheet 'Product specification: cement blends': http://www.e-creation.co.uk/demos/RMC/concrete_cement_blends.asp, last checked July 2005

[80] Kuennen T, 'Lithium admixtures scale ASR challenge', Concrete Products magazine, pp. 80-82, October 2000

[81] Bragg D, Foster K, 'Relationship between petrography and results of alkali-reactivity testing, samples from Newfoundland, Canada', Proc. 9th International Conference on Alkali-Aggregate Reaction (ICAAR), London, England, Ed. Poole AB, Concrete Society Publications, pp. 127-135, 1992

[82] British Standards Institution, BS 812-123: 1999, 'Testing aggregates – Method for determination of alkali-silica reactivity. Concrete prism method', BSI, London, 1999

[83] RILEM TC-ARP/01/20, 'AAR-4 – Detection of potential alkali reactivity. Accelerated method for aggregate combinations and concrete mix designs using concrete prisms', draft document for discussion

[84] Grattan-Bellew PE, 'A critical review of accelerated ASR tests', Proc. 10th International Conference on Alkali-Aggregate Reaction (ICAAR), Melbourne, Australia, Ed. Shayan A, pp. 27-38, 1996

[85] Nixon PJ, Simms I, 'RILEM TC 106 – AAR: Aggregates for alkali-aggregate reaction', Materials and Structures, Vol. 33, No. 226, pp. 88-93, 2000

[86] ASTM C1260 – 94, 'Standard test method for potential alkali reactivity of aggregates (Mortar bar method)', American Society for Testing and Materials, 1994

[87] Oberholster RE, 'Alkali reactivity of siliceous rock aggregates: Diagnosis of the reaction, testing of cement and aggregate and prescription of preventive measures', Proc. 6th International Conference on Alkali-Aggregate Reaction (ICAAR), Copenhagen, Denmark, Eds. Idorn GM, Rostain S, DBF Publishing (Danish Concrete Association) pp. 419-433, 1983

[88] Wigum BJ, French WJ, 'Sequential examination of slowly expanding alkali-reactive aggregates in accelerated mortar bar testing', Magazine of Concrete Research, Vol. 48, No. 177, pp. 281-292, Dec. 1996

[89] Mullick AK, Wason RC, 'NBRI tests on aggregate containing strained quartz', Proc. 10th International Conference on Alkali-Aggregate Reaction (ICAAR), Melbourne, Australia, Ed. Shayan A, pp. 340-347, 1996

[90] Ramezanianpour AA, Karimi M, 'Evaluation of aggregates for AAR using accelerated test methods', Proc. 10th International Conference on Alkali-Aggregate Reaction (ICAAR), Melbourne, Australia, Ed. Shayan A, pp. 348-354, 1996

[91] Blackwell BQ, Thomas MDA, Nixon PJ, Pettifer K, 'The use of fly ash to suppress deleterious expansion due to AAR in concrete containing greywacke aggregate', Proc. 9th International Conference on Alkali-Aggregate Reaction (ICAAR), London, England, Ed. Poole AB, Concrete Society Publications, pp. 102-109, 1992

[92] Hooton RD, Rogers CA, 'Development of the NBRI rapid mortar bar test leading to its use in North America', Proc. 9th International Conference on Alkali-Aggregate Reaction (ICAAR), London, England, Ed. Poole AB, Concrete Society Publications, pp. 461-467, 1992

[93] Shayan A, Ivanusec I, Diggins R, 'Comparison between two accelerated methods for determining alkali reactivity potential of aggregates', Proc. 9th International Conference on Alkali-Aggregate Reaction (ICAAR), London, England, Ed. Poole AB, Concrete Society Publications, pp. 953-957, 1992

[94] European Commission, 'Standard tests for alkali-reactive rocks, final report', DGXII contract no SMT4 - CT96 - 2128 STAR Project, 1999

[95] Poon CS, Peters CJ, Perry R, Barnes P, Barker AP, 'Mechanisms of metal stabilization by cement based fixation processes', The Science of the Total Environment', Vol. 41, pp. 55-71, 1985

[96] Cioffi R, Lavorgna M, Santoro L, 'Reuse of secondary lead smelter slag in the manufacture of concrete blocks', WASCON 2000, Waste Materials in Construction, Proc. Int. Conf. Science and engineering of recycling for environmental protection, Harrogate, England, Eds. Woolley GR, Goumans JJJM, Wainwright PJ, Pergamon Oxford/ Amsterdam, pp. 741-749, 2000

[97] Cote PO, Bridle TR, Hamilton DP, 'Evaluation of pollutant release from solidified aqueous wastes using a dynamic leaching test', Proc. Hazardous Wastes and Environmental Emergencies Conference, Houston, Texas, pp. 302-308, 1984

[98] Sharma RK, Kumar S, De AK, Ray PK, 'Use of flyash as an ion exchanger in water filtration studies for the removal of heavy metals', J. Environ. Sci. Health, Vol. A25, No. 6, pp. 637-651, 1990

99 Cho JW, Ioku K, Goto S, 'Effect of Pb^{II} and Cr^{VI} ions on the hydration of slag alkaline cement and the immobilization of these heavy metal ions', Advances in Cement Research, Vol. 11, No. 3, pp. 111-228, July 1999

100 van der Sloot HA, Hoede D, de Groot GJ, van der Wegen GJL, Quevauviller Ph, 'Intercomparison of leaching tests for stabilized wastes', Commission of the European Communities, EUR 16133 EN, 1995

101 van der Sloot HA, Heasman L, Quevauviller Ph, 'Harmonization of leaching/ extraction tests', Elsevier, Amsterdam, 1997

102 de Groot GJ, Wijkstra J, Hoede D, van der Sloot HA, 'Leaching characteristics of selected elements from coal fly ash as a function of the acidity of the contact solution and the liquid/ solid ratio', Environmental Aspects of Stabilization and Solidification of Hazardous and Radioactive Wastes, ASTM STP 1033. In Cote PL, Gilliam TM (Eds), American Society for Testing and Materials, Philadelphia, pp. 170-183, 1989

103 CEN/TC 292, Draft prEN XXXXX, 'Characterisation of waste - Leaching - Compliance test for leaching of monolithic waste of regular shape', European Committee for Standardisation, CEN Central Secretariat, Brussels, 2000

104 CEN/TC 154, Draft prEN 1744-3, 'Tests for chemical properties of aggregates – Part 3: Preparation of eluates by leaching of aggregates', European Committee for Standardisation, CEN Central Secretariat, Brussels, 2000

105 ASTM D3987 – 85 (Reapproved 1999), 'Standard test method for shake extraction of solid waste with water', American Society for Testing and Materials, 1999

106 British Standards Institution, BS EN 12457 parts 1-4: 2002, 'Characterisation of waste – Leaching – Compliance test for leaching of granular waste materials and sludges', BSI, London, 2002

107 Statutory Instrument 2004 No. 1375, 'The Landfill (England and Wales) (Amendment) Regulations 2004, HM Stationary Office Ltd, ISBN 0110493168, 2004

108 US Environmental Protection Agency, 'SW-846: Test methods for evaluating solid wastes, Physical/ Chemical methods. Method 1311 – Toxicity Characteristic Leaching Procedure (TCLP), Revision 0, July 1992

109 Eighmy TT, van der Sloot HA, 'A unified approach to leaching behaviour of waste materials', WASCON 1994, 'Environmental aspects of construction with waste materials', Eds. Goumans. JJJM, van der Sloot. HA, Aalbers. TG, Elsevier, Amsterdam, 1994, pp. 979-988

110 van der Sloot HA, 'Leaching behaviour of waste and stabilized waste materials; characterization for environmental assessment purposes', Waste Management & Research, Vol. 8. pp. 215-228, 1990

111 Thomas NL, Jameson DA, Double DD, 'The effect of lead nitrate on the early hydration of portland cement', Cement and Concrete Research, Vol. 11, pp. 143-153, 1981

112 Gress DL, El-Korchi T, 'Microstructural characterization of cement-solidified heavy metal wastes', in Spence. RD (Ed), 'The chemistry and microstructure of solidified waste forms', Lewis Publishers, pp. 169-185, 1993

[113] Cocke DL, Ortego JD, McWhinney HG, Lee K, Shukla S, 'A model for lead retardation of cement setting', Cement and Concrete Research, Vol. 19, No. 1, pp. 156-159, 1989

[114] Sugita S, Shoya M, Sugawara T, 'Study on the effective use of water-granulated slag as fine aggregates of concrete', CAJ Review, 1986

[115] Tashiro C, Takahashi H, Kanaya M, Hirakida I, Yoshida R, 'Hardening property of cement mortar adding heavy metal compound and solubility of heavy metal from hardened mortar', Cement and Concrete Research, Vol. 7 pp. 283-290, 1977

[116] Tashiro C, 'The effect of several heavy metal oxides on the hydration and the microstructure of hardened mortar of C_3S', Proc. 7th Int. Cong. on the Chemistry of Cement, Paris, Editions Septima, Vol. 11 pp. II 37-II 42, 1980

[117] Cocke DL, Mollah MYA, 'The chemistry and leaching mechanisms of hazardous substances in cementitious solidification/ stabilization systems', in Spence. RD (Ed), 'The chemistry and microstructure of solidified waste forms', Lewis Publishers, pp. 187-242, 1993

[118] Arliguie G, Ollivier JP, Grandet J, 'Etude de l'effet retardateur du zinc sur l'hydratation de la pate de ciment Portland' (Study of the retarding effect of zinc on the hydration of Portland cement paste), Cement and Concrete Research, Vol. 12, pp. 79-86, 1982

[119] Ortego JD, Jackson S, Yu GS, 'Solidification of hazardous substances – a TGA and FTIR study of Portland cement containing metal nitrates', Journal of Environmental Science and Health, Vol. 24, No. 6, pp. 589-602, 1989

[120] Lieber W, 'The influence of lead and zinc compounds on the hydration of Portland cement', Supplementary paper II-22, Proc. 5th Int. Cong. on the Chemistry of Cement, Tokyo, pp. 444-454, 1968

[121] Young JF, 'A discussion of the interactions between hydrating calcium silicates and set-modifying admixtures', Silicates Industriels, pp. 209-212, 1978

[122] Arliguie G, Grandet J, Duval R, 'Etude du contact zinc – Pâte de ciment Portland' (Study of the contact zone between zinc and Portland cement paste), Proc. 7th International Congress on the Chemistry of Cement, Paris, Editions Septima, VII-22 – VII-27, 1980

[123] Lieber W, 'Influence of zinc oxide on the setting and hardening or Portland cement', Zement-Kalk-Gips, Vol. 20, No. 3, pp. 91-95, 1967 (Translated from German into English)

[124] Hill J, Sharp JH, 'The hydration products of Portland cement in the presence of tin(II) chloride', Cement and Concrete Research, Vol. 33, pp. 121-124, 2003

[125] Hill J, Sharp JH, 'Heat evolution in composite cements with additions of Sn(II) and Sn(IV) chlorides', Advances in Cement Research, Vol. 15, No. 2, pp. 57-66, 2003

[126] Taplin JH, Discussion of paper by Vivian HE, Proc. 4th Int. Symp. Chemsitry of Cements, Washington DC, Vol II, pp. 924-925, 1962

[127] British Standards Institution, BS 812: Part 2: 1995, 'Testing aggregates – Methods of determination of density', BSI, London, 1995

[128] BRE Report, BR331, 'Design of normal concrete mixes', available online from the BRE bookshop via the BRE homepage at www.bre.co.uk, or from CRC Ltd, 151 Rosebery Avenue, London, EC1R 4QX

[129] British Standards Institution, BS 882: 1992, 'Specification for aggregates from natural sources for concrete', BSI, London, 1992

[130] British Standards Institution, BS EN 12620: 2002, 'Aggregates in Concrete', BSI, London, 2002

[131] British Standards Institution, BS 1881-125: 1986, 'Testing Concrete – Methods for mixing and sampling fresh concrete in the laboratory', BSI, London, 1986

[132] British Standards Institution, BS 1881-102: 1983, 'Testing Concrete – Method for determination of slump', BSI, London, 1983

[133] British Standards Institution, BS 1881-107: 1983, 'Testing Concrete – Method for determination of density of compacted fresh concrete', BSI, London, 1983

[134] British Standards Institution, BS 1881-116: 1983, 'Testing Concrete – Method for determination of compressive strength of concrete cubes', BSI, London, 1983

[135] British Standards Institution, BS EN 196-1: 1995, 'Methods of testing cement - Part 1: Determination of strength', BSI, London, 1995

[136] Sibbick RG, Page CL, 'Susceptibility of various UK aggregates to alkali-aggregate reaction', Proc. 9th International Conference on Alkali-Aggregate Reaction (ICAAR), London, England, Ed. Poole AB, Concrete Society Publications, pp. 980-987, 1992

[137] CEN/TC 292, Draft prEN XXXXX, 'Characterisation of waste – Leaching – Compliance test for leaching of monolithic waste of regular shape', European Committee for Standardisation, CEN Central Secretariat, Brussels, 2000

[138] Neville AM, Brooks JJ, 'Concrete Technology', Revised edition, Longman Scientific and Technical, 1990

[139] Bushnell-Watson SM, Sharp JH, 'The effect of temperature upon the setting behaviour of refractory calcium aluminate cements', Cement and Concrete Research, Vol. 16, pp. 875-884, 1986

[140] British Standards Institution, PD 6682-1: 2003, 'Aggregates – Part 1: Aggregates for concrete – Guidance on the use of BS EN 12620', BSI, London, 2003

[141] Paul A, 'Chemistry of Glasses', 2nd Edition, Chapmen and Hall Ltd, London, 1990

[142] Shayan A, Ivanusec I, 'Influence of NaOH on mechanical properties of cement paste and mortar with and without reactive aggregate', Proc. 8th International Conference on Alkali-Aggregate Reaction ICAAR, Kyoto, Japan, Eds. Okada K, Nishibayashi S, Kawamura M, Elsevier Applied Science Publications Ltd, pp. 715-720, 1989

[143] Dimic D, 'Gas forming admixtures', in Paillere. AM (Ed), 'Application of admixtures in concrete', E&FN Spon, 1995, pp. 95-103

[144] Short A, Kinniburgh W, 'Lightweight Concrete', 3rd Edition, Applied Science Publishers Ltd, London, 1978

[145] Pera J, Coutaz L, Ambroise J, Chababbet M, 'Use of incinerator bottom ash in concrete', Cement and Concrete Research, Vol. 27. No. 1, pp. 1-5, 1997

[146] Zhu H, Byars E, 'Post-consumer glass in concrete: Alkali-silica reaction and case studies', Proc. Int. Conf. on Sustainable Waste Management and Recycling: Glass Waste, Kingston University, London, Eds. Limbachiya MC, Roberts JJ, Thomas Telford Publishing Ltd, pp. 99-108, 2004

[147] Blackwell BQ, Pettifer K, 'alkali-reactivity of greywacke aggregates in Maentwrog Dam (North Wales)', Magazine of Concrete Research, Vol. 44, No. 161, pp. 255-264, Dec. 1992

[148] Bland CH, Sharp JH, 'The chemistry of Portland cement – gasifier slag interactions', Advances in Cement Research, Vol. 3, No. 11, pp. 91-98, 1990

[149] Ong. S, Diamond. S, 'Unexpected effects of alkali hydroxide added to cement mix water', Cement Based Materials: Present, Future and Environmental aspects, Moukwa. M. et al. (Ed), Ceramic Transactions, Vol. 37, American Ceramics Society, Westerville, OH, pp. 37-48, 1993

[150] Diamond. S, Ong. S, 'Effects of added alkali-hydroxides in mix water on long-term SO_4^{2-} concentrations in pore solution', Cement and Concrete Composites, Vol. 16, pp. 219-226, 1994

[151] Kondo R, Daimon M, Sakai E, Ushiyama H, 'Influence of organic salts on the hydration of tricalcium silicate', J. Applied Chemistry and Biotechnology, Vol. 27, pp. 191-197, 1977

[152] Weast RC (Ed), 'CRC Handbook of Chemistry and Physics', 58th edition, CRC Press Inc, 1977